The Thesis Committee for Nishant Bandaru
Certifies that this is the approved version of the following thesis:

Map Based Visual Design Process for Multi-Stage Gear Drives

APPROVED BY
SUPERVISING COMMITTEE:

Supervisor:

Delbert Tesar

Pradeepkumar Ashok

Map Based Visual Design Process for Multi-Stage Gear Drives

by

Nishant Bandaru, B.E.

Thesis

Presented to the Faculty of the Graduate School of

The University of Texas at Austin

in Partial Fulfillment

of the Requirements

for the Degree of

Master of Science in Engineering

The University of Texas at Austin

May 2011

Acknowledgements

I would like to thank Dr.Tesar for his constant guidance throughout the process of researching and the writing of this report. His exemplary work ethic and the enthusiasm he showed in my research have been a strong motivation for me. I would also like to thank Dr. Pradeepkumar Ashok, whose valuable support over the years is greatly appreciated.

I would also like to express my immense gratitude to my parents, Ramesh and Padmavathi Bandaru for always providing me with unconditional support and the freedom to pursue my own goals.

May 6, 2011

Abstract

Map Based Visual Design Process for Multi-Stage Gear Drives

Nishant Bandaru, MSE

The University of Texas at Austin, 2011

Supervisor: Delbert Tesar

The primary objective of this research is to develop a visual design process for gear trains with multiple stages of reduction and varying configurational architectures. One of the main challenges in the design of such gear trains is in the sizing of the individual gears such that high levels of performance are obtained in spite of constraints due to different gear configurations. Formal design procedures that successfully meet this challenge are developed. A key contribution of this research is the utilization of these design procedures to create sets of three-dimensional design maps. The design procedures help a designer manage more than 20 design parameters in designing for a broad range of gear train requirements (Rated torque capacity, Volume, Weight, Inertia, Responsiveness, Torque Density etc.) while accounting for assembly constraints. Each set of design maps corresponds to a given set of design parameters, some of which are held fixed and some of which are put in the hands of the designer. The latter set of design

parameters are termed in this research as design knobs. They can be ‘tuned’ by a designer in order to generate new sets of design maps. The idea is that a designer, using the design information conveyed to him/her graphically through a given set of design maps, is able to then tune the design knobs to generate an updated set of design maps which reflect design solutions that are more desirable in terms of the application requirements. By adjusting the design knobs and looking at updated design maps, a designer is able to quickly assess the effect of his/her design decisions. The end result is that a single designer is empowered with the ability to quickly arrive at a preliminary design of a gear train that satisfies the design requirements. This preliminary design would be a good starting point for more detailed design development.

Table of Contents

List of Tables

List of Figures

List of Illustrations

No table of contents entries found.

Chapter 1 : Introduction

In today's world, Electro-mechanical Actuators (EMA) have become critical elements in the design and development of open-architecture intelligent mechanical systems. There is a strong drive to replace traditional hydraulic or pneumatic actuators in applications such as vehicle drive wheels, aircraft and submarine control surfaces (Weimer 2003; Koran and Tesar 2008; Budinger et al.). An electro-mechanical actuator is an integrated unit consisting of an electric prime mover (motor), gear train, bearings, seals, sensors and a controller (Figure 1-1). Some of the features that make EMAs important are their compactness, power density, potential for advanced control, modularity, efficiency, ease of maintenance and eco-friendliness (Park 2005).

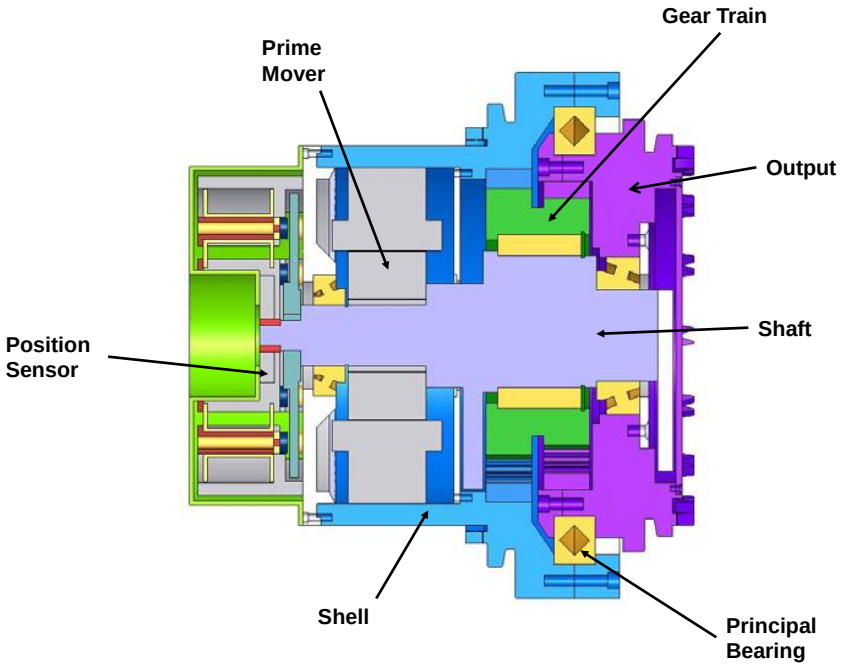

Figure 1-1: Major Electromechanical Actuator Components (Tesar, 2004)

1.1 MOTIVATION

The goal of this research is to develop a formal design process for a particular class of EMA termed as Low Complexity Rotary Actuators which can be mass produced at low cost while still delivering a high level of performance. The gear train is a key component in determining whether or not an actuator can meet these requirements. The use of Star Compound Gear Trains (SCGT's) (see Figure 2-16, Figure 2-22 and Figure 2-37) is a significant step towards achieving these requirements due to their remarkable characteristics. Star Compound Gear Trains are simple in structure, rugged and easy to manufacture and assemble. The present research will focus on the development of a design process for three types of SCGT's. The three types are:

1. One-Stage Star Compound Gear Train (1-Stage SCGT)
2. Pancake-Type Two-Stage Star Compound Gear Train (P-Type 2-Stage SCGT)
3. Coffee-Can type Two-Stage Star Compound Gear Train (C-Type 2-Stage SCGT)

Design procedures for these three SCGT's are developed in Chapter 2. For a complete understanding of the developed design procedures, a basic understanding of gear nomenclature is necessary. Therefore, a description of fundamental gear terminology is presented in Section 2.1. The strength equations provided by the AGMA (American Gear Manufacturers Association) are discussed in Section 2.2. The rest of Chapter 2 is devoted to developing systematic design procedures for each of the three types of SCGT's. The design procedures developed in Chapter 2 are the foundation for a visual design process.

1.2 FEATURES OF THE PROPOSED VISUAL DESIGN PROCESS

The proposed visual design process is meant to reduce the time and effort needed to obtain a preliminary design that satisfies all the basic requirements for a given application. The goal is that anyone with a Bachelor of Science in Mechanical

Engineering should be able to make use of the design process to quickly arrive at a set of preliminary actuator designs that meet his/her needs. Succeeding in this goal removes the need for teams of experts to be involved at the preliminary design stage. For a company that designs and manufactures actuators, this would mean a more efficient use of company resources.

The visual design process developed in this report is meant to both steer and be steered by the designer based on his/her choices of 'design knobs'; i.e., fundamental design parameters that a designer has the freedom to modify (See Section 3.2). Although different in implementation, the visual design process developed in this report reflects the basic motivation behind "computational steering". According to (Winer and Bloebaum 2001), the goal of the computational steering paradigm is to allow a researcher to make changes to the parameters of a problem to interactively "steer" the analysis to a solution, rather than let the solution algorithm run its course.

(Tong and Walton, 1987) described an interactive program to design internal gear pairs. The program was designed to be part of a suite of programs and is said to "make use of an extensive knowledge base allowing non-specialized users to achieve satisfactory designs". The authors state that the objective was to give maximum flexibility to the user, thus allowing him/her to direct the design rather than having the software make all of the decisions. As such, the design process developed in the current research will reflect this philosophy.

(Roos and Spiegelberg, 2005) made use of a graphical solution process as a design aid. Their work illustrated the value of plotting three-dimensional design surfaces to show how design parameter choices (gear ratio, center distances, ring gear radius, and face width) affect the performance parameters (gear size, weight, and inertia) (Vaculik and Tesar, 2008). The three-dimensional design surfaces are also used to compare simple

spur gear and planetary gear trains given the same materials, gear ratios and sets of constraints (see Figure 1-2).

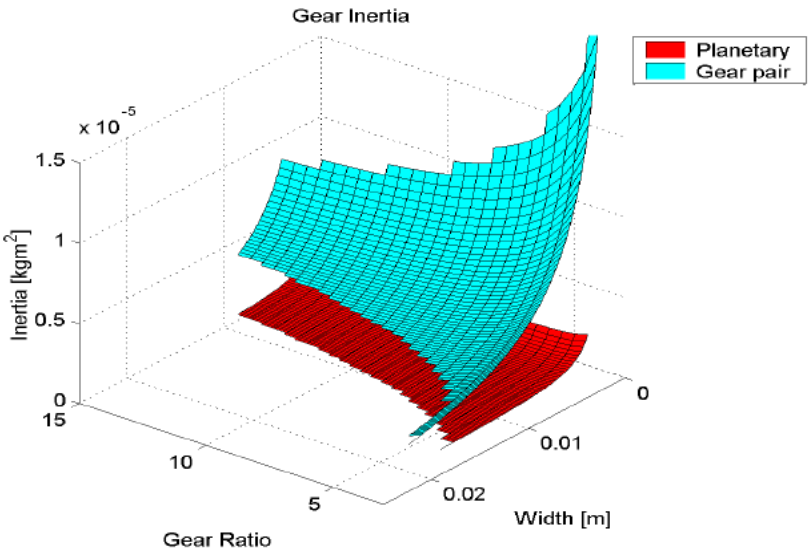

Figure 1-2: Gear Train Inertia as a Function of Tooth Numbers and Gear Ratio for Spur and Planetary Gear Trains, from Roos and Spiegelberg (2004)

In the current report, three-dimensional maps of design and performance parameters are used to graphically convey to the designer the state of a design. The benefits of such an approach will be illustrated clearly in Chapter 4, where three different design problems are presented. Solutions that satisfy all constraints and design requirements specified in each of the design problems are found by making use of design maps described in Chapter 3. The design maps make it easy for a novice designer to observe the effects of his/her design parameter choices on the actuator performance. In this way, it serves as a learning tool for inexperienced designers. This aspect is illustrated in Figure 1-3. Each of the design maps shown in Figure 1-3 on the left indicate the Rated Torque capacity T (vertical-axis) as a function of the gear train mesh diameter D_{gm} (see Section 2.4) and the gear ratio g. A horizontal reference plane is shown at 2000 *ft-lbf* for

convenience. The design map on the left corresponds to a set of design parameters that specify spur gearing (See Section 2.1.1). The design map on the right of Figure 1-3 corresponds to the same set of design parameters except that helical gearing is specified. By comparing the two design maps in Figure 1-3, a designer can quickly assess the relative benefit of specifying helical gearing rather than spur gearing. In the design maps shown in Figure 1-3, the designer may be able to deduce that the use of helical gearing approximately doubles the Rated Torque capacity in this case. The reader should also keep in mind that, although it cannot be demonstrated here due to the limitations of paper, the 3-D design maps are interactive. The designer is free to rotate the maps for viewing from any angle. By selecting various points on the design maps, a designer is also able to get accurate design information. This is illustrated in the design maps in Chapter 4. Some additional information regarding the visual design process developed in this report is presented in the following section.

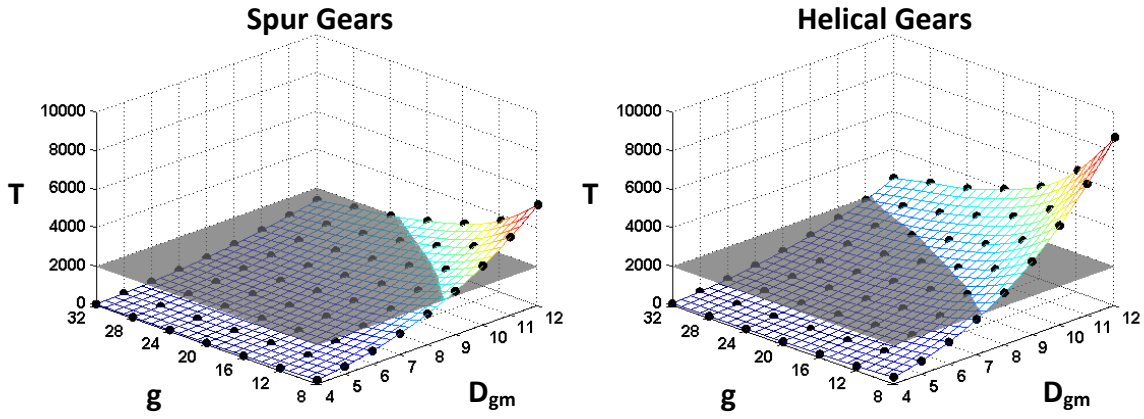

Figure 1-3: Design Map for Rated Torque (*ft-lbf*) - Spur versus Helical Gearing

(Chong 2002) recognized the shortcomings of traditional methods, provided by gear standards organizations and researchers, in estimating gear sizes and parameters for preliminary design. These methods 'do not take the configuration and the arrangement of the gear drive elements into consideration', although the configuration and arrangement of the gears have a significant effect on the gear dimensions. The authors then propose an algorithm that integrates and automates the dimensional and configuration design processes in order to help the designer at the preliminary design stage. The design process (Chapter 2) developed in the present research also succeeds in integrating the dimensional and configuration design processes. A major difference between the design procedures developed in this report and the work in (Chong 2002), is that gear design parameters such as pressure angles and helix angles are included in the preliminary design stage in this report, whereas (Chong 2002) defer the selection of these parameters to a more detailed design stage.

1.3 VISUAL DECISION-MAKING ENVIRONMENT

(Vaculik and Tesar, 2008) draw a parallel between the visual decision making framework for the operation of an EMA developed by (Ashok and Tesar, 2007) and EMA design. They note that, "In both operation and design, a human decision maker must make intelligent choices of the operational (or design) parameters in order to optimize (or manage) the performance parameters of the system". The design process developed in this research will therefore share some characteristics with the framework for actuator operation. Based on their review of literature relevant to the development of a visual decision-making environment, Vaculik and Tesar provide a list of key features that such a system must embody. Features from that list that are relevant to the current research are listed in Table 1-1 along with comments appropriate to the present research.

The reader is advised to refer to (Vaculik and Tesar, 2008) for the full list of key features. The comments make it clear that, although no specific visual decision-making tool was developed as part of the current research, the proposed visual design process is well-suited to being embedded in such a tool. The comments, together with the features described in the previous section, provide a full description of the features of the design process developed in the present research. The reader is encouraged to note how the developed design process is well-suited to being incorporated into a visual decision-making tool.

1.4 SUMMARY OF CHAPTERS

The motivation behind the creation of a visual design process for the gear trains studied in the current research, as well as the attributes and characteristics of such a design process were discussed in this chapter. The remaining chapters in this report are laid out as follows:

In Chapter 2, first gearing fundamentals and relevant terminology are presented. A description of the AGMA tooth strength equations, a key part of the gear train design procedures, is then provided. Design procedures (with integrated configuration and dimensional processes) are then systematically developed for each of the three types of SCGT's studied in the current research. Additional information that may be useful for a designer employing these design procedures are presented at the end.

In Chapter 3, an algorithm used to create three-dimensional design maps using the design procedures developed in Chapter 2 is presented. Next, the concept of 'design knobs'; i.e., design parameters that a novice designer may use to update design maps is described. Section 3.3 then lists some fundamental design characteristics of SCGT's. The

discussion in Section 3.3 is meant to aid the reader in understanding the reasons behind the shapes of the three-dimensional design maps presented in the following sections.

Table 1-1: Important Features of a Visual Decision Making Environment

Key Features	Comments
All of the information shown in different displays, windows or tabs should be linked such that choices made in one display are reflected in other displays.	A set of design maps are generated corresponding to a particular combination of a priori parameters and design knob values (See Section 3.2). Any change in the design knobs result in an updated set of design maps that correspond to the new values for the design knobs.
High- level information (e.g. overall performance metrics) should be available, particularly when non-experts will be viewing the information.	The design procedures developed in Chapter 2 involve the calculation of low-level information (e.g. contact ratios, resultant thrust load) as well as high-level information (e.g. rated torque, weight). For the majority of this report, only high-level information will be presented. However, as shown in 4.2.4, low-level information is also available at any time.
Low-level information (with more internal details) should be available for experts.	
The user should be able to drill down to the lower levels of the problem and be able to view/ modify internal parameters and any assumptions when necessary.	The design process developed in the present research empowers a designer to work only with high-level design parameters (e.g. overall geometry, gear ratio etc.) through the use of design knobs, or control more fundamental design parameters through *constraint addition* (See Section 2.7.5) and *filtration* of the Design Solution Set (See Section 2.2)
The interface should be interactive, allowing user input of independent parameters.	The user is in complete control of all design parameters and can choose to override suggested values at any time in the process (See 4.3)

Section 3.4, Section 3.5 and Section 3.6 show representative design maps for a 1-Stage SCGT, Pancake-Type 2-Stage SCGT and a Coffee-Can Type 2-Stage SCGT respectively. In order to provide the reader with a fundamental understanding of the relationships between the performance parameters (Rated Torque T, Weight W, Torque Density T_D, Inertia I and Responsiveness R) and the gear train geometry (mesh diameter D_{gm}, pitch diameters and face-widths of the gears, gear ratio g), an in-depth analysis of the design maps for a 1-Stage SCGT was done. Power laws relating the performance parameters to the primary design knobs D_{gm} and g (see Section 3.2) are provided.

In Chapter 4, the steps a designer may take in order to find a good preliminary design solution for a given set of design requirements are illustrated through the use of three different design problems. The approach used is summarized in Figure 4-30 (from Section 4.4). The design problems illustrate how a designer may *tune* design knobs to systematically update a set of design maps. From each design map, the designer gains visual information he/she can use to decide which design knobs to tune.

The design procedures (Chapter 2), design maps (Chapter 3) and the recommended approaches for the utilization of the maps (Chapter 4) are summarized in Chapter 5. Significant results and findings from the current research are also presented. Some recommendations for future work are also provided.

Chapter 2 : Methodology for Design Map Generation

This chapter describes the methodology used to generate the design maps shown in Chapter 3. In this study, the design and analysis of the gearing conforms to those in standards ANSI/AGMA 2001-D04 *Fundamental Rating Factors and Calculation Methods for Involute Spur and Helical Gear Teeth*. It should be noted that the use of American National Standards is completely voluntary; a designer can choose to either conform to or ignore these standards. Before the AGMA methodology for gear design can be presented, it is necessary to have some basic understanding of gearing and gear terminology.

2.1 FUNDAMENTALS OF GEAR TERMINOLOGY

2.1.1 Gear Types

The Star Compound Gear Train (SCGT) contains only parallel-shaft gear types i.e. the axes of meshing gears are parallel to each other and are in fixed rigid structures. Therefore, intersecting-axes gears such as bevel gears and non-intersecting, non-parallel axes gears such as worm gears, hypoid gears etc. are not discussed in the current research. The two primary types of parallel-shaft gears used in the SCGT are spur and helical gears.

Spur gears are the most common type of gear used in industry because they are relatively simple to design and manufacture. Spur gears have teeth cut parallel to the axis of rotation and, as a result, impose only radial loads on supporting bearings. Spur gears are generally limited to pitch-line-velocities around 4000 fpm (approximately 2500 rpm for a 6” diameter gear) to avoid high-frequency vibrations and unacceptable noise levels (Collins 2002).

Helical gears are similar to spur gears except that their teeth are cut at an angle (known as the helix angle ψ) to the axis of rotation. The angled teeth produce both radial and axial (thrust) loads on supporting bearings, with the axial loads increasing with helix angle. The advantage of helical gear teeth is that mating teeth come into contact gradually leading to smoother and quieter operation, especially at high speeds. Helical gears have therefore been used in applications where the pitch line velocities were in excess of 10,000 fpm (approximately 6500 rpm for a 6" diameter gear). Helical gears also have a greater load-carrying capacity than equivalently sized spur gears. The reasons for this will become obvious in the following sections.

2.1.2 Tooth Profile

Currently, the most commonly used tooth profile is the involute, which can be described as the curve traced by the end of a taut string as it is unwrapped from a cylinder (Figure 2-1).

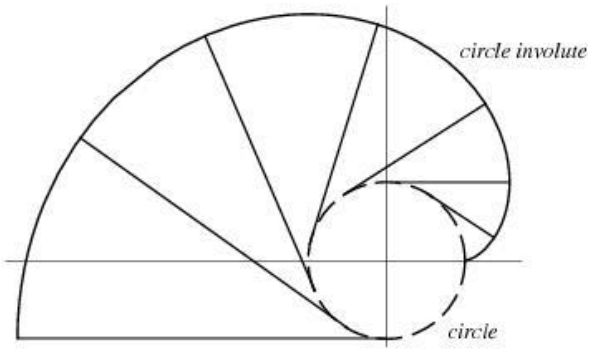

Figure 2-1: Generation of an involute curve (Weisstein, Eric W. "Involute." From *MathWorld*--A Wolfram Web Resource)

(Park and Tesar, 2005) listed the benefits of using circular-arc gear teeth in an internal-external gear mesh. However, there is a limit (0.28) for the ratio of pitch diameter of the external gear to the pitch diameter of the internal gear below which circular-arc gears cannot be used. For the current study of Star Compound Gear Trains,

this constraint severely restricts the set of possible designs. For this reason, throughout this study, involute gear teeth will be used.

2.1.3 Basic Gear Nomenclature

Chapter 12 from (Budynas and Nisbett 2010) and Chapter 15 from (Collins 2002) provide a comprehensive introduction to gear nomenclature. A full discussion on gear terminology is not in the scope of this text but the reader may refer to the references mentioned above for information not included here. A brief summary of relevant gear terminology important to an understanding of the current research is presented here. With regard to Figure 2-2 and Figure 2-3, the following can be stated:

- The smaller of two mating gears is called the *pinion*. The larger is referred to as the *gear*. For all the designs in this study, the pinion is the driving member and the gear is the driven member.
- The *pitch diameter D* is the diameter of the *pitch circle*, which is a theoretical circle that serves as a basis for most gear calculations. The pitch circle may be thought of as the "effective working circle of a gear that would be obtained if a pair of gears were replaced with disks that transmitted the same motion in the same package space through contact friction" (Anon)
- The *base circle* is an invisible circle from which the involute tooth profile is generated (Figure 2-2). It is important to note that the involute tooth profile exists only outside of the base circle (See *Interference*).
- The *addendum a* and *dedendum b* are the distances between the pitch circle and the *top land* and *bottom land* of a gear tooth respectively. The *whole depth* of a tooth h_t equals the sum of the addendum and dedendum. The diameter of the addendum circle is known as the *Addendum Diameter* D_a (Outer Diameter). The

diameter of the dedendum circle is known as the *Dedendum diameter* D_b (Root Diameter).

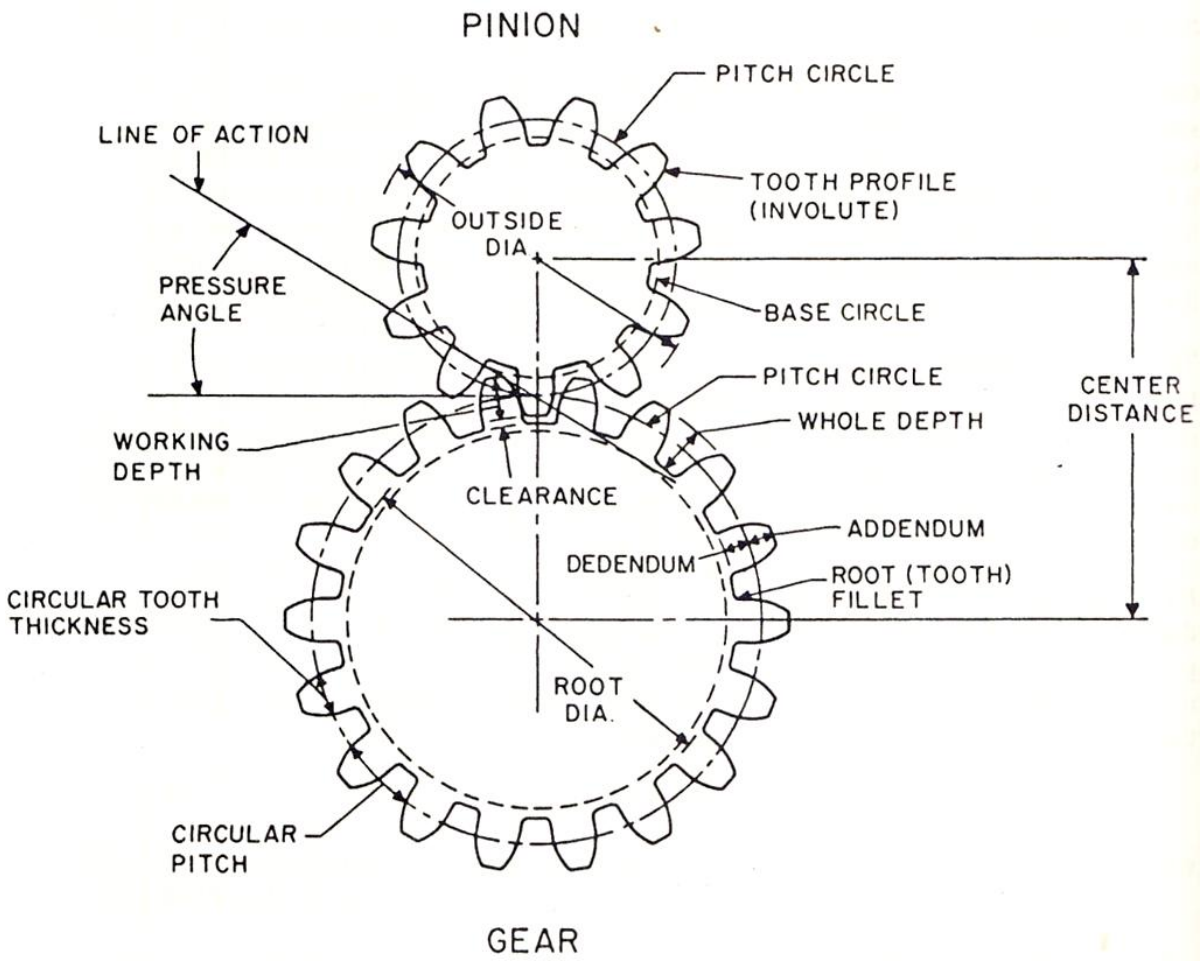

Figure 2-2: Basic Gear Nomenclature (Wilson and Sadler)

- The theoretical *center distance* equals the sum of the pitch radii of the pinion and gear. The *operating center distance* is not the same as the theoretical due to manufacturing and assembly inaccuracies. Operating center distance may also be changed to obtain a required *backlash* (See below).

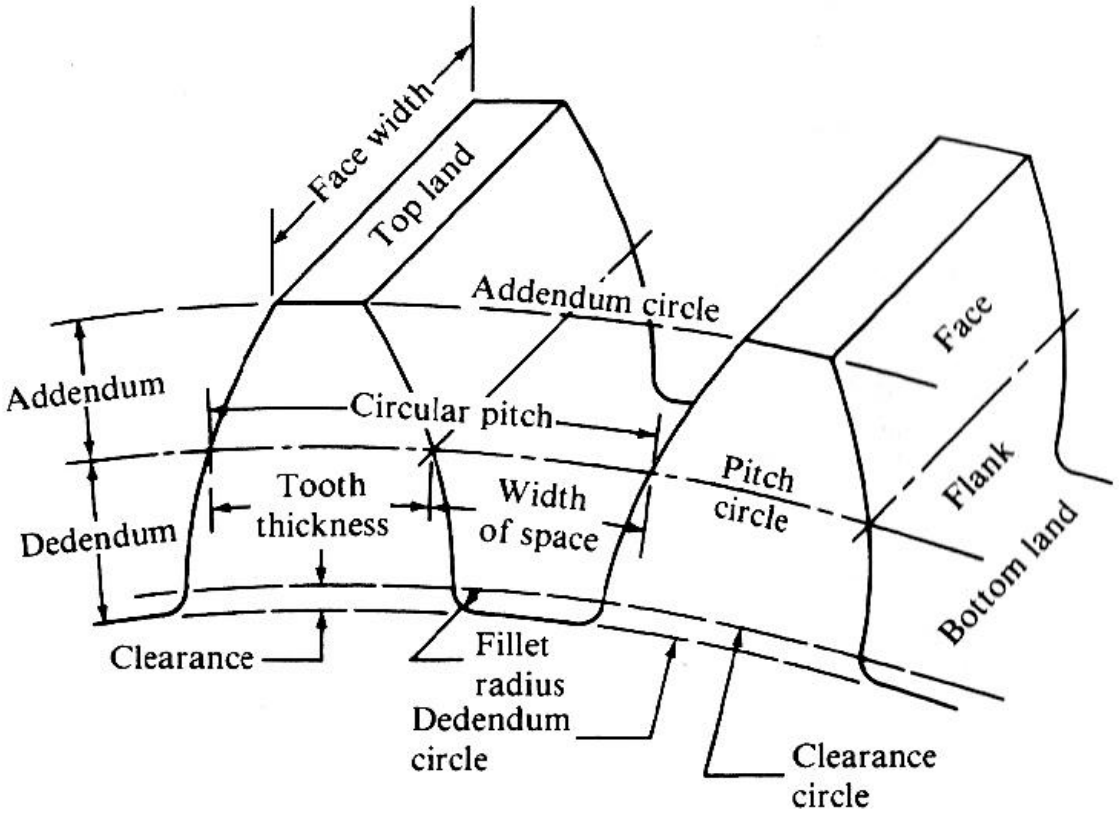

Figure 2-3: Basic Gear Nomenclature (Mott 2003)

- The *line of action* (Figure 2-4) is a line normal to the mating gear teeth at the point of contact and tangent to the base circles. For a pair of meshing gears, the normal force applied by the driving member on the driven member acts along this line. The *length of contact* (Z) is the length of the segment of the line of action during which teeth from mating gears are in contact. The *base pitch* p_b is the distance along the base circle from a point on one tooth to the corresponding point on an adjacent tooth. It is thus similar to the circular pitch except that it is measure along the base circle.

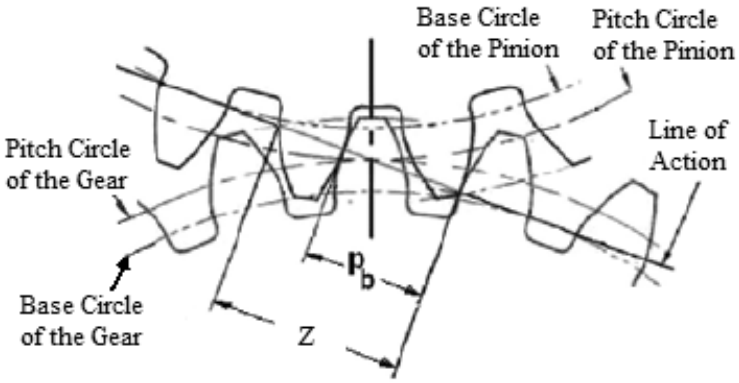

Figure 2-4: Line of Action (Gonzalez, 2009)

The ratio of the length of contact Z to the base pitch p_b is known as the *Contact Ratio* p_b.

$$m_p = \frac{Z}{p_b} \tag{2.1}$$

It is a measure of the average number of driving teeth in contact with driven teeth. The reader may refer to (Budynas and Nisbett 2010) for details on the calculation of Z. Higher contact ratio implies better load sharing and lower noise due to smoother meshing. The minimum preferred contact ratio is 1.4 (Norton 2010). This means that two pairs of teeth are in contact 40% of the time and one pair of teeth are in contact 60% of the time. Gears with contact ratios greater than 2 are known as high-contact ratio gears.

- The pressure angle φ is the angle between the line of action and the common tangent to the pitch circles of the mating gears (see Figure 2-2). From Figure 2-2, it should be apparent that all other parameters being the same, an increase in the pressure angle results in a reduced base circle diameter. The Figure 2-5 illustrates the fact that reduction in the base diameter results in an increased tooth thickness at the base circle and thus a stronger tooth i.e. a tooth with a higher bending-load-

carrying capacity (Collins 2002). However, higher pressure angles also cause increased radial loads on the shafts and bearings and higher noise levels as a result of decreased contact ratio. Gears and cutting tools with pressure angles of 20^o are commonly available in the market.

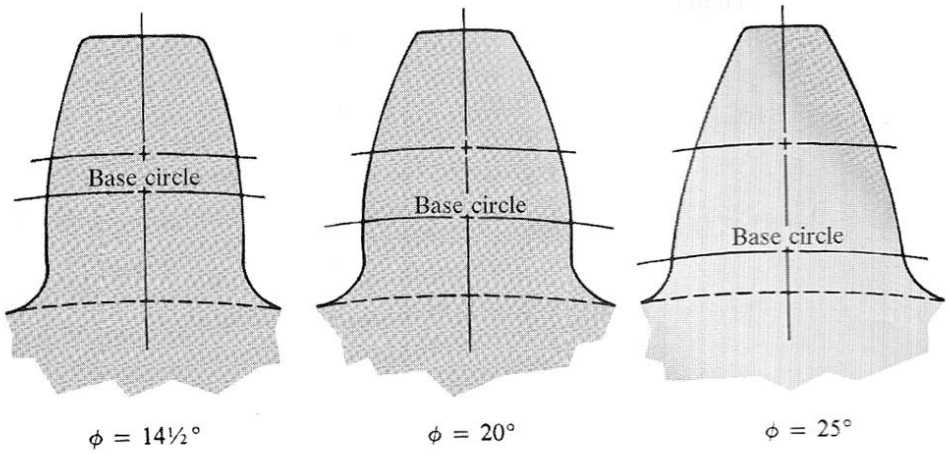

Figure 2-5: Full-depth, Involute Tooth Form for varying Pressure angles (Mott 2003)

The three following terms relate to the size of teeth:

- The circular pitch p is the distance along the pitch circle from a point on one tooth to the corresponding point on an adjacent tooth.
- The module m, a measure of tooth size used in SI[1], is the ratio of the pitch diameter in millimeters (mm) to the number of teeth.
- The diametral pitch P_d, a measure of tooth size used in the U.S. system is the ratio of the number of teeth on the gear to the pitch diameter in inches (in) i.e. it is the reciprocal of the module.

[1] SI is the abbreviation for the International System of Units

[2] The *clearance circle* is a circle tangent to the addendum circle of the mating gear. The *clearance* c (see Figure 2-3) is the amount by which the dedendum in a gear exceeds the addendum of its mating gear

The relations between the three parameters above are shown in Table 2-1. For the current study, the U.S. system of units will be used; i.e., tooth size will be expressed in terms of the diametral pitch. Common diametral pitches and modules which most gear manufacturers have in stock are shown in Table 2-2. However, it must be clear that a designer may specify *any* value of diametral pitch if warranted by an application.

Table 2-1: Relations between Diametral Pitch, Circular Pitch and Module

To obtain	P known	Formula
Diametral Pitch P_d	Module m	$P_d = \frac{25.4}{m}$
Diametral Pitch P_d	Circular Pitch p	$P_d = \frac{\pi}{p}$
Diametral Pitch P_d	No. of Teeth N and Pitch Diameter D	$P_d = \frac{N}{D}$
Module m	No. of Teeth N and Pitch Diameter D	$m = \frac{D}{N}$
Circular Pitch p	No. of Teeth N and Pitch Diameter D	$p = \frac{\pi D}{N}$
Circular Pitch p	Module m	$p = \pi m$

Table 2-2: Commonly used Diametral Pitches and Modules (Reproduced from (Shigley, Mischke, and Brown))

Diametral Pitches in General Use	
Coarse pitch	2, 2¼, 2½, 3, 4, 6, 8, 10, 12, 16
Fine pitch	20, 24, 32, 40, 48, 64, 96, 120, 150, 200
Modules in General Use	
Preferred	1, 1.25, 1.5, 2, 2.5, 3, 4, 5, 6, 8, 10, 12, 16, 20, 25, 32, 40, 50
Next Choice	1.125, 1.375, 1.75, 2.25, 2.75, 3.5 , 4.5, 5.5, 7, 9, 11, 14, 18, 22, 28, 36, 45

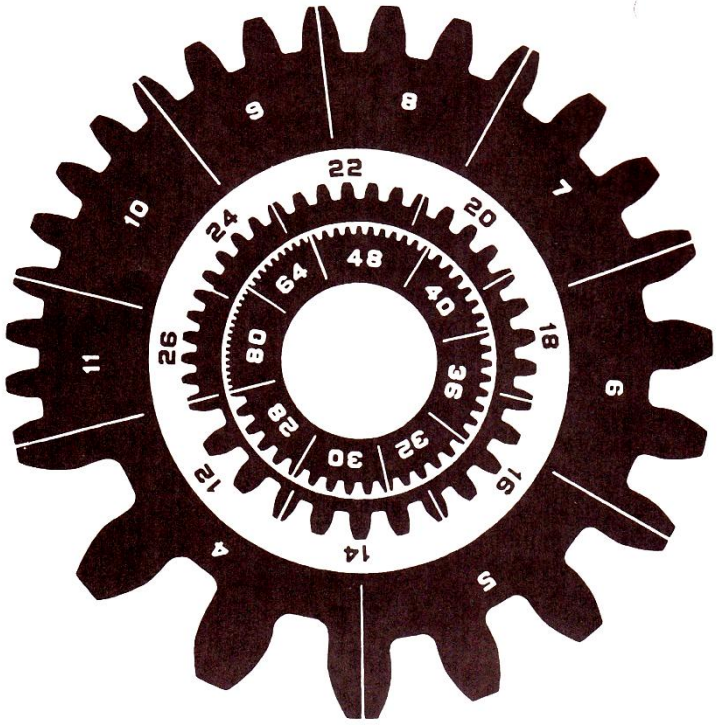

Figure 2-6: Actual Gear Tooth Size as a function of Diametral Pitch (Barber-Colman Company, Loves Park, IL)

We can see from Figure 2-6 that, for the same pitch circle diameter, smaller diametral pitches result in fewer and hence larger gear teeth. Therefore, lower diametral pitches allow high torque transmission. Also, as a general rule, diametral pitches should decrease as we move from the input side to the output side of a gear train to account for increasing tooth loads.

To facilitate interchangeability the gear industry has adopted some standardized tooth systems defined by specific values for pressure angles, addendum and dedendum dimensions, whole depth, and minimum tip clearance (related to tool geometry) (Collins 2002).

Table 2-3: Standard Proportions - AGMA Full-Depth Gear Teeth (inch) (Collins, 2002)

	Coarse Pitch $P_d < 20$	Fine Pitch $P_d \geq 20$
Pressure Angle	20^o or 25^o	20^o
Addendum	$1.000/P_d$	$1.000/P_d$
Dedendum	$1.250/P_d$	$(1.200/P_d)+0.002(\text{min})$
Whole Depth	$2.250/P_d$	$(2.200/P_d)+0.002(\text{min})$
Working Depth	$2.000/P_d$	$2.000/P_d$
Clearance[2] (basic)	$0.250/P_d$	$(0.200/P_d)+0.002(\text{min})$
Clearance (shaved or ground teeth)	$0.350/P_d$	$(0.350/P_d)+0.002(\text{min})$
Circular Tooth Thickness	$1.571/P_d$	$1.571/P_d$

For the current research, Standard Full-Depth Teeth with the dimensions as in Table 2-3 will be used. Non-standard teeth may be used for special applications if necessary.

- Backlash, shown in Figure 2-7, can be thought of as the amount of freedom of one gear to move while the mating gear is held fixed (Collins 2002). It is the amount by which the width of tooth space (See Figure 2-2) exceeds the thickness of the

[2] The *clearance circle* is a circle tangent to the addendum circle of the mating gear. The *clearance* c (see Figure 2-3) is the amount by which the dedendum in a gear exceeds the addendum of its mating gear (Collins, 2002).

tooth of the mating gear along the pitch circle. Although zero-backlash gears are necessary in some applications such as precision positioning mechanisms, in most applications some backlash is recommended to account for manufacturing tolerances, temperature effects and tooth lubrication. Table 2-4 shows the recommended backlash (extracted from AGMA 2002-B88 Standard) corresponding to certain diametral pitches and center distances (Mott 2003).

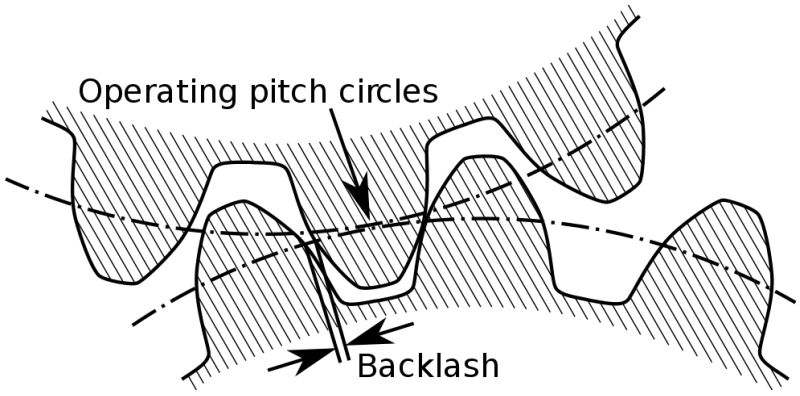

Figure 2-7: Illustration of Backlash in a gear pair

Table 2-4: Recommended minimum backlash (in) for coarse pitch gears (Mott 2003)

Diametral Pitch	Circular Pitch	Center Distance, C (in)				
P_d	p_c	2	4	8	16	32
18	0.17	0.005	0.006			
12	0.26	0.006	0.007	0.009		
8	0.39	0.007	0.008	0.010	0.014	
5	0.63		0.010	0.012	0.016	
3	1.05		0.014	0.016	0.020	0.028
2	1.57			0.021	0.025	0.033
1.25	2.51				0.034	0.042

- Interference between gear teeth occurs when the addendum of one gear tooth makes contact with the non-involute portion of the mating tooth's flank. Interference leads to the undercutting of teeth when a generation process such as hobbing is used for gear manufacture. Undercutting is the removal of material at the interfering portion of the flank and it significantly weakens the tooth (Collins 2002). Although there are many ways to overcome interference (increasing the number of pinion teeth, increasing center distance, tooth modification etc.), the simplest way is to never use less than the minimum number of teeth necessary to avoid interference (See Table 2-5). To ensure that no interference occurs between any two gears in a particular tooth system, the minimum number of teeth necessary on the pinion is:

$$N_{\min} = \frac{2}{\sin^2 \varphi} \qquad (2.2)$$

Table 2-5: Recommended minimum number of pinion teeth (Mott 2003)

Tooth Form	Minimum number of teeth
14.5^o, involute, full-depth	32
20^o, involute, full-depth	18
25^o, involute, full-depth	12

The reader should note that the minimum number of pinion teeth necessary to avoid interference reduces as the pressure angle increases. As discussed earlier, an increase in the pressure angle results in a smaller base circle, leading to a larger involute region which helps avoid interference. In the discussion on diametral pitch earlier, it was stated that smaller diametral pitches were favorable for high torque transmission. Thus, in order to satisfy the need for small diametral pitches

i.e. smaller number of teeth, without the occurrence of interference, a higher pressure angle is used when high torque transmission or higher torque density is required.

Although much of the nomenclature discussed so far was in reference to spur gears, the terms are also valid for helical gears. As mentioned earlier, helical gears are similar to spur gears, the only difference being that instead of having their teeth straight and parallel to the axis of rotation, helical gears have their teeth at an angle (known as the helix angle ψ) to the axis of rotation (See Figure 2-8).

With reference to Figure 2-8, the following can be stated:

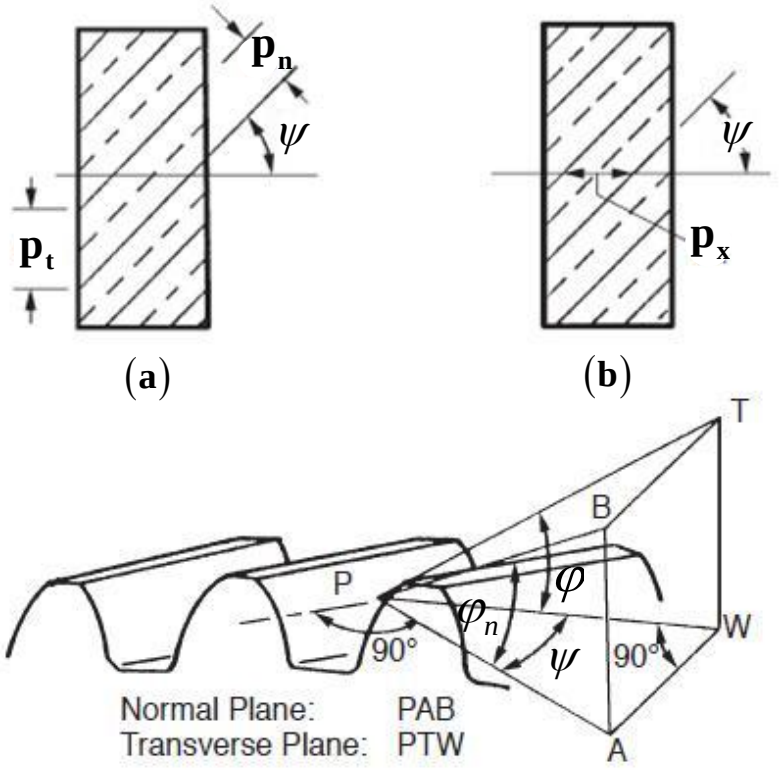

Figure 2-8: Helical Gear Nomenclature [Courtesy of Quality Transmission Components]

- In addition to the diametral and circular pitches defined for spur gears, helical gears have two additional pitches associated with them. These are associated with the two planes shown in Figure 2-8(c), namely, the transverse plane PTW which is perpendicular to the axis of gear rotation and the normal plane PAB which is perpendicular to the tooth surface.
- The transverse diametral pitch P_t is the ratio of number of teeth in the gear to the pitch diameter. It applies when the teeth are being considered in the transverse plane. The diametral pitch defined for spur gears earlier is therefore the same as the transverse diametral pitch.

$$P_t = P_d = \frac{N}{D} \tag{2.3}$$

- The normal circular pitch p_n is the distance between corresponding points on adjacent teeth measure on the pitch surface in the normal plane. It is related to the circular pitch p_c (which equals the transverse circular pitch p_t as it is measured in the transverse plane) by

$$p_n = p_c \cos\psi = p_t \cos\psi \tag{2.4}$$

- The normal diametral pitch P_{nd} is the diametral pitch in the normal plane. The normal diametral pitch is related to the normal circular pitch p_n in the same way that diametral pitch P_d is related to circular pitch p in the case of spur gears.

$$P_d p_c = \pi \text{ (Spur)} \tag{2.5}$$

$$P_{nd} p_n = \pi \text{ (Helical)} \tag{2.6}$$

- The axial pitch is the distance between corresponding points on adjacent teeth, measured in the axial direction i.e. along the axis of rotation. In order to ensure smooth transfer of load as teeth come into mesh, it is recommended (Mott 2003; Collins 2002) that the face width F be at least 2 times the axial pitch p_x. The axial pitch is given by

$$p_x = \frac{p_t}{\tan\psi} = \frac{p_n}{\sin\psi} \tag{2.7}$$

The contact ratio m_p defined earlier for spur gears is valid for helical gears and is labeled the transverse contact ratio. In addition, helical gears have an axial contact ratio, which is given by the relation:

$$m_F = \frac{F}{p_x} \tag{2.8}$$

A larger transverse contact ratio implies better load sharing among multiple teeth simultaneously in contact, and a larger axial contact ratio implies a distribution of tooth loading along a greater contact length (Collins 2002).The total contact ratio, an indication of the overall load sharing among helical teeth, equals the sum of the transverse and axial contact ratios.

- Two pressure angles are associated with helical teeth, namely, the transverse pressure angle φ_t measured in the transverse plane (equal to the pressure angle defined for spur gears) and the normal pressure angle φ_n measured in the normal plane. They are related through the helix angle as shown below:

$$\tan\varphi_n = \left(\tan\varphi_t\right)\left(\cos\psi\right) \tag{2.9}$$

Standard full-depth helical gears have the same tooth proportions as those for spur gears (Table 2-3) with the important difference that the diametral pitch and pressure angle are those measured in the normal plane; i.e., the normal diametral pitch and the normal pressure angle.

Table 2-6: Standard Proportions for AGMA Full-Depth Helical Gear Teeth (Collins 2002)

	Coarse Pitch $P_n < 20$	Fine Pitch $P_n \geq 20$
Addendum	$1.000/P_n$	$1.000/P_n$
Dedendum	$1.250/P_n$	$(1.200/P_n) + 0.002(\text{min})$
Whole Depth	$2.250/P_n$	$(2.200/P_n) + 0.002(\text{min})$
Working Depth	$2.000/P_n$	$2.000/P_n$
Clearance (basic)	$0.250/P_n$	$(0.200/P_n) + 0.002(\text{min})$
Clearance (shaved or ground teeth)	$0.350/P_n$	$(0.350/P_n) + 0.002(\text{min})$
Circular Tooth Thickness	$1.571/P_n$	$1.571/P_n$

From Figure 2-8(a), it is clear that the tooth thickness measured in the transverse plane is greater than the tooth thickness in the normal plane. Since torque transmission occurs in the transverse plane (due to tangential load on the gear teeth), this implies that helical teeth are stronger than equivalent spur teeth; i.e., spur teeth with the same normal diametral pitch and pitch diameter. Thus, due to increased tooth strength and increased contact ratio, helical gears have greater load-carrying capacity than equivalently sized spur gears.

2.2 AGMA METHODOLOGY FOR GEAR DESIGN

The AGMA approach to gear tooth design against failure makes use of numerous empirical modifying factors that account for factors such as assembly, geometry, loading and material inconsistencies. Although a large number of charts, graphs and tables of supporting data are published by the AGMA, the current research will make use of an abridged selection of supporting data (as published in (Budynas and Nisbett 2010; Collins 2002). For the goals of the current research, this simplified AGMA approach is sufficient. When a more detailed design is sought, a designer is advised to use the full standards. Table 2-7 lists all of the symbols used in the AGMA procedure and their meanings. A brief summary of the meaning of the terms and their recommended values (where applicable) is provided in Section 2.2.1.

The AGMA methodology for design of a gear pair uses two fundamental stress equations, one for bending stress (s_t) in a gear tooth and another for contact stress (s_c), which relates to the pitting resistance in a gear tooth. Pitting is one kind of failure of the surface of a gear tooth as a result of repeated contact stresses of high magnitude. The two fundamental equations (taken from (Budynas and Nisbett 2010)) are:

$$s_t = f^t K_o K_v K_s \frac{P_d}{F} \frac{K_m K_B}{J} \tag{2.10}$$

and,

$$s_c = C_P \sqrt{f^t K_o K_v K_s \frac{K_m}{d_p F} \frac{C_f}{I}} \tag{2.11}$$

Table 2-7: Summary of AGMA Terminology

Nomenclature			
Symbol	Description	Symbol	Description
C_e	Mesh alignment correction factor	d_p	Pitch diameter of pinion (in)
C_f	Surface condition factor	L	Life (cycles)
C_{ma}	Mesh alignment factor	m_p	Transverse contact ratio
C_{mc}	Lead correction factor	m_F	Axial contact ratio
C_{mf}	Face load distribution factor	n_P	Pinion speed (rpm)
C_{mf}	Pinion Proportion Modifier	P	Transmitted power (hp)
C_P	Elastic co-efficient ($\sqrt{lbf/in^2}$)	P_{nd}	Normal diametral pitch (in^{-1})
C_H	Hardness ratio factor for pitting resistance	p_c	Circular pitch (in)
F	Net face width (in)	m_n	Normal module (mm)
f^t [3]	Tangential load transmitted (lb)	S_F	Safety factor - bending
I	Geometry factor - pitting	S_H	Safety factor - pitting
J	Geometry factor - bending	s_{ac}	Allowable contact stress number (lb/in^2)
K_B	Rim thickness factor	s_{at}	Allowable bending stress number (lb/in^2)
K_m	Load distribution factor	s_c	Contact stress number (lb/in^2)
K_o	Overload factor	s_t	Bending stress number (lb/in^2)
K_R	Reliability factor	ψ	Helix angle (^{o})
K_s	Size factor	φ_n	Normal pressure angle (^{o})
K_T	Temperature factor	Y_N	Stress cycle factor -bending stress
K_v	Dynamic factor	Z_N	Stress cycle factor- contact stress

[3] AGMA uses the symbol W^t instead. f^t is used in this study to avoid confusion with Weight (W)

According to AGMA, the calculated bending stress and contact stress should satisfy the following conditions,

$$s_t \le \frac{s_{at}}{S_F}\frac{Y_N}{K_T K_R} \tag{2.12}$$

$$s_c \le \frac{s_{ac}}{S_H}\frac{Z_N}{K_T}\frac{C_H}{K_R} \tag{2.13}$$

Combining Equations 1.1 and 1.7 and Equations 1.2 and 1.8 we get,

$$s_t = f^t K_o K_v K_s \frac{P_d}{F}\frac{K_m K_B}{J} \le \frac{s_{at}}{S_F}\frac{Y_N}{K_T K_R} \tag{2.14}$$

$$s_c = C_P\sqrt{f^t K_o K_v K_s \frac{K_m}{d_p F}\frac{C_f}{I}} \le \frac{s_{ac}}{S_H}\frac{Z_N C_H}{K_T K_R} \tag{2.15}$$

Equations 2.14 and 2.15 seem a little overwhelming at first glance. The following section will provide a brief summary of the choices available for these terms and simplify the equations.

2.2.1 Description of Terms Used in the AGMA Stress Equations

Out of the terms in Equations 2.14 and 2.15, F and P_d relate directly to tooth geometry and will be discussed in Section 2.3. A clear and comprehensive description of the terms used in the AGMA stress equations is provided in (Budynas and Nisbett 2010) and it serves as the primary reference for this section.

2.2.1.1 Overload Factor K_o

The overload factor K_o is meant to account for momentary loads that exceed the nominal tangential load f^t during normal operation. It can also be thought of as accounting for the degree of shock expected in the loading. (McCarthy 1996) notes that

using a value of $K_o = 1$ gives a gear mesh the capability to sustain momentary overloads of up to 200% of the nominal load for brief periods of time. This value is used throughout this research.

2.2.1.2 Dynamic Factor K_v

The dynamic factor K_v accounts for the dynamic augmentation of transmitted load due to manufacturing inaccuracies and may be calculated analytically. The reader is referred to the Appendix A for details on the calculation of K_v.

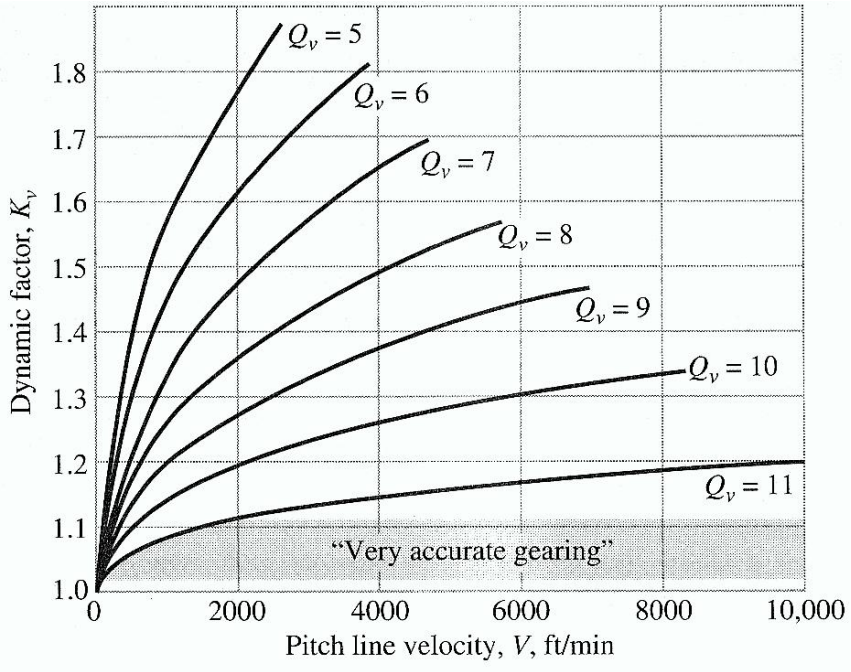

Figure 2-9: Dynamic factor K_v versus Pitch Line Velocity for different gear quality values (Collins 2002)

2.2.1.3 Size Factor K_S

The AGMA suggests that, until further information is available, the size factor K_s can be taken to be 1.00 for most gears.

2.2.1.4 Load Distribution Factor K_m

The load distribution factor K_m accounts for non-uniform distribution of load across the face width due to shaft misalignments, manufacturing defects etc. This research uses the analytical method provided by the AGMA to calculate K_m .

$$K_m = 1.0 + C_{mc}\left(C_{pf}C_{pm} + C_{ma}C_e\right) \tag{2.16}$$

The meanings of the terms in Equation 2.16 are shown in Table 2-7. The Appendix A contains additional information for the calculation of each of the terms based on empirical and analytical information. A value of 1 for the load distribution factor K_m implies ideal conditions where load is equally distributed along the entire face-width of mating gear teeth. Table 2-8 shows typical values for this factor based on mounting conditions and gear quality. Broadly speaking, a designer can minimize K_m by using high quality teeth, narrow face widths, straddle-mounted gears rather than overhung gears, small shaft spans between bearings and housings with high stiffness.

Table 2-8: Load Distribution Factor K_m (From (Budynas and Nisbett 2010))

Support Properties and Gear Quality	Face Width, in			
	0 to 2	6	9	≥16
Accurate mountings, small bearing clearances, minimum deflections, precision gears	1.3	1.4	1.5	1.8
Less rigid mountings, more bearing clearance, less accurate gears, contact across full face	1.6	1.7	1.8	2.2
Combinations of mounting properties and gearing precision that produce less than full face contact	2.2 or higher			

2.2.1.5 Rim-thickness Factor K_B

The rim-thickness factor K_B is used to adjust the estimated bending stresses for thin-rimmed gears. For the purposes of this research, the external gears are assumed to be solid disks with integral mounting shafts (Figure 2-10 (a)) or disks with internally

supporting bearings (Figure 2-10 (b)). Internal gears and the latter type of external gears are designed such that the rim-thickness factor K_B equals 1. This requires that the backup ratio m_B, defined as the ratio between the rim-thickness t_R to the total tooth height h_t, is greater than 1.2.

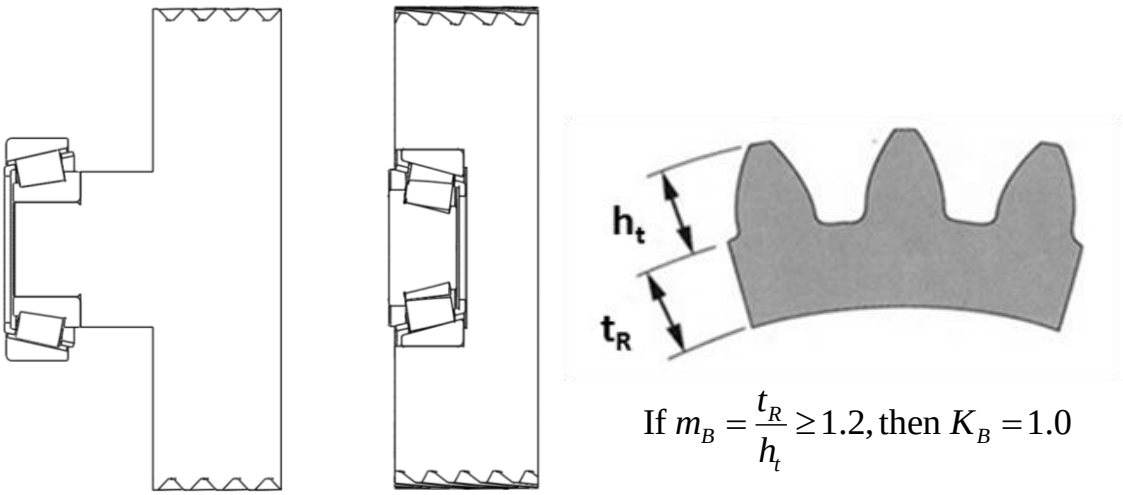

Figure 2-10: (a) External Gear with integral mounting shaft for press-fit bearings (b) External gear with internally supported bearing (c) Backup Ratio

When using webs and thin rims to save weight, it is important for a designer to account for rim stresses. Reference (Letaief, Chaari, and Haddar 2008) and addresses this issue.

2.2.1.6 Surface Condition Factor C_f

Currently, the AGMA does not provide recommendations for this factor so it will be set equal to 1. (Budynas and Nisbett 2010) suggest that if poor surface condition is expected, a higher value may be used.

2.2.1.7 Geometry Factors J (Bending Strength) and I (Surface Strength)

Geometry Factors J and I account for factors such as the shape and size of mating teeth, extent to which load sharing occurs and the point of application of the load on the tooth. The AGMA provides look-up tables, charts and semi-analytical methods to find values for J. However, in order to make use of charts in a computer program, curve-fitting is necessary (Arikan 2002). The semi-analytical method "involves an iterative procedure very tedious to implement in a computer program" and is also time-consuming when used repeatedly (Pedrero, Fuentes, and Estrems 2000). For these reasons, some researchers (Arikan 2002; Pope 1996; Pedrero, Fuentes, and Estrems 2000) have proposed alternative methods to calculate J. However, the first and third references above only dealt with spur teeth. The present research deals with both spur and helical gears and therefore these methods were not used. The procedure developed by (Pedrero, Fuentes, and Estrems 2000) is valid for all tooth profiles but requires knowledge about cutting tool geometry. The goal of the present research is to develop preliminary designs only. Hence, advanced manufacturing decisions such as cutting tool geometry are not considered here. Instead, regression techniques were used to fit surfaces to relevant data from the AGMA look-up tables. The generated surfaces were then mathematically described using quadratic polynomials. To illustrate, Table 2-9 shows a look-up table to find J for spur teeth with a 25^o pressure angle. Figure 2-11 shows the surface fit to the J data for the pinion. For reasons stated in Section 2.2.2, only the pinion data needs to be considered. The polynomial equation representing the surface along with the corresponding residual-least-squares (R^2) error is shown in Table 2-10 (when $\varphi = 25^o$ and $\psi = 0^o$)

The pitting strength geometry factor I is calculated analytically using the procedure described in the AGMA 908-B89 Information Sheet.

Table 2-9: Typical look-up table for *J* ((Oberg 2000))

Number of Gear Teeth		25 -deg Pressure Angle 0.0-deg Helix Angle 0.027 Tool Edge Radius		2.350 Whole Depth Factor 0.024 Tooth Thinning for Backlash Loaded at Tip of Gears													
		Number of Pinion Teeth															
		12		14		17		21		26		35		55		135	
		P	G	P	G	P	G	P	G	P	G	P	G	P	G	P	G
Equal Addendum Coefficients ($x_1 = x_2 = 0$)																	
14	*I*			0.086													
	J			0.28	0.28												
17	*I*			0.091		0.090											
	J			0.28	0.30	0.30	0.30										
21	*I*			0.095		0.096		0.092									
	J			0.28	0.31	0.30	0.31	0.31	0.31								
26	*I*			0.100		0.101		0.099		0.094							
	J			0.28	0.33	0.30	0.33	0.31	0.33	0.33	0.33						
35	*I*			0.106		0.109		0.108		0.104		0.095					
	J			0.28	0.34	0.30	0.34	0.31	0.34	0.33	0.34	0.34	0.34				
55	*I*			0.113		0.119		0.121		0.119		0.112		0.095			
	J			0.28	0.36	0.30	0.36	0.31	0.36	0.33	0.36	0.34	0.36	0.36	0.36		
135	*I*			0.123		0.132		0.139		0.142		0.141		0.131		0.096	
	J			0.28	0.38	0.30	0.38	0.31	0.38	0.33	0.38	0.34	0.38	0.36	0.38	0.49	0.49

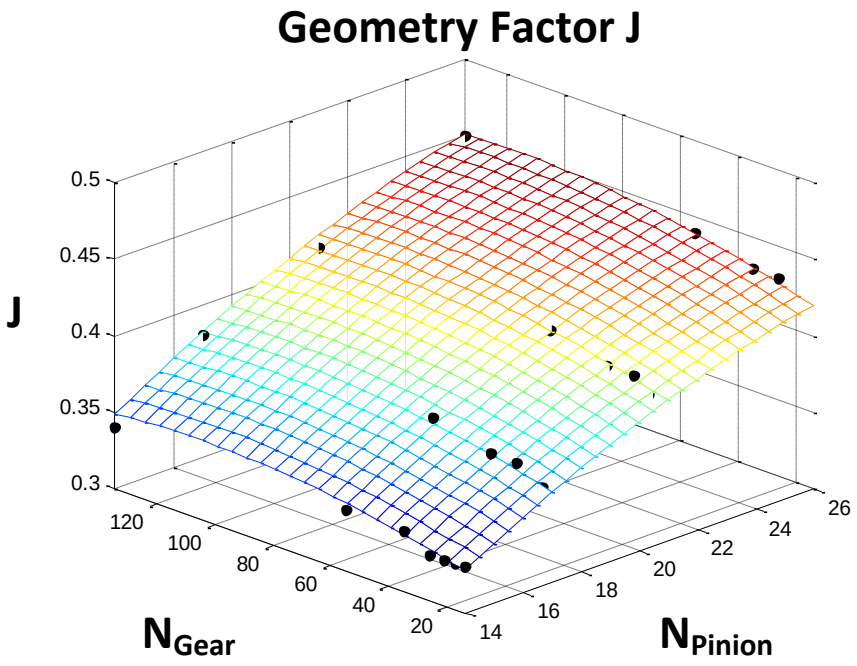

Figure 2-11: Illustration of a surface fit to the *J* values for the pinion (from Table 2-9)

Table 2-10: Polynomial Equations representing J for various Pressure and Helix Angles

φ	ψ	Equation	R^2
25°	0°	$J = 0.1083 + (0.01915)x + (5.144e^{-4})y - (2.889e^{-4})x^2 \ldots$ $\cdots + (6.554e^{-6})xy - (2.896e^{-6})y^2$	0.9951
	10°	$J = 0.1891 + (0.02476)x + (1.255e^{-3})y - (3.851e^{-4})x^2 \ldots$ $\cdots - (2.597e^{-6})xy - (5.649e^{-6})y^2$	0.995
	15°	$J = 0.2073 + (0.0255)x + (1.012e^{-3})y - (4.211e^{-4})x^2 \ldots$ $\cdots + (3.609e^{-6})xy - (5.201e^{-6})y^2$	0.9947
	20°	$J = 0.2126 + (0.02627)x + (8.99e^{-4})y - (4.52e^{-4})x^2 \ldots$ $\cdots + (5.8e^{-6})xy - (4.575e^{-6})y^2$	0.9948
	25°	$J = 0.2368 + (0.02386)x + (9.554e^{-4})y - (4.12e^{-4})x^2 \ldots$ $\cdots + (8.884e^{-7})xy - (4.596e^{-6})y^2$	0.9934
	30°	$J = 0.2666 + (0.02033)x + (8.792e^{-4})y - (3.54e^{-4})x^2 \ldots$ $\cdots - (3.448e^{-7})xy - (4.118e^{-6})y^2$	0.9898
20°	0°	$J = 0.2365 + (0.00379)x + (2.986e^{-4})y + (1.852e^{-5})xy - (3.272e^{-6})y^2$	0.9783
	10°	$J = 0.3469 + (0.004184)x + (1.153e^{-3})y + (1.484e^{-5})xy - (7.296e^{-6})y^2$	0.9917
	15°	$J = 0.3104 + (0.006066)x + (1.463e^{-4})y + (3.965e^{-6})xy - (7.615e^{-6})y^2$	0.983
	20°	$J = 0.337 + (5.276e^{-3})x + (9.875e^{-4})y + (9.221e^{-5})xy - (5.46e^{-6})y^2$	0.9845
	25°	$J = 0.301 + (0.00637)x + (1.368e^{-3})y - (4.352e^{-6})xy - (6.234e^{-6})y^2$	0.9839
	30°	$J = 0.3094 + (5.141e^{-3})x + (1.082e^{-3})y - (2.394e^{-6})xy - (4.919e^{-6})y^2$	0.9741

2.2.1.8 Temperature Factor K_T

The value of K_T is set to 1 in this research. This corresponds to gear or oil temperatures less than 250^oF. Heavy power transmitted over time may raise the temperatures beyond this value. For such applications, the full AGMA standards must be consulted for the value of this factor.

2.2.1.9 Reliability Factor K_R

The reliability factor accounts for the effect of statistical distributions of material fatigue failures. The published allowable stress numbers are based on a reliability of 99% for which $K_R = 1$. See Appendix A for more details.

2.2.1.10 Safety Factor S_F and S_H

These safety factors are incorporated to account for unpredicted or unquantifiable properties. The values for these factors depend upon the type of application, experience of the designer, nature of the designer (risk-averse or aggressive) etc. For the purposes of this research, the safety factors will be set to 1.3. A conservative designer may use a safety factor of 1.7 to be very safe.

2.2.1.11 Stress - Cycle Factors Y_N and Z_N

The stress cycle factors adjust the fatigue limit stress values (s_{at} and s_{ac}), which correspond to 10^7 mesh cycles, for a required number of cycles of operation.

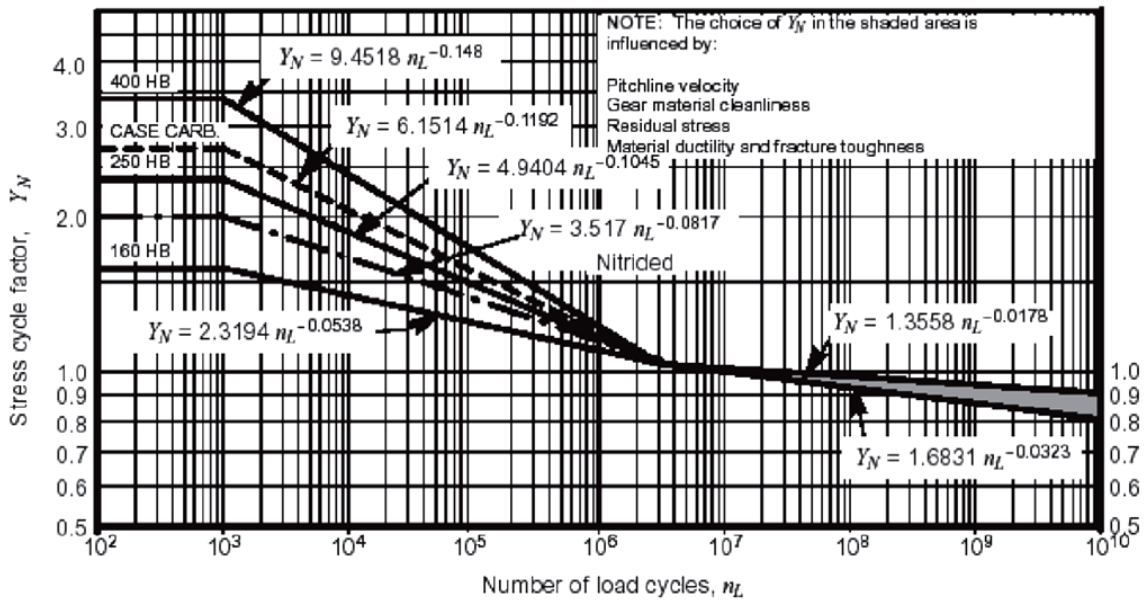

Figure 2-12: Bending Strength Stress Cycles Factor Y_N (Gonzalo et al., 2007)

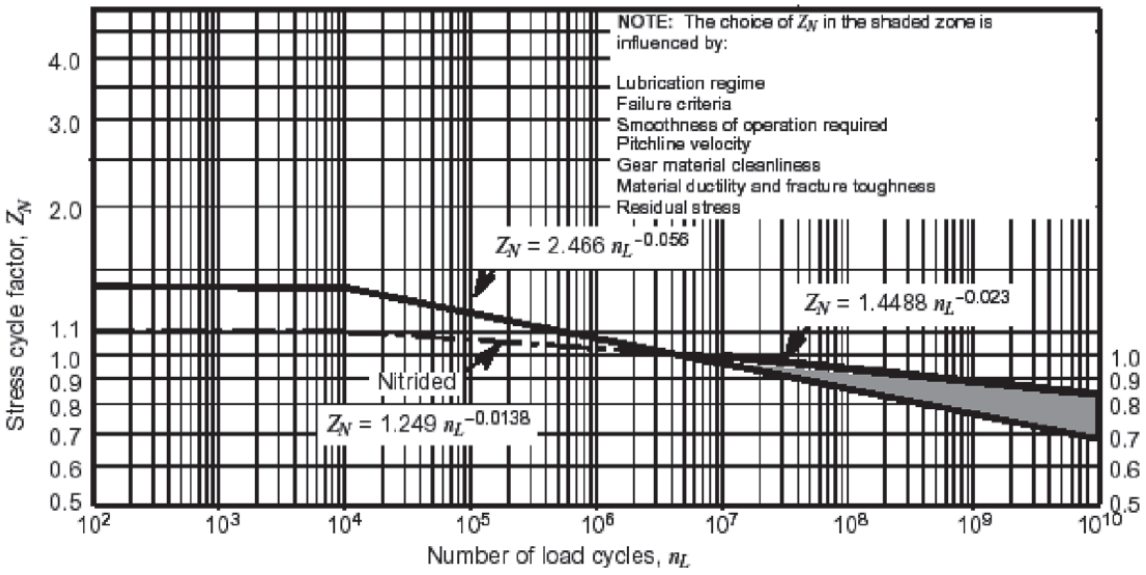

Figure 2-13: Pitting Resistance Stress Cycles Factor Z_N (Gonzalo, Frechilla Fernández, and José García Martín 2007)

From Figure 2-12 and Figure 2-13, it is clear that, for low lives, the stress values in gear teeth can be substantially higher than those for nominal life. For example, Figure

2-12 indicates that if only 1000 mesh cycles are required of a gear pair, the stress levels can be as much as 3 times the nominal bending stress values (for case-carburized gears).

2.2.1.12 Allowable Stress Numbers

According to tables published by AGMA [2001-D04] for bending and fatigue strengths for carburized and case-hardened steel gear materials:

Table 2-11: Allowable Stress Numbers for various Steel Quality Grades

	Grade 1	Grade 2	Grade 3
Max. Allowable bending stress number (ksi)	55	70	75
Max. Allowable surface stress number (ksi)	180	225	275

The three material 'grades' have the following characteristics (Collins 2002):

Table 2-12: Description of AGMA Quality Grades

Quality Grade		Characteristics
0	Ordinary Quality	No gross defects; no close control of quality items[4]
1	Good Quality	Modest control of most important quality items; typical industrial practice.
2	Premium Quality	Close control of all critical quality items; results in improved performance but increases material cost
3	Super Quality	Absolute control of all critical quality items; results in ultimate performance but high material cost; rarely required

(Kawalec, Wiktor, and Ceglarek 2006) compared tooth-root stresses calculated using AGMA standards, ISO standards and FEM based models and simulation. Based on their study, they say that:

> In all performed computations, tooth-root stresses obtained according to the ISO standard were greater than the tooth-root stress calculated according to the AGMA standard.

[4] Quality items include surface hardness, core hardness, case structure, core structure, steel cleanliness, flank surface condition, root-fillet surface condition, grain size, and non-uniform hardness or structure.

> Stresses computed with the use of finite element method were in-between; i.e., were greater than stresses according to the AGMA and smaller than stresses according to the ISO standard.

Based on their findings, the AGMA approach to gear design may be considered more aggressive than ISO standards. From plots published in (Kawalec, Wiktor, and Ceglarek 2006) for gear teeth subjected to the same load, the calculated stresses according to finite element methods were roughly 10 % to 25 % greater than those calculated by AGMA methods. Put differently, this means that for a given gear tooth stress, the AGMA standards give a higher torque rating than ISO standards.

(Lewicki et al. 2007) performed surface durability tests on face gears in support of the RDS-21 (U.S. Army Rotorcraft Drive Systems for the 21st Century) program. They found that "the test results support use of the AGMA spur-helical method for estimating the pitting resistance of face gear sets".

The designer is advised to weigh all of this information in deciding what values of allowable bending and pitting stress values to use. For the current study, the allowable bending stress numbers used will generally correspond to Grade 2, carburized and case-hardened steel with 58 R_C (Rockwell C scale).

Allowable bending stress number - 70 ksi

Allowable contact stress number - 225 ksi

As discussed earlier, the overload factor K_o is used to account for the fact that peak loads during operation may be greater than the nominal load due to shock, vibrations, speed changes etc. An overload factor of 1 allows momentary overloads of up to 200% of the nominal load; i.e., they may induce stresses of up to 150 ksi on the teeth.

2.2.1.13 Face-width

As seen from the AGMA Stress equations (Equations 2.14-2.15), an increase in gear face-width leads to greater torque capacity for a gear mesh. However, long, thin pinions are prone to misalignment issues, leading to non-uniform loading across the width of a gear tooth, ultimately leading to reduced gear life. For this reason, experts in the field suggest a maximum allowable face-width for a given gear mesh. A common recommendation from gear design literature is that the maximum face width for a gear pair must not exceed twice the pinion pitch diameter (Tong and Walton 1987). The AGMA equation for calculation of the load distribution factor K_m (Section 2.2.4) is valid only if this condition is true. In most literature on gear design, it is recommended that the face width should be between 3 and 5 times the circular pitch of the pair of gears in mesh (Budynas and Nisbett 2010)(Mott 2003).

$$3 \leq \frac{F}{p_c} \leq 5 \tag{2.17}$$

Put in terms of diametral pitch, the recommended face width limits are

$$9 \leq FP_d \leq 16 \tag{2.18}$$

However, in a recent AGMA technical paper (Schultz 2009), the author notes that, in his experience, when pinions with a face width to diameter ratio of two were used, "it became apparent that torsional deflection adversely affected the life of these drives". The author then suggests that a face width to diameter ratio of 1-1.25 was found to be most beneficial.

In order to develop a good understanding of what these different recommendations mean, a critical comparison between the three 'thumb rules' is now presented. The 1st thumb rule is embodied in Equation 1.18. The 2nd and 3rd thumb rules

suggest that the face width F should be limited to the pinion pitch diameter d_p times a multiplication factor. This multiplication factor is designated as F_{rule}. Using the definition of diametral pitch (with reference to the pinion) and considering only the upper limit in Equation 1.18, the following can be derived:

$$FP_d \leq 16 \;\Rightarrow\; F\frac{N}{D} \leq 16 \;\Rightarrow\; F_{rule}N \leq 16 \;\Rightarrow\; F_{rule} \leq \frac{16}{N}$$

Table 2-13 compares the 3 different recommendations for maximum face width. The first thumb rule is dependent on the number of pinion teeth. Table 2-14 lists a set of representative designs for a one-stage SCGT for various gear ratios and a fixed diameter. It is seen that the number of pinion teeth usually varies between 14 and 16. Substituting these values for *N* into Table 2-13 gives us the final maximum recommended values for face width according to the three rules. These are shown in Table 2-15.

Table 2-13: Comparison of the upper limits on Face Width according to 3 thumb rules

S.No	Rule for upper limit on Face Width	F_{rule}
1	5 times the circular pitch	$\frac{16}{N}$
2	Twice the pinion pitch diameter	2
3	1 - 1.25 times the pinion pitch diameter	1- 1.25

Table 2-14: Representative Designs for a One-Stage SCGT

N_P	N_{LS}	N_{SS}	N_R	P_{d1}	P_{d2}	g	D_g	T
15	60	14	63	22.50	14.70	18	6	988.5
15	56	14	60	21.17	13.71	16	6	1055.2
16	53	14	59	20.33	13.26	14	6	1202.9
15	45	14	56	17.50	12.25	12	6	1369.3
15	39	14	54	15.50	11.48	10	6	1615.3
14	31	15	54	12.67	10.98	8	6	1917.7

Table 2-15: Comparison of the upper limits on Face Width according to 3 thumb rules

S.No	Rule for upper limit on Face Width	F_{rule}
1	5 times the circular pitch	1 to 1.15
2	Twice the pinion pitch diameter	2
3	1.25 times the pinion pitch diameter	1 to 1.25

Based on the values in the table above, the recommendation for the current study is to use an upper limit of $F_{rule} = 1$ i.e. face-width equal to the pinion pitch diameter for nominal conditions. An aggressive designer, by specifying high quality gears and bearings and small manufacturing tolerances on all drive components, may decide to use $F_{rule} = 1.25$.

2.2.2. Summary

This section described the significance of important terms used in the AGMA strength equations. Guidelines regarding the choice of the empirical modifying factors were provided. Table 2-16 provides a summary of the values that will be used throughout this research for the terms discussed above as well as some additional terms.

By substituting the values from Table 2-16 into Equations 2.10 and 2.11, the final strength equations (Equations 2.18 and 2.19) are obtained.

$$s_t = f^t K_v K_m \frac{P_d}{FJ} \leq s_{at} Y_N \tag{2.19}$$

$$s_c = 2300 \sqrt{f^t K_v \frac{K_m}{d_p FI}} \leq s_{ac} Z_N \tag{2.20}$$

It can be mathematically proved that, when the same material is used for both gear and pinion, the pinion will always be the weaker component (Budynas and Nisbett 2010). Since the AGMA strength equations are based on fatigue loading, and by

definition the pinion is the smaller of two mating gears, the pinion teeth will undergo more load cycles than the gear teeth and therefore be the first to fail.

Table 2-16: Summary of the AGMA Stress Modifying Factors and their Values

Symbol	Term	Value
K_o	Overload Factor	1
K_v	Dynamic Factor	Calculated analytically
K_s	Size Factor	1
K_m	Load Distribution Factor	Calculated analytically
K_B	Rim Thickness Factor	1
C_f	Surface Condition Factor	1
K_T	Temperature Factor	1
K_R	Reliability Factor	1
S_F and S_H	Safety Factors	1.3
Y_N and Z_N	Stress Cycles Factors	Calculated corresponding to 10^7 mesh cycles at the output gear
J and I	Geometry Factors	Calculated analytically
C_P	Elastic Co-efficient	2300 (Both pinion and gear made of Steel)
C_H	Hardness Ratio Factor	1 (Pinion and gear equally strong)

Therefore, in practice the pinion is often made harder than the gear in order to balance the stresses in each of them (see Table 2-17). For preliminary design, it is sufficient to assume that the pinion and gear are made of identical materials; i.e., $C_H = 1$ (See Table 2-16). Based on calculated stresses, the materials for the gear and pinion can then be modified when a more detailed design is sought.

Table 2-17: Suggestions for choice of Pinion and Gear materials (Wilson and Sadler)

Ratio	Pinion and Gear Material
1:1 to 2:1	Pinion and gear of the same hardness
2:1 to 8:1	Pinion hardness 40 BHN higher than gear hardness
Over 8:1	Pinion hardness more than 40 BHN higher than gear hardness

2.3 PARAMETRIC DESIGN OF STAR COMPOUND GEAR TRAINS

In this section, parametric models and design procedures for three types of Star Compound Gear Trains (SCGT's) are developed. The three types are:

1. One-Stage Star Compound Gear Train (1-Stage SCGT)
2. Pancake-Type Two-Stage Star Compound Gear Train (P-Type 2-Stage SCGT)
3. Coffee-Can type Two-Stage Star Compound Gear Train (C-Type 2-Stage SCGT)

For each of the types listed above, design procedures that enable a designer to arrive at a set of design configurations that satisfy certain geometric (diameter, length etc.), strength (bending and pitting) and functional constraints (life, reliability etc.) are developed. These sets of design configurations are termed as 'Design Solution Sets'. Thus, the geometric, strength and functional constraints act as inputs to the design procedures and the Design Solution Sets are the outputs. The individual designs in a Design Solution Set may be compared based on performance criteria and secondary criteria such as aspect ratio or contact ratio. The performance criteria used in the present research are:

1. Nominal Torque Capacity (T)
2. Weight (W)
3. Effective Inertia (I)
4. Torque Density (T_D)
5. Responsiveness (R)

A detailed discussion on the performance criteria is presented in Section 3.4.

The geometric, strength and functional constraints are termed the *design parameters*. (Budynas and Nisbett 2010) divide the design parameters into two sets, 'a priori decisions' and 'design decisions'. For the design procedures proposed here, slight modifications to these two sets are necessary. The reader is referred to Section 14-19 of

[1] for the original decision set classification. With regard to the methodology proposed in the next section, the a priori decisions include:

- Functional parameters: speed, reliability, life, overload factor, etc.
- Risk parameters: safety factors
- Tooth system: φ (pressure angle), ψ (helix angle), addendum, dedendum, etc.
- Quality number Q_v
- Material properties: material, core hardness, case hardness

Some of the a priori decisions depend on the application requirements (speed, overload factor, pressure angle, etc.), some are dependent on designer preferences (safety factors) and some (Quality number, material, etc.) relate to cost. The current research will make recommendations for these parameters but the final choice is left to the designer. For instance, for low noise, it is recommended that helical gears with low pressure angles be used. However, the user may opt for spur gear teeth to keep costs low.

The design decision set includes:

- Diametral pitches P_d for each gear mesh
- Pitch Diameters D for each of the gears
- Numbers of teeth N on each of the gears
- Face-widths F for each gear mesh
- Gear Ratio g
- Diameter D_{gm}

Among the design decisions listed above, the gear ratio g and the diameter D_g are unique in that, they act as inputs to the design procedures developed later in this chapter, but are also design decisions with regard to the design process developed in Chapter 3. This will become clear to the reader in Chapter 3.

The process by which design maps are created will be discussed in detail in a later section, but a brief summary is presented here. Given a set of design parameters, a Design Solution Set is found. Then, based on relevant performance criteria, only the *best* solution from the Design Solution Set is picked. Thus, a given set of design parameters results in a corresponding set of performance parameters. If two of the design parameters are varied over a range (all others being held constant), a corresponding range of performance parameters are obtained. When these design parameters are plotted on the *x-axis* and *y-axis* respectively, and a performance parameter of interest is plotted on the *z-axis*, an array of points to which a surface can be fit is obtained. The surface fitted is termed a *design map*. To illustrate, consider the case of a 1-Stage SCGT. Two design parameters, g and D_{gm} are varied as follows:

g - 8 , 16 , 24, 32
D_{gm} - 4", 8", 12"

For each set of design parameters, the corresponding Nominal Torque Capacity is tabulated as shown in the table below.

Table 2-18: Sample Data for the creation of a Design Map

D_{gm} (inches)	g	T (ft - lbs)
12	32	2484
12	24	4057
12	16	6328
12	8	12423
8	32	743
8	24	1218
8	16	1905
8	8	3757
4	32	93
4	24	153
4	16	241
4	8	479

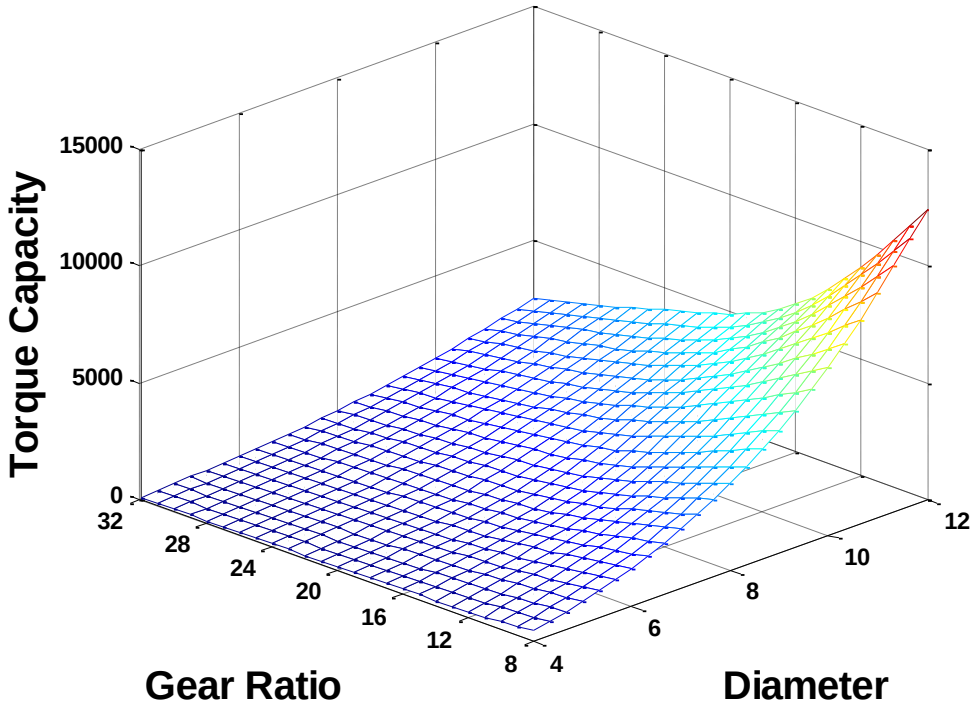

Figure 2-14: Design Map – Nominal Torque Capacity vs. Diameter and Gear Ratio

Figure 2-14 shows the design map created from the data in Table 2-18. The significance of such design maps will become apparent in Chapter 3, where design processes for each of the three gear train types mentioned earlier will be developed. The following sections will present the development of design procedures for each of the gear train types. To facilitate understanding, the reader is advised to note parallels between the design procedures developed in the following sections and Figure 2-15. This figure presents a high level summary of the basic methodology employed to obtain the Design Solution Set for a given set of input parameters. The procedure showed here acts as a template for the three individual SCGT design procedures.

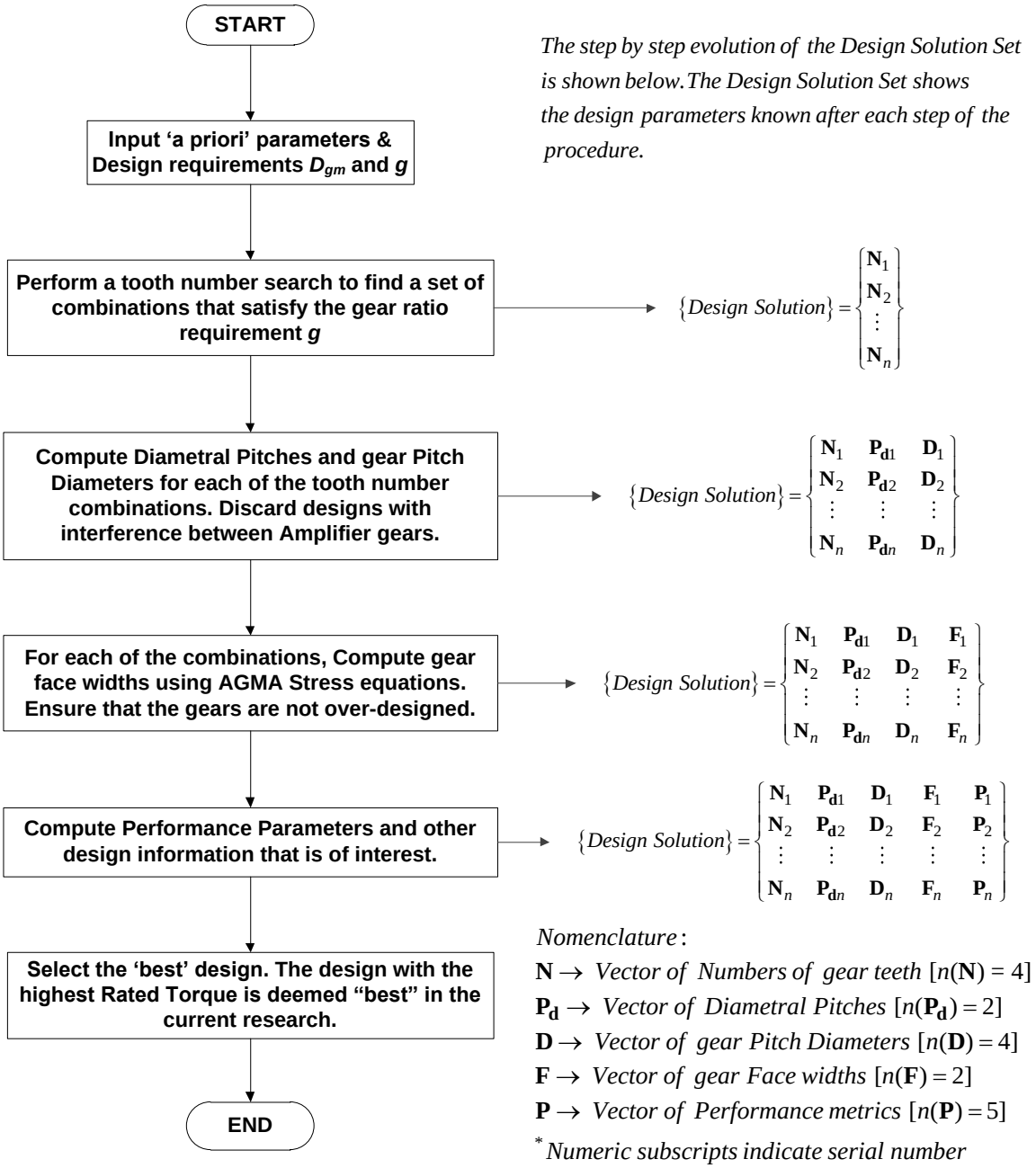

Figure 2-15: High Level Summary of the SCGT Design Procedures

2.4 Design Procedure for a One-Stage Star Compound Gear Train

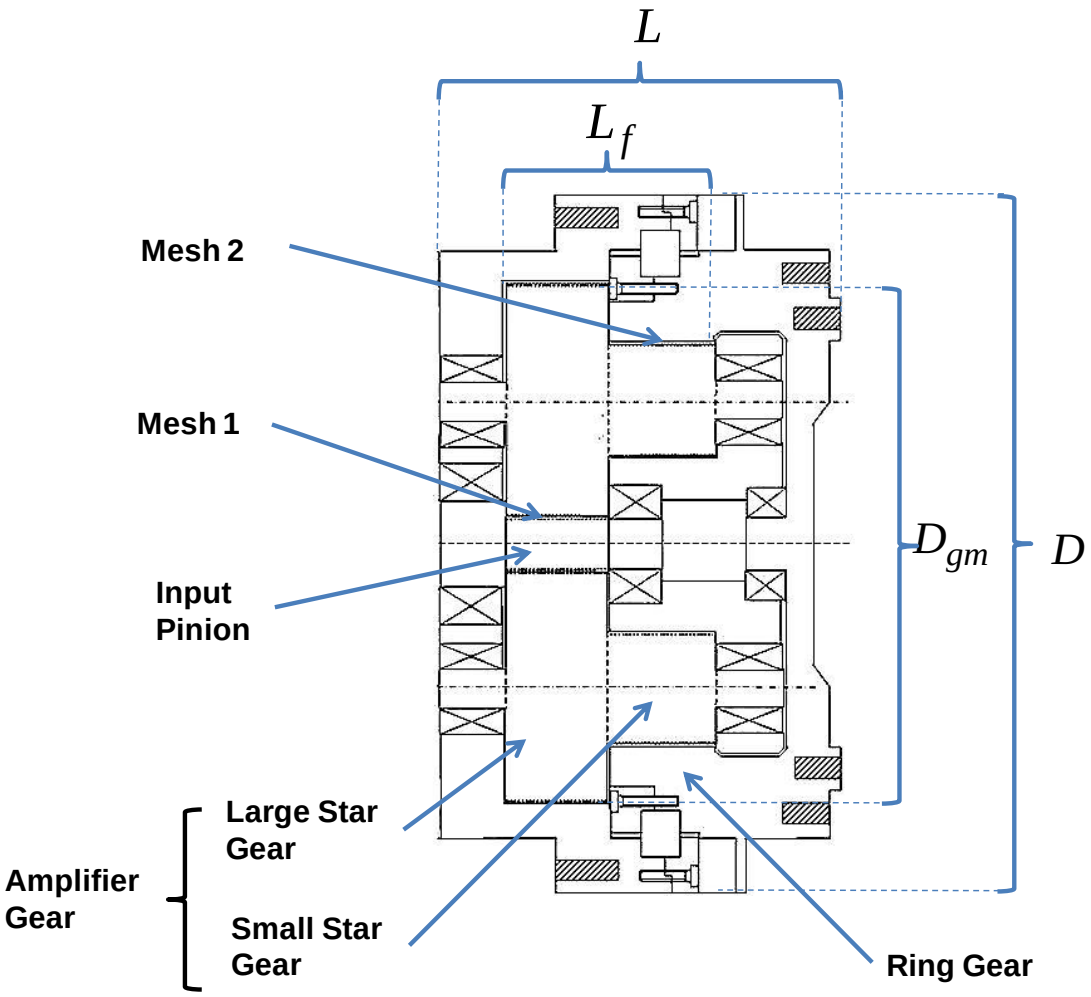

Figure 2-16: One-Stage Star Compound Gear Train

The Table 2-19 lists the design parameters (both a priori and design decisions) and other terminology that relate to the gears in a 1-stage SCGT (see Figure 2-16). Design parameters specific to the backbone, bearing cage, bearings etc. are not shown here and are addressed in a later section. Note the distinction between the term "gear mesh", which refers to gears *only* and "gear train" which refers to the gears along with

supporting components i.e. the bearings, bearing cage, backbone and shell structure, seal and output plate.

Table 2-19: Terminology for a One-Stage Star Compound Gear Train

Nomenclature			
Symbol	**Description**	**Symbol**	**Description**
Design Decisions			
D_P	P.D. of the Input Pinion	g	Reduction in the gear train
D_{LS}	P.D. of the Large Star gear	g_1	Reduction in Mesh 1
D_{SS}	P.D. of the Small Star gear	g_2	Reduction in Mesh 2
D_R	P.D. of the Ring gear	P_{d1}	Transverse Diametral pitch of gears in Mesh 1
D	Diameter of gear train	P_{d2}	Transverse Diametral pitch of gears in Mesh 2
D_{gm}	Diameter of gear mesh	L	Length of gear train
N_P	No. of teeth on the Input Pinion	L_f	Length of gear meshes
N_{LS}	No. of teeth on the Large Star gears	F_1	Face width of gears in Mesh 1
N_{SS}	No. of teeth on the Small Star gears	F_2	Face width of gears in Mesh 2
N_R	No. of teeth on the Ring gear	A	Aspect Ratio of gear train
n	Output Speed (rpm)		
A Priori Decisions			
φ_1	Pressure Angle (Transverse) in Mesh 1	ψ_1	Helix Angle in Mesh 1
φ_2	Pressure Angle (Transverse) in Mesh 2	ψ_2	Helix Angle in Mesh 2
General			
Mesh 1	Mesh between Input Pinion and Large Star gears	Mesh 2	Mesh between Small Star gears and the Ring gear

2.4.1 Design Procedure Development for a 1-Stage SCGT

The gear train diameter D_{gm} and gear ratio g serve as the primary input parameters to the proposed methodology.

The gear train reduction ratio g is a product of the reduction ratio in each plane of gears (See Figure 2-16).

$$g = g_1 g_2 = \frac{N_{LS}}{N_P}\frac{N_R}{N_{SS}} = \frac{\prod N_{Driven\ Gears}}{\prod N_{Driving\ Gears}} \tag{2.21}$$

where,

g_1 - Reduction in mesh 1
g_2 - Reduction in mesh 2
N_P - No. of teeth of Pinion
N_{LS} - No. of teeth on Large Star Gear
N_{SS} - No. of teeth on Small Star Gear
N_R - No. of teeth on Ring Gear

From the definition of diametral pitch and from simple geometry (see Figure 2-17), we have the relations:

$$D_{gm} = D_P + 2 \times D_{LS} \tag{2.22}$$

$$D_{gm} = \frac{N_P}{P_{d1}} + 2 \times \frac{N_{LS}}{P_{d1}} \tag{2.23}$$

Equation 2.22 arises from the fact that all gears in mesh must have the same diametral pitch. Re-arranging, we get

$$P_{d1} = \frac{N_P + 2 \times N_{LS}}{D_{gm}} \tag{2.24}$$

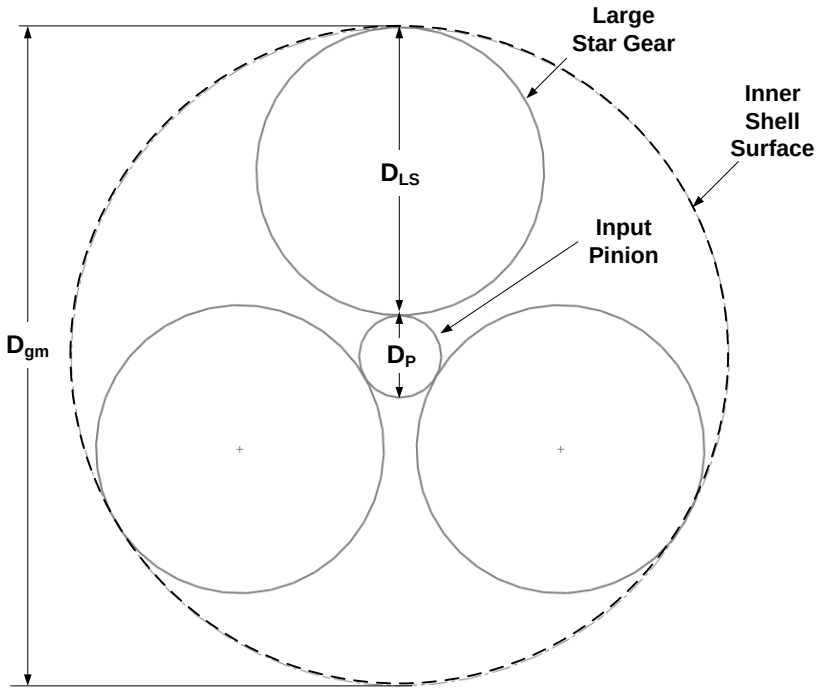

Figure 2-17: Simplified layout of the gears in Mesh 1

However, since the addendum of a gear protrudes outside of the pitch circle, Equation 2.23 must be modified such that the tips of the gear teeth lie just inside the inner surface of the shell (see Figure 2-18). Using the standard value of addendum for full-depth gear teeth (see Table 2-3), Equation 2.22 is modified as such.

$$D_{gm} = \frac{N_P}{P_{d1}} + 2 \times \left(\frac{N_{LS}}{P_{d1}} + \frac{1}{P_{d1}} \right) + x_{gap} = \frac{\left(N_P + 2\left(N_{LS} + 1 \right) \right)}{P_{d1}} + x_{gap} \qquad (2.25)$$

In Equation 2.25, the second term in the brackets accounts for the addendum of the Large Star Gear. The term x_{gap} is used to create a small gap between the tips of the large star gear teeth and the inner surface of the shell (See Figure 2-18).

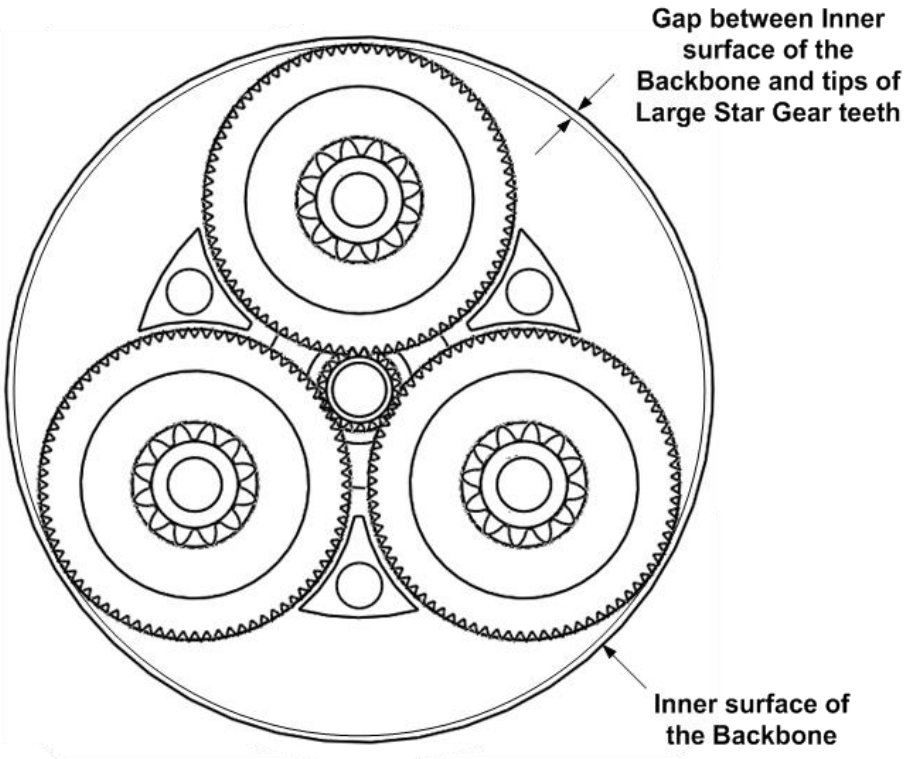

Figure 2-18: Shows the size of the gap between the Large Star Gear teeth tips and the Inner surface of the Backbone structure

Re-arranging Equation 2.24, the final equation for the diametral pitch for the gears in the first mesh is obtained:

$$P_{d1} = \frac{N_P + 2 \times (N_{LS} + 1)}{D_{gm} - x_{gap}} \tag{2.26}$$

Assuming that x_{gap} is fixed based on manufacturing tolerances, the diametral pitch in the first plane (P_{d1}) is thus a function only of the input design parameters D_{gm} and gear ratio g; and the numbers of teeth on the gears in the first mesh; i.e., N_P and N_{LS}. Using the definition of diametral pitch, the pitch diameters of the first plane of gears (D_P and D_{LS}) can then be calculated.

From Figure 2-16, it can be deduced that

$$D_P + D_{LS} + D_{SS} = D_R \tag{2.27}$$

Re-arranging the equation above and putting it in terms of the number of teeth and diametral pitch, the following equation can be derived

$$P_{d2} = \frac{N_R - N_{SS}}{D_P + D_{LS}} \tag{2.28}$$

The diametral pitch in the second plane (P_{d2}) is thus a function of the numbers of teeth on the gears in the second plane and the pitch diameters of the first plane of gears. With the diametral pitches in both gear meshes as well as the number of teeth known, the pitch diameters of *all of the gears* in a star compound gear train are obtained. The pitch diameters are purely functions of the input parameter D_g, gear ratio g and the numbers of teeth on the gears.

In summary, it is sufficient to conduct an exhaustive search of gear tooth numbers that yield the required gear ratio g in order to arrive at a set of gear pitch diameters that satisfy the geometric constraint of D_{gm}. Among this set of designs, solutions which lead to interference between the amplifier gears can be found and eliminated. The necessary condition for avoiding interference between amplifier gears is that the distance between two adjacent amplifier gears must be more than twice the addendum diameter of the large star gears. Figure 2-19 shows the limiting condition at which interference between the amplifier gears occurs. In Figure 2-19, the following are true:

$$O_1O_2 = 2 \times R_{LS}^o \tag{2.29}$$

$$O_1O = O_2O = R_P + R_{LS} \tag{2.30}$$

where,

R_{LS}^o is the addendum radius of the Large Star Gear

R_P is the pitch radius of the Pinion

R_{LS} is the pitch radius of the Large Star Gear

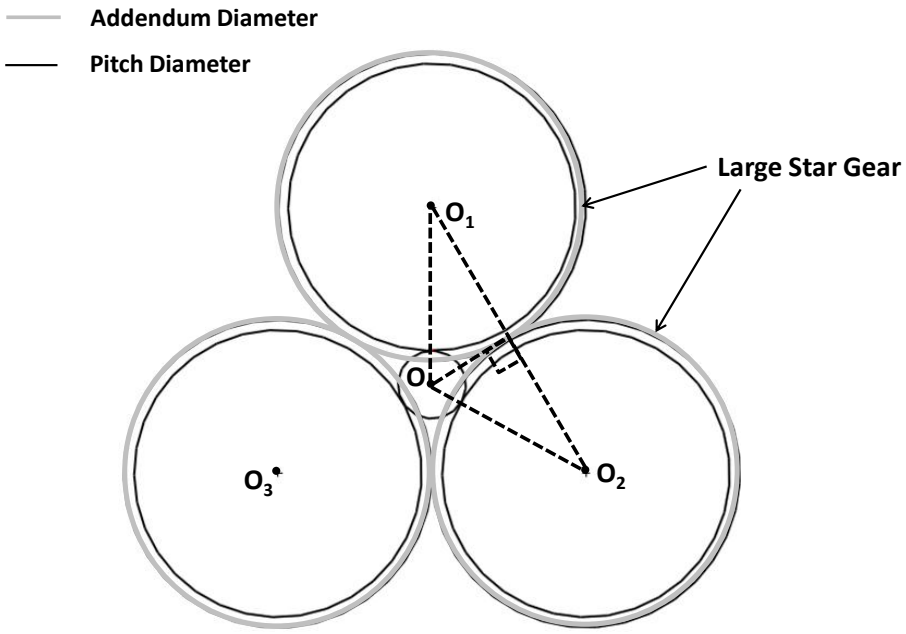

Figure 2-19: Simplified view of Plane 1 of the gear train

From basic geometry,

$$\sin\left(\frac{\angle O_1OO_2}{2}\right)=\frac{R_{LS}^o}{R_P+R_{LS}} \tag{2.31}$$

The condition for avoiding interference is obtained by simply replacing the equality in Equation 1.9 with an inequality.

$$\sin\left(\frac{\angle O_1OO_2}{2}\right)>\frac{R_{LS}^o}{R_P+R_{LS}} \tag{2.32}$$

It is obvious that, for the case of three equally spaced amplifier gears, $\angle O_1OO_2=120^o$. Substituting this value in Equation 2.31 and reducing it, we arrive at a final equation for avoiding amplifier gear interference in a one-stage star compound gear train.

$$\frac{\sqrt{3}}{2} > \frac{R_{LS}^{o}}{R_P + R_{LS}} \tag{2.33}$$

In general, for equally spaced amplifier gears,

$$\angle O_1 O O_2 = \frac{360^o}{no.ofPlanets} \tag{2.34}$$

At this stage of the design procedure, with the pitch diameters and number of gear teeth for all gears known, the only gear level design parameter left to calculate is the face width.

2.4.1.1 Determination of Face widths

Equations 2.18 and 2.19 from Section 2.1.12 are shown below:

$$s_t = f^t K_v K_m \frac{P_d}{FJ} \leq s_{at} Y_N \tag{2.35}$$

$$s_c = 2300 \sqrt{f^t K_v \frac{K_m}{d_p FI}} \leq s_{ac} Z_N \tag{2.36}$$

Before the procedure for determining F_2 can be presented, some new nomenclature and design aspects must be addressed. With reference to the equations above:

- The stress-cycle factors Y_N and Z_N are functions of the number of mesh cycles. As such, each gear in an SCGT has a stress-cycle factor associated with it. However, it seems reasonable to assume identical materials for the pinion and gear for a preliminary design. As mentioned in Section 2.1.12, under this assumption, the pinion will *always* be the weaker component. Therefore, it is only necessary to check bending and contact stresses in two components; i.e., the input pinion and the small star gear. For the rest of the study, calculated stresses in the input pinion

will be designated with the subscript '1' (Mesh 1) and calculated stresses in the small star gear will be designated with the subscript '2' (Mesh 2). For example, s_{c2} implies the calculated contact stress in the small star gear.

- The allowable stress numbers (s_{at} and s_{ac}) are modified by the stress-cycle factors Y_N and Z_N to give modified allowable stress numbers which are a more accurate reflection of the allowable stress considering operating conditions. These modified allowable stress numbers for bending and contact will be designated as S_{at} and S_{ac} in this study.

- For a design to be considered acceptable, the calculated stresses should be less than or equal to the modified allowable stress numbers i.e. $s_t \le S_{at}$ and $s_c \le S_{ac}$.

- The tangential loads on the large star gears are equal and opposite to the tangential load on the input pinion f_1^t. This load can be used to find the load on the small star gear f_2^t. From the principle of conservation of energy, we have

$$\tau_{LS}\omega_{LS} = \tau_{SS}\omega_{SS} \tag{2.37}$$

The large star and small star gears are integral parts of the amplifier gear and hence have the same angular velocity i.e. $\omega_{LS} = \omega_{SS}$. This implies that the torque on them is the same i.e. $\tau_{LS} = \tau_{SS}$. Expanding the torque terms in terms of tooth loads, Equation 1.25 becomes

$$\left(\frac{D_{LS}}{2}\right)\times f_1^t = \left(\frac{D_{SS}}{2}\right)\times f_2^t \Rightarrow f_2^t = \frac{D_{LS}}{D_{SS}}\times f_1^t \tag{2.38}$$

Equation 2.40 explains why the compound gear consisting of the large star gear and the small star gear is known as the amplifier gear. The tangential transmitted tooth load in the second gear mesh f_2^t is equal to the tangential transmitted tooth

load in the first mesh f_1^t multiplied by an amplification factor r_A. This amplification factor is simply the ratio of the pitch diameter of the large star gear to the small star gear.

$$r_A = \frac{D_{LS}}{D_{SS}} \tag{2.39}$$

With the modified allowable stresses and amplification factor defined, the procedure for the determination of face-widths F_1 and F_2 can be presented.

Since gear design is an iterative process, initial values for the face-widths are required. The value can then be changed as required. In the methodology proposed, the face-widths F_1 and F_2 are initially set equal to the maximum allowable face width; i.e., equal to the pitch diameter of the pinion namely, the Input Pinion for Mesh 1 and the Small star gear for Mesh 2. The reader should note that this is a result of using $F_{rule} = 1$ (Section 2.2.1.13).

By re-arranging Equation 2.36 and using the limiting condition; i.e., $s_t = S_{at}$ the following expression for allowable tangential transmitted load (based on bending stress) on a gear tooth in the first mesh is obtained:

$$f_1^t = \frac{S_{at1} F_1 J_1}{K_{v1} K_{m1} P_{d1}} \tag{2.40}$$

The corresponding load on the gear teeth in the second mesh will be

$$f_2^t = f_1^t \times r_A \tag{2.41}$$

The bending stress in Mesh 2 corresponding to this load is then

$$s_{t2} = f_2^t K_{v2} K_{m2} \frac{P_{d2}}{F_2 J_2} \tag{2.42}$$

This calculated bending stress is then compared with the allowable bending stress in the 2nd gear mesh, S_{at2}. If the calculated bending stress s_{t2} exceeds the allowable bending stress S_{at2}, the transmitted load in the 1st gear mesh f_1^t (and as a result f_2^t) is reduced as shown below:

$$Updated\ f_1^t = \frac{S_{at2}}{s_{t2}} \times f_1^t \ \ if\ \ s_{t2} > S_{at2} \tag{2.43}$$

The rationale behind Equation 2.44 is that, since all other tooth level parameters (diametral pitch, geometry factor etc.) have been fixed, and maximum allowed face-width is used, the only way to reduce stress in the gear teeth is by reducing the allowed tangential transmitted load. It is important that f_2^t is updated whenever f_1^t is updated.

This rationale is then applied to the contact stresses in the gear meshes as shown below:

$$s_{c1} = 2300\sqrt{f_1^t K_{v1} \frac{K_{m1}}{d_{p1} F_1 I_1}} \tag{2.44}$$

$$\text{Updated}\ f_1^t = \left(\frac{S_{ac1}}{s_{c1}}\right)^2 \times f_1^t \ \ \text{if}\ \ s_{c1} > S_{ac1} \tag{2.45}$$

$$s_{c2} = 2300\sqrt{f_2^t K_{v2} \frac{K_{m2}}{d_{p2} F_2 I_2}} \tag{2.46}$$

$$\text{Updated}\ f_1^t = \left(\frac{S_{ac2}}{s_{c2}}\right)^2 \times f_1^t \ \ \text{if}\ \ s_{c2} > S_{ac2} \tag{2.47}$$

The value for f_1^t from Equation 2.47 and the corresponding f_2^t, give the final values of the tangential load that can be transmitted through the two gear meshes respectively. The corresponding gear tooth stresses at this stage of the design procedure are either less than or equal to the allowable stresses. The next step in the procedure is to

ensure that neither gear mesh is over-designed. Put differently, we seek a design where both Mesh 1 and Mesh 2 are at their limiting stress values (either in bending or in contact). The term 'Limiting Face-width', designated as F and defined as that value of face-width at which the actual stress becomes equal to the allowed stress, is used for this purpose. With reference to the bending and contact stresses in the two gear meshes, four Limiting Face-width values may be found:

$$F_{t1} = \left(\frac{s_{t1}}{S_{at1}} \right) \times F_1 \quad \& \quad \mathrm{F}_{t2} = \left(\frac{s_{t2}}{S_{at2}} \right) \times F_2$$

$$F_{c1} = \left(\frac{s_{c1}}{S_{ac1}} \right)^2 \times F_1 \quad \& \quad F_{c2} = \left(\frac{s_{c2}}{S_{ac2}} \right)^2 \times F_2$$

The equations above have the following significance:

- If the actual stress is equal to the allowed stress, the Limiting Face-width equals the face-width.
- If the actual stress is less than the allowed stress, the Limiting Face-width indicates the value to which the face-width may be reduced such that the actual and allowed stresses are equal.

The last step of the gear design procedure is to update the face widths based on the Limiting Face-width's. This is shown below:

$$F_1 = \text{ Greater of } F_{t1} \text{ and } F_{c1}$$
$$F_2 = \text{Greater of } F_{t2} \text{ and } F_{c2}$$

The design decision set (Tooth numbers, diametral pitches, pitch diameters and face-widths) corresponding to the gears, for a given set of a priori decisions (see Section

2.3), is then completely known. The reader should note that for a given gear ratio g , there may exist numerous configurations of gear teeth that satisfy the gear ratio requirement. It is for this reason that a *set* of designs (Design Solution Set) rather than a single design can be found for a given set of inputs. The design procedure for the 1-Stage SCGT is summarized in Figure 2-20 and Figure 2-21. The reader is advised to refer to Figure 2-15 and note how the high level ideas shown there are embodied in the design procedure just developed.

With reference to Figure 2-20 and Figure 2-21, the asterisk's beside the boxes indicated by the letters 'C' and 'F' are to indicate that all steps in between (steps 'C' and 'F' included) apply to *each* of the tooth number combinations found in step 'B'. Steps labeled A-G will be discussed in more detail in Section 2.7.

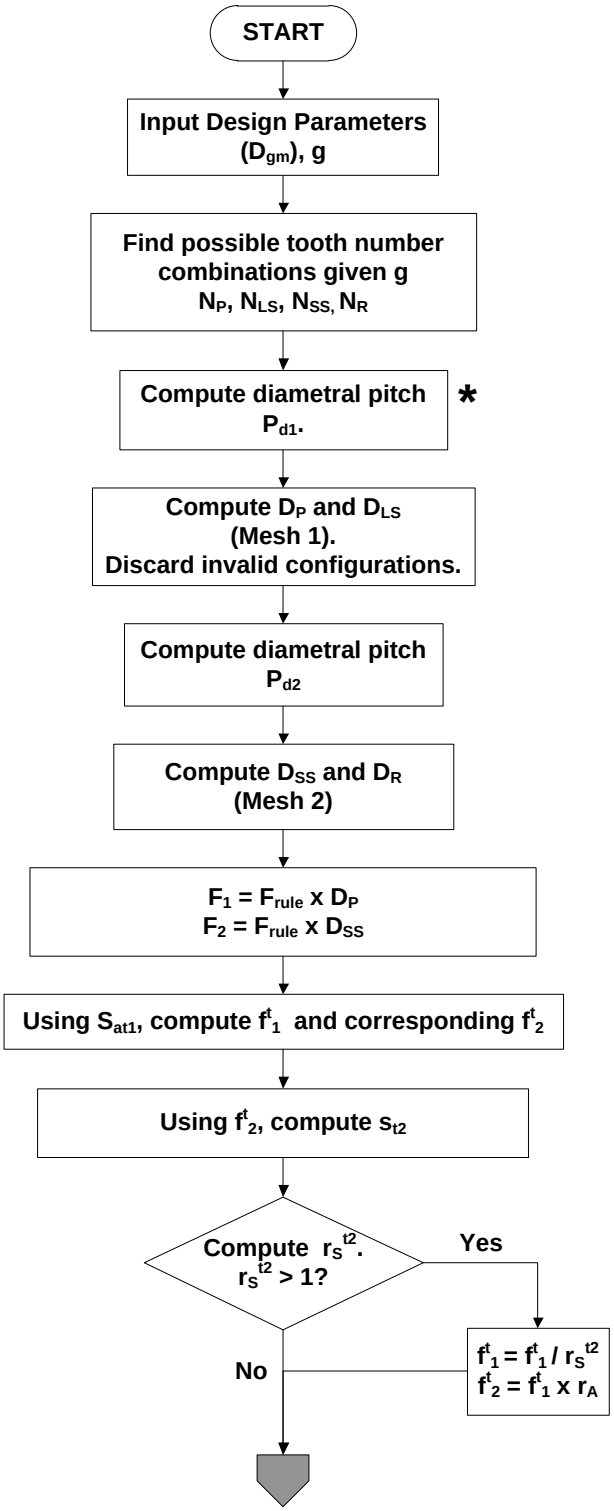

Figure 2-20: Design Procedure for a One-Stage Star Compound Gear Train

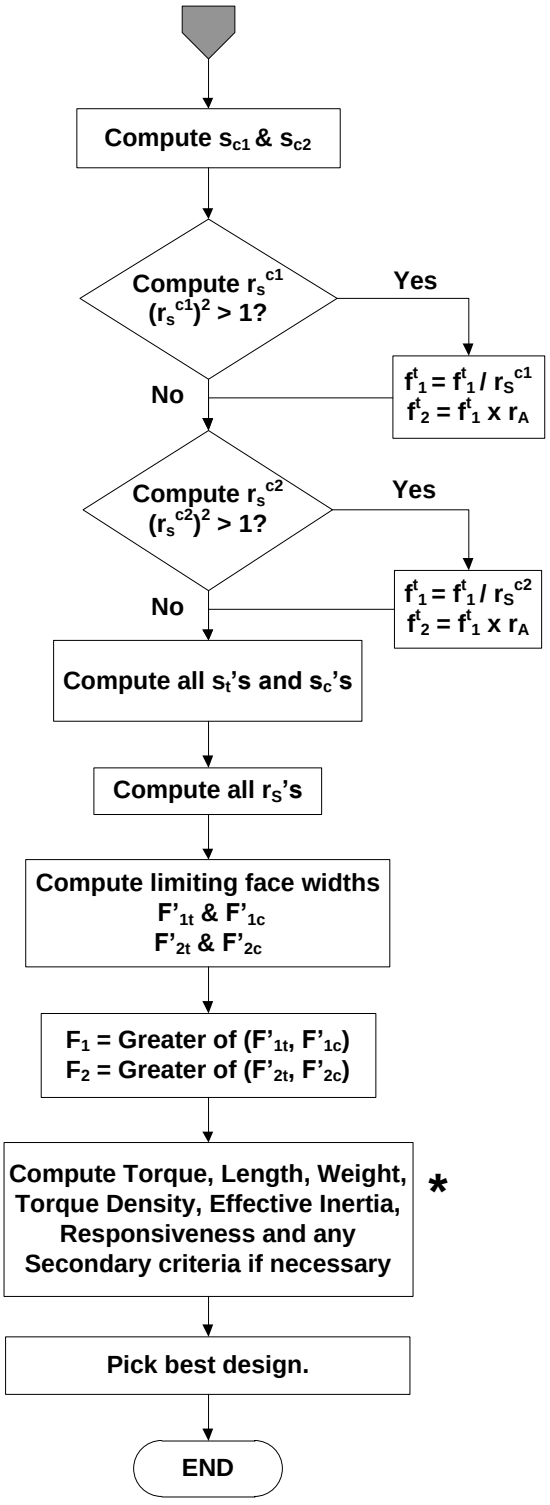

(E)

(F)

(G)

Figure 2-21: Design Procedure for a One-Stage Star Compound Gear Train (Continued)

2.5 Design Procedure for a Pancake-Type Two-Stage SCGT

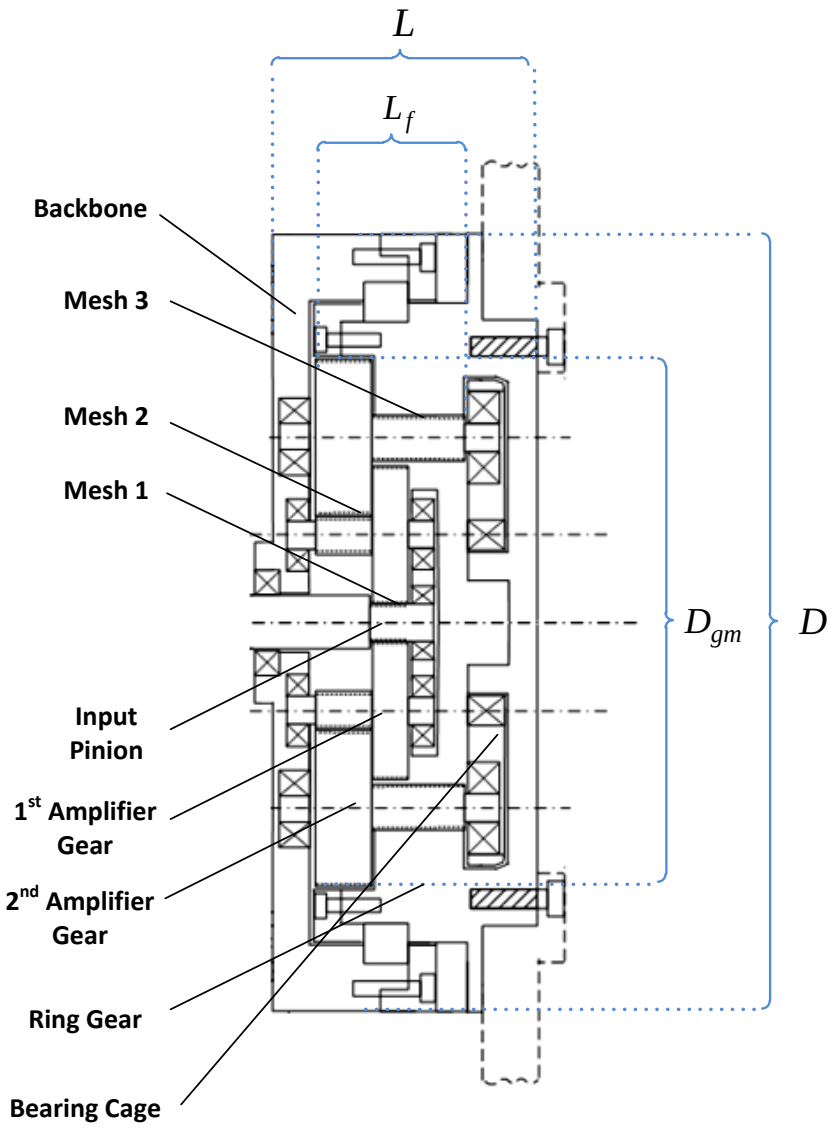

Figure 2-22: Pancake-Type Two-Stage Star Compound Gear Train

Figure 2-22 shows a representative layout of a typical Pancake-Type Two-Stage SCGT. The relevant nomenclature is listed in Table 2-20. The development of the design procedure for this gear train is presented next.

Table 2-20: Nomenclature for a Pancake Type 2-Stage SCGT

Nomenclature			
	Description		**Description**
Design Decisions			
D_P	P.D. of the Input Pinion	g	Reduction in the gear train
D_{LS1}	P.D. of the Large Star gear (Mesh1)	g_1	Reduction in Mesh 1
D_{SS1}	P.D. of the Small Star gear (Mesh 2)	g_2	Reduction in Mesh 2
D_{LS2}	P.D. of the Large Star gear (Mesh 2)	g_3	Reduction in Mesh 3
D_{SS2}	P.D. of the Small Star gear (Mesh 3)	P_{d1}	Transverse Diametral pitch of gears in Mesh 1
D_R	P.D. of the Ring gear	P_{d2}	Transverse Diametral pitch of gears in Mesh 2
D	Diameter of gear train	P_{d3}	Transverse Diametral pitch of gears in Mesh 3
D_{gm}	Diameter of gear mesh	L	Length of gear train
N_P	No. of teeth on the Input Pinion	L_f	Length of gear meshes
N_{LS1}	No. of teeth on $LS1$	F_1	Face width of gears in Mesh 1
N_{SS1}	No. of teeth on $SS1$	F_2	Face width of gears in Mesh 2
N_{LS2}	No. of teeth on $LS2$	F_3	Face-width of gears in Mesh 3
N_{SS2}	No. of teeth on $SS2$	A	Aspect Ratio of gear train
N_R	No. of teeth on the Ring gear		
n	Output Speed (rpm)		
A Priori Decisions			
φ_1	Transverse Pressure angle in Mesh 1	ψ_1	Helix Angle in Mesh 1
φ_2	Transverse Pressure angle in Mesh 2	ψ_2	Helix Angle in Mesh 2
φ_3	Transverse Pressure angle in Mesh 3	ψ_3	Helix Angle in Mesh 3

2.5.1 Design Procedure Development for a Pancake-Type 2-Stage SCGT

The first step in the design procedure is to perform a tooth number search such that the required gear ratio g is attained. In this case, g is given by

$$g = g_1 g_2 g_3 = \frac{N_{LS1}}{N_P}\frac{N_{LS2}}{N_{SS1}}\frac{N_R}{N_{SS2}} \tag{2.48}$$

As mentioned earlier, a number of tooth number combinations may give the required gear ratio g. The steps that follow are in reference to *each* individual combination of tooth numbers. The approach following for the P-Type 2-Stage SCGT is to work backwards; i.e., beginning with the calculations for the gears in Mesh 3 and ending with those for the gears in Mesh 1.

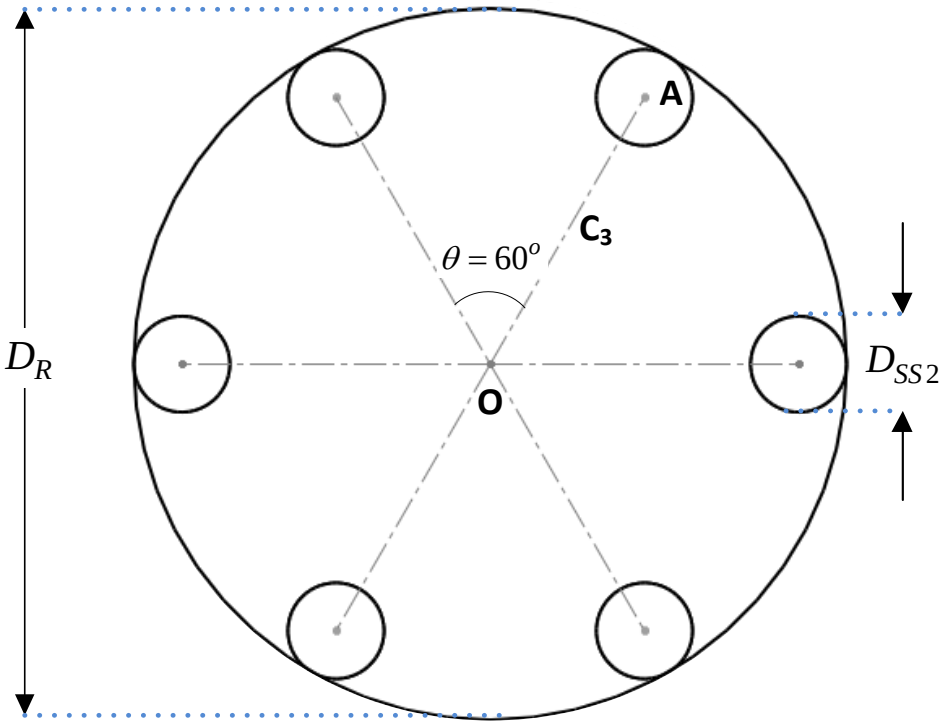

Figure 2-23: Sketch showing the arrangement of the gears in Mesh 3

The sketch in Figure 2-23 shows the pitch diameters of the gears in Mesh 3; i.e., the 2nd Small Star gears (SS2) and the Ring gear. Instead of using the gear mesh diameter D_{gm}, the following design procedure will use the pitch diameter of the Ring gear D_R as a starting point. The relationship between D_R and D_{gm} will be established at the end of this section. Given D_R, the diametral pitch for the gears in Mesh 3 can be found:

$$P_{d2} = \frac{N_R}{D_{gm}} \tag{2.49}$$

The pitch diameter of the 2nd Small Star gears can then be found using the equation:

$$D_{SS2} = \frac{N_{SS2}}{P_{d3}} \tag{2.50}$$

The pitch diameters and diametral pitches of the gears in Mesh 3 are therefore known. The Mesh 3 center distance C_3 can then be found (See line OA in Figure 2-23).s

$$C_3 = \frac{D_R}{2} - \frac{D_{SS}}{2} \tag{2.51}$$

The 2nd Large Star Gears (LS2's) are concentric with the 2nd Small Star gears (SS2's) as both are integral components of the 2nd Amplifier gears (see Figure 2-22). The limiting condition for the maximum pitch diameter of the LS2 gears is shown in Figure 2-24. At the limiting condition, the addendum diameters of the LS2 gears *just* begin to interfere with each other. As shown in Figure 2-24, this occurs when the central angle θ subtended by the 2nd Amplifier gears is 60°. In order to avoid interference, the central angle θ will be set to 59° in this report. From Figure 2-24, using the formula for the chord ($A'A$) of a circle with radius C_3 (OA), we have the relation:

$$A'A = D^o_{LS2} = 2 \times OA \times \sin\left(\theta/2\right) = 2C_3 \sin\left(\theta/2\right) \tag{2.52}$$

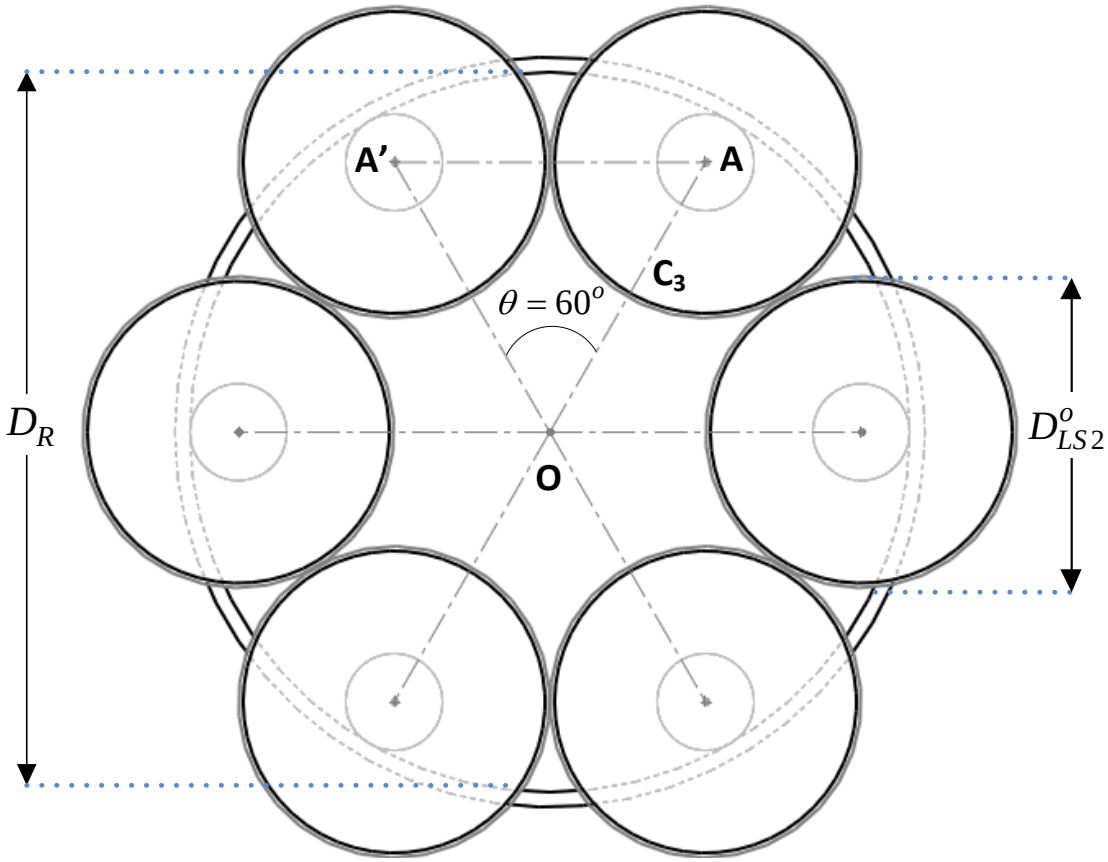

Figure 2-24: Sketch showing the limiting condition for the 2nd Large Star gears

The addendum diameter D_{LS2}^{o} can be expressed in terms of the number of teeth and diametral pitch to derive the following formula for P_{d2}:

$$\begin{aligned} D_{LS2}^{o} &= 2C_3 \sin\left(\theta/2\right) \\ \Rightarrow \frac{N_{LS2}+2}{P_{d2}} &= 2C_3 \sin\left(\theta/2\right) \\ \Rightarrow P_{d2} &= \frac{N_{LS2}+2}{2C_3 \sin\left(\theta/2\right)} \end{aligned} \tag{2.53}$$

The reader should note from Equation 2.52 and Figure 2-24 the angle θ dictates the maximum possible value for D_{LS2}. A decrease in Θ results in a smaller D_{LS2}, which

results in a decrease in g_2 $\left(g_2 = D_{LS2}/D_{SS1}\right)$. The result is that the maximum g that can be obtained is also reduced. This issue will be addressed in more detail at the end of this section.

With the diametral pitch in Mesh 2 known, the pitch diameters of the gears in Mesh 2; i.e., D_{SS1} and D_{LS2} can be found:

$$D_{SS1} = \frac{N_{SS1}}{P_{d2}}$$

$$D_{LS2} = \frac{N_{LS2}}{P_{d2}}$$

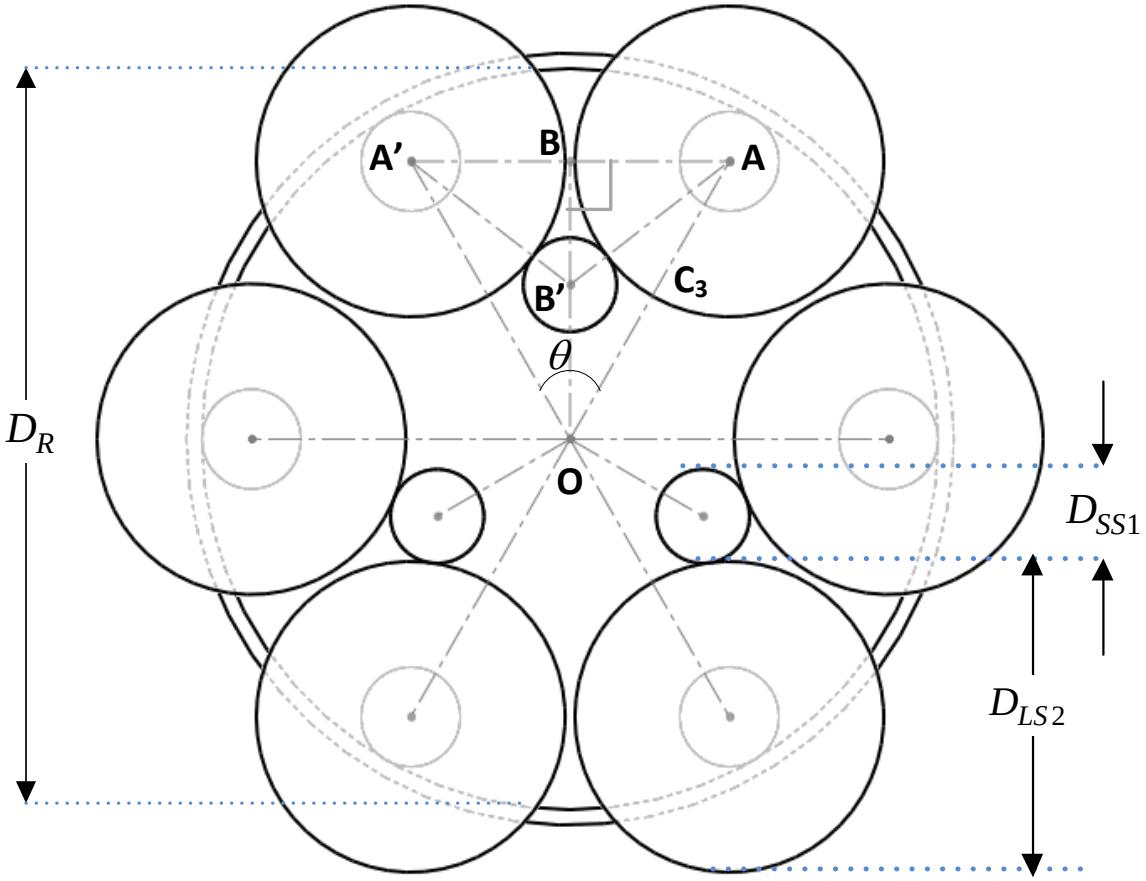

Figure 2-25: Sketch showing the arrangement of the gears in Mesh 2 and Mesh 3

The resulting gear train configuration at this stage of the design procedure is shown in Figure 2-25. With the LS2 and SS1 gears arranged as shown in the figure above, the fact that LS1 and SS1 are concentric (they are integral components of the 1st Amplifier gear) can be used to calculate C_1, the center distance in Mesh 1. In Figure 2-25, the length of the line segment OB' equals C_1. Using basic geometric concepts, the following relations are derived:

$$OB = OA\cos\left(\theta/2\right) = C_3\cos\left(\theta/2\right) \tag{2.54}$$

$$BB' = \sqrt{\left(AB'\right)^2 - \left(AB\right)^2} = \sqrt{\left(D_{SS1} + D_{LS2}\right)^2 - \left(D^o_{LS2}\right)^2} \tag{2.55}$$

$$C_1 = OB' = OB - BB' \tag{2.56}$$

With the Mesh 1 center distance known, it is possible to calculate the diametral pitch P_{d1} and the pitch diameters D_P and D_{LS1} as shown below:

$$\begin{aligned} P_{d1} &= \frac{N_P + N_{LS1}}{2C_1} \\ D_P &= \frac{N_P}{P_{d1}} \\ D_{LS1} &= \frac{N_{LS1}}{P_{d1}} \end{aligned} \tag{2.57}$$

The sketch in shows the arrangement of all the gears in a P-Type 2-Stage SCGT with six amplifier gears (P-Type-6) in the 2nd Stage. At this stage of the Pancake-Type Two-Stage SCGT design procedure, the diametral pitches and pitch diameters of all the gears are known. The next step in the design procedure is the calculation of the face-widths in the three gear meshes. However, before presenting the face-width determination procedure, two assembly constraints must be addressed.

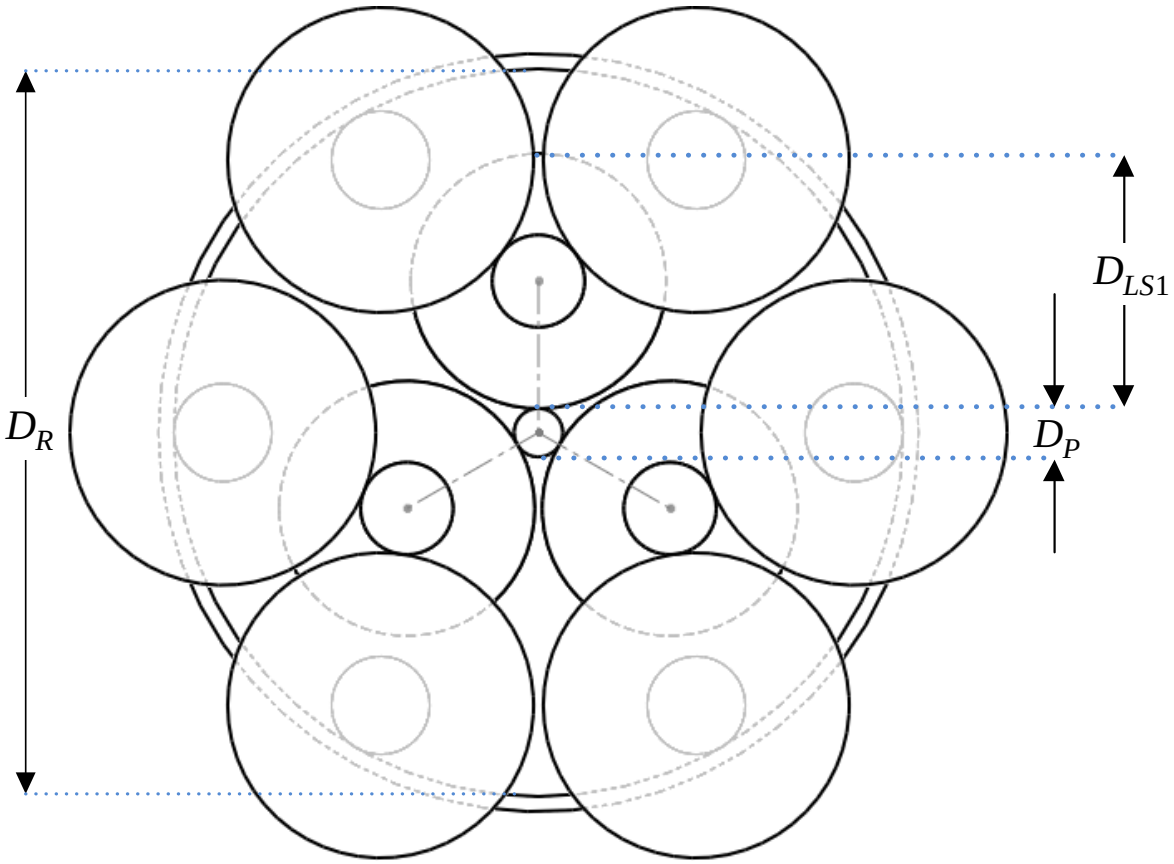

Figure 2-26: Sketch showing all of the gears in a P-Type 2-Stage SCGT

The first issue is the constraint on the pitch diameters of the gears to avoid interference. Interference between the 1st stage amplifier gears is handled in the same way as with the 1-stage SCGT (See Equation 2.32). An additional constraint in the P-Type 2-Stage SCGT is:

$$D_{SS1} + D_{LS2} > D^o_{LS1} + D^o_{SS2} \tag{2.58}$$

From Figure 2-27, it can be seen that if the condition in Equation 2.58 is not met, the LS1 and SS2 gears interfere with one another. It is helpful to look at Figure 2-22 , which

shows the cross-sectional view of the gear train, to understand this constraint more clearly.

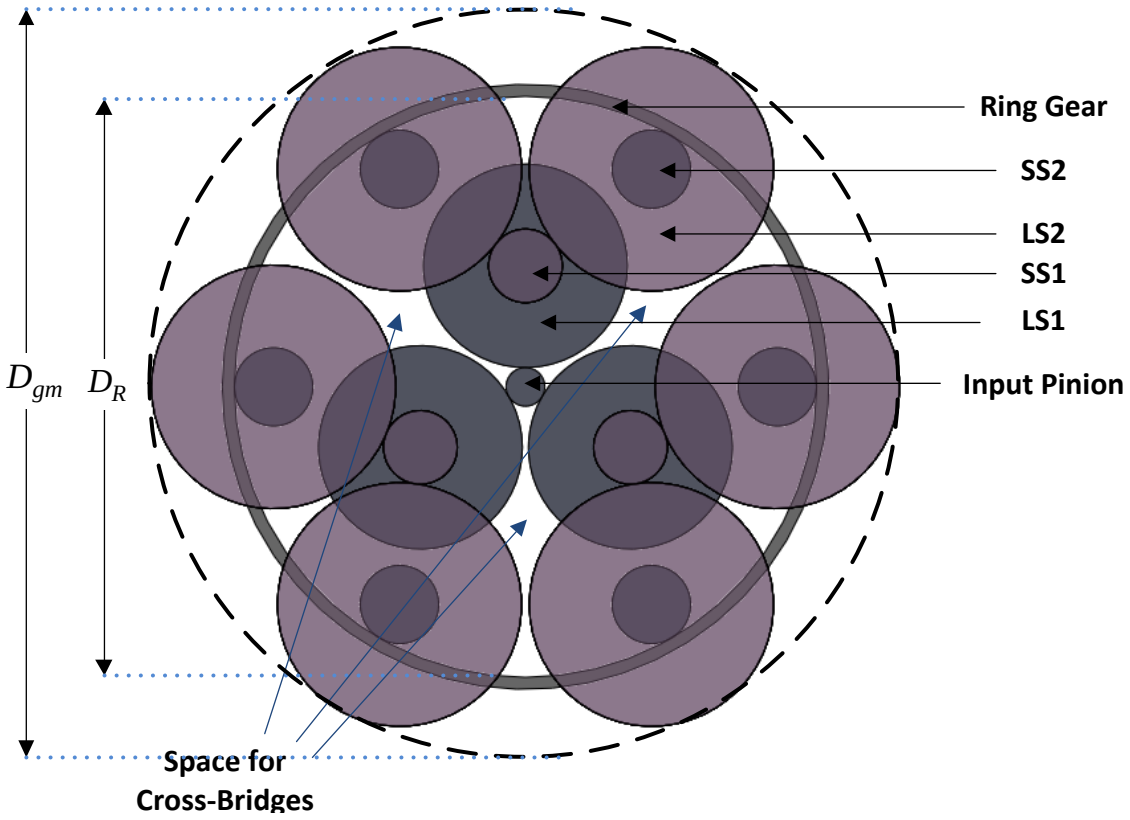

Figure 2-27: Layout of gears in a P-Type 2-Stage SCGT (6 Second Stage Amplifier Gears)

The second issue relates to the amount of space available for the cross-bridges connecting the rigid backbone to the bearing cage (See Figure 2-27). At a more advanced stage of design, if it is found that the space available for the cross-bridges is inadequate, the space can be increased by decreasing the value of central angle θ. As mentioned earlier, doing this decreases the maximum value of D_{LS2} thereby providing more room for

the cross-bridges (See Figure 2-27). However, the maximum gear ratio that can be obtained from the P-Type 2-Stage SCGT is also reduced. Taking the pitch diameter constraints into account, the maximum gear ratios that can be achieved corresponding to relevant values for Θ are shown in Table 2-21.

Table 2-21: Maximum obtainable Gear ratio for various values of Θ

Θ	Maximum obtainable Gear ratio g
59^o	240
57.5^o	220
55^o	190
52.5^o	160

From Figure 2-26 , the gear mesh diameter can be calculated as follows:

$$D_{gm} = D_R - D_{SS2} + D_{LS2} \tag{2.59}$$

Since, for a designer, the gear mesh diameter D_{gm} is a more intuitive starting point than D_R, it is useful to know how the two relate to each other. It is found that the two terms are related through gear ratio g as shown in Figure 2-28. The ripple in the plot shown in Figure 2-28 appears due to whole number constraints on the numbers of teeth. A 6th degree polynomial equation was fitted to the curve in Figure 2-28:

$$\frac{D_R}{D_{gm}} = -1.1e^{-13}g^6 + 1e^{-10}g^5 - 3.9e^{-8}g^4 + \ldots \tag{2.60}$$
$$\ldots + 7.3e^{-6}g^3 - 7.2^{e-4}g^2 + 0.03g + 0.1$$

Thus, for a given gear mesh diameter D_{gm} and gear ratio g, the corresponding value for the Ring pitch diameter D_R can be calculated using Equation 2.60. As discussed in the beginning of this Section, D_R is used as the starting point for the current design procedure. The procedure for the face-width determination is now presented.

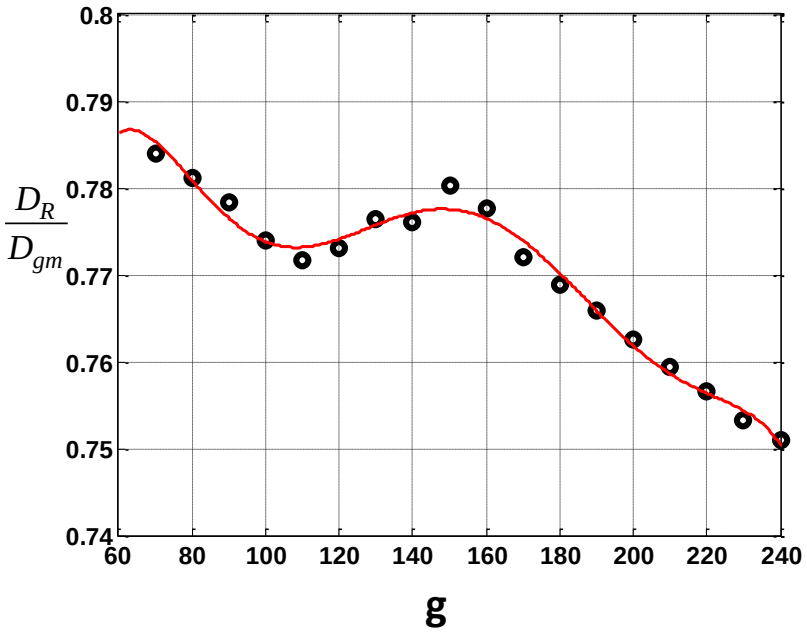

Figure 2-28: Ratio of Ring Diameter to Gear Mesh Diameter as a function of g

2.5.1.1 Determination of Face-Widths F_1, F_2 and F_3

The rationale and therefore the steps employed in the determination of F_1, F_2 and F_3 are similar to the steps employed in the determination of F_1 and F_2 in the design process for the 1-Stage SCGT (see Section 2.4.1.1); the only difference being that here there are three gear meshes instead of two.

The tangential transmitted load through the 1st gear mesh, based on the allowable bending stress S_{at1} is given by (See Equation 2.40):

$$f_1^t = \frac{S_{at1} F_1 J_1}{K_{v1} K_{m1} P_{d1}} \tag{2.61}$$

The tangential load on the first Small Star Gear SS1 (in Mesh 2) is then

$$f_2^t = f_1^t \times r_{A1} \tag{2.62}$$

where the amplification factor r_{A1} is given by,

$$r_{A1} = \frac{D_{LS1}}{D_{SS1}} \tag{2.63}$$

The bending stress in Mesh 2, s_{t2}, under the load f_2^t is given by,

$$s_{t2} = f_2^t K_{v2} K_{m2} \frac{P_{d2}}{F_2 J_2} \tag{2.64}$$

If s_{t2} exceeds S_{at2}, f_1^t (and therefore f_2^t) is updated as shown:

$$Updated\ f_1^t = \frac{s_{t2}}{S_{at2}} \times f_1^t \tag{2.65}$$

The corresponding transmitted loads through the 2nd and 3rd gear meshes are then found:

$$\begin{aligned} f_2^t &= f_1^t \times r_{A1} \\ f_3^t &= f_2^t \times r_{A2} \end{aligned} \tag{2.66}$$

where the amplification factor r_{A2} is given by,

$$r_{A2} = \frac{D_{LS2}}{D_{SS2}} \tag{2.67}$$

The bending stress in Mesh 3, s_{t3}, under the load f_3^t is given by,

$$s_{t3} = f_3^t K_{v3} K_{m3} \frac{P_{d3}}{F_3 J_3} \tag{2.68}$$

If s_{t3} exceeds S_{at3}, f_1^t (and therefore f_2^t and f_3^t) is updated as shown:

$$Updated\ f_1^t = \frac{s_{t3}}{S_{at3}} \times f_1^t \tag{2.69}$$

The transmitted loads through the 2nd and 3rd gear meshes are updated using Equation 2.65. At this stage of the procedure, it has been ensured that the bending stresses in all gear meshes are within allowable limits. The steps laid out below are performed in order to ensure that the contact stresses in the gear meshes also do not exceed the allowable

limits. The rationale is the same as with the bending stresses. Although it will not be shown in the equations below, the reader must keep in mind that whenever the load f_1^t is updated, the loads f_2^t and f_3^t must also be updated using Equation 2.65.

$$s_{c1} = 2300\sqrt{f_1^t K_{v1} \frac{K_{m1}}{d_{p1} F_1 I_1}} \tag{2.70}$$

$$\text{Updated } f_1^t = \left(\frac{S_{ac1}}{s_{c1}}\right)^2 \times f_1^t \quad \text{if } s_{c1} > S_{ac1} \tag{2.71}$$

$$s_{c2} = 2300\sqrt{f_2^t K_{v2} \frac{K_{m2}}{d_{p2} F_2 I_2}} \tag{2.72}$$

$$\text{Updated } f_1^t = \left(\frac{S_{ac2}}{S_{c2}}\right)^2 \times f_1^t \quad \text{if } s_{c2} > S_{ac2} \tag{2.73}$$

$$s_{c3} = 2300\sqrt{f_3^t K_{v3} \frac{K_{m3}}{d_{p3} F_3 I_3}} \tag{2.74}$$

$$\text{Updated } f_1^t = \left(\frac{S_{ac3}}{s_{c3}}\right)^2 \times f_1^t \quad \text{if } s_{c3} > S_{ac3} \tag{2.75}$$

The value for f_1^t from Equation 2.74 and the corresponding values for f_2^t and f_3^t give the final values of the transmitted load through each of the three gear meshes respectively. The stresses corresponding to these loads can be calculated using Equations 2.69, 2.71 and 2.73 respectively. Then, in order to ensure that none of the gear meshes are over designed, the Limiting Face-Widths are found. The six Limiting Face-Widths are calculated as shown below:

$$F_{t1} = \left(\frac{s_{t1}}{S_{at1}}\right) \times F_1 \qquad F_{t2} = \left(\frac{s_{t2}}{S_{at2}}\right) \times F_2 \qquad F_{t3} = \left(\frac{s_{t3}}{S_{at3}}\right) \times F_3$$

$$F_{c1} = \left(\frac{s_{c1}}{S_{ac1}} \right)^2 \times F_1 \qquad F_{c2} = \left(\frac{s_{c2}}{S_{ac2}} \right)^2 \times F_2 \qquad F_{c3} = \left(\frac{s_{c3}}{S_{ac3}} \right)^2 \times F_3$$

The face-widths F_1, F_2 and F_3 are then updated as shown below:

$F_1 =$ Greater of F_{t1} and F_{c1}

$F_2 =$ Greater of F_{t2} and F_{c2}

$F_3 =$ Greater of F_{t3} and F_{c3}

The design procedure for the Two-Stage Pancake-Type SCGT is summarized in the figures below. The reader should note the similarities between the design procedures for the 1-Stage SCGT presented earlier and the 2-Stage P-Type SCGT presented here. The reader is also encouraged to note how the developed procedure is in keeping with the ideas presented in Figure 2-15.

With reference to Figure 2-29, Figure 2-30 and Figure 2-31, the asterisk's beside the boxes indicated by the letters 'C' and 'F' are to indicate that all steps in between (steps 'C' and 'F' included) apply to *each* of the tooth number combinations found in step 'B'. Steps labeled A-G will be discussed in more detail in Section 2.7.

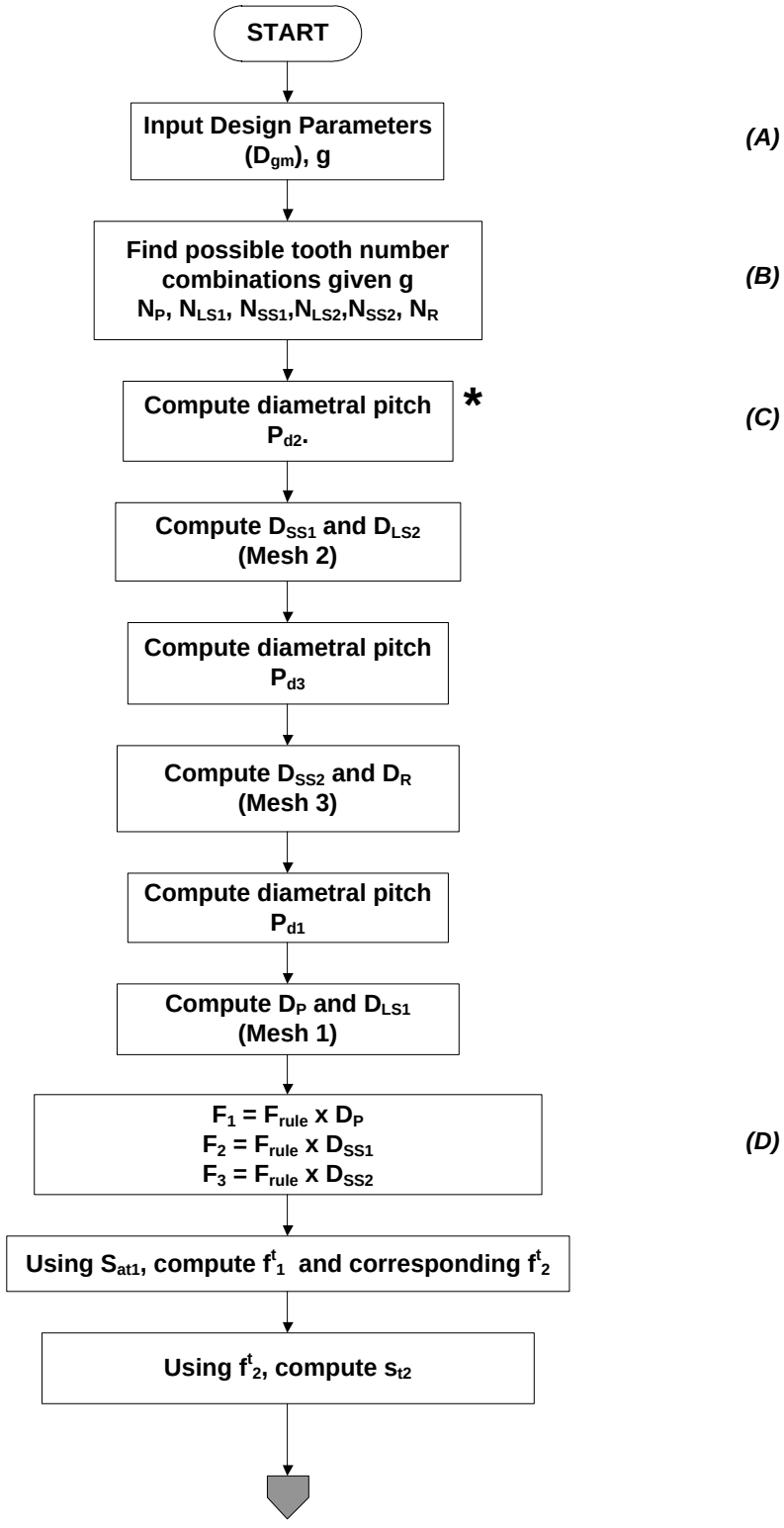

Figure 2-29: Two-Stage Pancake-Type SCGT Design Procedure

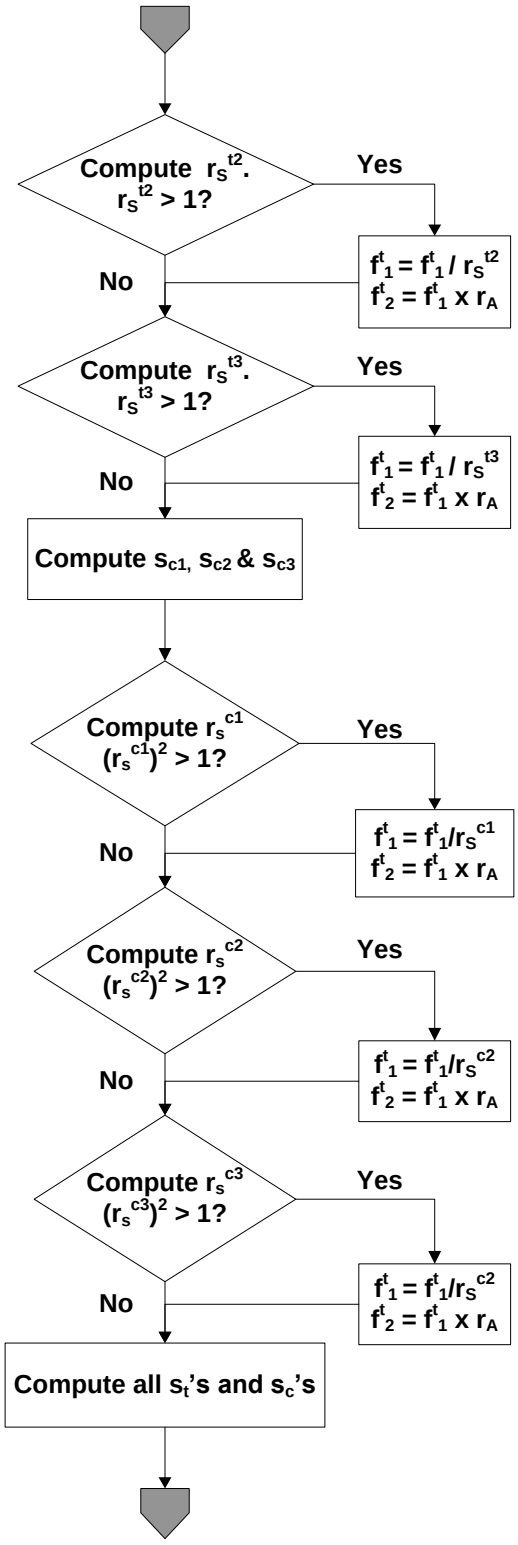

Figure 2-30: Two-Stage Pancake-Type SCGT Design Procedure (Continued)

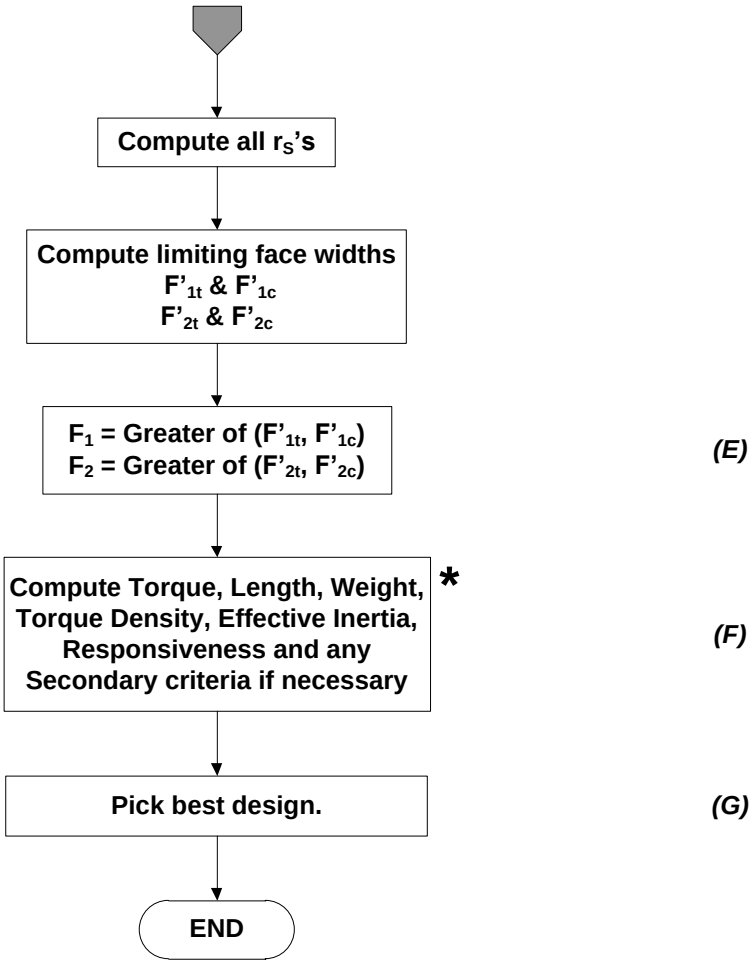

Figure 2-31: Two-Stage Pancake-Type SCGT Design Procedure (Continued)

2.5.2 Pancake-Type Two-Stage SCGT with three 2nd Stage Amplifier Gears

The P-Type 2-Stage SCGT discussed in the previous section contained six amplifier gears in the 2nd stage; i.e., in Mesh 2 and Mesh 3. If a design of lesser complexity is sought, or if the performance requirements are not high, a simpler design using only three amplifier gears in the 2nd stage (P-Type -3) may be used. This is shown in Figure 2-32.

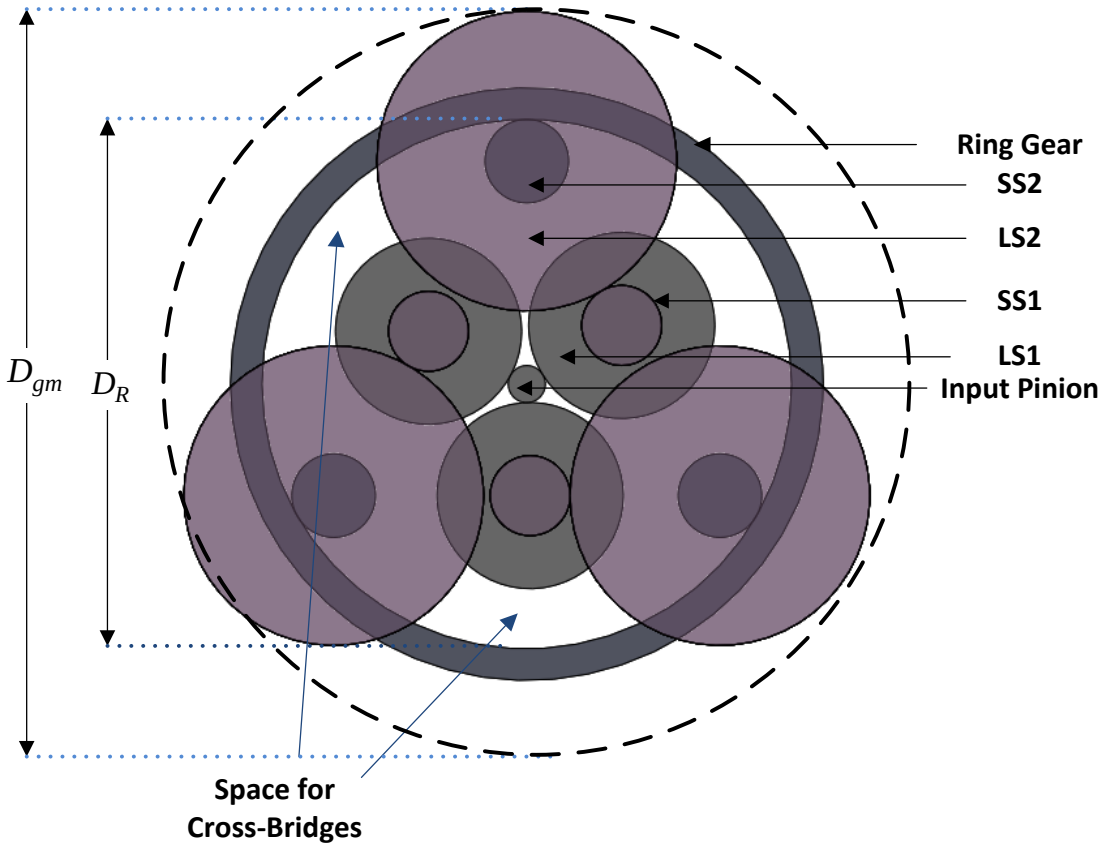

Figure 2-32: Layout of gears in a P-Type 2-Stage SCGT (3)

As Figure 2-32 shows, in this type of gear train, the 1st and 2nd Amplifier gears are offset relative to one another in order to achieve a compact gear mesh diameter D_{gm}. The two assembly constraints discussed with regard to the P-Type 2-Stage SCGT with six 2nd Stage Amplifier gears (see Equation 2.32 and Equation 2.58) must also be met in this case. The relation between the Ring gear diameter D_R and the gear mesh diameter D_{gm} is found in exactly the same manner as discussed earlier. The relationship obtained is:

$$\frac{D_{gm}}{D_R} = 8.117e^{-4}g + 1.301 \tag{2.76}$$

As with the former version of the P-Type 2-Stage SCGT, the first step in the design procedure is to perform a tooth number search such that the required gear ratio *g* is attained. The gear ratio g is given by Equation 2.48. As mentioned earlier, a number of tooth number combinations may give the required gear ratio *g*. The steps that follow are in reference to *each* individual combination of tooth numbers.

For a given D_{gm} and *g*, the corresponding value for the Ring gear diameter D_R is found from Equation 2.76.

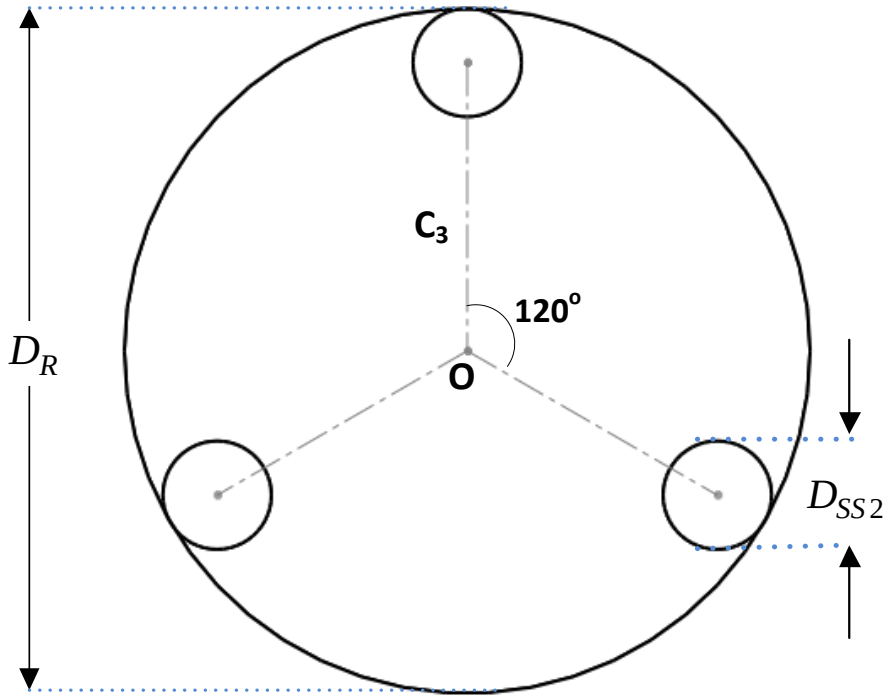

Figure 2-33: Sketch showing the gears in Mesh 3 of a P-Type 2-Stage SCGT (3)

The diametral pitch in Mesh 3 P_{d3} and the pitch diameter of the 2nd Small Star gear D_{SS2} are found:

$$P_{d3} = \frac{N_R}{D_R} \tag{2.77}$$

$$D_{SS2} = \frac{N_{SS2}}{P_{d3}} \tag{2.78}$$

The Mesh 3 center distance C_3 (See Figure 2-33) is then found using:

$$C_3 = \frac{D_R}{2} - \frac{D_{SS2}}{2} \tag{2.79}$$

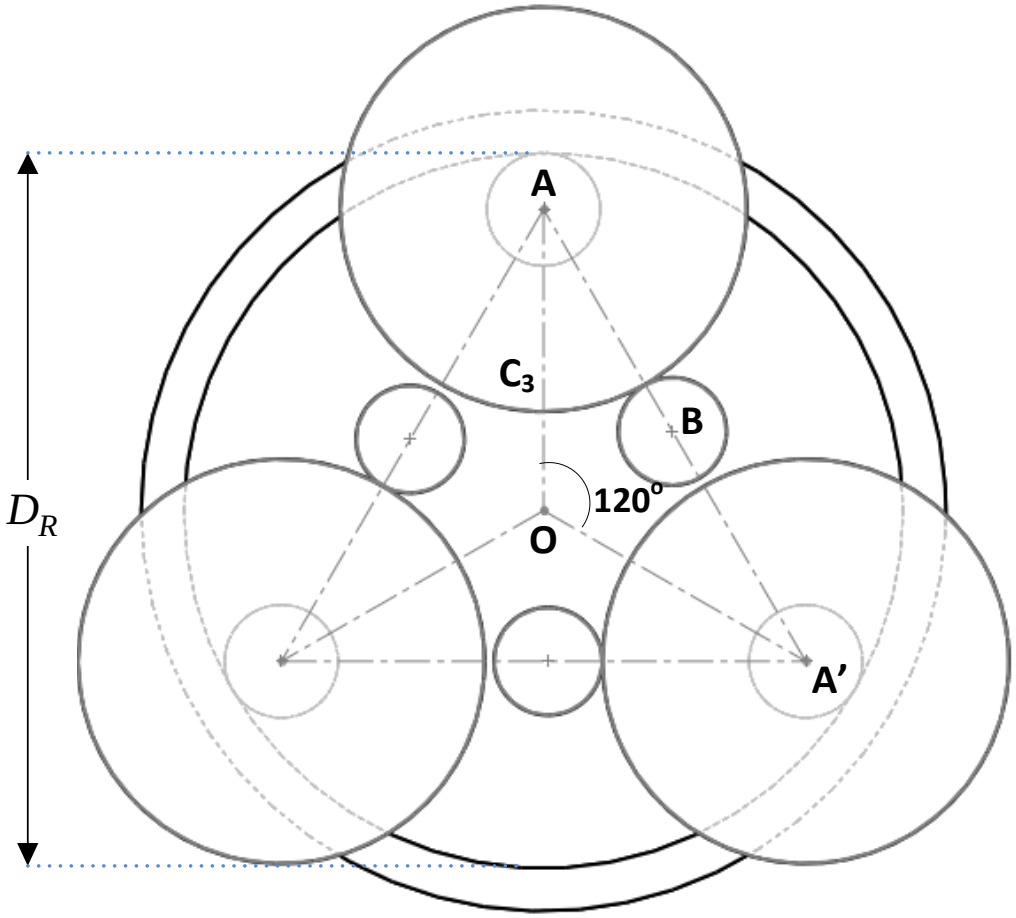

Figure 2-34: Sketch showing the gears in Mesh 2 and Mesh 3 (P-Type 2-Stage (3))

In Figure 2-34, consider the line segment AA'. The following relation can be seen:

$$AA' = AB + BA' \tag{2.80}$$

The line segment AB equals the sum of the pitch diameters of the gears in Mesh 2.

$$AB = \frac{D_{SS1} + D_{LS2}}{2} \tag{2.81}$$

The line segment BA' on the other hand, needs to be greater than or equal to the sum of the addendum diameters of the gears in Mesh 2 so as to avoid interference between the gears. This can be stated mathematically as:

$$BA' = \frac{D^o_{SS1} + D^o_{LS2}}{2} + x_{gap} \tag{2.82}$$

Note that the term x_{gap} can be used to provide a small clearance between the gears in Mesh 2 that are *not* in mesh. For instance, in Figure 2-34, the LS2 centered at A is in mesh with the SS1 centered at B. The LS2 centered at A' must not interfere with the SS1 centered at B. When x_{gap} is set equal to zero, interference *just* begins to occur. The x_{gap} value used in this report will be equal to the tooth addendum. Using the formula for the chord AA' of a circle with radius C_3 and Equations 2.80, 2.81 and 2.82, we get

$$AA' = \frac{D_{SS1} + D^o_{SS1}}{2} + \frac{D_{LS2} + D^o_{LS2}}{2} + x_{gap} \tag{2.83}$$

$$AA' = \frac{N_{SS1} + \left(N_{SS1} + 1\right)}{2P_{d2}} + \frac{N_{LS2} + \left(N_{LS2} + 1\right)}{2P_{d2}} + \frac{1}{P_{d2}} \tag{2.84}$$

$$AA' = 2C_3 \sin\left(\frac{120^o}{2}\right) = \frac{N_{SS1} + N_{LS2} + 2}{P_{d2}} \tag{2.85}$$

$$P_{d2} = \frac{N_{SS1} + N_{LS2} + 2}{C_3\sqrt{3}} \tag{2.86}$$

With P_{d2} known, the pitch diameters D_{SS1} and D_{LS2} can be found.

$$D_{SS1} = \frac{N_{SS1}}{P_{d2}}$$

$$D_{LS2} = \frac{N_{LS2}}{P_{d2}}$$

A close-up view of $\Delta AOA'$ is shown in Figure 2-34. The point B' bisects line segment AA'. The line segment OB equals the center distance in Mesh 1; i.e., C_1.

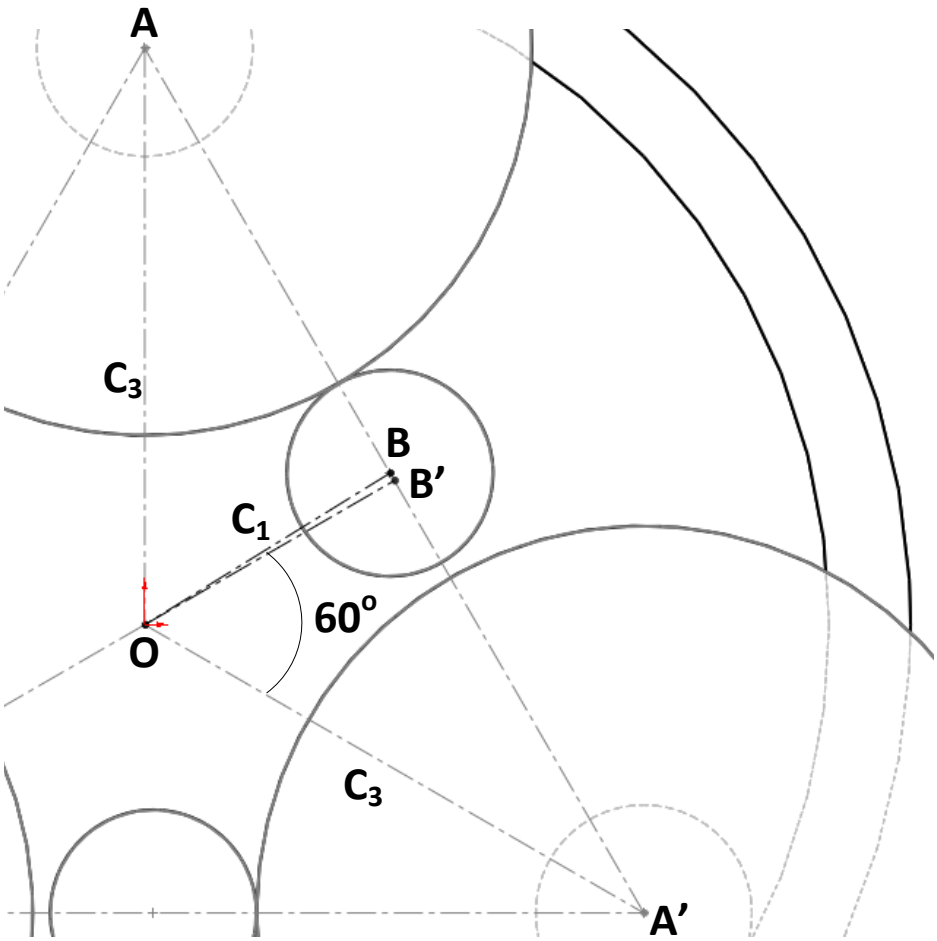

Figure 2-35: Close-up view of $\Delta AOA'$ from Figure 2-34

From Figure 2-35, it is clear that is the perpendicular bisector of line B'. Therefore, $\Delta AOA'$ is a right triangle. From Figure 2-36 , it can also be seen that $\Delta OB'B$ is a right triangle.

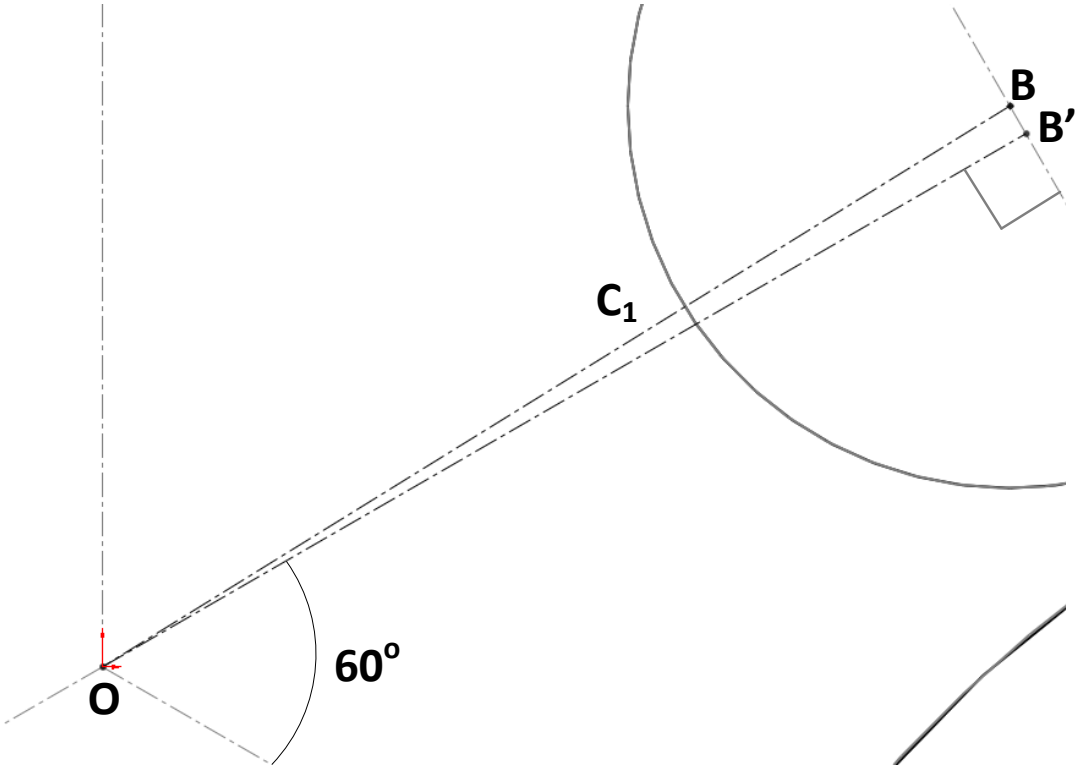

Figure 2-36: Close-up view of $\Delta OB'B$ from Figure 2-35

From Figure 2-35, the following relation can be stated:

$$OB' = C_3 \cos\left(60^o\right) = \frac{C_3}{2} \tag{2.87}$$

$$AB' = C_3 \sin\left(60^o\right) = \frac{C_3\sqrt{3}}{2} \tag{2.88}$$

The length of line segment AB is already known (Equation 2.81). Thus, the length BB' can be calculated.

$$BB' = AB' - AB \tag{2.89}$$

Finally, the Mesh 1 center distance C_1 can be calculated:

$$C_1 = \sqrt{(OB')^2 + (BB')^2} \tag{2.90}$$

It then becomes possible to calculate the pitch diameters and diametral pitch of the gears in Mesh 1.

$$\begin{aligned} P_{d1} &= \frac{N_P + N_{LS1}}{2C_1} \\ D_P &= \frac{N_P}{P_{d1}} \\ D_{LS1} &= \frac{N_{LS1}}{P_{d1}} \end{aligned} \tag{2.91}$$

At this stage, the diametral pitches and pitch diameters of all the gears in the P-Type 2-Stage with three 2nd stage amplifier gears SCGT are known. The only remaining design parameters to be determined are the face-widths. The procedure for the determination of the face-widths is the same as the procedure for the P-Type 2-Stage SCGT with six 2nd stage amplifier gears (see Section 2.5.1.1). The P-Type 2-Stage SCGT design procedure outlines in Figure 2-29, Figure 2-30 and Figure 2-31 is valid for both variations of the P-Type 2-Stage SCGT.

An interesting point to note is that the maximum obtainable gear ratio in a P-Type 2-Stage SCGT with three 2nd Stage Amplifier Gears is 320. As showed, in the case of the six Amplifier version of the P-Type 2-Stage SGCT, the maximum obtainable gear ratio is 240. Therefore, in order to be able to compare the two versions, the gear ratios for the design maps for both versions of the P-Type 2-Stage SCGT (See Section 3.5) will be limited to 240.

2.6 Design Procedure for a Coffee-Can Type Two-Stage SCGT

Figure 2-37 shows a Coffee-Can Type Two-Stage SCGT (C-Type 2-Stage SCGT). The reader is encouraged to review the 1-Stage SCGT shown in Figure 2-16 and note that the 2nd stage of the C-Type 2-Stage SCGT is exactly the same as the 1-Stage SCGT.

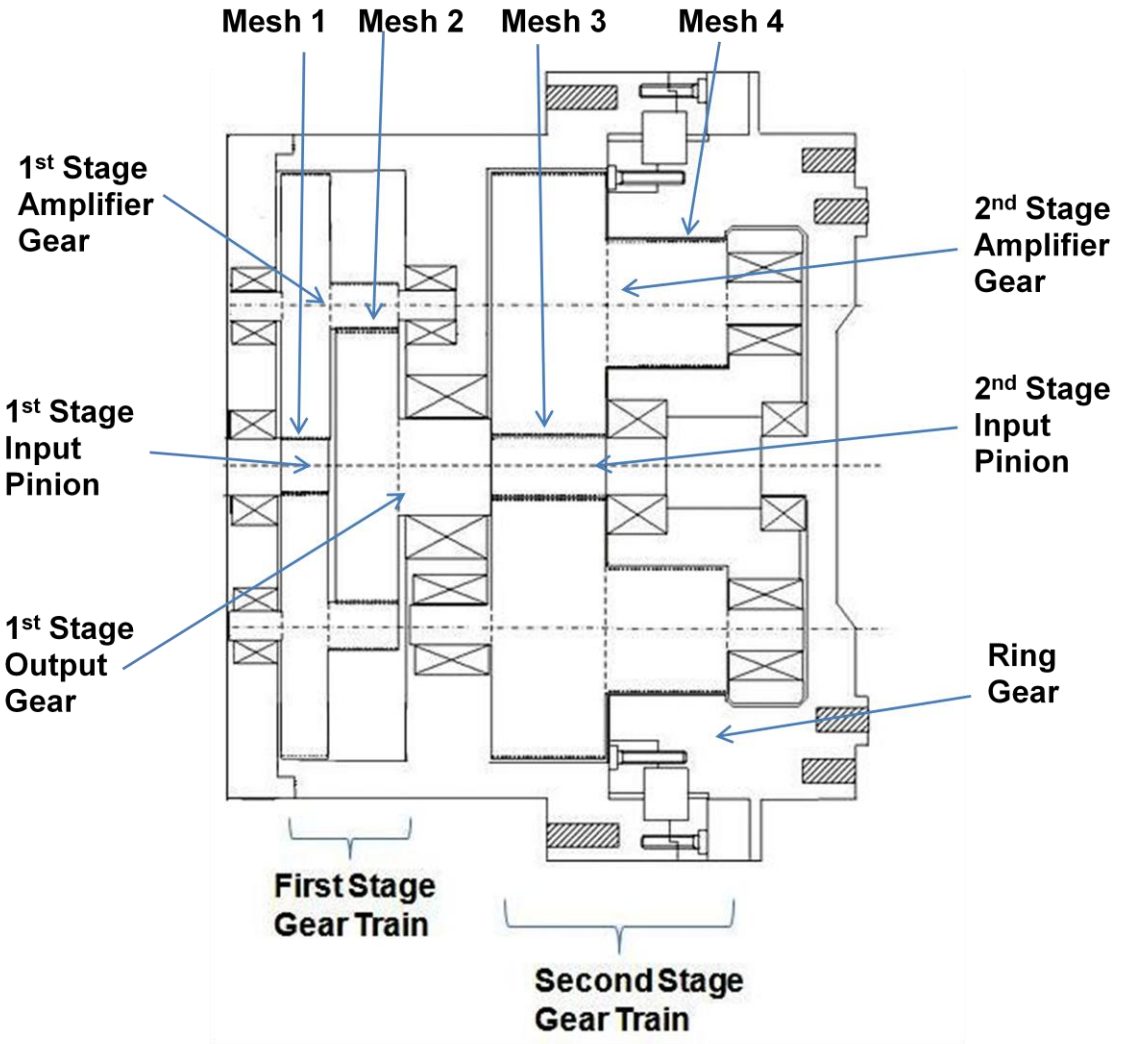

Figure 2-37: Coffee-Can Type Two-Stage Star Compound Gear Train

It is also not difficult to see that the 1st stage of the C-Type 2-Stage SCGT is the same as the 2nd stage except that the output gear is an external gear rather than an internal Ring gear. These commonalities between the two stages result in a significant reduction in design complexity. For instance, the 1st and 2nd Stages of the C-Type 2-Stage SCGT may be designed separately, one after the other. Visual design maps introduced in Chapter 3 prove to be very useful in the design of C-Type 2-Stage SCGT's. Therefore, a full discussion on the design procedure will be deferred to Chapter 4. At this juncture, only a brief description of the suggested approach is presented:

1) The Rated Torque T of the C-Type 2-Stage SCGT will be treated as the primary performance parameter of interest. The recommended approach is to first design the 2nd Stage gear train to meet a given torque requirement along with any geometric constraints. The design procedure to obtain a single design for the 2nd Stage is the same as that for the 1-Stage SCGT. The design process which, through the use of visual design maps, enables a designer to design a 1-Stage SCGT given certain performance/geometric goals is discussed in Chapter 4.
2) The 1st stage of the C-Type 2-Stage SCGT is a reverted gear train whose output acts as input to the 2nd stage. With the 2nd Stage design complete, the suggested approach is to then design the 1st stage such that it meets the input torque requirements for the 2nd stage. The design procedure for the reverted 1st stage varies only slightly from the design procedure for the 1-Stage SCGT and is presented in the next section. The 1st Stage gear train also has a significant impact on lowering the inertia of the C-Type 2-Stage SCGT. This aspect, as well as the process by which an appropriate 1st Stage gear train can be designed for a given 2nd Stage gear train, is deferred to Chapter 4.

The design procedure for a Reverted Star Compound Gear Train (R-SCGT), which forms the 1st stage of the C-Type 2-Stage SCGT, is now presented.

2.6.1 Design Procedure for a Reverted Star Compound Gear Train

Figure 2-38 shows a representative R-SCGT. As it is the same as a 1-Stage SCGT except for the output being an external gear instead of an internal ring gear, the terminology laid out in Table 2-19 is also valid here. The only modifications necessary are shown below:

N_R is replaced by N_O – Number of teeth on the Output Gear

D_R is replaced by D_O – Pitch Diameter of the Output Gear

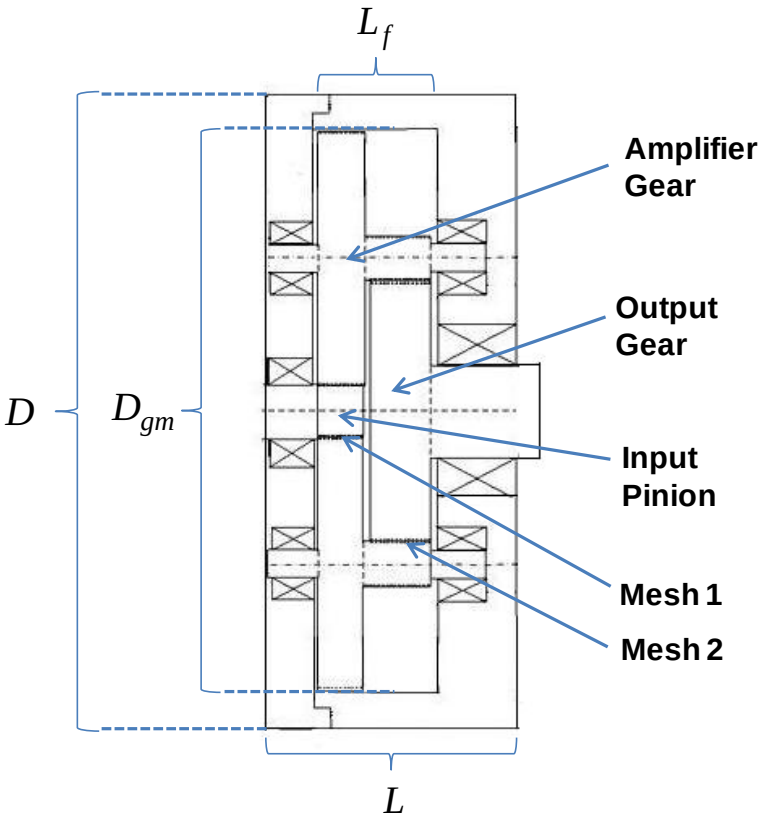

Figure 2-38: Reverted Star Compound Gear Train (R-SCGT)

Equations 2.21-2.47 from Section 2.4.1, with the exceptions of Equation 2.27 and Equation 2.28, may also be used for the R-SCGT. Equation 2.27 and Equation 2.28 are modified as follows:

$$D_P + D_{LS} = D_{SS} + D_O \tag{2.92}$$

Re-arranging the equation above and expressing it in terms of number of teeth and diametral pitches, we get

$$P_{d2} = \frac{N_O + N_{SS}}{D_P + D_{LS}} \tag{2.93}$$

With Equations 2.27-2.28 replaced by Equations 2.80-2.81, the R-SCGT design procedure is exactly the same as the 1-Stage SCGT design procedure.

2.7 Additional Information on the Design Process Flowcharts

The flowcharts summarizing the design procedures for the 1-Stage SCGT (Figures 2.20-2.21) and the P-Type 2-Stage SCGT (Figures 2.27-2.29) included steps labeled A-E. This section will elaborate upon those steps in order to provide an understanding of some of the intricacies.

2.7.1 Step 'A'

The first step in the design procedure is to provide the Input Design Parameters D_g and g. As explained earlier, a Design Solution Set is found for each set of input parameters. If only a single design from the Design Solution Set is chosen, there exists a one-to-one relationship between the input set and the output. In other words, one set of input design parameters lead to a set of performance parameters. For instance, suppose that the Torque Capacity T is the performance parameter of interest. Then, for a set of inputs D_g and g, there exists a corresponding T. If each is plotted on a different axis, a single point in space is obtained. Thus, by repeatedly running through the design

procedure with varying input sets, a set of points may be obtained. A surface fit to this set of point's results in the creation of a design or performance map. A more detailed set of instructions for the creation of design and performance maps is provided in Chapter 3.

2.7.2 Step 'B'

The second step in the design procedure requires a search for all sets of tooth numbers that result in the desired gear ratio. As mentioned earlier, there exist minimum numbers of teeth that may be used on a gear in order to avoid interference. The minimum number of teeth varies based on the pressure and helix angles (See Table 2-5). In the current research, the minimum number of teeth for gears with a 25^o pressure angle is either 12 or 14 depending on the helix angle. For gears with a 20^o pressure angle, the minimum number is 14, 17 or 21 depending on the helix angle. Although theoretically there is no maximum number of teeth that may be used on a gear, the maximum number must be practical. Tables for AGMA Geometry Factors list a maximum of 135 and this number will be used for the 1-Stage SCGT and the C-Type 2-Stage SCGT. For the P-Type 2-Stage SCGT, up to 160 teeth will be used. In summary, the values that will be used for the current research are:

Min. No. of Teeth	12,14,17 or 21 (depending on Pressure and Helix Angles)
Max No. of Teeth	135,160

Suppose a minimum of 14 and a maximum of 135 teeth may be used. For a 1-stage SCGT, which consists of 4 different gears, the total number of teeth number combinations is 121^4. For a 2-Stage SCGT, the total number of teeth number combinations is 121^6. These numbers may help the reader to appreciate the enormity of the design task. However, the current research will provide design insight that will help a

designer reduce the size of the search space considerably. This will be discussed in Chapter 3.

2.7.3 Step 'C'

The third step in the design procedure is the calculation of the diametral pitch of a particular mesh of gears. As Table 2-2 showed, there exist common diametral pitches for which gear manufacturers usually have cutting tools in stock. However, diametral pitch is simply an indication of tooth size and so uncommon or non-standard diametral pitches may be specified if necessary for a particular application. Therefore, no effort will be made in the current research to ensure that the diametral pitches are of a standard value. However, in Section 2.7.5, a method by which the designer can specify only standard diametral pitches is described.

2.7.4 Step 'D'

The face-width of the gears is calculated in Step D. Maximum recommended values for F_{rule} were provided in Section 2.2.13. However, a designer may use a higher value of F_{rule} based on his or her preferences.

2.7.5 Step 'E'

In addition to the five performance parameters calculated in this step, several other useful secondary criteria may also be calculated at this stage. Some of these secondary criteria may be used to discard some designs from the Design Solution Set before the next step; i.e., where the 'best' design is picked.

The most important of these secondary criteria is the length of the gear train L (see Chapter 3). Often times, it is not a fixed aspect ratio that a designer wants; instead, it is a particular length. For instance, the designer may have a constraint on the maximum length of the gear train. Solutions from the Design Solution Set which have a length

greater than the allowed maximum should then be discarded, and only then should the best design be picked. If a designer wishes to compare actuators of varying diameters, it may be helpful to keep the aspect ratio constant. In this case, design configurations on the Design Solution Set that are not equal to the desired aspect ratio may be discarded. One last example is that the Design Solution Set may be 'filtered' based on diametral pitch values. Only solutions with standard diametral pitches can be retained while the others are discarded.

A list of useful secondary criteria based on which the Design Solution Set may be filtered is shown below:

- Length of the gear train
- Standard Diametral Pitches
- Aspect Ratio
- Contact Ratios in the gear meshes
- Constraint on minimum pitch diameters allowable

Chapter 4 includes some sample SCGT design problems. The secondary criteria mentioned above will be used to filter designs in some of the design problems presented in Chapter 4.

2.8 CHAPTER SUMMARY

This chapter introduced the reader to some fundamental terminology related to gear design. A discussion on the stress equations used by the AGMA to design gear teeth against failure was presented. Design procedures that made use of the AGMA stress equations were then developed for three types of SCGT's; namely, 1-Stage SCGT's, Pancake-Type 2-Stage SCGT's and Coffee-Can-Type 2-Stage SCGT's. Each of the design procedures allowed *design decisions* to be made, allowing one to obtain a Design

Solution Set for a given set of inputs. Some preliminary understanding of how the design procedure facilitates the creation of visual design and performance maps was provided.

Chapter 3 will discuss the creation of visual design maps. Design maps for 1-stage SCGT's will be discussed in detail for a complete understanding of the fundamental characteristics of SCGT's.

Chapter 3 : Visual Design and Performance Maps

Design procedures for three main types of SCGT's; namely, One-Stage SCGT's, Pancake-Type Two-Stage SCGT's, and a Coffee-Can Type Two-Stage SCGT's were presented in Chapter 2. The design procedures facilitate the creation of visual design and performance maps which, as will be shown in the present chapter, serve as useful tools in the development of an overall design process for the SCGT's dealt with in the current research. The visual maps are basically 3-D plots of design and performance data, with the parameters on the axes chosen by the designer (Vaculik and Tesar 2008). The present research identifies sets of design maps that are critical to the design process.

3.1 Creation of Design Maps

Figure 3-1 outlines the procedure for the creation of the visual design/performance maps discussed above. As mentioned in Section 2.7.1, there exists a one-to-one relationship between a set of design decisions D_{gm} and g and a set of corresponding performance parameters *if* only one solution from the Design Solution Set is picked. For instance, Table 3-1 shows a representative set of design and performance parameter data. Corresponding to each set of input design parameters D_{gm} and g, there is a set of performance parameters that correspond to the *best design* from the Design Solution Set. As mentioned in Chapter 2, the design solution which achieves the highest Rated Torque for a given set of inputs will be deemed the "best" solution in the current research. A three-dimensional plot of the Rated Torque Capacity T (z-axis) as a function of the mesh diameter D_{gm} and gear ratio g (x- and y- axis respectively) is shown in Figure 3-2. When a surface is fit to the points shown in Figure 3-2, a design map such as that shown in Figure 3-3 is obtained. As stated in Chapter 1, design maps are a key feature of a future visual decision-making tool for actuator design.

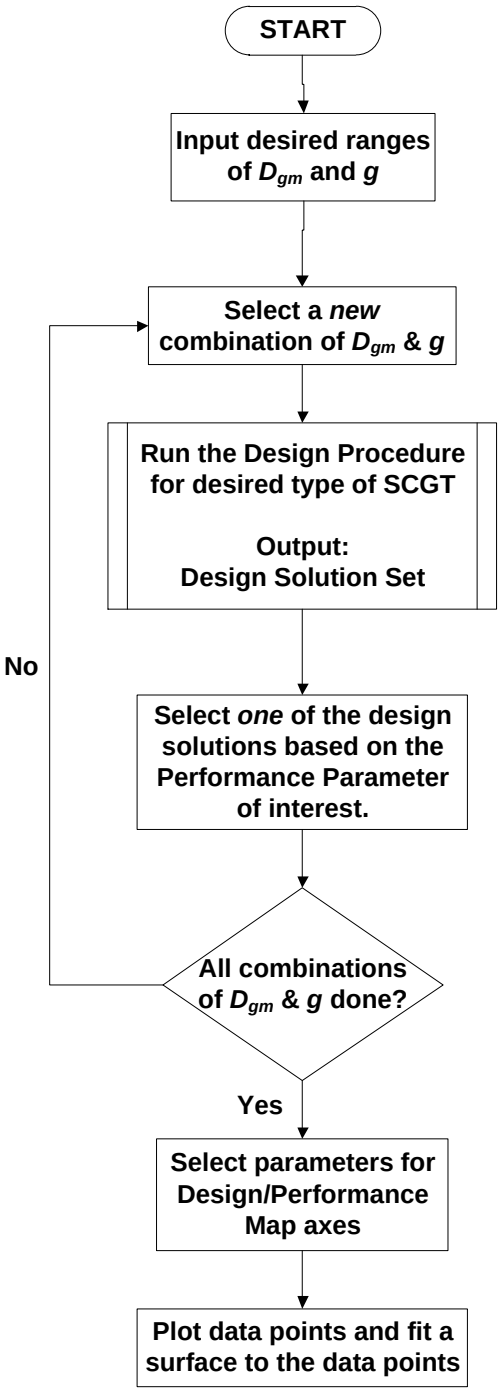

Figure 3-1: Flowchart for the creation of visual design/performance maps

Table 3-1: Representative Design/Performance Data Set

Design Parameters		Performance Parameters					
Diameter	Gear Ratio	Torque	Weight	Inertia	Torque Density	Reponsiveness	Aspect Ratio
D_{gm}	g	T	W	I	T_d	R	AR
12	32	2555.5	100.5	4.17E-01	25.4	6128.2	0.2
12	28	3387.0	115.1	6.20E-01	29.4	5461.1	0.2
12	24	4266.3	138.1	9.80E-01	30.9	4355.1	0.3
12	20	5126.3	160.8	1.41E+00	31.9	3642.7	0.3
12	16	6333.0	184.3	1.79E+00	34.4	3538.9	0.3
12	12	8280.2	224.3	2.49E+00	36.9	3329.2	0.4
10	32	1486.7	58.2	1.69E-01	25.6	8804.7	0.2
10	28	1972.3	66.6	2.51E-01	29.6	7848.9	0.2
10	24	2485.7	80.0	3.97E-01	31.1	6265.5	0.3
10	20	2988.3	93.1	5.69E-01	32.1	5249.4	0.3
10	16	3691.6	111.3	7.40E-01	33.2	4989.0	0.4
10	12	4822.0	129.6	1.01E+00	37.2	4785.7	0.4
8	32	764.6	29.8	5.59E-02	25.7	13672.0	0.2
8	28	1016.2	34.1	8.33E-02	29.8	12199.4	0.2
8	24	1281.4	41.0	1.32E-01	31.3	9743.0	0.3
8	20	1541.3	47.7	1.89E-01	32.3	8157.5	0.3
8	16	1905.5	57.0	2.46E-01	33.4	7748.0	0.4
8	12	2484.7	66.2	3.35E-01	37.5	7424.3	0.4

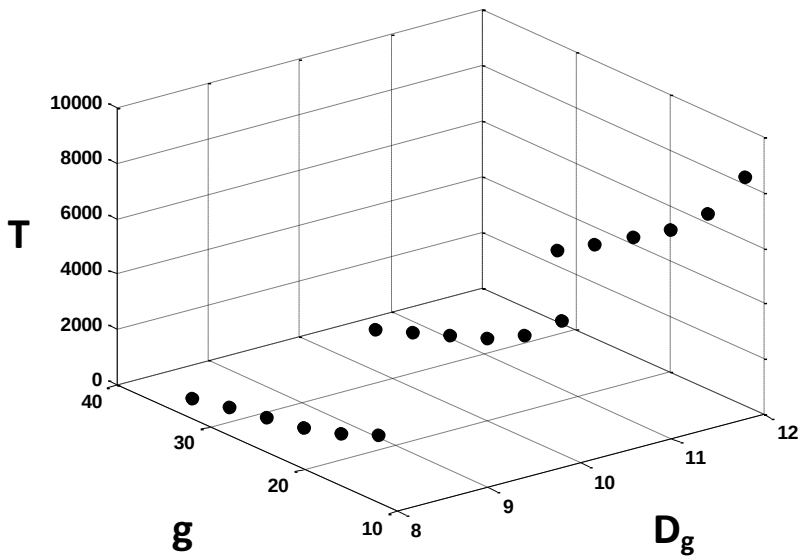

Figure 3-2: 3-D Plot of Representative Design/Performance Data

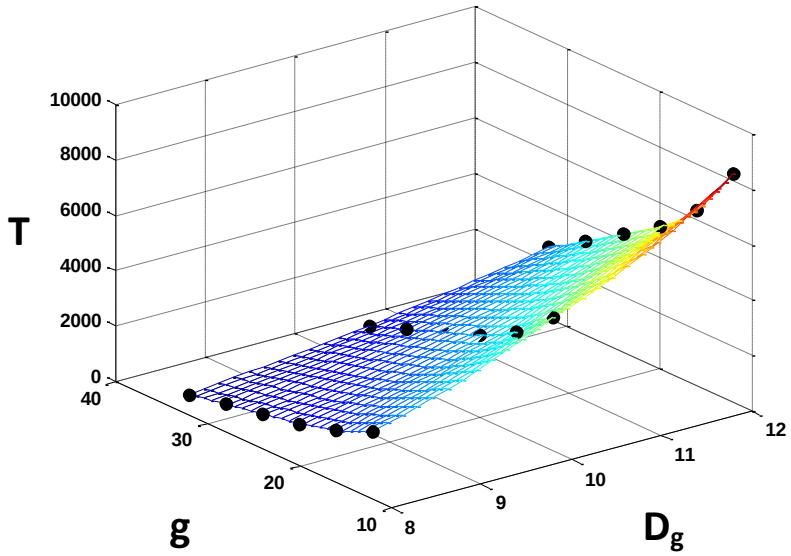

Figure 3-3: Representative Design Map

3.2 DESIGN KNOBS

It is stressed at this point that a design map is associated with a set of "a priori" decisions (see Section 2.3) as well as ranges of two design decisions; usually the two design decisions are D_{gm} and g. When the a priori decisions or design decisions are changed, a new design map is obtained. Some a priori decisions might become fixed based on design requirements. For instance, if a designer seeks to build an actuator with a certain output speed (rpm) and a certain life requirement (no. of mesh cycles), then two of the a priori decisions are fixed. Then, the designer is free to modify other decision parameters in order to obtain a satisfactory design. Those design decision parameters, which a designer has the freedom to modify/choose, are termed *design knobs*. The purpose of this research is to guide the designer in choosing values for these design knobs such that a desirable solution is obtained.

The design knobs may be divided into different categories based on their effect on the design solution. The design knobs that will be important in the present research, as well as the categories they fall under, are shown below:

- Geometric:
    1. Ratio of face-width to pinion pitch diameter F_{rule}
    2. Gear Mesh Diameter D_{gm}
- Tooth System:
    1) Pressure Angle φ
    2) Helix Angle ψ
- Functional:
    1) Gear Ratio g
- Material
    1) Allowable Stresses (S_t and S_c)

The gear mesh diameter D_{gm}, and the gear ratio g, will very often be mentioned as a pair. Therefore, for convenience, these two parameters will be referred to as the 'primary design knobs' for the rest of the report.

In summary, a set of 'a priori' and 'design knob' values have a unique design map associated with them. By 'tuning' one or more of the design knobs; i.e., changing their values, updated design maps corresponding to the new values of the design knobs are generated. The following sections will provide a designer with a list of useful design maps as well as a full description of how the design maps are affected by the design knobs. Whenever possible, some guidelines on how the design maps should be interpreted by the designer will also be provided.

3.2.1 Design Knob values for Preliminary Set of Design Maps

For the initial design maps, it is suggested that the design knobs be set as follows:

- Gear Mesh Diameter D_{gm}: A range of diameters of interest must be chosen by the designer. The range may be dictated by relevant geometric constraints. For instance, if an application requires that the gear train diameter be smaller than 10", the designer may choose a range of say, 6" to 10" for the first design map. If no restrictions on the diameter are made, then the designer may choose a wide range of diameters over which to plot the rated torque. Note that the 'granularity' of the range may also be chosen by the designer. For instance, he/she may choose to plot the rated torques over 5 diameter values; i.e., 4",6",8",10" and 12" or he/she may choose to plot rated torques over 9 diameter values; i.e., 4", 5", 6", 7", 8", 9", 10", 11" and 12". It is suggested that a 'coarse' granularity be used for the initial few design maps, and a 'finer' granularity be used as a designer narrows down to a final design solution.
- Gear Ratio g: The designer may choose a range of gear ratio's of interest. Different gear ratio choices will significantly affect the size of the motor for a particular application (Vaculik and Tesar, 2008)Therefore, by specifying a range of gear ratio's instead of a fixed gear ratio, a designer can get an idea of what gear ratio choices are available. For the initial design maps, the range of gear ratios in this report will be 8, 12, 16, 20, 24, 28 and 32. As with the diameter range discussed above, the granularity of the gear ratio range may also be made finer as the designer narrows down on a desired design solution.
- $F_{rule}{}'s$: As discussed in Chapter 2, these design knobs control the allowable face-width relative to the key value of the pinion pitch diameter. It is recommended that the F_{rule}'s for all of the gear meshes be set to their maximum value, i.e. 1 for

the first design map. The reader may recognize this as a "best first" strategy. A best first strategy implies that the design knobs are initially set to values that yield the *best proven* performance. Unless stated otherwise, this report will consider the best solution to be the one that achieves the highest rated torque.

- Pressure Angles φ : For maximum torque density, it is recommended that pressure angles of 25^o be used. The designer may use a value of 20^o if the design goals are not very aggressive. Gears with 20^o pressure angles are widely used in industry and may be more easily available than gears with 25^o pressure angles. In keeping with the best first strategy, the pressure angles will be set to 25^o initially.
- Helix Angles ψ : It is suggested that a designer set the design knobs for the helix angles in each gear mesh equal to zero; i.e., the designer is looking at a design map for spur gears. If a higher level of performance is required, the designer may then specify non-zero helix angles; i.e., helical gears, where required. This idea will become clear upon further reading. The reader may note that, with regard to the helix angles, the best first approach is not our recommended starting point in this case.
- Allowable Stresses (s_t and s_c): In keeping with the idea of the best first approach, it is suggested that the designer begin with 'AGMA Grade 2 material'. The corresponding allowable stresses are 70 ksi and 225 ksi for bending (s_t) and pitting (s_c) respectively. Note that the reason AGMA Grade 3 materials ($s_t = 75ksi$, $s_c = 275ksi$) are not suggested here is because Grade 3 Steel is usually reserved for aerospace applications or other demanding applications.

A summary of the fixed a priori parameters and initial design knob values is shown in Table 3-2. As per their definitions, the a priori parameters will be kept constant throughout the following development, whereas the design knobs will change.

Table 3-2: Summary of A Priori and Initial Design Knob Parameters

A Priori Parameters		
K_o	Overload Factor	1
K_v	Dynamic Factor	Calculated analytically
K_s	Size Factor	1
K_m	Load Distribution Factor	Calculated analytically
K_B	Rim Thickness Factor	1
C_f	Surface Condition Factor	1
K_T	Temperature Factor	1
K_R	Reliability Factor	1
S_F and S_H	Safety Factors	1.3
Y_N and Z_N	Stress Cycles Factors	Calculated corresponding to 10^7 mesh cycles at the output gear
J and I	Geometry Factors	Calculated analytically
C_P	Elastic Co-efficient	2300 (Both pinion and gear made of Steel)
C_H	Hardness Ratio Factor	1 (Pinion and gear equally strong)
Q_v	AGMA Accuracy Number	11
Design Knobs		
D_{gm}	Diameter	4” to 12” in increments of 1”
g	Gear Ratio	8 to 32 in increments of 4
F_{rule1}, F_{rule2}	Rule for max. face-width	1,1
φ_1, φ_2	Pressure Angles	25^o,25^o
ψ_1, ψ_2	Helix Angles	0^o,0^o
s_t	Allowable Bending Stress	70,000 psi
s_c	Allowable Pitting Stress	225,000 psi

3.3 FUNDAMENTAL DESIGN CHARACTERISTICS OF A 1-STAGE SCGT

In order for the reader to be able to interpret and utilize the design maps effectively, it is necessary to have a fundamental understanding of the design characteristics of the 1-Stage SCGT and the design procedure used. The following text aims at providing the reader with that knowledge. An explanation of how the proposed design procedures facilitate the optimum selection of a set of gear design parameters (number of teeth, face-widths and diametral pitches/modules) for a given diameter and gear ratio is elaborated upon. The gear design parameters are selected such that assembly feasibility is maintained i.e., center distances are equal where required and interference between two or more compound gears is avoided. The following text will also illustrate how the designer can control the choice of the gear design parameters mentioned above through constraint application.

A key idea in the developed design procedure is the coupling between the external geometry (the Gear Mesh Diameter D_{gm}) with the internal gear design parameters (the tooth numbers and diametral pitches). Equations 2.22 and 2.28, and Figure 2-17 in Chapter 2 illustrate this coupling. The geometric constraint of the Gear Mesh Diameter is thus transformed into constraints on the numbers of teeth and diametral pitches (Li, Symmons, and Cockerham 1996) and consequently, the pitch diameters of the gears. This report will not place any constraints on the diametral pitches initially. For a designer who seeks only standard or integer values for diametral pitches, a method by which this constraint can be incorporated (based on the discussion in Section 2.7.5). Thus, it can be said that, given a certain Gear Mesh Diameter (external geometry), the gear pitch diameters and diametral pitches are driven by the choice of numbers of teeth on the four gears of a 1-Stage SCGT. The feasible combinations of numbers of teeth are limited by the constraint of the gear ratio requirement. With regard to the face-width, fixing the

face-width to pinion pitch diameter ratio i.e., F_{rule} is a common approach in gear design [Symmons and Cockerham][Chong] and is used in this report. Using the design knob values specified by the designer, the torque capacity of all of the geometrically feasible combinations of numbers of gear teeth can be evaluated, and the one with the highest Rated Torque capacity picked. Note that, as a last step, the proposed design procedure modifies the face-widths such that neither of the gear meshes is over-designed relative to the other. The ideas mentioned above are illustrated in Figure 3-4.

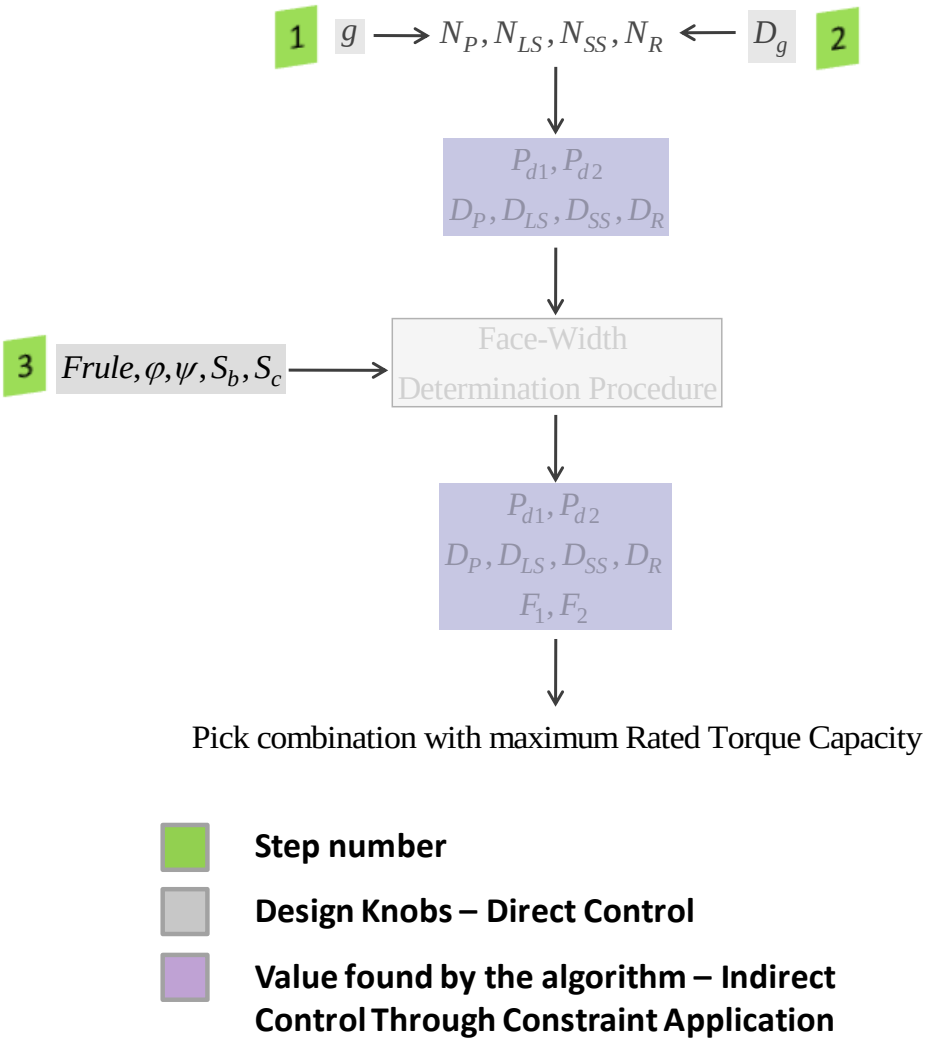

Figure 3-4: Graphical Summary of the Proposed Design Procedure

The reader is advised to compare the graphical summary shown above with the summary shown in Figure 2-15 and note that they are consistent with each other.

An example is presented here for the benefit of the reader's understanding of the proposed design procedure. For a Gear Mesh Diameter of 8" and a required Gear Ratio of 20, 3 sample combinations of numbers of gear teeth that give geometrically feasible combinations of diametral pitches and pitch diameters are shown in the table below.

N_P, N_{LS}, N_{SS}, N_R	g_1, g_2	P_{d1}, P_{d2}	D_P, D_{LS}, D_{SS}, D_R	F_1, F_2
17,93,37,135	5.47,3.64	25.38,22.615	0.67", 3.66",1.64", 5.97"	0.67", 1.64"
31,131,22,104	4.22,4.727	36.63,18.545	0.84",3.57",1.18",5.60"	0.84",1.18"
41,123,18,120	3.00,6.66	35.88,22.32	1.14",3.42",0.80",5.37"	1.14",0.80"

The 3 geometric configurations are also shown in the upper half of (Ring gear is not shown). The face-width determination procedure described in Section 2.4.1.1 is then performed and the final geometric configurations are shown in the lower half of Figure 3-5 is obtained. The reader should note that the *only* difference between the former and latter configurations is the face-widths. As explained in Section 2.4.1.1, the face-widths in the two gear meshes are adjusted such that the stresses (Bending or Pitting) in each of the gear meshes are at their maximum allowed value. The Rated Torque capacities of all three configurations is evaluated and compared against each other. The Rated Torque capacities will depend upon the design knob values specified by the designer. As mentioned earlier, the geometric configuration with the maximum Rated Torque capacity is chosen as the design solution for the given Gear Mesh Diameter and Gear Ratio combination. In addition to the rated torque capacity, the length, weight, torque density and effective inertia at the input and input responsiveness are also calculated and plotted as design maps.

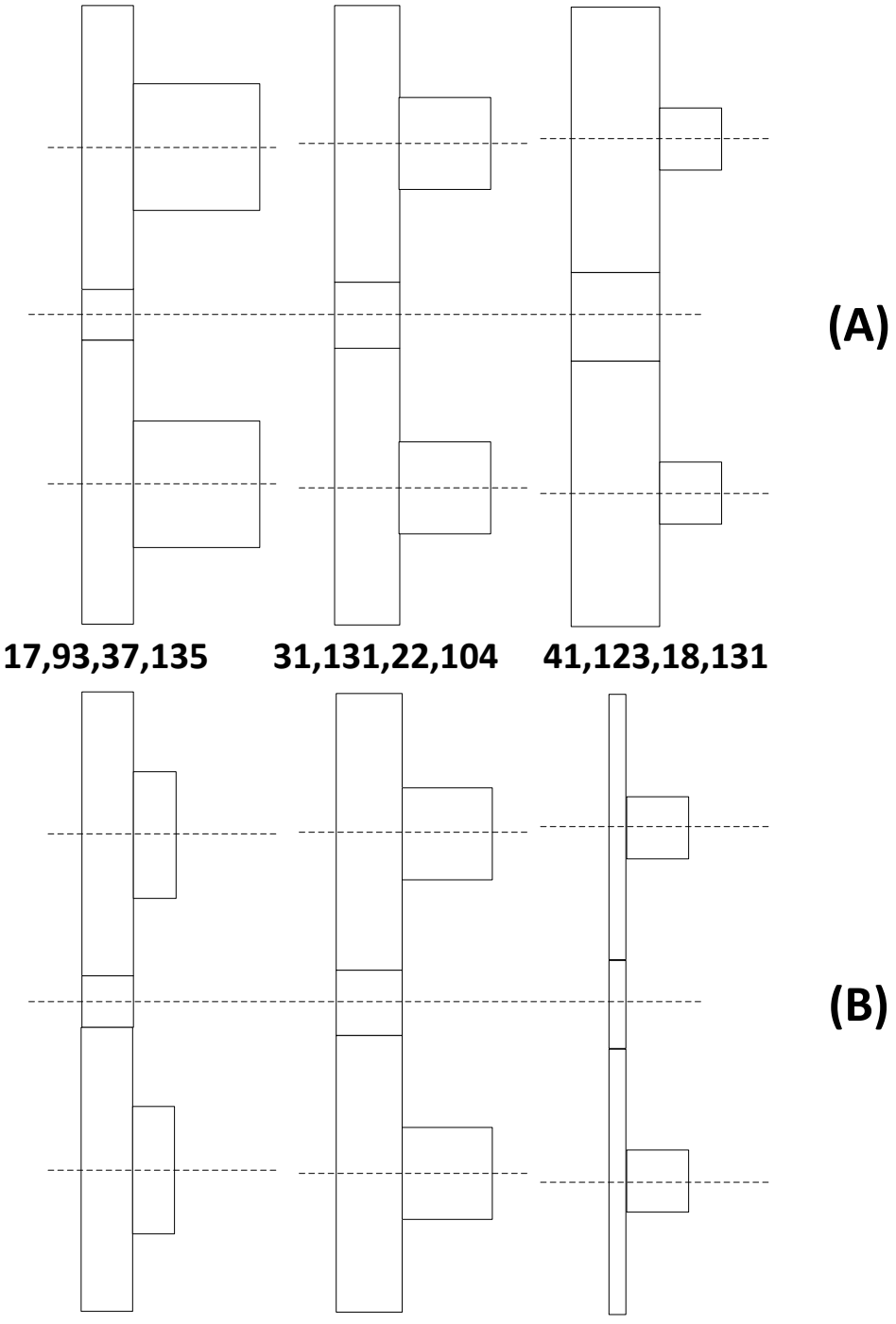

Figure 3-5: Sample Geometric Configurations before (A) and after (B) face-width determination procedure.

Referring to Figure 3-5, it is observed that the configuration obtained from the first combination of numbers of gear teeth (far left) results in Mesh 2 being over-designed relative to Mesh 1. This conclusion is drawn by noting that, for this geometric configuration, the face-width in Mesh 2 is reduced while Mesh 1 is unchanged from (A) to (B). By the same reasoning, it is concluded that the geometric configuration obtained from the third combination of numbers of gear teeth (far right) results in Mesh 1 being over-designed relative to Mesh 2. The geometric configuration obtained from the second combination of numbers of gear teeth (middle) on the other hand, remains almost unchanged before and after the face-width determination procedure; thus indicating that the two gear meshes are nearly balanced in strength. It is observed that, more often than not, such combinations of numbers of teeth offer the maximum rated torque capacity for a given Gear Mesh diameter and gear ratio.

3.3.1 Design Characteristics

It is essential to understand the fundamental characteristics of the star compound gear train layout to be able to understand the design maps presented later in the report. One of the fundamental characteristics is that, for a fixed Gear Mesh Diameter D_{gm}, the size of the Input Pinion decreases as the reduction ratio in Mesh 1 increases. This characteristic is clearly illustrated in Figure 3-6 and represented mathematically in Figure 3-7. As Figure 3-7 shows, the decrease in D_P relative to a fixed D_{gm} is non-linear and satisfies the equation shown in the upper right corner of the plot. The reader may also note that, since the face-width of Mesh 1 is fixed relative to the pitch diameter of the Input Pinion, the width of the 1st mesh of gears decreases proportionally with D_P.

A second noteworthy characteristic is that the center distance between the gears in Mesh 2 is decided by the reduction ratio in Mesh 1. The reader may recognize that this is

because the large star and small star gears are concentric with each other on the compound gear. Figure 3-5 shows how C_2 increases with a decrease in g_1.

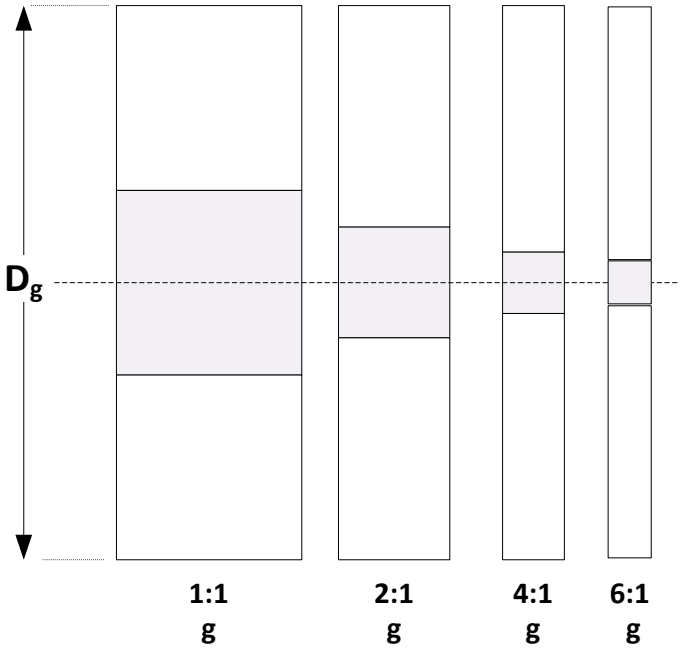

Figure 3-6: Illustration of the decrease in size of Input Pinion with increase in g_1

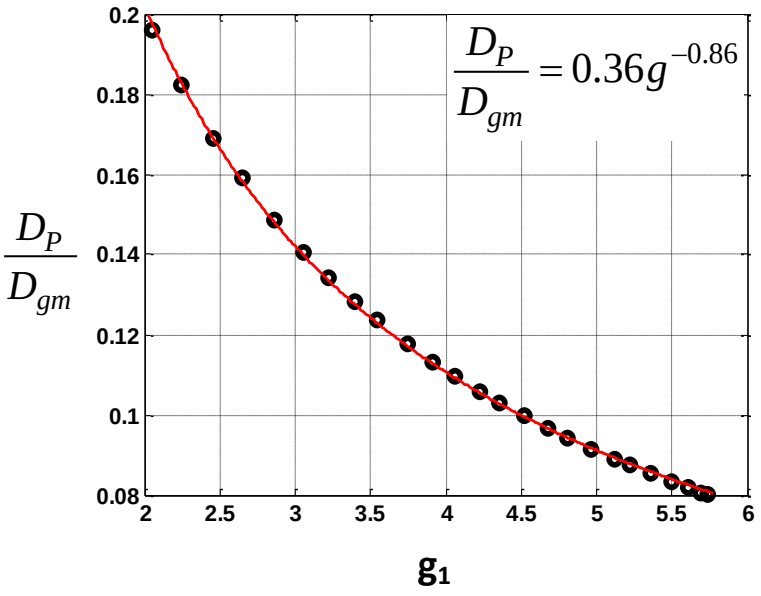

Figure 3-7: Variation of D_P with the reduction ratio in Mesh 1 g_1

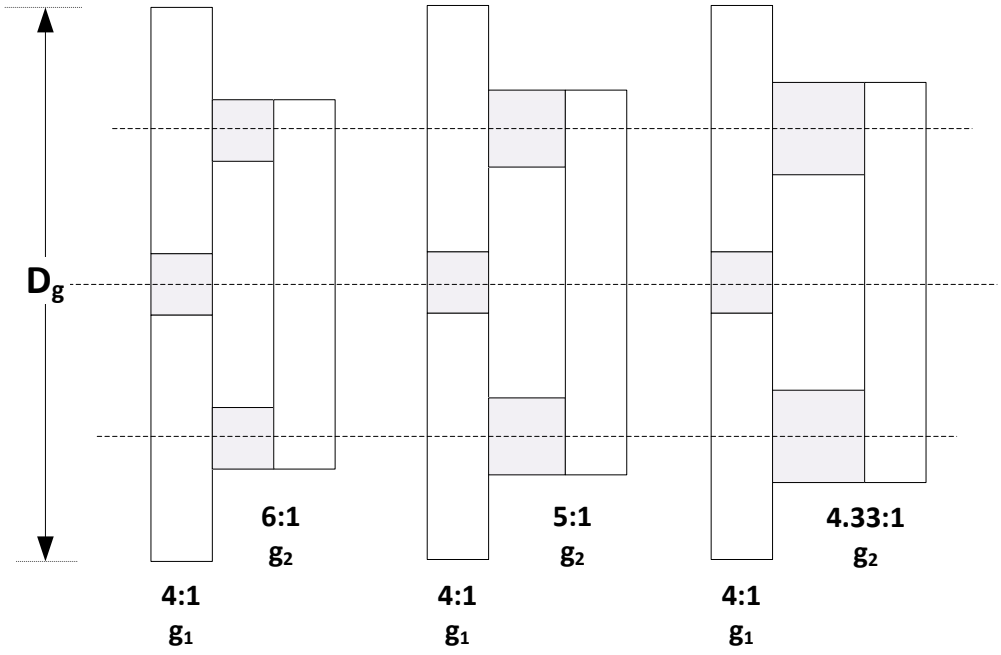

Figure 3-8: Illustration of (a) the decrease in size of Small Star Gear with increase in g_2 and (b) Center Distance C_2 is fixed by g_1

In Figure 3-8, it is observed that the center distance C_2 remains the same because the reduction ratio in Mesh 1 i.e., g_1 remains the same. Also, a third characteristic, similar to the first, is observed; namely, that for a fixed C_2 the pitch diameter D_{SS} (and proportionally, the face-width F_2**)** decrease with an increase in the reduction ratio in Mesh 2 i.e., g_2. This characteristic is shown graphically in Figure 3-8 . Mathematically, it is embodied by the curve shown in Figure 3-9. Again, as with the plot in Figure 3-7, the relationship is non-linear and is given by the equation shown in the upper right corner of the plot in Figure 3-9.

These non-linear relationships between the pitch diameters of the gears with respect to the reduction ratios per mesh result in complex relationships between performance criteria and the overall gear ratio as will be seen upon further reading.

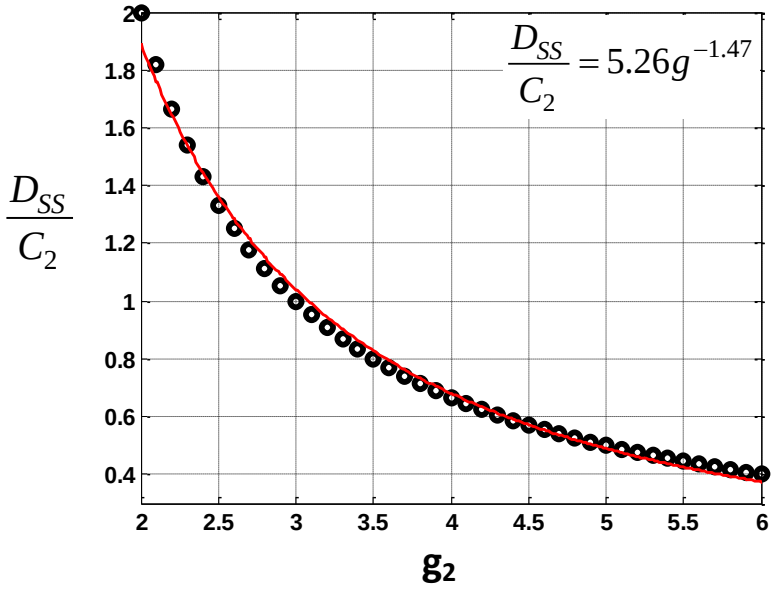

Figure 3-9: Variation of D_{SS} with reduction ratio on Mesh 2 g_2

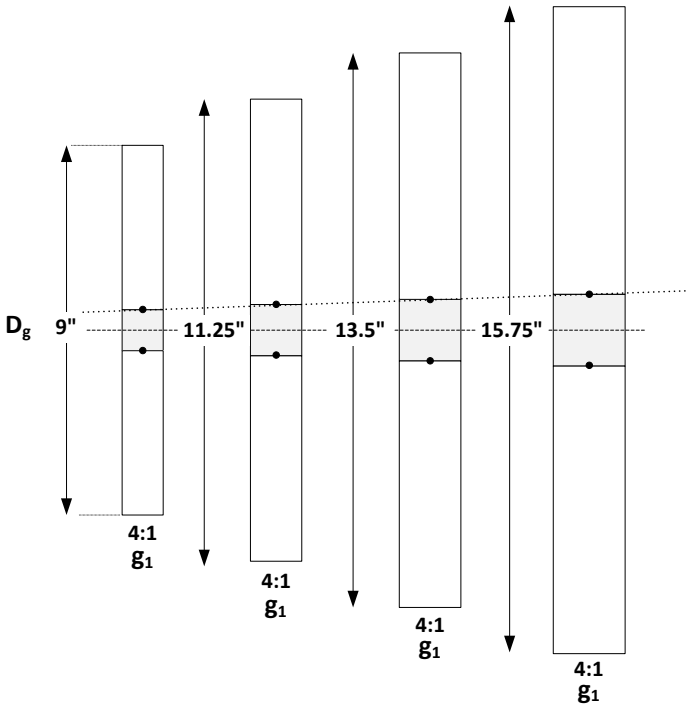

Figure 3-10: Illustration of the linear relationship between Gear Mesh diameter D_{gm} and size of Input Pinion for a fixed gear ratio g

The fourth characteristic that is useful to know is illustrated in Figure 3-10. The reasoning is fairly intuitive and shows that the pitch diameter of the Input Pinion D_P (and face-width F_1) increases linearly with the gear mesh diameter D_{gm}, provided that the gear ratio g is fixed.

Finally, it is important to understand keep in mind that gear tooth size decreases with an increase in number of teeth, for a gear mesh with a fixed center distance and reduction ratio. This characteristic is illustrated in Figure 3-11 which shows 4 gear pairs that achieve the same reduction (2 to 1), but have different numbers of teeth on the pinion and gear. Essentially, it is the diametral pitch that changes with changing number of teeth; as per its definition, the diametral pitch is directly proportional to the number of teeth for a given pitch diameter. In general, finer (higher) diametral pitches result in increased contact ratios and therefore lower contact stresses, whereas, coarse (lower) diametral pitches are favorable for increased bending strength in a gear tooth.

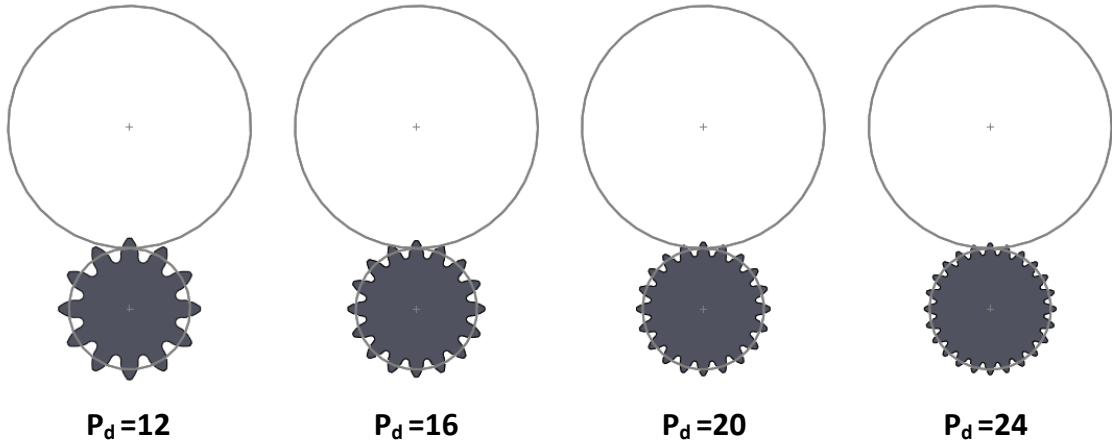

Figure 3-11: Illustration of varying tooth size with varying Diametral Pitches

The 5 characteristics discussed above should convince the reader that it is essential to find the optimum set of teeth numbers for the 4 gears (in a 1-Stage SCGT) that result in the highest rated torque for a given diameter and gear ratio combination.

This is accomplished by sweeping through all *practical* combinations (See Section 2.7.2) of numbers of gear teeth, each of which have gear geometry that satisfies the Gear Mesh diameter and gear ratio constraints, and evaluating the combinations based on performance metrics such as the maximum rated torque capacity. As an example, Table 3-3 shows six sample combinations of gear tooth numbers along with the rated torque they achieve. The data is also represented on a parallel co-ordinates plot (Figure 3-12). Each line type on the parallel co-ordinates plot corresponds to a row in Table 3-3. Each vertical line in the parallel co-ordinates plot corresponds to a design parameter (in this case, tooth number on a gear) with parameter values varying linearly along the vertical line, from the lower and upper limits shown below and above the vertical lines respectively.

Table 3-3: Rated Torque as a function of gear tooth numbers for D_{gm} = 8" and $g = 14$

N_P	N_{LS}	N_{SS}	N_R	T $(ft-lb)$
18	51	24	119	751.4
23	61	25	132	647.4
24	63	22	117	650.3
24	68	17	84	712.1
24	79	23	98	1008.6
25	72	23	112	833.7

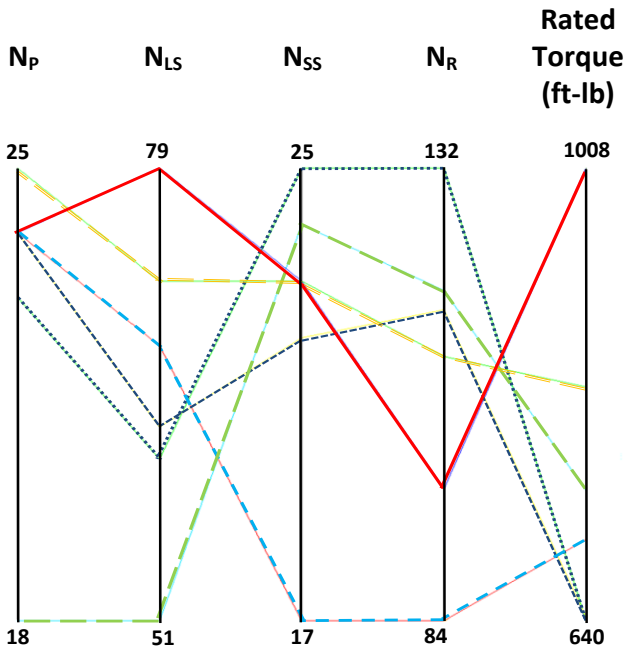

Figure 3-12: Parallel Coordinates Plot corresponding to data in Table 3-3

Design maps that are deemed critical for effective selection of gear train type/geometry are now presented. The physical reasoning behind the shape of each of the design maps is also explained. The reader is encouraged to try and relate the 5 characteristics discussed earlier with the shape of the design maps.

3.3.2 Fundamental Results

Two fundamental results in the design of a 1-Stage SCGT for maximum rated torque capacity are presented first. The first is the relationship between the Amplification Ratio r_A and the primary design knobs i.e., Gear Mesh diameter D_{gm} and gear ratio g. The reader may recall from Section 2.4.1.1 that the Amplification Ratio is defined as the ratio of the pitch diameter of the Large Star gear to the pitch diameter of the Small Star gear. It indicates the degree to which the tangential transmitted load in Mesh 2 (f_2^t) is amplified relative to the tangential transmitted load in Mesh 1 (f_1^t). The design map in Figure 3-13 shows a very important result; namely, that when designing for maximum

rated torque for a given $D_{gm} - g$ combination, the amplification ratio is *independent* of the Gear Mesh diameter.

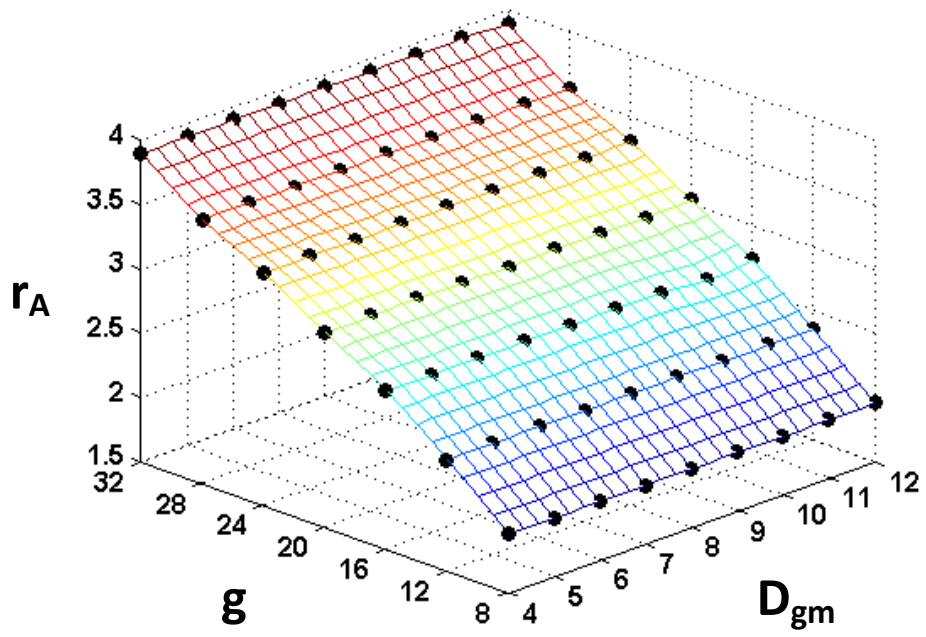

Figure 3-13: Amplification Ratio r_A vs. Primary Design Knobs

Therefore, a 2-D plot of r_A versus g was created (See Figure 3-14). A polynomial of the 'power-law" type; i.e., a standard low-order polynomial type generally used in two-dimensional plots and three dimensional surfaces (Vaculik and Tesar, 2008) was fit to the data points in Figure 3-14. The polynomial equation along with the R^2-error is shown below:

Table 3-4: Power Law - Amplification Ratio vs. Gear Ratio

Power Law	R^2
$r_A = 0.703g^{0.487}$	0.9985

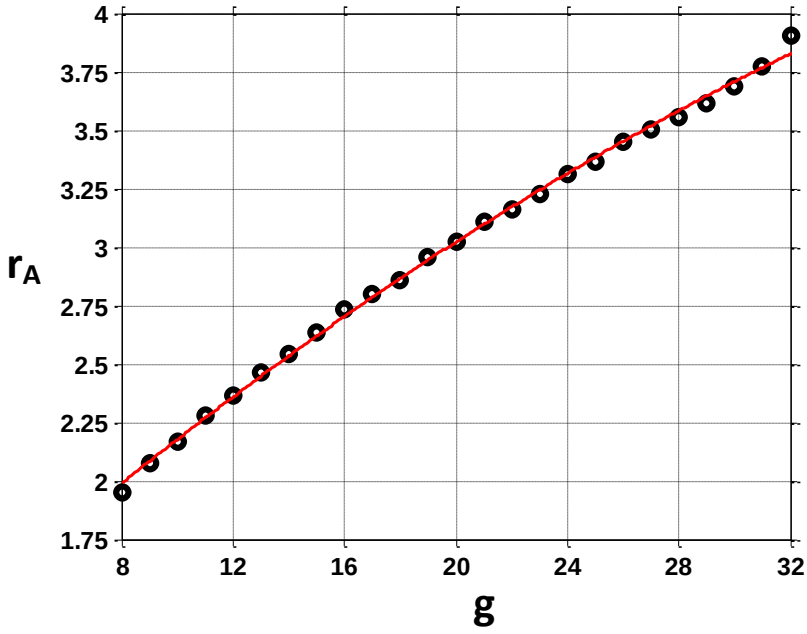

Figure 3-14: Plot of Amplification Ratio r_A vs. Gear Ratio g

Looking at Figure 3-13 and Figure 3-14, it is understood that, when designing for maximum rated torque capacity, the pitch diameter of the Large Star and Small Star gears are fixed relative to each other, depending upon the required gear ratio. For example, suppose that a designer is to design a 1-stage SCGT with a gear ratio of 20 to 1. To achieve the maximum rated torque capacity for any diameter with this gear ratio, the designer may use Figure 3-14 to infer that the pitch diameter of the Large Star gear should be 3 times larger than the pitch diameter of the Small Star gear. The reader may realize that the amplification ratios shown in the plot are those that result in geometric combinations with well balanced stresses in the Mesh 1 and Mesh 2 gears, thereby leading to greater rated torque capacities. In order to understand the significance of the previous statement, it is useful to investigate the variation of the bending and contact stresses with the primary design knobs. Design maps showing four Stress Fraction's (SF), defined as the ratio of the actual stress on a gear tooth to the allowable stress, are shown

in Figure 3-15 and Figure 3-16. The two subscripts after the 'SF' term indicate the type of stress (bending or contact) and the mesh number (1 or 2). For instance, SF_{b2} implies the ratio of the actual bending stress in mesh 2 to the allowable bending stress in Mesh 2.

$$SF_{b2} = \frac{S_{b2actual}}{S_{b2allowable}} \tag{3.1}$$

An important point to note is that the 'actual stress' referred to here is the calculated stress in the gear teeth *before* the face-widths are adjusted at the end of the gear design procedures. This is because, *after* the face-widths are adjusted to avoid either gear mesh being over-designed relative to the other, all the Stress Fraction's will be equal to 1.00, indicating that they are at their maximum allowable values. For the current investigation, we need to check the stresses before the face-widths are adjusted, in order to know which gear mesh is limiting the rated torque capacity, and whether it is the bending or the contact stress that is limiting. From Figure 3-15, the reader can see that in general, the bending stresses in the 2nd gear mesh are very close to their allowable limits; SF_{b2} values are in general close to 1.00. However, values for SF_{b1} decrease steadily as the gear ratio increases, indicating that the bending stresses in Mesh 1 are *not* limiting. From Figure 3-16, it can be said that with regard to the contact stresses, both gear meshes are close to their maximum allowable limits, indicating that the torque capacities in both gear meshes are limited by their contact stresses.

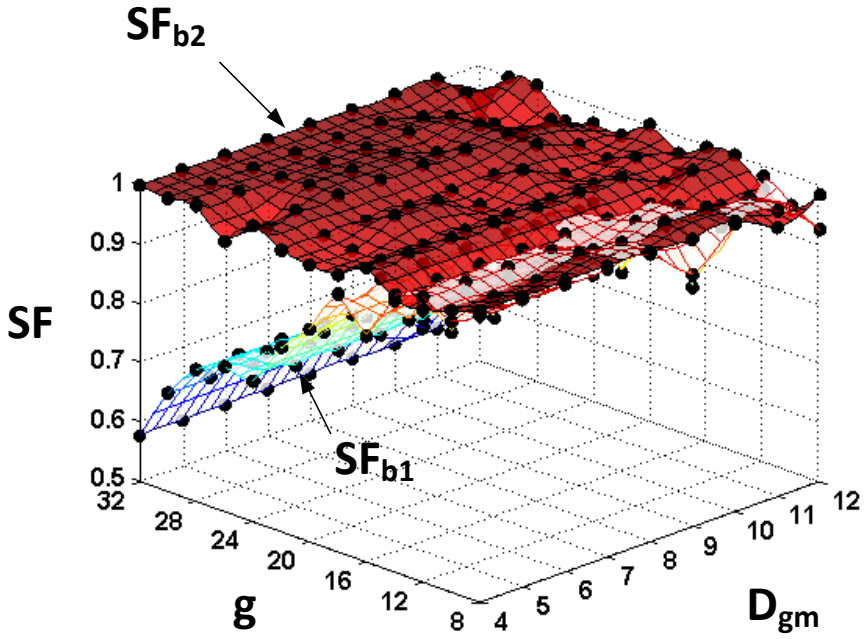

Figure 3-15: Design map - Bending Stress Ratio vs. Primary Design Knobs

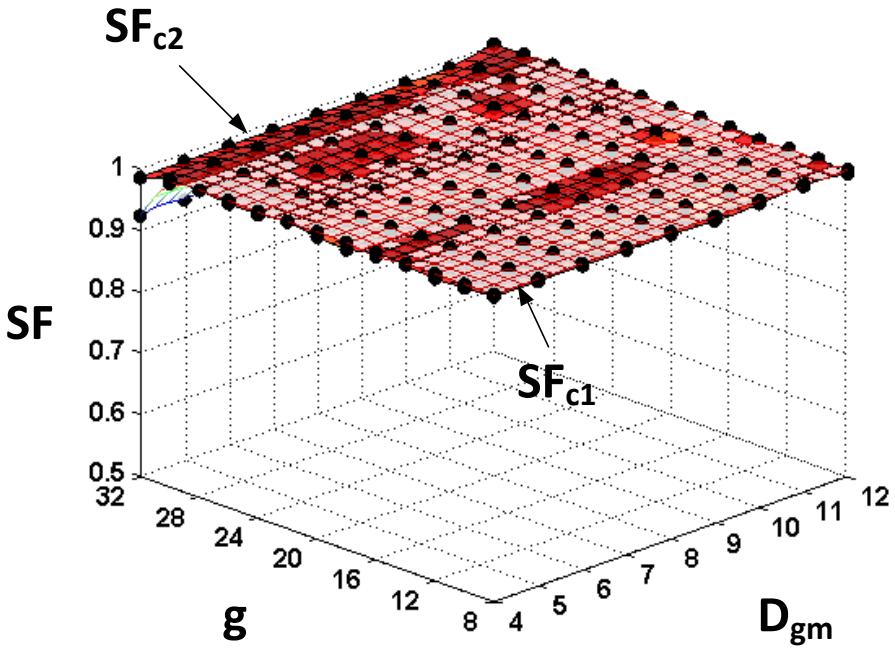

Figure 3-16: Design Map - Contact Stress Fraction vs. Primary Design Knobs

The important detail to note from Figure 3-15 and Figure 3-16 is that the bending stresses in the 2nd mesh (Small Star gear) are close to or at their limits but the bending stresses in the 1st mesh (Input pinion) are not. From the fundamental AGMA stress equations (Equation 2.10 and 2.11), it is clear that the bending stresses in a gear tooth increase linearly with the tangential transmitted load whereas the contact stresses increase with the *square root* of the tangential transmitted load. The reader should recall that the tangential transmitted load in mesh 2 is related to the tangential transmitted load in mesh 1 through the amplification ratio:

$$f_2^t = f_1^t \times r_A \tag{3.2}$$

Figure 3-8 showed that the amplification ratio must increase in order to get a higher gear ratio g. From Equation 3.2 and the discussion preceding it, the reader should be convinced that it is beneficial if the amplification ratio increases with the square root of the gear ratio rather than linearly with the gear ratio. Looking at the power law relating the amplification ratio to the gear ratio (shown above Figure 3-14), it is seen that the exponent for the gear ratio is 0.487; i.e., reasonably close to 0.5. Thus, the fundamental reason for the shape of the plot in Figure 3-14 is that Mesh 2 is limited by the bending stress but Mesh 1 is not.

A corollary of the result for the amplification ratio is the result that the gear reduction taking place in Mesh 1(g_1) relative to that in Mesh 2(g_2) is fixed for a given overall required gear ratio g and is independent of D_{gm}. The design map in Figure 3-17 and the 2-D plot in Figure 3-18 are proof that the previous statement is true.

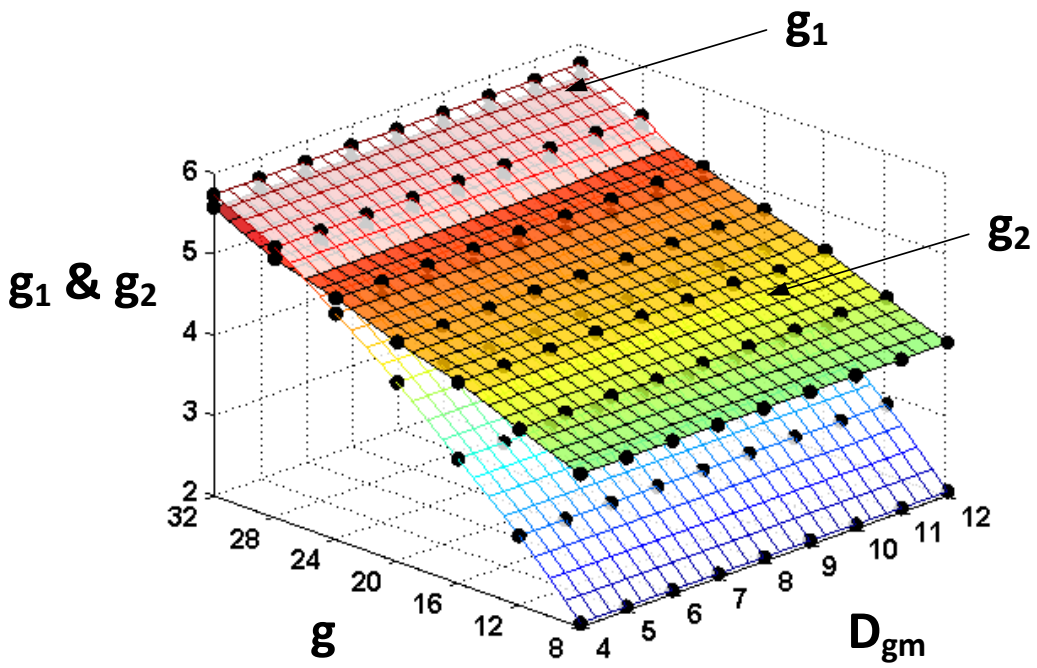

Figure 3-17: Gear Reductions g_1 and g_2 vs. Primary Design Knobs

A designer may look at the plot in Figure 3-18 and infer the best possible combination of Mesh 1 and Mesh 2 reductions i.e., g_1 and g_2 for a given required overall gear ratio g. For example, a designer should see that, in order to get the maximum rated torque capacity for a chosen overall gear ratio of 16 (see Figure 3-18) , he/she must design such that g_1 and g_2 are 3.55 and 4.5 respectively. Again, the choices for g_1 and g_2 shown in Figure 3-18 result in geometric combinations with well balanced stresses in the Mesh 1 and Mesh 2 gears, thereby leading to greater rated torque capacities.

An interesting characteristic to note in Figure 3-18 is that, with an increase in the overall gear ratio, the reduction in Mesh 1 (g_1) approximately increases with the square root of g whereas the reduction in Mesh 2(g_2) is almost linear with respect to g. These observations are made by looking at the exponent of g in the power laws shown in Figure 3-5.These characteristics concur with the fact that the gears in Mesh 1 are limited

only by the contact stress whereas the gears in Mesh 2 are limited by both bending and contact stresses.

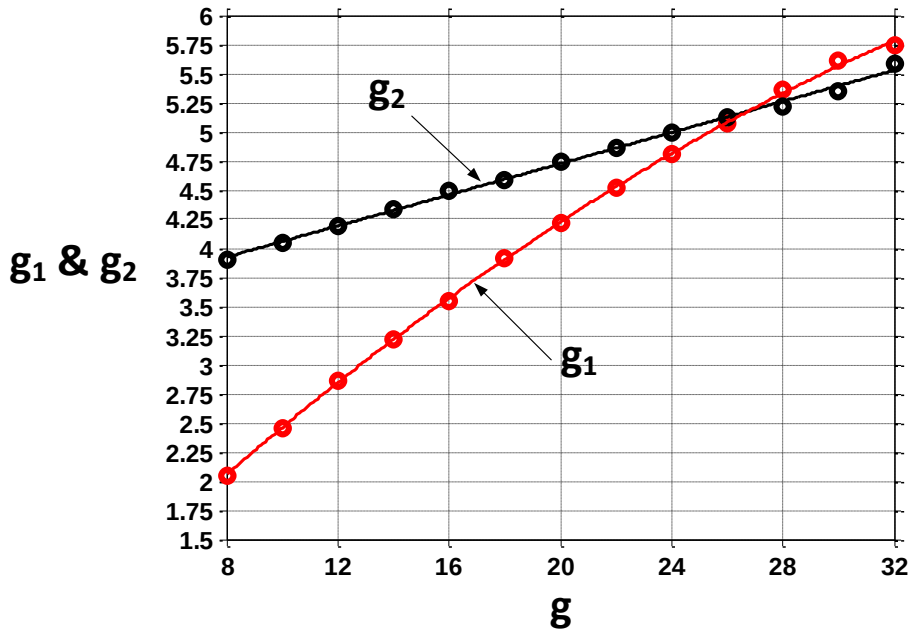

Figure 3-18: Plot of mesh reductions g_1 and g_2 vs. Gear ratio g

Table 3-5: Mesh reductions vs. Gear ratio Power Law ($ax^b + c$)

Parameter	Power Law	R^2
g_1	$g_1 = 1.211g^{0.52} - 1.55$	0.9994
g_2	$g_2 = 0.08g^{0.93} + 3.30$	0.9972

The two fundamental results just discussed, in conjunction with the five fundamental design characteristics discussed in the previous section, make it possible to understand the more advanced design maps shown next. The design maps presented next show the relationship between the performance parameters and the design knobs.

3.4 Design Maps for a 1-Stage Star Compound Gear Train

3.4.1 Rated Torque (T) versus Gear Mesh Diameter (D_{gm}) and Gear Ratio (g)

For a 1-Stage SCGT, the Rated Torque is given by the total tangential transmitted load through the gears in Mesh 2 f_2^t times the pitch diameter of the ring gear D_R. Since there are three Small Star gears in mesh with the internal ring gear, the Rated Torque (ft-lbf) is given by following equation:

$$T = 3 \times f_2^t \times D_R \tag{3.1}$$

Figure 3-19 shows the design map obtained with the design knobs set to the values shown in Table 3-2. Note the ranges of values for the Primary Design Knobs (See Table 3-2)

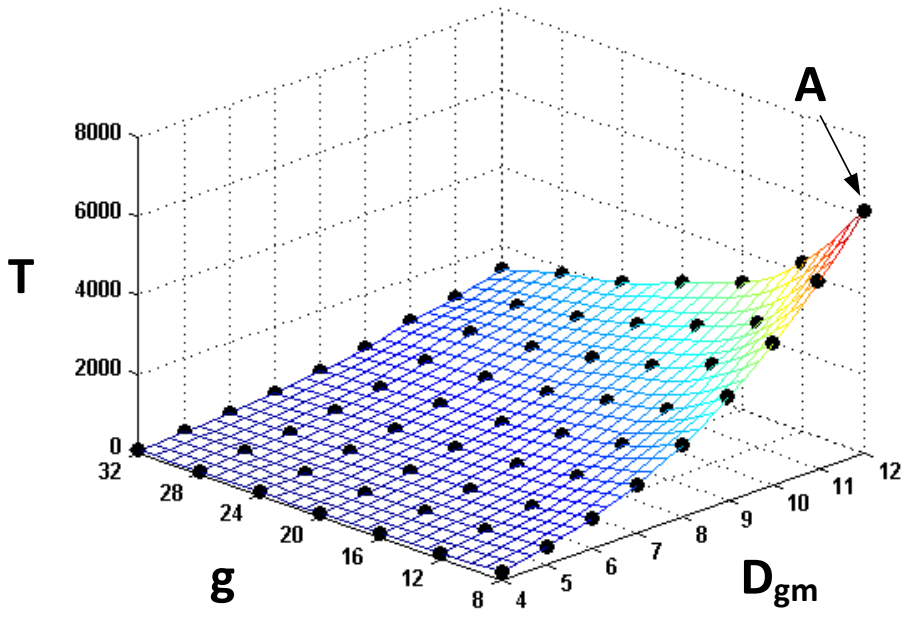

Figure 3-19: Design Map - Torque T vs. Primary Design Knobs

The reader should note that these ranges are not restrictive; i.e., it is possible to design outside these ranges as well. Examples of design maps with different ranges will

be discussed in Chapter 4. These specific ranges are chosen only because they are deemed to be representative of the requirements for most common applications.

Each of the data points in Figure 3-19 represents the Rated Torque corresponding to a particular '$D_{gm} - g$' combination. For instance, the maximum torque of 6149 ft-lbs corresponds to a '12"-8' combination; i.e., a Gear Mesh Diameter D_{gm} of 12" and a gear ratio of 8:1 (point A on plot). Each $D_{gm} - g$ combination has a complete design solution associated with it (See Chapter 2). To illustrate, the design parameters for the solution associated with the '12"-8' combination are listed in Table 3-6.

Table 3-6: Design Solution corresponding to the 12"-8 Diameter-Gear Ratio combination

D_P	Pitch Diameter of the Input Pinion	2.3997	inch
D_{LS}	Pitch Diameter of the Large Star gear	4.7994	inch
D_{SS}	Pitch Diameter of the Small Star gear	2.3997	inch
D_R	Pitch Diameter of the Ring gear	9.5988	inch
N_P	No. of teeth on the Input Pinion	32	
N_{LS}	No. of teeth on the Large Star gears	64	
N_{SS}	No. of teeth on the Small Star gears	32	
N_R	No. of teeth on the Ring gear	128	
F_1	Face width of gears in Mesh 1	2.3997	inch
F_2	Face width of gears in Mesh 2	2.3602	inch
T	Rated Torque Capacity	2844	ft-lbf
L	Length	4.7599	inch
W	Approximate Weight	304	lbf
TD	Torque Density	9.41	ft-lbf/lbf
I	Inertia	0.0348	lbm-in^2
R	Input Responsiveness	82,339	rad/s^2

A reference plane indicating a required Rated Torque may also be added to the design map for enhanced clarity. This is shown in Figure 3-20. A designer should

interpret the design map in Figure 3-20 as follows: Any point lying above the reference plane (shown in translucent grey) refers to a design solution that achieves a rated torque greater than or equal to the required rated torque of 2000 ft-lb.

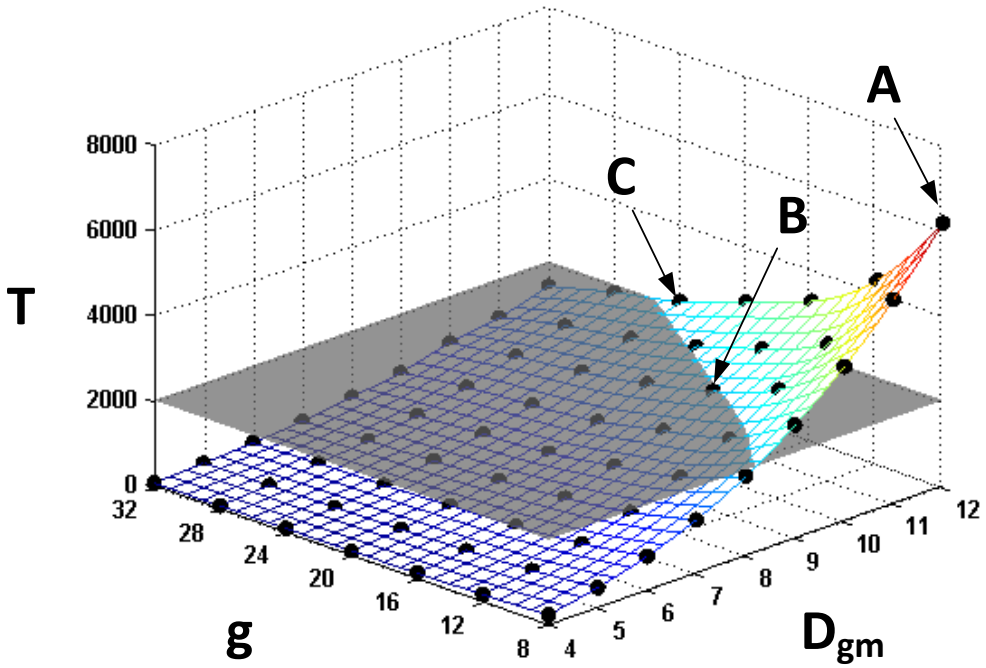

Figure 3-20: Design Map -Torque T (*ft-lbf*) vs. Primary Design Knobs

For instance, Figure 3-20 shows that there are a total of 11 neighboring design solutions that achieve a rated torque greater than or equal to the required rated torque. Any points lying below the translucent reference plane refer to complete design solutions that do not achieve the required rated torque. Using this design map, one can state that, given the current values for the design knobs, if a gear ratio g of 24 is required, then the minimum Gear Mesh Diameter D_{gm} required is 12"(Point C is the only available solution on the design map). This is because, all other points corresponding to a gear ratio of 24 lie below the reference plane. A designer should also note that the point B, corresponding to

a D_{gm}-g combination of 10"-16, appears to lie *just* below the reference plane. As discussed in Chapter 2, an increase in face-width proportionally increases the rated torque capacity. An experienced designer may look at point B and, in order to bring point B above the reference plane, choose to increase the value for F_{rule} slightly; i.e., set F_{rule} to a value slightly greater than 1 even though it is not recommended at first. The nature of design is such that, at times, design solutions just outside the recommended ranges may be useful (Tong and Walton 1987).

3.4.1.1 Physical Reasoning behind the design map

For a given gear ratio g, the 'T - D_{gm}' relationship shown in Figure 3-19 can be explained using Equations 2.40 and 2.41 from Chapter 2, shown below for convenience.

$$f_1^t = \frac{S_{at1} F_1 J_1}{K_{v1} K_{m1} P_{d1}} \tag{3.2}$$

$$f_2^t = f_1^t \times r_A \tag{3.3}$$

The tangential force transmitted through Mesh 2 (f_2^t), is linearly related to the tangential force transmitted through Mesh 1(f_1^t) through the amplification ratio r_A (Equation 3.3). Here, f_1^t is inversely proportional to the diametral pitch P_{d1}. Since the diametral pitch is inversely proportional to the pitch diameter, this implies that f_1^t is proportional to the pitch diameter of the input pinion (D_P). Additionally, since F_{rule} equals' unity for the design map under consideration, the face-width F_1 may also be replaced by D_P. Thus, f_1^t and therefore f_2^t are proportional to the square of the pinion pitch diameter D_P. Since the rated torque T is directly proportional to f_2^t (Equation 3.1) the conclusion is that the rated torque for a given gear ratio g is proportional to the square of the pinion pitch diameter D_P. For a given gear ratio g, D_P increases with an increase in D_{gm} (see Figure 3-10). Finally, the design characteristics discussed in Section

3.3.1 predict that D_R will increase proportionally with D_{gm}. The result is that the Rated Torque T is proportional to the cube of the gear mesh diameter. In order to validate these conclusions, rated torques were plotted against diameter for four different gear ratios; namely, 8:1, 16:1, 24:1 and 32:1 (See Figure 3-21). 'Power laws' fit to the curves in Figure 3-21 are shown in Table 3-7. The cubic relation between the Rated Torque and the gear mesh diameter can be seen from the values of the exponents (b) in the power laws.

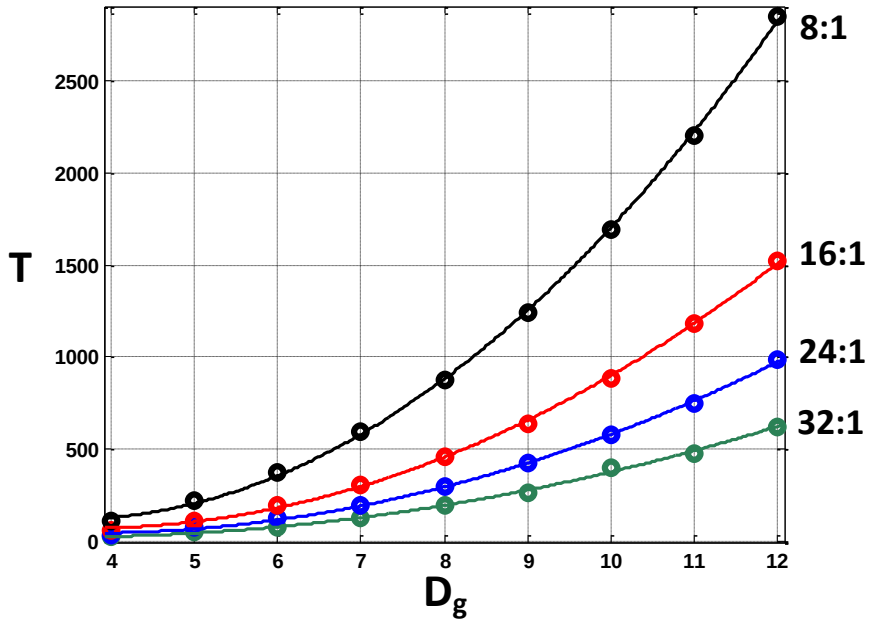

Figure 3-21: Rated Torque (*ft-lbf*) vs. Gear Mesh Diameter for 4 gear ratios

Table 3-7: Power Law - Rated Torque (*ft-lbf*) vs. Gear Mesh Diameter (ax^b)

Gear Mesh Diameter	a	b	R^2
6"	2.1	2.9	0.9986
8"	0.95	2.96	0.9984
10"	0.62	2.96	0.9994
12"	0.49	2.87	0.9993

The reader may note that the 'R^2' values in Table 3-7 are very close to 1, indicating that the quadratic equations listed are a good fit to the data.

The '$T-g$' relationship, for a given diameter D_{gm}, are more complex compared to the $T-D_{gm}$ relationship. The reason for this is that, although the pitch diameters of the pinion gears increase fairly linearly with D_{gm}, their relationship with the gear ratio is non-linear. This non-linearity was evident in the variation of the amplification ratio and the individual mesh reduction ratios (both affect the pitch diameters) with the overall gear ratio (See Section 3.3.2). Therefore, power laws for the relationships between the performance parameters with the gear ratio will be presented without a detailed explanation for the value of the exponent. The decrease in the Rated Torque (indicated by a negative exponent b in Table 3-8) with increasing gear ratio (Figure 3-22) is expected because the size of the pinions in both Mesh 1 and Mesh 2 decrease with increasing gear ratio. Therefore, the transmitted load and consequently, the Rated Torque decrease.

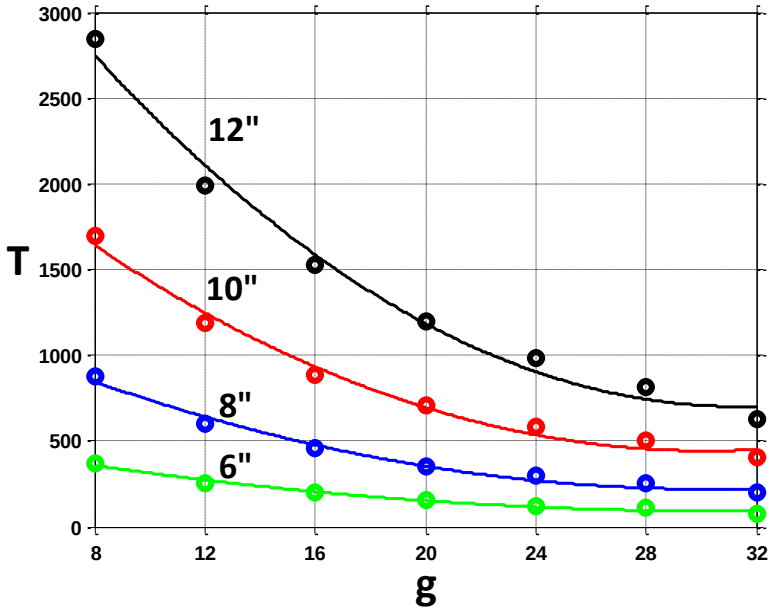

Figure 3-22: Rated Torque (*ft-lbf*) vs. Gear Ratio for 4 Gear Mesh Diameters

The plots in Figure 3-21 and Figure 3-22 should help the reader understand the reasons behind the shape of the design map for Rated Torque vs. Primary Design knobs that was shown in Figure 3-19.

Table 3-8: Power Law - Rated Torque (*ft-lbf*) vs. Gear Ratio (ax^b)

Gear Ratio	a	b	R^2
8	3006	-0.99	0.9938
16	7151	-1.00	0.9968
24	13120	-0.97	0.9973
32	22490	-0.98	0.9937

In Figure 3-6 through Figure 3-10 , the face-width F_1 increased linearly with an increase in diameter D_{gm} for a fixed gear ratio g. This was because the face-width to pinion pitch diameter ratio; i.e., F_{rule1} and F_{rule2} were set equal to unity for the discussion on these initial design maps. However, since the face-width is modified automatically in order to balance the bending and pitting stresses in each of the gear meshes, some method must be provided to keep the designer in control of the choice for the face-widths for each gear mesh. The length of the gear train along its centerline is often an important consideration in the selection/design of a gear train and is primarily dependant on the face-widths of the gears in the first and second gear meshes; i.e., F_1 and F_2. Therefore, the next type of design map discussed is the gear train length L plotted as a function of the primary design knobs.

3.4.2 Gear Train Length (L) versus Gear Mesh Diameter (D_{gm}) and Gear Ratio (g)

As mentioned earlier, each D_{gm}-g combination has a complete design solution associated with it. The design map for the length is obtained by plotting the length of

each of those design solutions against the primary design knobs. Suppose that the length L_f equals the sum of the face-widths of the gears in Mesh 1 and Mesh 2.

$$L_f = F_1 + F_2 \tag{3.4}$$

The actual length of the gear train L would include the widths of the backbone, the bearing cage and the output plate, along with any clearances between components.

$$L = L_f + F_{Backbone} + F_{BearingCage} + F_{OutputPlate} + Clearance \tag{3.5}$$

The ratio of the actual gear train length L to the length L_f typically ranges from 1.5 to 2.0 and depends upon factors such as the magnitude of resultant thrust load on gear shafts, bearing selection and type of mounting at the output. For a preliminary estimate of the actual length, it is recommended that a multiplication factor of 1.75 be used:

$$L = 1.75 \times L_f \tag{3.6}$$

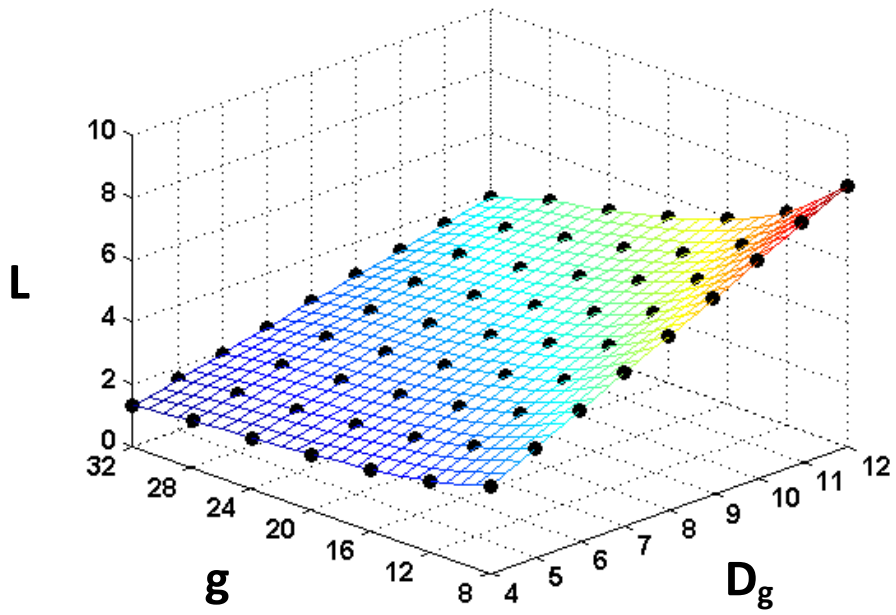

Figure 3-23: Design Map – Length (*in*) vs. Primary Design Knobs

A design map showing the length L as a function of the Primary Design Knobs is shown in Figure 3-23. For the rest of the report, design maps for the estimated actual length L will be shown and used for other performance criteria such as the weight and aspect ratio. However, in order to understand the reason for the shape of the design map in Figure 3-23, the length L_f will be considered.

3.4.2.1 Physical Reasoning behind the design map

The variation of length L_f with the Gear Mesh diameter D_{gm} for four gear ratios is shown in Figure 3-24. It is apparent that L_f varies linearly with D_{gm} given a fixed gear ratio g. This can be explained as follows. From Figure 3-10, it is clear that the Input Pinion pitch diameter D_P increases proportionally with D_{gm}. Since F_{rule} equals one, this means that the maximum allowable face-width for F_1 also increases proportionally with D_{gm}. Next, making use of the two fundamental results discussed in Section 3.3.2, it can

be stated that as D_P increases, D_{SS} (and therefore F_2) increases proportionally. Since L_f is defined as the sum of the face-widths F_1 and F_2, we can conclude that the relationship between L_f and D_{gm} is linear, as shown in Figure 3-24. The linear relationship is confirmed with the observation that the exponent in the power law equations (See Table 3-9) is very close to 1 in all cases.

Table 3-9: Power Law - Length (*in*) vs. Gear Mesh Diameter (ax^b)

Gear Ratio	a	b	R^2
8	0.402	0.997	0.9999
16	0.285	0.994	0.9995
24	0.230	0.999	1.0000
32	0.186	1	1.0000

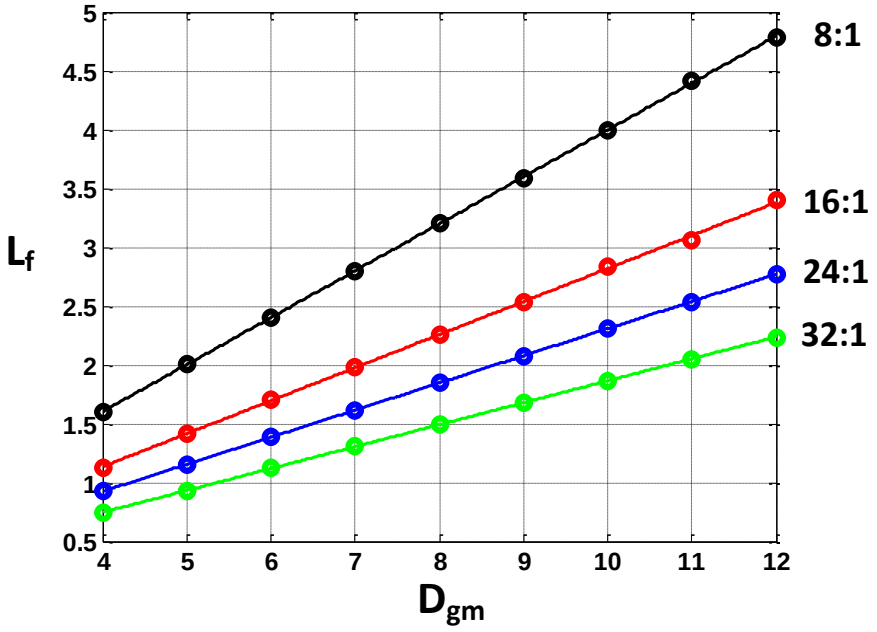

Figure 3-24: Plot of Length L_f (*in*) vs. Gear Mesh Diameter for 4 Gear Ratios

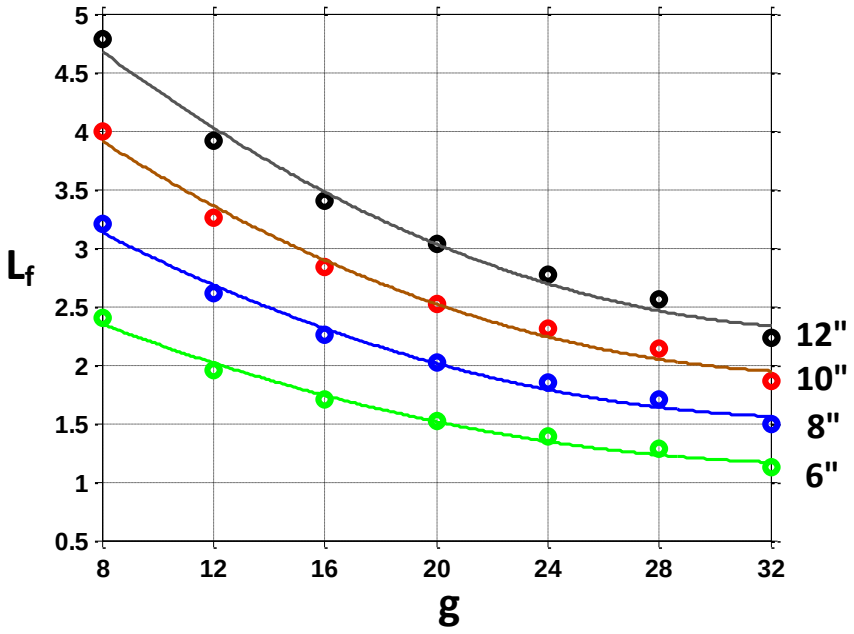

Figure 3-25: Plot of Length L_f (in) vs. Gear Ratio g for 4 different Diameters

Table 3-10: Power Law - Length L_f (*in*) vs. Gear Ratio

Gear Mesh Diameter	a	b	R^2
6”	7.07	-0.5172	0.9958
8”	9.43	-0.5181	0.9964
10”	11.78	-0.5173	0.9955
12”	13.99	-0.5135	0.9960

The reason for the decrease in the Length L_f with increasing gear ratio is the same as that for the decrease in the Rated Torque T with increasing gear ratio (See Section 3.4.1.1).

By dividing the Length L, shown in Figure 3-23 by the Gear Mesh diameter D_{gm}, it is possible to obtain the aspect ratio A ($A = L/D_{gm}$), for the design solutions in that design map. A plot of the aspect ratio A against gear ratio g is shown in Figure 3-26.

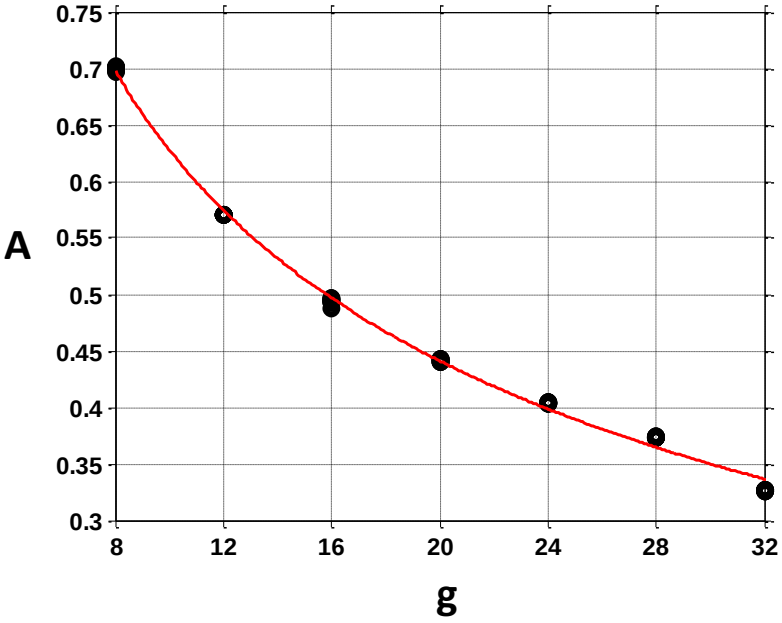

Figure 3-26: Plot of Aspect Ratio A vs. Gear ratio g

It is observed that the length L in the design map shown in Figure 3-23 corresponds to the *maximum* possible length for a given D_{gm}-g combination. This is not surprising as for a given D_{gm}-g combination, the solution with the maximum rated torque capacity is picked. It is to be expected that designs with the maximum rated torque capacity have face-widths that are at their maximum allowable limit; i.e., close to or equal to the pinion pitch diameter since F_{rule} equals one. Therefore, the plot in Figure 3-26 is an indication of the *maximum* aspect ratio that can be achieved for a given gear ratio g. For example, a designer may infer from the plot that if he/she wanted to design for an aspect ratio of 0.4, then the gear ratios 28 and 32 cannot be obtained, if the recommended maximum value for F_{rule} ; i.e., one, is used. As mentioned in Section 2.7.5, the Design Solution Set can be filtered such that only design solutions with a fixed aspect ratio are obtained. Some sample design problems when such filtered designs are necessary will be presented in Chapter 4.

3.4.3 Weight (W) versus Gear Mesh diameter (D_{gm}) and Gear ratio (g)

The actual weight of a 1-Stage SCGT gear train would include the weights of the Input Pinion, amplifier gears, ring gear (output), backbone, shell, bearing cage, bearings (including the primary bearing) as well as supporting structures for the primary bearing.

$$W = W_{InputPinion} + 3\times(W_{Amplifier\ Gears}) + W_{Ring} + W_{BearingCage} \cdots \\ \cdots + W_{Backbone} + W_{bearings\&support} \tag{3.7}$$

However, as dimensions and therefore weights for components such as the bearing cage, backbone, bearings and bearing supports can only be obtained at a more advanced stage of design, an accurate value for the gear train weight cannot be obtained at the preliminary design stages. However, it is possible to get a reasonably good estimate of the gear train weight by using the following formula for the weight W:

$$W = \frac{\pi\left(D_{gm}\right)^2 L}{4}\times\rho\times f_f \tag{3.8}$$

In the expression above, ρ refers to the density of the material used in the gear train (usually steel with a density of 0.283 $lbin^{-3}$) and f_f is the material filling factor, defined as the percentage of gear train volume V that is filled with material. The reader may recognize from Equation 3.8 that the volume of the gear train V is calculated by approximating the gear train volume to that of a solid cylinder with a diameter equal to the Gear Mesh diameter D_{gm} and a length L. The material filling factor f_f is used to account for the fact that this volume is not, in fact, a solid cylinder and it is typically about 85-90% for a 1-Stage SCGT. A value of 85% will be used in this report.

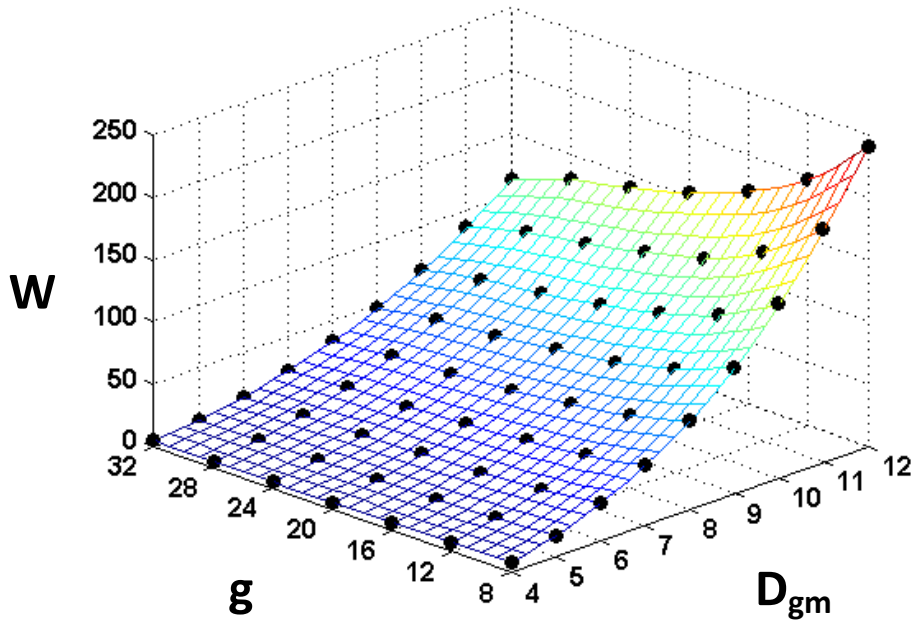

Figure 3-27: Design Map – Weight (*lbf*) vs. Primary Design Knobs

3.4.3.1 Physical Reasoning behind the design map

The design map in Figure 3-27 shows the variation of the weight W with the primary design knobs. From Equation 3.9, it is clear that the weight increases with the square of the Gear Mesh diameter; i.e., they have a quadratic relationship. However, as shown in Figure 3-24, the length L is directly proportional to the Gear Mesh diameter. The relationship between the weight and the gear mesh diameter is therefore cubic as seen in Table 3-11 and Figure 3-28.

Table 3-11: Power Law –Weight (*lbf*) vs. Gear Mesh diameter (in) (ax^b)

Gear Ratio	a	b	R^2
8	0.14	2.994	1
16	0.09	3.001	0.9999
24	0.08	3.004	1
32	0.06	2.998	1

For a fixed Gear Mesh diameter, it is clear (see Equation 3.8) that the weight is directly proportional to the length L. From Table 3-10, the length is proportional to the inverse square root of the gear ratio g. Since the gear mesh diameter D_{gm} is fixed, it is expected that the weight W should also be proportional to the inverse square root of the gear ratio. This is confirmed by the value of the exponent b in Table 3-12. A plot of the weight against the gear ratio is shown in Figure 3-29.

Table 3-12: Power Law – Weight (*lbf*) vs. Gear Ratio (ax^b)

Gear Mesh Diameter	a	b	R^2
6”	89.1	-0.5172	0.9958
8”	211.4	-0.5181	0.9964
10”	412.3	-0.5173	0.996
12”	705.1	-0.5135	0.9955

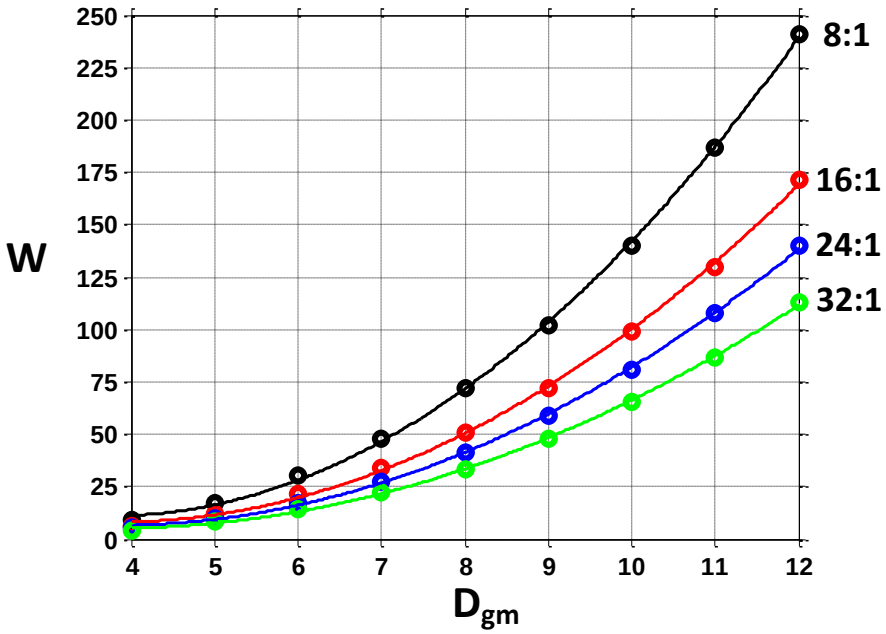

Figure 3-28: Plot of Weight (*lbf*) vs. Gear Mesh diameter for 4 gear ratios

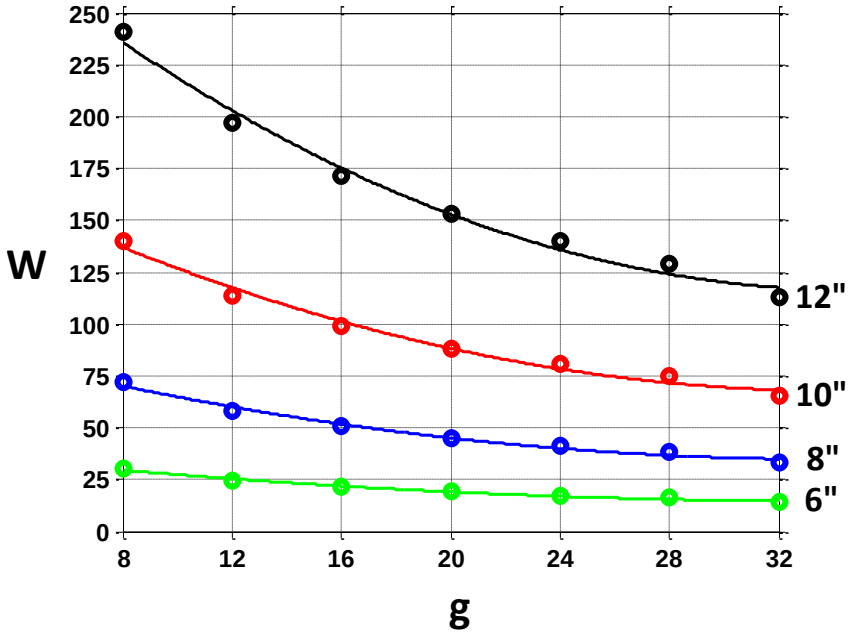

Figure 3-29: Plot of Weight (*lbf*) vs. Gear ratio for 4 Gear Mesh Diameters

3.4.4 Torque Density (T_D) versus Gear Mesh diameter (D_{gm}) and Gear ratio (g)

The Torque Density T_D, defined as the ratio of a gear train's Rated Torque to its weight, is a useful metric when comparing gear trains of different types.

$$T_D = \frac{Rated\ \ Torque\ \ (ft-lbf)}{Weight(lbf)} \tag{3.9}$$

The higher the torque density for a gear train or actuator, the smaller is the package necessary to achieve the same rated torque requirements. The design map for the torque density of a 1-Stage SCGT is shown in Figure 3-30. The reader must note that the design map is rotated 180^{o} (note the direction in which D_{gm} and g values are increasing) for a clear view of the design map.

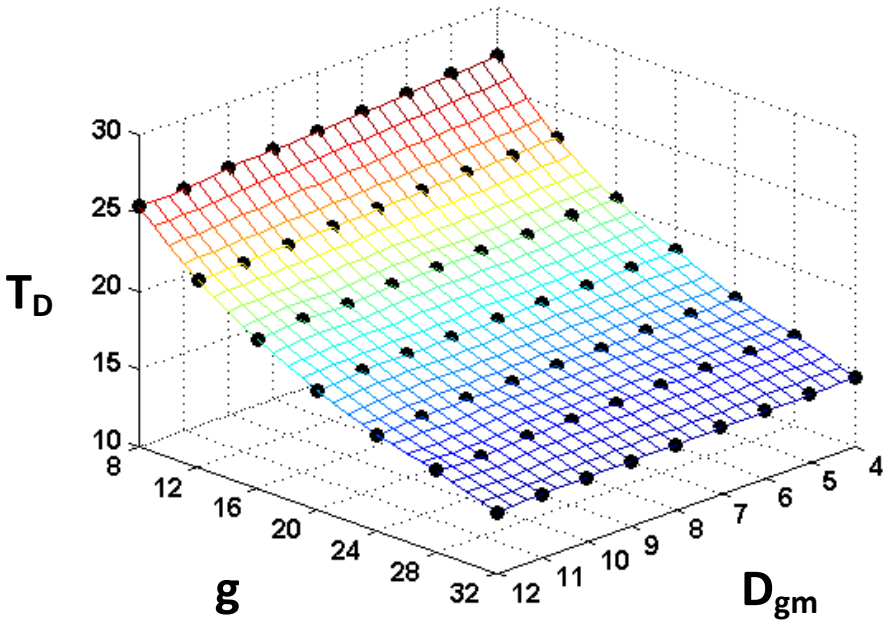

Figure 3-30: Design map - Torque Density (*ft-lbf/lbf*) vs. Primary Design Knobs

3.4.4.1 Physical Reasoning behind the design map

The design map above reveals that the torque density is almost independent of the Gear Mesh diameter D_{gm}. Note that since both Rated Torque and Weight are proportional to the cube of the gear mesh diameter, this is to be expected. As Figure 3-31 shows, the torque density decreases very slightly with an increase in D_{gm}. This can be attributed to the difference in co-efficient values in the power laws relating the Rated Torque and Weight to the gear mesh diameter. The values of the exponent *b* in Table 3-13 are almost zero, again indicating that the torque density is almost independent of the gear mesh diameter.

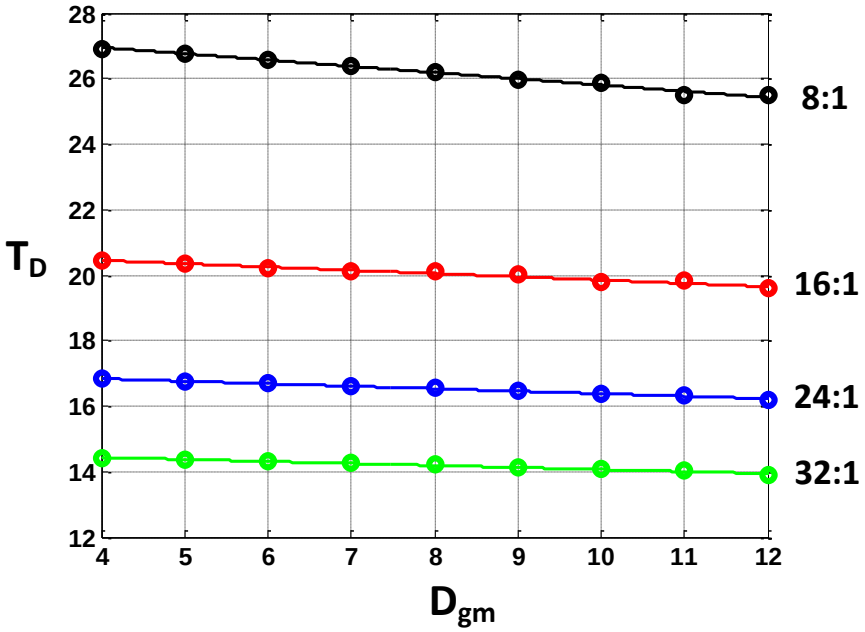

Figure 3-31: Torque Density (*ft-lbf/lbf*) vs. Gear Mesh Diameter for 4 gear ratios

Table 3-13: Power Law - Torque Density (*ft-lbf/lbf*) vs. Gear Mesh Diameter (*in*) (ax^b)

Gear Ratio	a	b	R^2
8	29.13	-0.052	0.9562
16	21.57	-0.036	0.9198
24	17.68	-0.033	0.9465
32	15.11	-0.031	0.9237

The torque density decreases with an increase in the gear ratio for a given gear mesh diameter, as Figure 3-32 shows. By comparing the values of the exponent b in Table 3-8 (Rated Torque vs. Gear Ratio power law) with those in Table 3-12, the reader should see that this is justified. With increasing gear ratio, the rated torque decreases at a faster rate than the weight leading to the T_D-g relationship shown in Figure 3-32 and mathematically represented in Table 3-14.

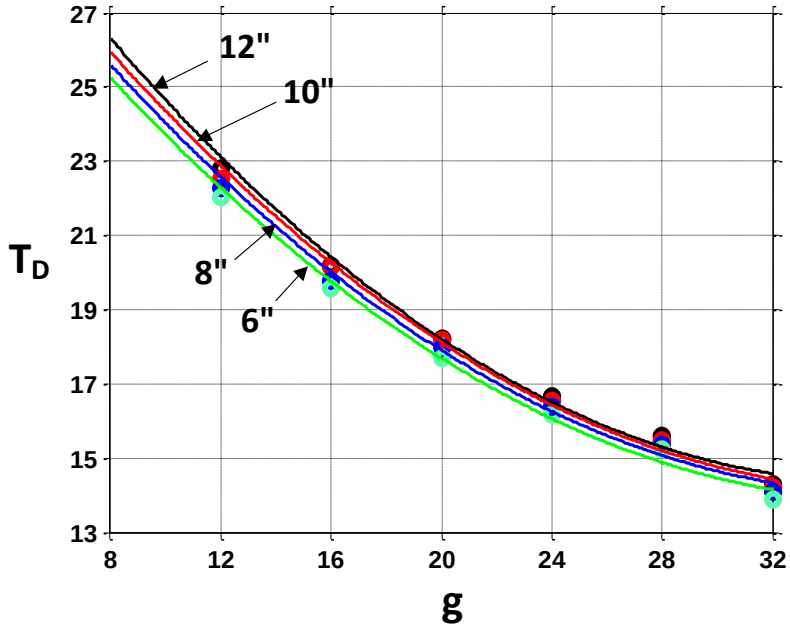

Figure 3-32: Torque Density (*ft-lbf/lbf*) vs. Gear ratio for 4 Gear Mesh diameters

Table 3-14: Power Law - Torque Density (*ft-lbf/lbf*) vs. Gear ratio (ax^b)

Gear Mesh Diameter	a	b	R^2
6”	66.19	-0.433	0.9959
8”	64.52	-0.427	0.9946
10”	63.18	-0.424	0.9952
12”	62.20	-0.422	0.9944

3.4.5 Inertia (I) versus Gear Mesh diameter (D_{gm}) and Gear ratio (g)

The Inertia of a gear train, reflected to the input is an important criterion in the selection of an optimum motor- gear train combination (F Roos, Johannson, and Wikander 2006). (Vaculik and Tesar, 2008)note that some authors recommend that the reflected inertia be equal to the motor inertia, but agree that inertia mismatches of up to 4 to 1 may be tolerated. The Inertia I (reflected to the input; i.e., motor shaft) for a 1-stage SCGT is given by the following equation:

$$I = I_P + 3 \times \frac{(I_{LS} + I_{SS})}{g_1^2} + \frac{I_R}{g^2} + I_{bearings} \tag{3.10}$$

Treating the gears and bearings as either solid or hollow cylinders, the inertia of each component may be calculated using the formula:

$$I = \frac{\rho \pi \left(d_o^4 - d_i^4 \right) L}{32} \tag{3.11}$$

The terms in Equation 3.11 have the following meanings: ρ = material density, d_o = outer diameter, d_i = inner (bore) diameter, L = Length or face-width.

The bearing inertias are often insignificant in comparison with the other components and may be neglected [Vaculik and Tesar, 2008]. Note that the gear train inertia may also be reflected to the output using the following equation:

$$I = I_P g^2 + 3 \times (I_{LS} + I_{SS}) g_2^2 + I_R + I_{bearings} \tag{3.12}$$

The gear train inertia reflected to the output is useful to calculate the Output Responsiveness of an actuator. The Output Responsiveness is a measure of the acceleration at the output. The rest of this report will refer to the inertia reflected to the input simply as Inertia I. The inertia reflected to the output will be used only in the calculation of the Output Responsiveness.

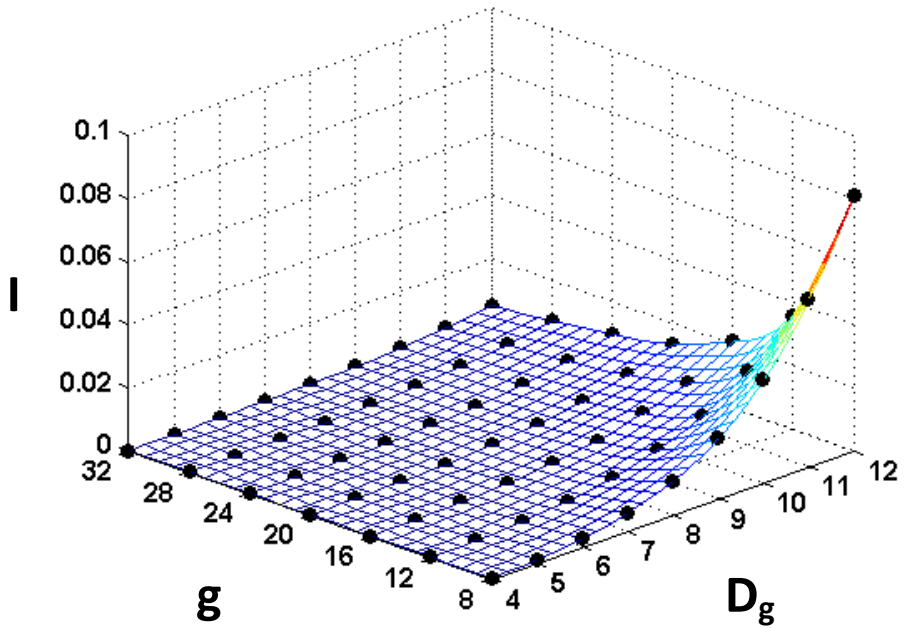

Figure 3-33: Design Map - Inertia ($lbm\text{-}in^2$) vs. Primary Design Knobs

As Figure 3-33 shows, the Inertia is highly non-linear with respect to the primary design knobs.

3.4.5.1 Physical Reasoning behind the design map

The variation of the inertia I with the gear mesh diameter D_{gm} can be explained by analyzing Equation 3.10 and Equation 3.11. As seen in Figure 3-17, g_1 is fixed for a given g unless otherwise constrained. Therefore, for a fixed gear ratio g, the variation of inertia I can be explained based on the effect D_{gm} has on Equation 3.11. As mentioned earlier, with increasing gear mesh diameter D_{gm}, the pitch diameters as well as face-widths increase proportionally. Therefore, from Equation 3.11, it is expected that the inertia increase with the fifth power of D_{gm}. From the plot in Figure 3-34 and the associated power law fits shown in Table 3-16, this is found to be true.

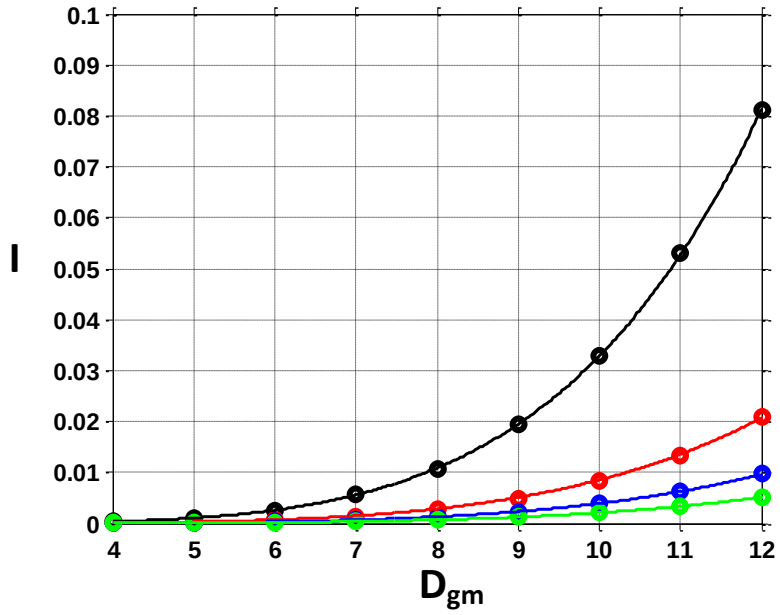

Figure 3-34: Plot of Inertia ($lbm\text{-}in^2$) vs. Gear Ratio for 4 Gear Mesh Diameters

Table 3-15: Power Law - Inertia ($lbm\text{-}in^2$) vs. Gear Mesh diameter (in) (ax^b)

Gear Ratio	a	b	R^2
8	$3.6e^{-7}$	4.96	1.000
16	$1.1e^{-7}$	4.87	0.9997
24	$4.8e^{-8}$	4.91	0.9998
32	$2.5e^{-9}$	4.91	1.000

The mass of the ring gear is in general much higher in comparison with the other components that contribute to the inertia. Therefore, the third term in Equation 3.10 may be said to dominate the others. From Equation 3.10, it is thus reasonable to expect that the inertia should approximately decrease with the square of the overall gear ratio g. This is confirmed by looking at the values for the exponent b in Table 3-16. A plot of the inertia I as a function of the gear ratio is shown in Figure 3-35.

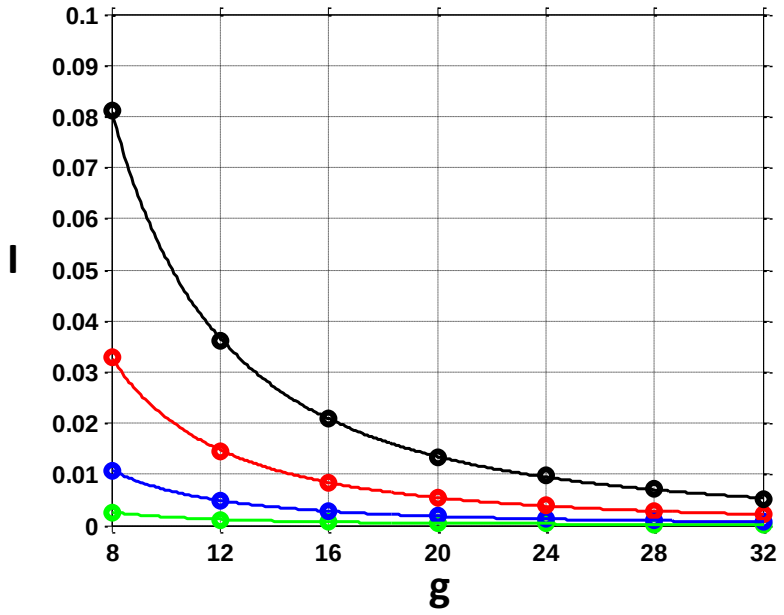

Figure 3-35: Plot of Inertia (*lbm-in*^{2}) vs. Gear Mesh diameter (*in*) for 4 Gear ratios

Table 3-16: Power Law – Inertia (lbm-in^2) vs. Gear ratio (ax^b)

Gear Mesh Diameter	a	b	R^2
6”	0.116	-2.20	0.9997
8”	0.483	-2.20	0.9997
10”	1.458	-2.19	0.9996
12”	3.715	-2.21	0.9997

3.4.6 Responsiveness (R) versus Gear Mesh diameter (D_{gm}) and Gear ratio (g)

Responsiveness R, defined as the ratio of torque to inertia is a useful metric to compare the acceleration (responsiveness) of an actuator.

$$R = \frac{Rated\ \ Torque\ (ft-lbf)}{Inertia(lbm-in^2)} \tag{3.13}$$

Since the inertia can be reflected to the input or output side, both Input Responsiveness as well as Output Responsiveness are presented in this report.

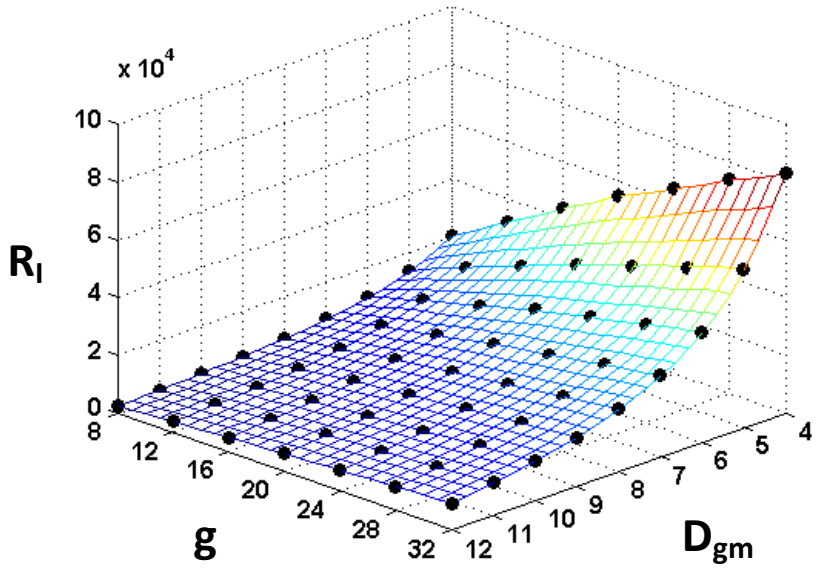

Figure 3-36: Design map - Input Responsiveness (*rad/s*) vs. Primary Design Knobs

3.4.6.1 Physical Reasoning behind the design map

The design map in Figure 3-36 shows the variation of the Input Responsiveness R_I with the primary design knobs. It must be noted that the design map is rotated so as to give the reader a clear view of the map (Note the direction of the x- and y-axes). A plot of the Input Responsiveness versus the gear mesh diameter is shown in Figure 3-37. The corresponding power law fits are shown in Table 3-17. Since the Rated Torque was proportional to the cube of D_{gm} and the Inertia was proportional to the fifth power of D_{gm}, the values of the exponent b in Table 3-17 are reasonable (approx. equal to two).

Table 3-17: Power Law - Input Responsiveness (*rad/s*) vs. Gear Mesh Diameter (ax^b)

Gear Ratio	a	b	R^2
8	$2.96e^5$	-1.921	0.9995
16	$6.37e^5$	-1.931	0.9998
24	$9.57e^5$	-1.944	0.9998
32	$1.24e^6$	-1.946	0.9998

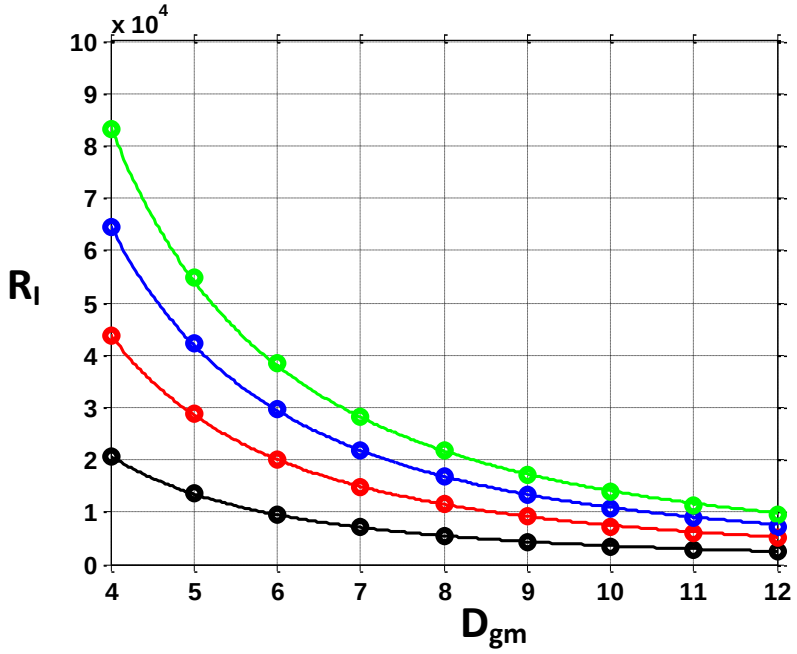

Figure 3-37: Input Responsiveness (*rad/s*) vs. Gear Mesh Diameter for 4 gear ratios

The plot in Figure 3-38 shows the variation of the Input Responsiveness as a function of increasing gear ratio. The relationship is approximately linear and may be deduced by looking at the power laws for the Rated Torque and Inertia with respect to the gear ratio (Table 3-7 and Table 3-16 respectively). The power law fits to the curves shown in Figure 3-38 are presented in. The power law fits agree with the expectation that the relationship is approximately linear.

Table 3-18: Power Law - Input Responsiveness (*rad/s*) vs. Gear Ratio (ax^b)

Gear Mesh Diameter	a	b	R^2
6”	1423	0.95	0.9981
8”	816.2	0.95	0.9980
10”	511.5	0.95	0.9982
12”	350.9	0.96	0.9979

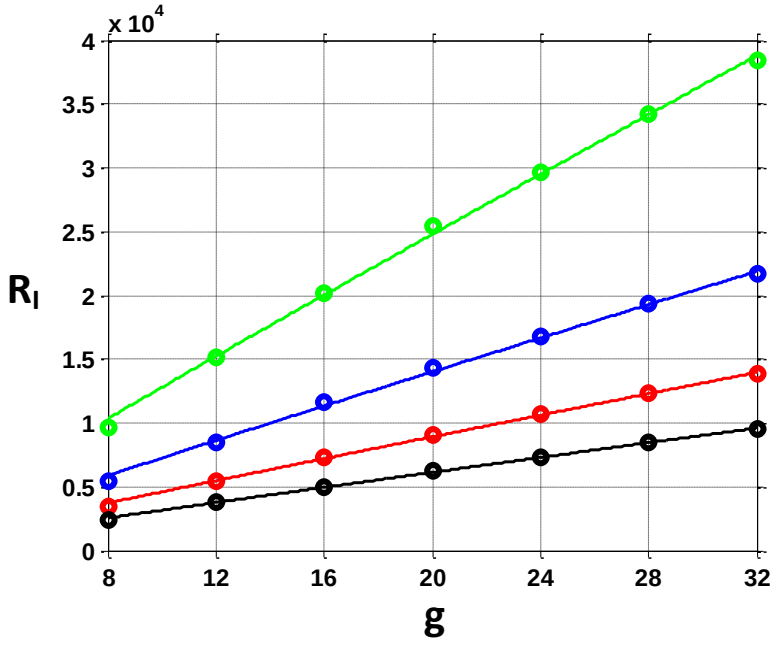

Figure 3-38: Input Responsiveness (*rad/s*) vs. Gear ratio for 4 Gear Mesh diameters

The design map for the Output Responsiveness R_o; i.e., the ratio of the rated torque to the inertia reflected to the output is shown in Figure 3-39. With regard to the relationship between the output responsiveness and the gear mesh diameter (See Figure 3-40), it may be deduced (see Equation 3.10, Equation 3.11 and Equation 3.12) that the output responsiveness is simply the input responsiveness scaled down by the square of the gear ratio. This may be observed by looking at the power laws in Table 3-17 and comparing them with those for the Output responsiveness in Table 3-19, which shows the power law fits to the curves in Figure 3-40.

Table 3-19: Power Law - Output Responsiveness (*rad/s*) vs. Gear Mesh Diameter (ax^b)

Gear Ratio	a	b	R^2
8	5063	-2.04	1
16	3038	-2.03	1
24	1961	-2.02	1
32	1430	-2.02	1

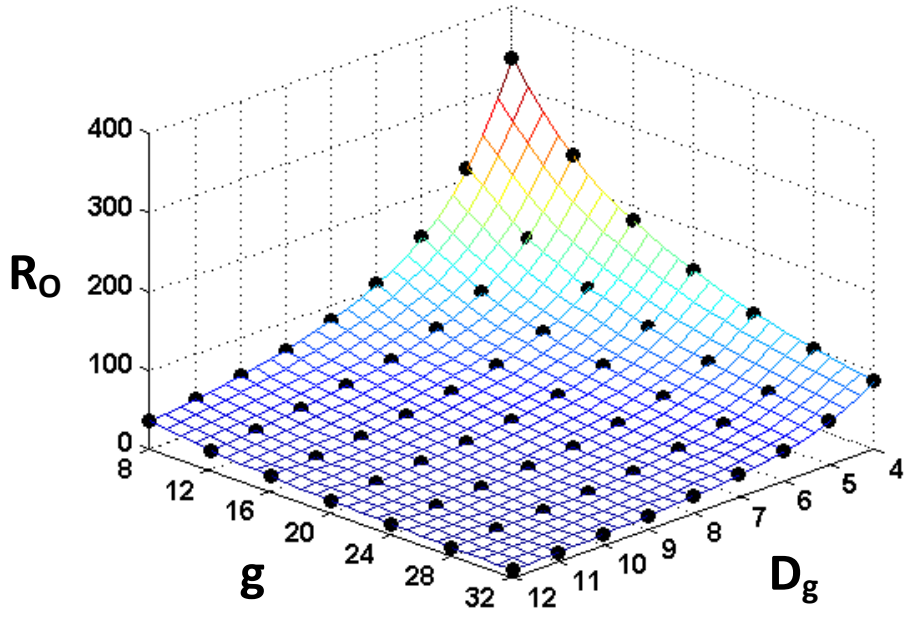

Figure 3-39: Design map - Output Responsiveness (*rad/s*) vs. Primary Design Knobs

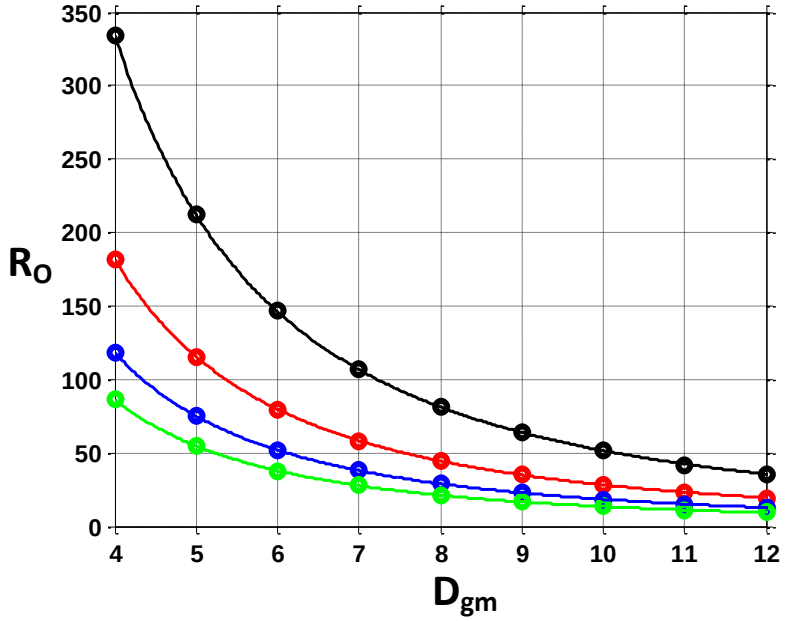

Figure 3-40: Plot of Output Responsiveness vs. Gear Mesh diameter for 4 Gear ratios

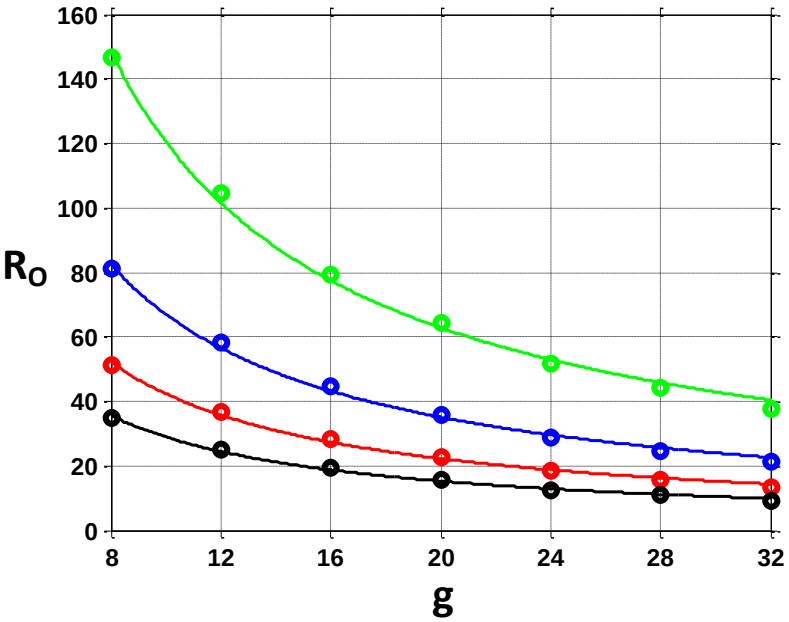

Figure 3-41: Plot of Output Responsiveness vs. Gear Ratio for 4 Gear Mesh diameters

Table 3-20: Power Law - Output Responsiveness vs. Gear Ratio (ax^b)

Gear Mesh Diameter	a	b	R^2
6”	1423	0.95	0.9981
8”	816.2	0.95	0.9980
10”	511.5	0.95	0.9982
12”	350.9	0.96	0.9979

Unlike the Input Responsiveness which increased with increasing gear ratio, the Output Responsiveness decreases with increasing gear ratio (See Figure 3-41). By looking at Equation 3.10 and Equation 3.12, this characteristic makes sense. The inertia reflected to the input decreases with increasing gear ratio, whereas the converse is true for the inertia reflected to the output. Therefore, the Input Responsiveness and the Output Responsiveness vary conversely with increasing gear ratio. The power law fits for the curves in Figure 3-41 are shown in Table 3-20.

3.5 DESIGN MAPS FOR THE FRONT END (1ST STAGE) OF A C-TYPE 2-STAGE SCGT

The design maps for the 1st stage of a C-Type 2-Stage SCGT follow similar trends as in the design maps for the 1-Stage SCGT from the previous section. This is because, as mentioned in Section 2.6, the front end of a C-Type 2-Stage SCGT is exactly the same as a 1-Stage SCGT except that the output gear is an external gear and not an internal ring gear. Therefore, the design maps for the front end will be presented below with only brief discussions on the design maps when necessary.

The ‘a priori’ and design knob values used for the design maps in this section will be the same as those shown in Table 3-2 except for the gear ratio g. The gear ratio range for the Front End of the C-Type 2-Stage SCGT will be from 2 to 16 in steps of 2. Thus, the maximum gear ratio achievable from a C-Type 2-Stage SCGT is 512 (16 times 32).

3.5.1 Rated Torque (T) versus Diameter (D_{gm}) and Gear Ratio (g)

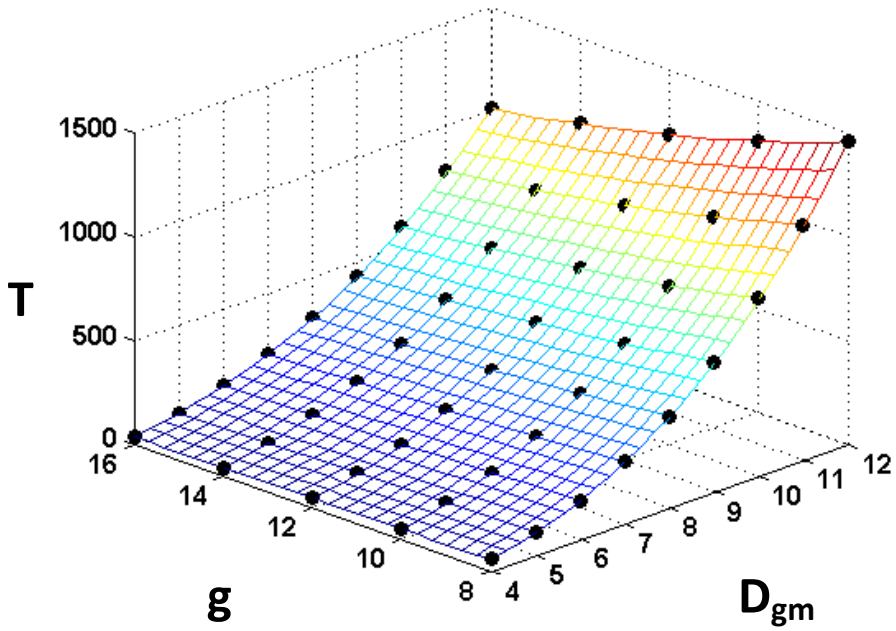

Figure 3-42: Design Map - Rated Torque (*ft-lbf)* vs. Primary Design Knobs

The Rated Torque values for the Front End gear train (shown in Figure 3-42) may be compared to their corresponding values for the Back End gear train; i.e., the 1-Stage SGCT (see Figure 3-19). The gear mesh diameter ranges for both the front end and back end are the same. The gear ratios from 8 to 16 are common to the front end and back end. Therefore, Rated Torques for common D_{gm}-g combinations are shown in Figure 3-43.

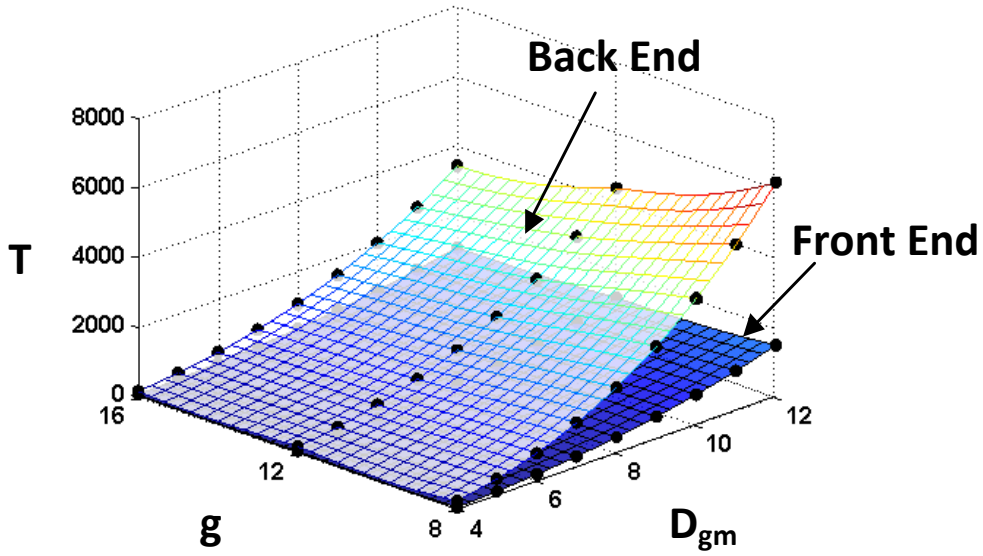

Figure 3-43: Rated Torque (*ft-lbf*) vs. Primary Design Knobs

As Figure 3-43 shows, for the same D_{gm}-g combination, the Rated Torque for the Back End is significantly higher than that for the Front End (about 3.75 times on average). This can be attributed to the single fact that the Back End uses an internal gear as the output whereas the Front End uses an external gear. For the same D_{gm}-g combination, the pitch diameter of the ring gear (Back End) is greater than the pitch diameter of an output external gear (Front End). A second factor is that internal gear teeth can, in general, carry more load than external gear teeth.

3.5.2 Gear Train Length (L) versus Diameter (D_{gm}) and Gear Ratio (g)

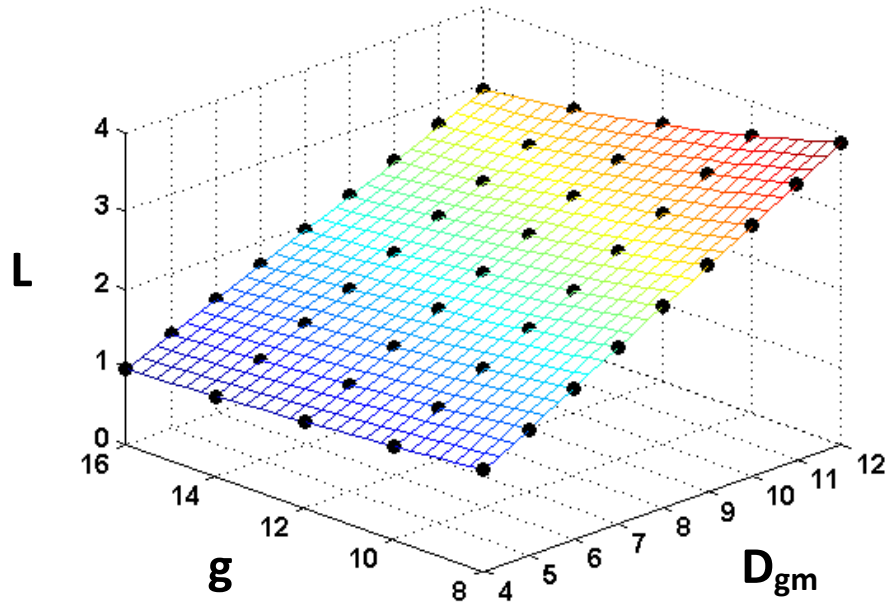

Figure 3-44: Design Map - Rated Torque (*in*) vs. Primary Design Knobs

$$L = 1.1 \times L_f \tag{3.14}$$

When considering the Front End, it is observed (see Figure 2-37) that a good estimate of the actual length L can be obtained by multiplying the length L_f by a factor of 1.1. In other words, the actual length of the Front End is generally about 10% longer than the sum of the face-widths of the gears in the two gear meshes. This estimate of the actual Front End gear train length is also used in the calculation for the weight *W*.

3.5.3 Weight (W) versus Gear Mesh diameter (D_{gm}) and Gear ratio (g)

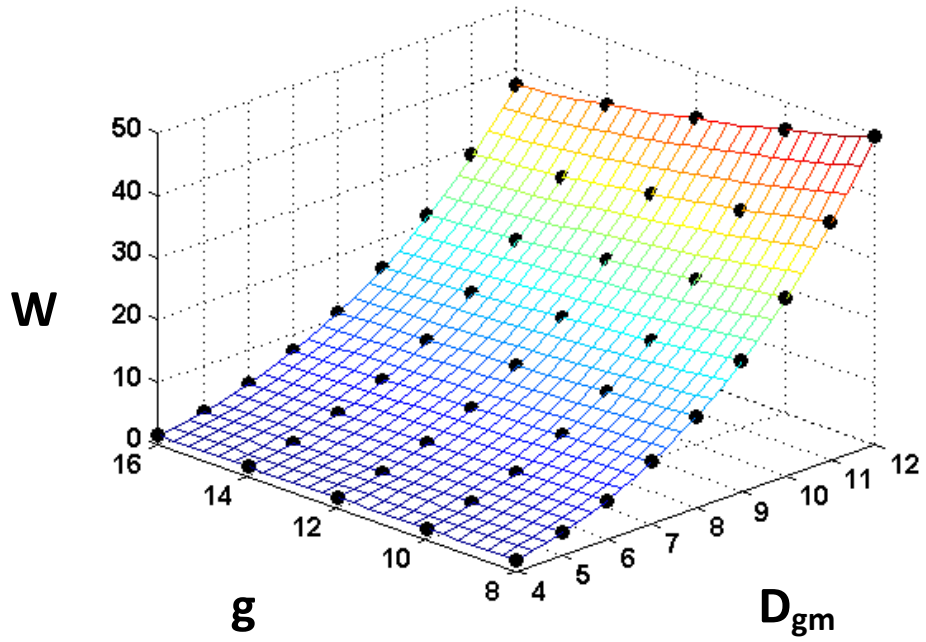

Figure 3-45: Design Map - Weight (*lbf*) vs. Primary Design Knobs

The actual Front End gear train weight is given by:

$$W = W_{InputPinion} + 3\times(W_{Amplifier\ Gears}) + W_{Ring} + \ldots + W_{Backbone} + W_{bearings\&support} \tag{3.15}$$

However, for the preliminary design stage, it is sufficient to estimate the weight using Equation 3.7. The filling factor in the case of the Front End Gear Train is found to be approximately 35-45%. A value of 40% is used in this report.

3.5.4 Torque Density (W) versus Gear Mesh diameter (D_{gm}) and Gear ratio (g)

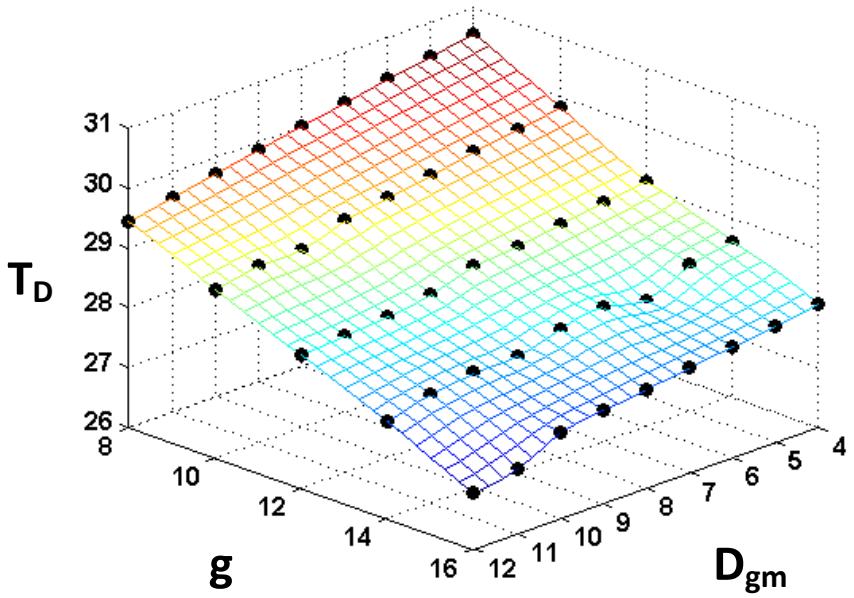

Figure 3-46: Design Map - Torque Density (*ft-lbf/lbf*) vs. Primary Design Knobs

The reader may compare the values for the Torque Density for the 1-Stage SCGT (Back End) (Figure 3-30) with the Torque Density values for the Front End gear train (Figure 3-46). The reason that the Torque Density in the front end is significantly higher than that in the back end is because the weight of the back end is higher than that for the front end. This is because the weights of primary gear train backbone as well as the bearing cage are included in the weight of the Back End. The size of the Front End Backbone relative to that of the Back End is significantly smaller.

3.5.5 Inertia (I) versus Gear Mesh diameter (D_{gm}) and Gear ratio (g)

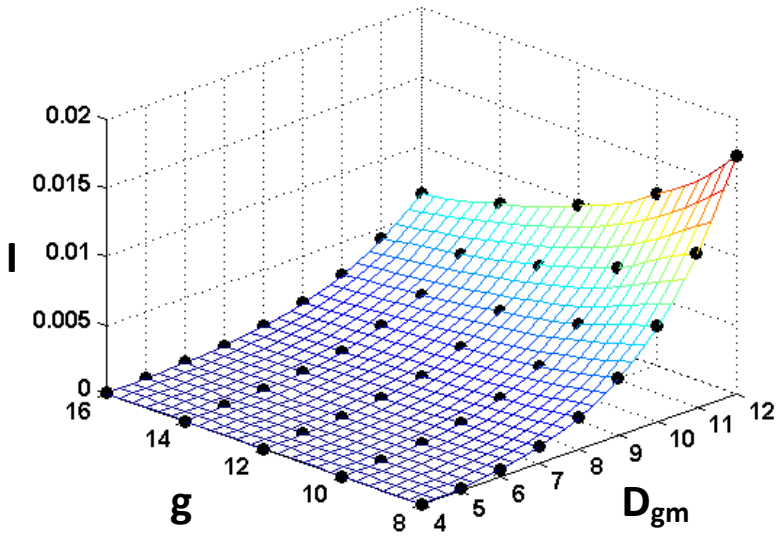

Figure 3-47: Design Map - Inertia (*lbm-in*^{2}) vs. Primary Design Knobs

The trends in the Inertia, Input Responsiveness and Output Responsiveness are similar to those in the 1-Stage SCGT discussed earlier. Therefore, these maps are presented without further discussion.

3.5.6 Responsiveness (R) vs. Gear Mesh diameter (D_{gm}) and Gear ratio (g)

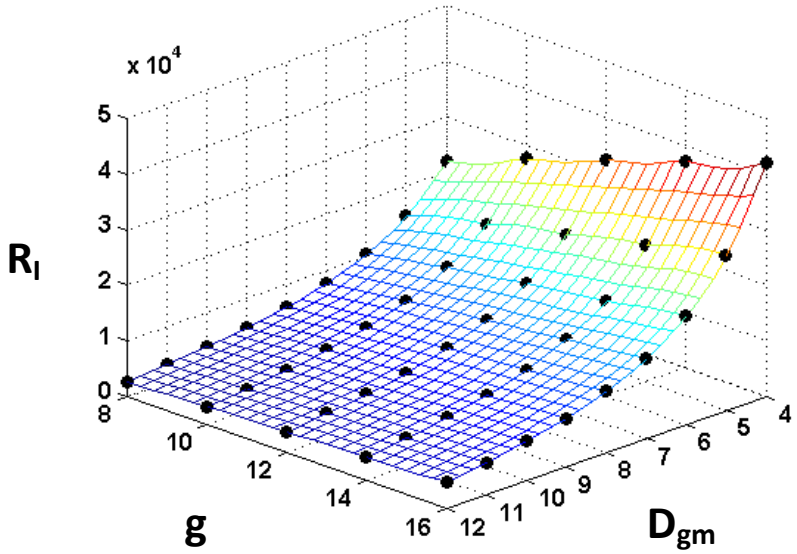

Figure 3-48: Design Map - Input Responsiveness (rad/s) vs. Primary Design Knobs

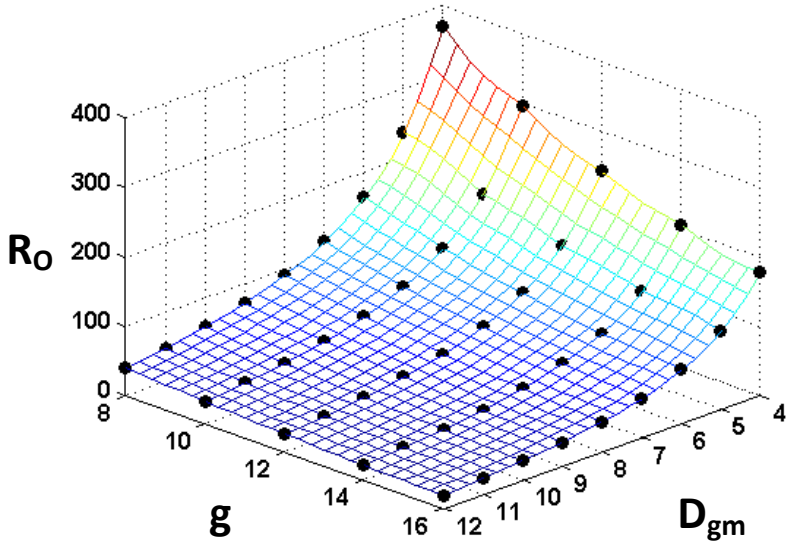

Figure 3-49: Design Map - Output Responsiveness (rad/s) vs. Primary Design Knobs

3.6 DESIGN MAPS FOR THE P-TYPE 2-STAGE SCGT

In Section 2.5, two variants of the P-Type 2-Stage SCGT were discussed; one with six 2nd stage amplifier gears and the second with three 2nd stage amplifier gears. These two variants will be referred to from this point onwards as P-Type-6 and P-Type-3 respectively. It is important to be able to judge the relative merits of each of the variants. Therefore, for the design maps for the P-Type 2-Stage SCGT's presented in this section, the aspect ratio will be fixed. The Aspect Ratio A is defined as the ratio of the length L to the Gear Mesh Diameter D_{gm}. An aspect ratio of 0.3 was chosen for the design maps in this section. The reader may recall from Section 2.4.2.1 that, because of the constraint on maximum face-width ($F_{rule} = 1$), there exists a maximum aspect ratio for a given D_{gm}-g combination. This idea will be elaborated upon in Section 3.5.2.

Another important detail is that regarding the gear ratio range. As mentioned in Section 2.5, due to assembly constraints, the maximum gear ratio achievable in a P-Type-6 gear train is 240. The maximum gear ratio achievable in the case of a P-Type-3 gear train is 320. In order to be able to compare the two variants, the gear ratio range for the design maps that follow will be from 60 to 240 in increments of 30. The gear mesh diameter range is the same; i.e., 4" to 12" in increments of one. The rest of the 'a priori' and design knobs are set to the values listed in Table 3-2.

Each type of design map is presented on a single page for easy visual comparison. The design map in the upper half of the page will correspond to the P-Type-3 SCGT and the one on the lower half of the page will correspond to the P-Type-6 SCGT.

3.6.1 Rated Torque versus the Primary Design Knobs

In a P-Type-6 gear train, the Rated Torque is produced by six 2nd Stage amplifier gears in mesh with the output ring gear. In a P-Type-3 gear train, the number of 2nd Stage amplifier gears is 3. Therefore, the Rated Torque T can be expressed as:

$$T = (Number\ of\ \ 2nd\ Stage\ Amplifier\ Gears) \times f_2^t \times D_R \qquad (3.16)$$

The design maps for the Rated Torques for both variants of the P-Type SCGT are shown in Figure 3-50. The upper design map corresponds to the P-Type-3 SCGT and the lower design map corresponds to the P-Type-6 SCGT. A translucent reference plane is shown at a torque of 1000 ft-lbs in both design maps. From Figure 3-50, it is apparent that the P-Type-6 SCGT has significantly larger Rated torque capacity in comparison to the P-Type-3 SCGT. This is visually noticeable by comparing the size of the portion of each design map that lies above the reference plane. In general, it is observed that the Rated Torque capacity of a P-Type-6 SCGT is anywhere between 1.9 to 2.3 times that of a P-Type-3 SCGT.

The reader may also note that, as a consequence of the assembly constraints discussed in Section 2.5, small ‘bumps’ or ‘waves’ are noticed in these design maps. It is in cases such as this that a visual decision making framework such as the one developed in this report becomes very important.

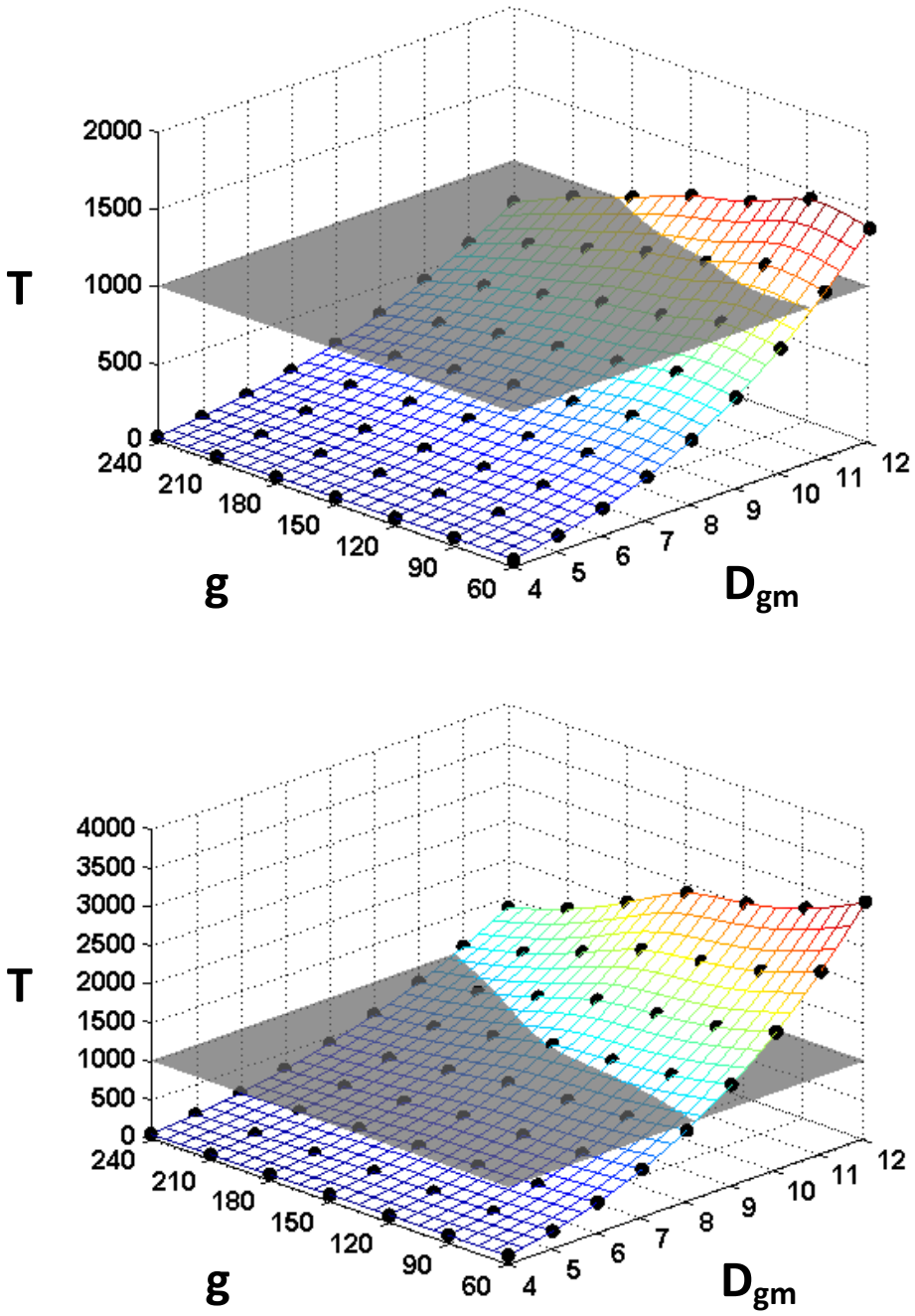

Figure 3-50: Rated Torque (*ft-lbf*) vs. Primary Design Knobs

3.6.2 Length versus the Primary Design Knobs

As mentioned earlier, in order to be able to compare the two variants of the P-Type SCGT, an aspect ratio of 0.3 is chosen. However, as seen in the design maps in Figure 3-51, it may not always be possible to obtain the given aspect ratio. From the design map in the upper half of Figure 3-51, it is observed that in the case of the P-Type-3 SCGT, when the gear ratio is 240, the aspect ratio is below 0.3. In the lower half of Figure 3-51, it is observed that design solutions with gear ratios 240, 210 and 180 all have aspect ratios below 0.3. This is a consequence of the fact that the assembly constraints for a P-Type-3 SCGT and a P-Type-6 SCGT are different.

The observations regarding the Length L mentioned above are also reflected in the design maps for Aspect Ratio as a function of the primary design knobs. These are shown in Figure 3-52.

3.6.3 Weight versus the Primary Design Knobs

As with the weight calculation for a 1-Stage SCGT, the weights W for the two variants of the P-Type 2-Stage SCGT are estimates obtained using Equation 3.8. The filling factor used is 0.8. The reader may note that the design maps for the weights (in Figure 3-53) reflect the variation of the length L with the primary design knobs.

3.6.4 Torque Density versus the Primary Design Knobs

The design maps for Torque Density for the two P-Type SCGT variants (see Figure 3-54) reflect the statement in Section 3.5.1 that the Rated Torque for a P-Type-6 SCGT is about 1.9 to 2.3 times that of a similarly sized P-Type-3 SCGT. Thus, a rule of thumb is that the torque density of a P-Type-6 SCGT is twice that for a P-Type-3 SCGT.

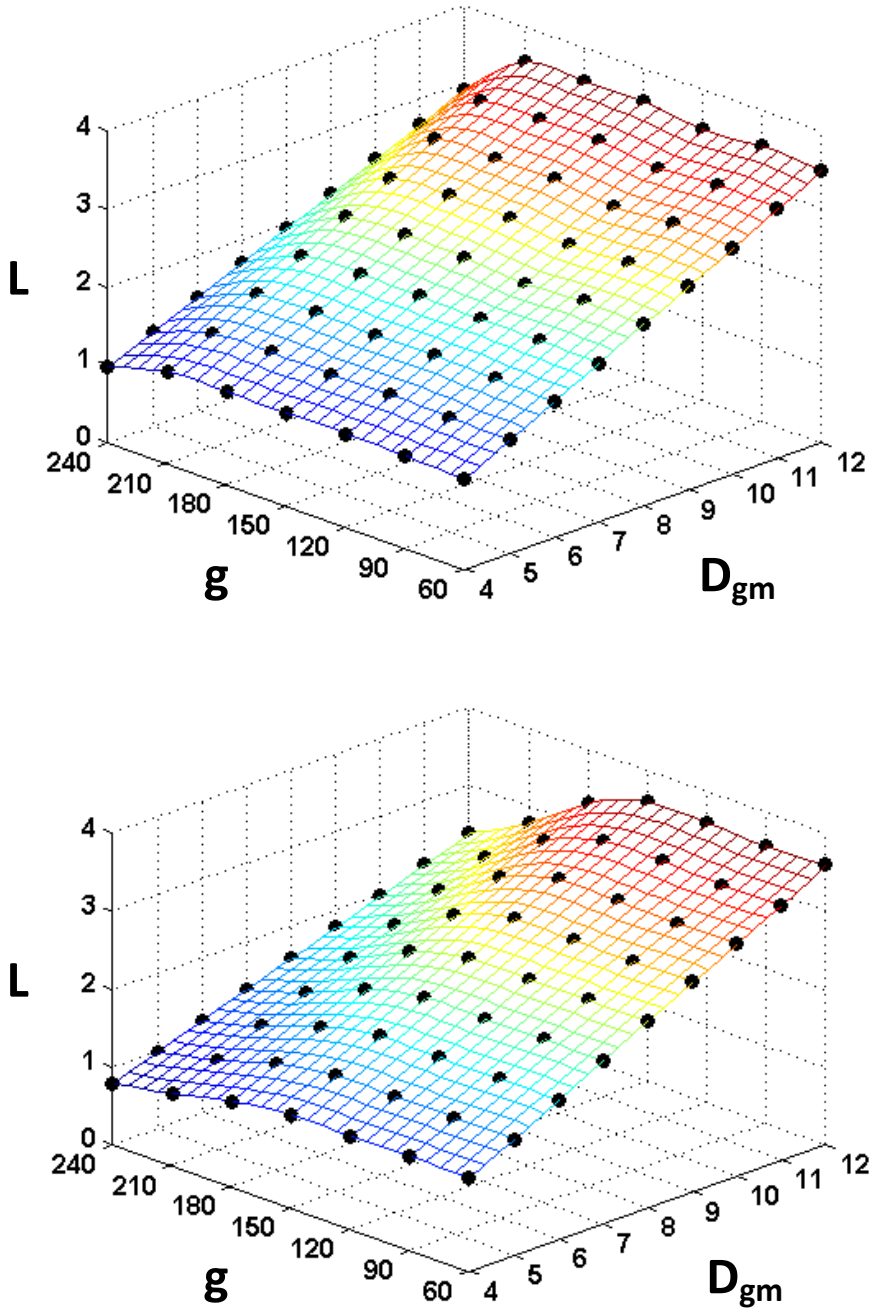

Figure 3-51: Length (*in*) vs. Primary Design Knobs

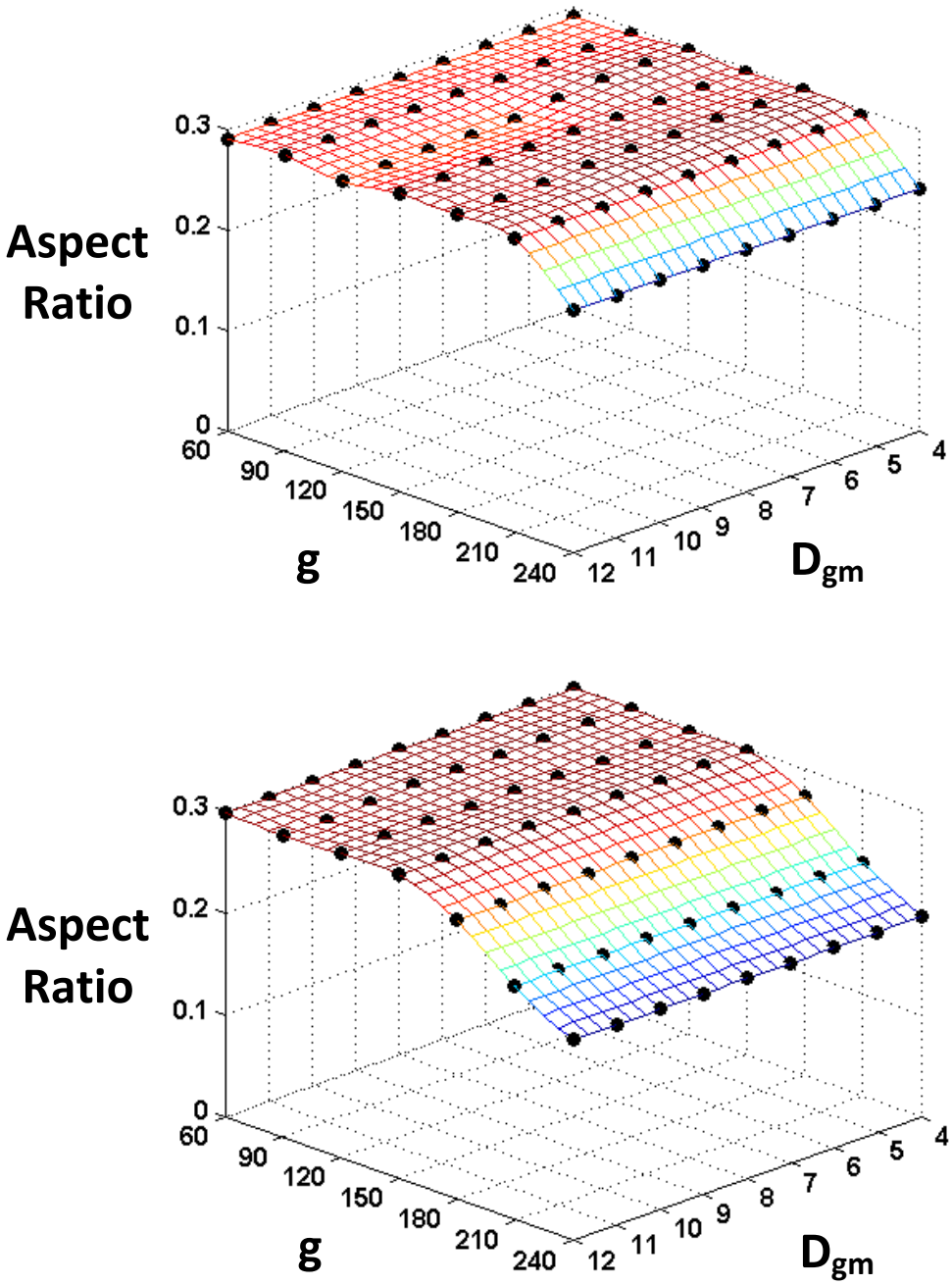

Figure 3-52: Aspect Ratio *A* vs. Primary Design Knobs

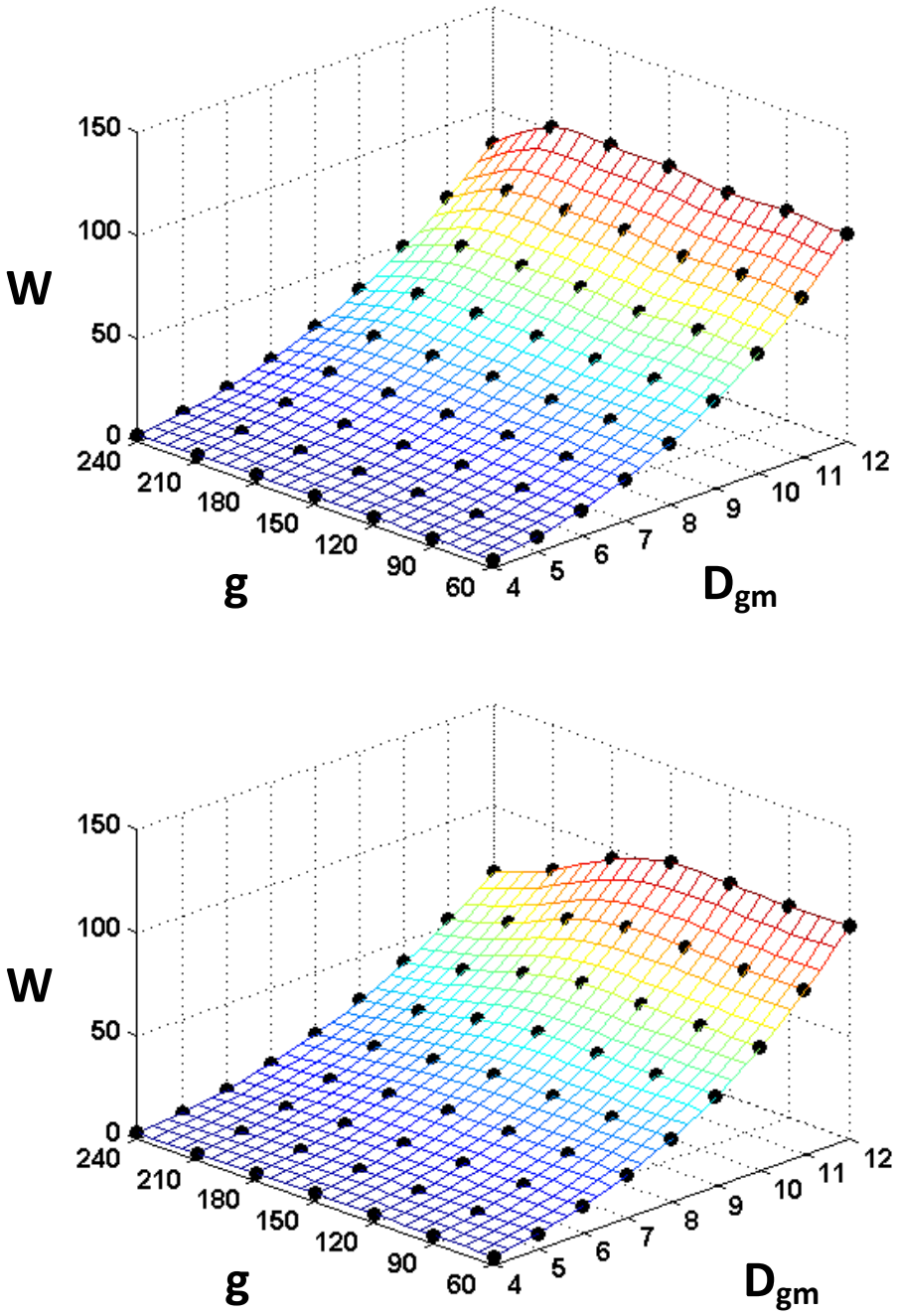

Figure 3-53: Weight (*lbf*) vs. Primary Design Knobs

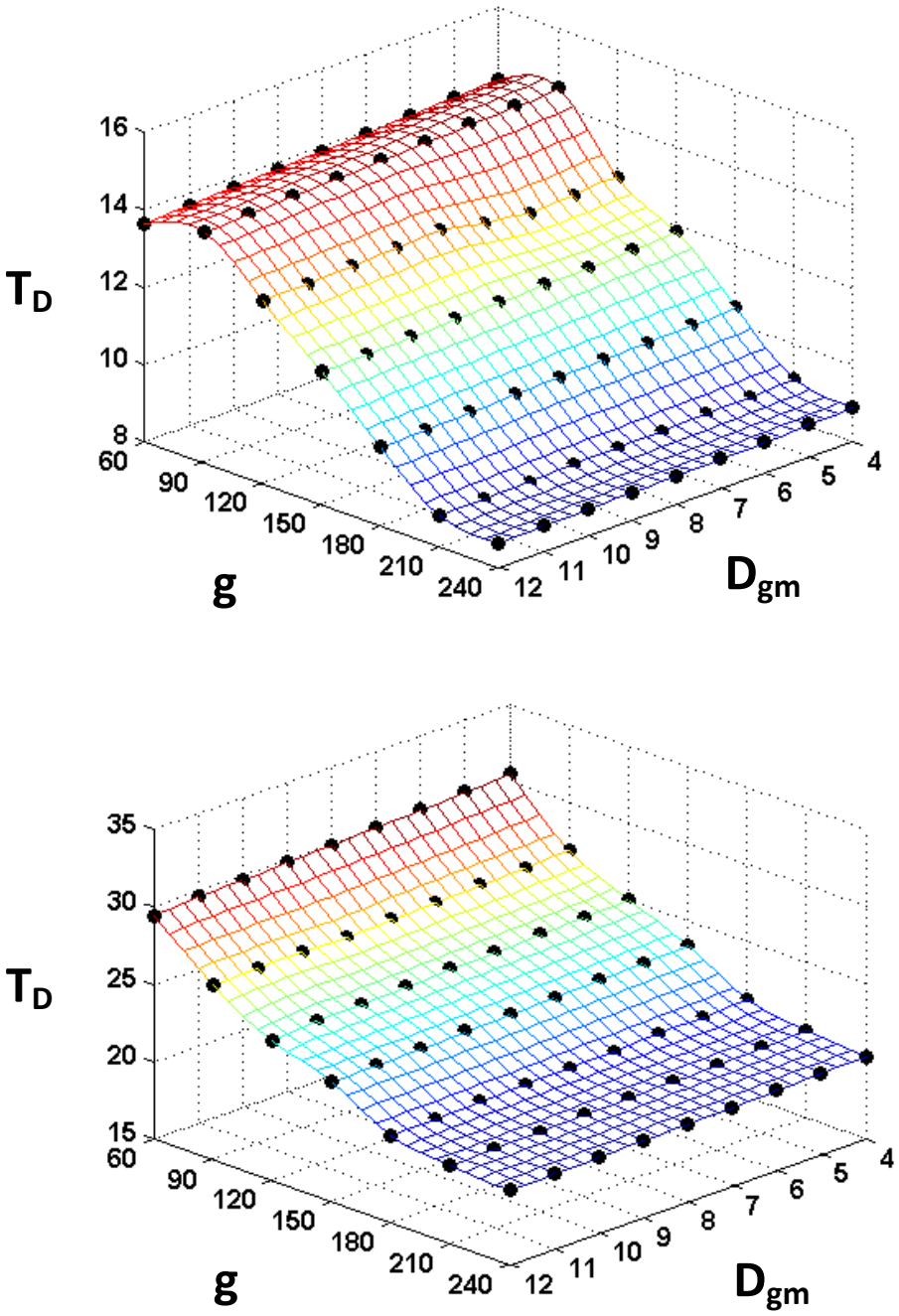

Figure 3-54: Torque Density (*ft-lbf/lbf*) vs. Primary Design Knobs

3.6.5 Inertia versus the Primary Design Knobs

The Inertia I in the case of the P-Type-3 SCGT is given by:

$$I = I_P + 3\times\frac{(I_{LS1}+I_{SS1})}{g_1^2} + 3\times\frac{(I_{LS2}+I_{SS2})}{(g_1 g_2)^2} + \frac{I_R}{g^2} + I_{bearings} \qquad (3.17)$$

For a P-Type-6 SCGT, the inertia I is given by:

$$I = I_P + 3\times\frac{(I_{LS1}+I_{SS1})}{g_1^2} + 6\times\frac{(I_{LS2}+I_{SS2})}{(g_1 g_2)^2} + \frac{I_R}{g^2} + I_{bearings} \qquad (3.18)$$

Design maps for the Inertia versus the Primary Design Knobs for the P-Type SCGT variants are shown in Figure 3-55. The reader is encouraged to compare the inertia values shown in Figure 3-55 with those in Figure 3-33. The higher gear ratios in the P-Type SCGT's produce significantly smaller inertias when compared to the 1-Stage SCGT. From Figure 3-55, it is also noticeable that, as expected, the inertia in a P-Type-6 SCGT is more than that in a P-Type-3 SCGT.

3.6.6 Responsiveness versus the Primary Design Knobs

Design Maps for the Input and Output Responsiveness for the two variants of the P-Type 2-Stage SCGT are shown in Figure 3-56 and Figure 3-57 respectively. It is important to note from these figures that the responsiveness of the P-Type-6 SCGT is greater than that for a P-Type-3 SCGT. This is not intuitive and is an important result. In spite of the increased mass in a P-Type-6 SCGT, the responsiveness is greater than that for a P-Type-3 SCGT.

With the design maps discussed in this chapter, it becomes possible to use a visual design approach towards multi-stage gear train design problems. This is illustrated in Chapter 4.

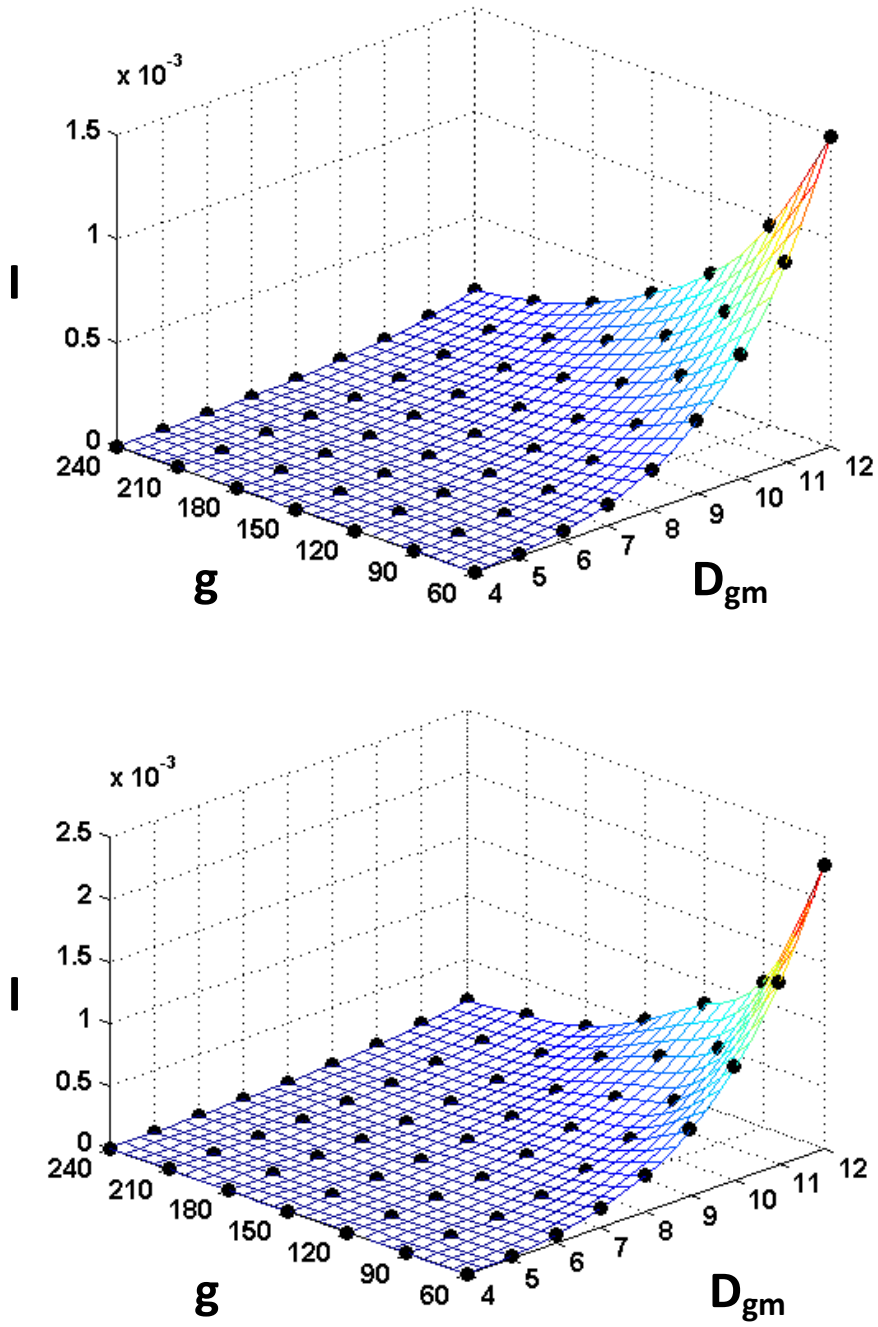

Figure 3-55: Inertia (*lbm-in*^{2}) vs. Primary Design Knobs

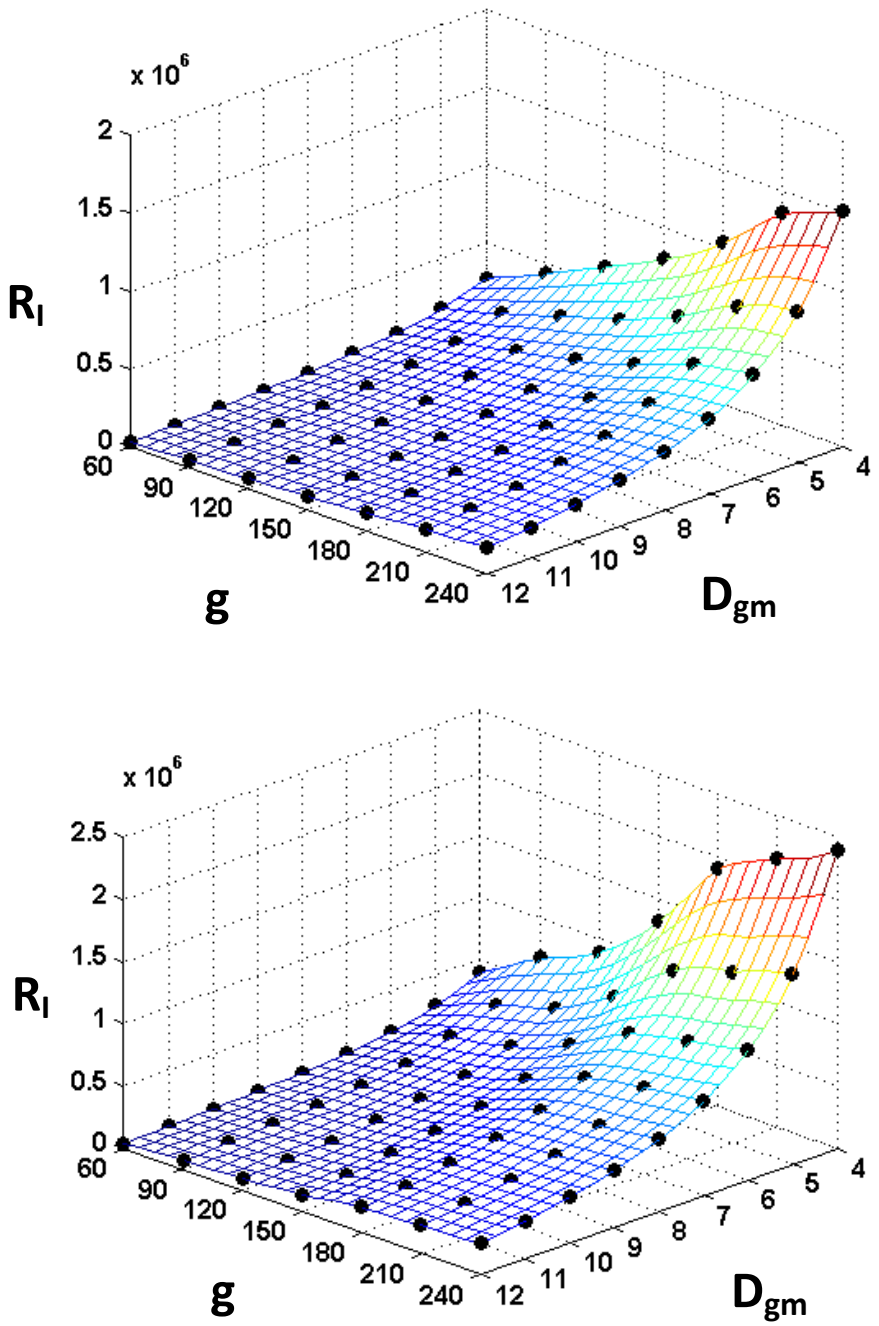

Figure 3-56: Input Responsiveness (*rad/s*) vs. Primary Design Knobs

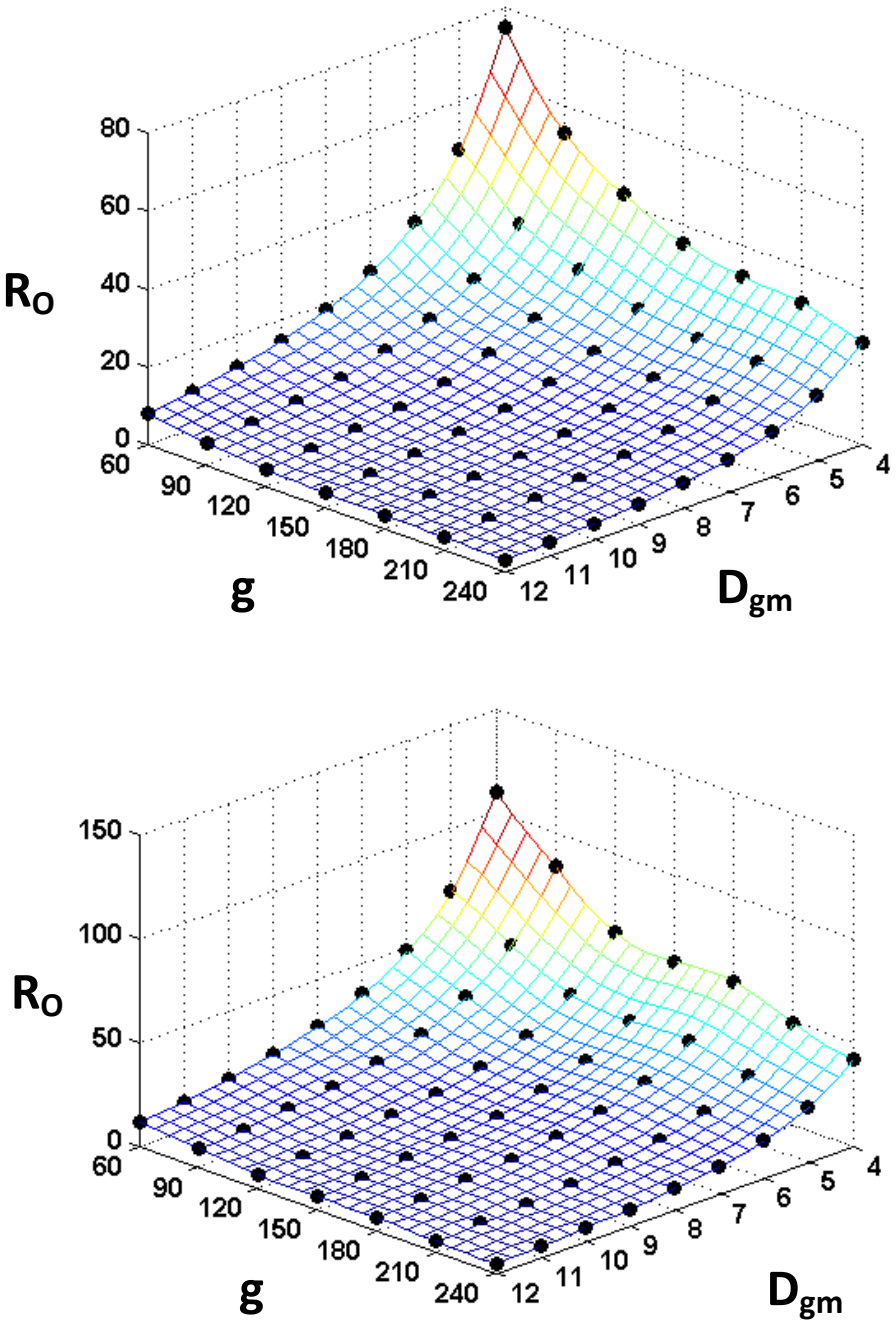

Figure 3-57: Output Responsiveness (*rad/s*) vs. Primary Design Knobs

Chapter 4 : Design Map Utilization

Design procedures for three main types of SCGT's; namely, a One-Stage SCGT's, Pancake-Type Two-Stage SCGT's, and a Coffee-Can Type Two-Stage SCGT's were presented in Chapter 2. In Chapter 3, a procedure for creating design maps using the design procedures from Chapter 2 was shown. Design maps for the three types of SCGT's were presented. In-depth discussions on the 1-Stage SCGT design maps were presented. The fundamental concepts behind the shape of the 1-Stage SCGT design maps are valid for the other SCGT types. The current chapter is aimed at demonstrating to the reader, the efficacy of the visual design maps in gear-train design problems. For this purpose, realistic sample gear train design problems will be posed. For each design problem, first, a nominal set of geometric constraints and required performance criteria will be listed. The geometric constraints and/or performance criteria will then gradually be made more and more demanding. For example, initially the nominal geometric constraints may specify a maximum gear train diameter of 10" and gear train length of 6". The first steps needed to tackle this initial design problem will be presented. Then, the constraint on the maximum gear train diameter will be reduced to 9.5", thereby making it a more difficult design problem. The process by which a designer can quickly redesign for the new constraints will therefore be demonstrated.

A point to be noted is that, as mentioned in Chapter 2, the gear mesh diameter D_{gm} is used in the design procedures developed for the SCGT's in this report. The design problems however, will provide constraints based on the actual gear train diameter D. Experience suggests that the actual gear train diameter D is, in general, around 10%-15% larger than the gear mesh diameter D_{gm}. Constraints on the diameter D will be mapped to constraints on the gear mesh diameter D_{gm} using this value.

4.1 DESIGN PROBLEM 1 – VALVE ACTUATOR

4.1.1 Nominal Design Requirements

A gear train with low complexity is to be designed for use in an electric valve actuator. The desired rated torque is 833 ft-lbf. The nominal output speed is a low 7.5 rpm and a total of 10^7 revolutions at the output are required. A gear ratio of 18 to 1 is required. The maximum diameter and length for the gear train are 11" and 5" respectively. A summary of the gear-train design requirements is shown in Table 4-1.

Table 4-1: Summary of Design Requirements - Design Problem 1

Design Requirement	Value
Rated Torque	833 *ft-lbf*
Output RPM	7.5 RPM
Gear Ratio	18
Max. Diameter	11 in
Max. Length	5 in
Life	10^7 revolutions at the output

Consider the a priori and design knob values listed in Table 3-2. For the initial set of design maps, the same values as those listed in Table 3-2 will be used except for the gear ratio range. The gear ratio range for the initial set of design maps will be 14 to 24 in increments of 1. Although the gear ratio required is given, a range of gear ratios (bounded by 14 to 24 in increments of 1) will be used for the design maps.

Table 4-2: Tuned Design Knobs - Gear Ratio *g* (Functional)

Design Knob	Previous Range	New Value
g	8 to32	14 to 24

This allows a designer to not only see the desired solution, but also to gain some insight regarding neighboring solutions. At times, a neighboring solution may be found be acceptable or perhaps even better. The output speed requirement affects the design maps through the dynamic factor K_v (See 2.2.1.2). For the design map of the Rated

Torque versus the primary design knobs, a reference plane will be drawn at 833 ft-lbf to reflect the required rated torque. Thus, any of the design solutions that lie above the reference plane may possibly be chosen as the solution for the given design problem. Initially, the diametral pitches will not be constrained to only commonly available values (See Table 2-2). The relevant design maps are shown in Figure 4-1. Note that only the design solutions with rated torques greater than what is required (833 ft-lbs) are shown in the design map for length *L*.

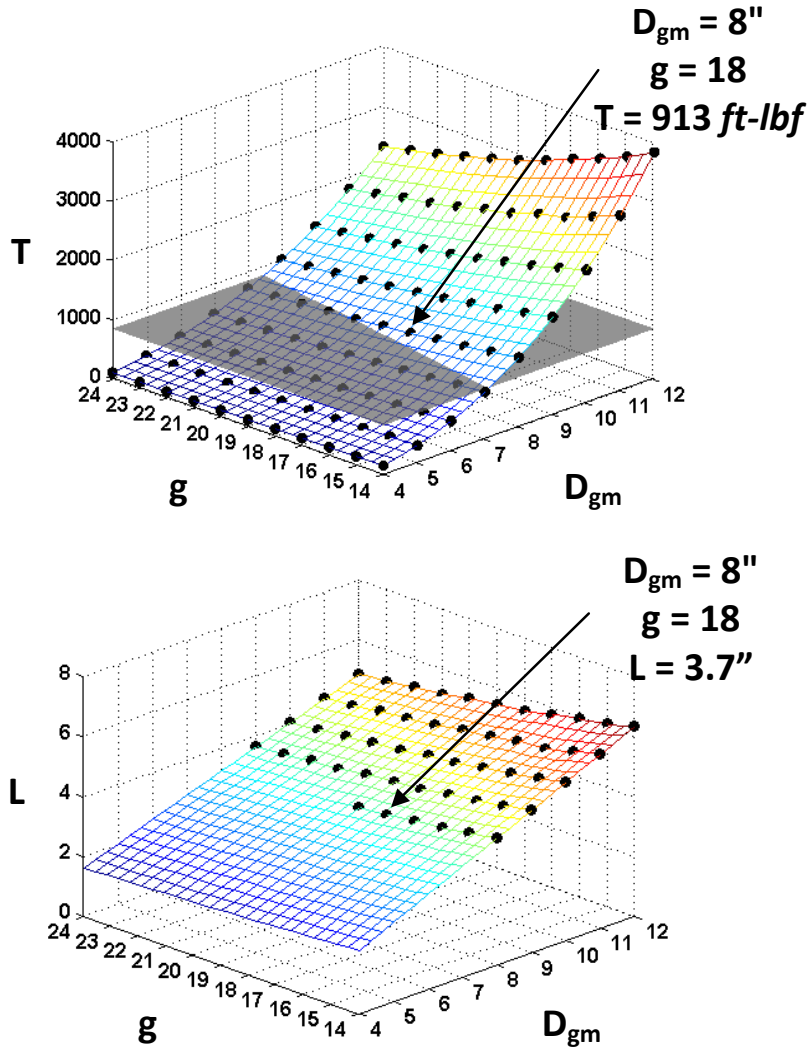

Figure 4-1: Design Maps - Rated Torque (above) and Length (below)

The two design maps shown in Figure 4-1 are sufficient to choose a design solution based on the nominal set of design requirements shown in Table 4-1. Major design parameters corresponding to the chosen design solution are listed in Table 4-3.

Table 4-3: List of Design Parameters corresponding to the chosen Design Solution

N_P	No. of teeth on the Input Pinion	34	
N_{LS}	No. of teeth on the Large Star gears	133	
N_{SS}	No. of teeth on the Small Star gears	22	
N_R	No. of teeth on the Ring gear	101	
D_P	Pitch Diameter of the Input Pinion	0.91	inch
D_{LS}	Pitch Diameter of the Large Star gear	3.55	inch
D_{SS}	Pitch Diameter of the Small Star gear	1.24	inch
D_R	Pitch Diameter of the Ring gear	5.69	inch
P_{d1}	Diametral Pitch in Mesh 1	37.505	$inch^{-1}$
P_{d2}	Diametral Pitch in Mesh 2	17.745	$inch^{-1}$
F_1	Face width of gears in Mesh 1	0.906	Inch
F_2	Face width of gears in Mesh 2	1.210	inch
D_{gm}	Gear Mesh Diameter	8.0	inch
g	Gear Ratio	18	
T	Rated Torque Capacity	913.58	ft-lbf
L	Length	3.71	inch
W	Approximate Weight	47.44	lbf
TD	Torque Density	19.26	ft-lbf/lbf
I	Inertia	2.19E-03	$lbm\text{-}in^4$
R_I	Input Responsiveness	1.30E+04	rad/s^2
R_O	Output Responsiveness	39.89	rad/s^2
A	Aspect Ratio	0.46	

It is also possible to *see* from the design map for rated torque in Figure 4-1, that the rated torque corresponding to the chosen solution (913 ft-lbf) is well above what is required (833 ft-lbf). It appears that the reference plane cuts across the design map between D_{gm} values of 7" and 8" for a gear ratio of 18. Therefore, a designer could choose to narrow down and refine the D_{gm} range. For example, the range could be from

7” to 8” in increments of 0.2”. With the D_{gm} design knobs set to the new range mentioned above, the design maps obtained are as shown in Figure 4-2.

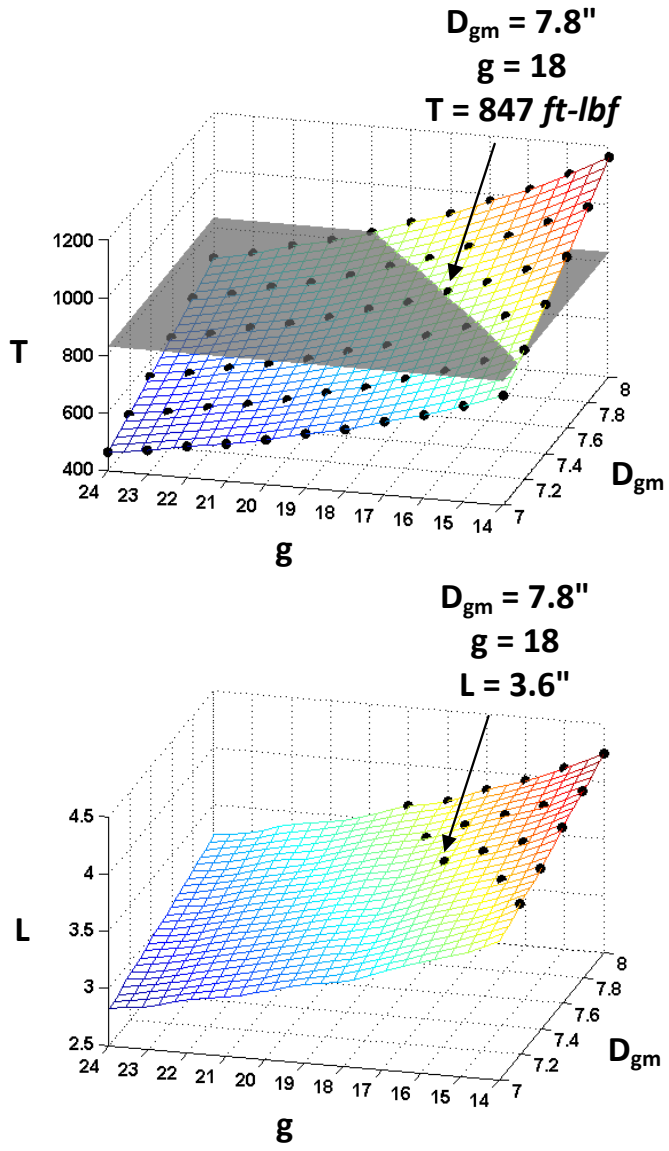

Figure 4-2: Design Maps (With design knob D_{gm} tuned) - Rated Torque (above) and Length (below)

Thus, by simply *looking* at the design maps in Figure 4-1, it is possible to deduce how to tune a design knob (D_{gm}) so that a more appealing final design solution is obtained. The design solution chosen from the design maps in Figure 4-2 is smaller in diameter as well as length compared to the design solution obtained from the design maps in Figure 4-1, but still achieves an adequate rated torque capacity.

For further discussion, the D_{gm} design knobs are reset to their original values in Table 3-2; i.e., 4" to 12" in increments on 1".

4.1.2 Addition of Material Constraints for Reduced Cost

For the design maps shown in Figure 4-1, the material used was AGMA Grade 2 carburized and hardened steel (s_t = 70 ksi and s_c = 225 ksi). As Table 2-12 showed, Grade 1 material is typically used in industrial practice. The geometric dimensions; i.e., diameter D and length L for the design solution from Figure 4-1 were well within the geometric constraints defined (see Table 4-1). Therefore, it is worth investigating if Grade 1 material is sufficient for the current design requirements. The reader should recognize that by using AGMA Grade 1 steel rather than AGMA Grade 2 steel, the cost is reduced (see Table 2-12). The design knobs s_t and s_c from Table 3-2 are therefore modified to correspond to carburized and hardened AGMA Grade 1 steel (s_t = 55 ksi and s_c = 180 ksi). This will be treated as a material constraint for the all of the following design maps in Section 4.1.

Table 4-4: Tuning of Design Knobs – Allowable Stresses (Material)

Design Knob	Previous value	New Value
s_t	70 ksi	55 ksi
s_c	225 ksi	180 ksi

All the other design knobs are kept same as those in Table 3-2. The updated design maps for rated torque and length are shown in Table 4-3.

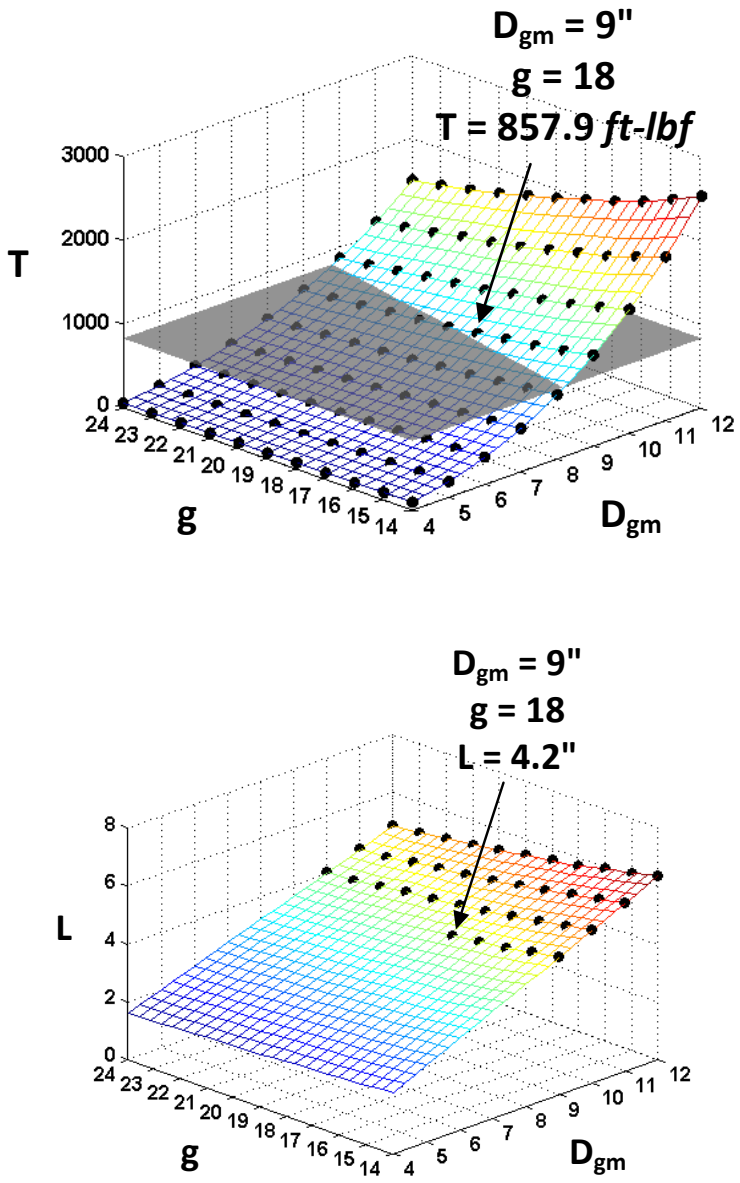

Figure 4-3: Design Maps (With design knobs st and sc tuned) – Rated Torque (above) and Length (below)

As Figure 4-3 shows, the gear mesh diameter D_{gm} as well as the length L of the chosen design solution are larger than those in Figure 4-1, but still within the nominal geometric constraints (see Table 4-1) By visually comparing the area of the rated torque

design map from Figure 4-1 with that in Figure 4-3, it is possible for a designer to get a quick assessment of the drop in performance as a result of using material of a lower AGMA grade. The design procedures developed in Chapter 2, allow the creation of new design maps (corresponding to newly tuned design knobs) within seconds.

4.1.3 Demand for Increased Performance – Weight

Up to this point, only design maps for the Rated Torque T and the Length L were provided. The reader should note however, that as Table 4-3 shows, each data point on a design map has a *complete* design solution associated with it. Thus, even though only design maps for rated torque and length were presented, design maps for any of the other performance parameters are also available at all times. It is up to the designer to decide which design maps are sufficient for a particular application.

The design map for weight W corresponding to the chosen design solution in Figure 4-3 is shown in Figure 4-4 (only solutions with adequate rated torque are shown).

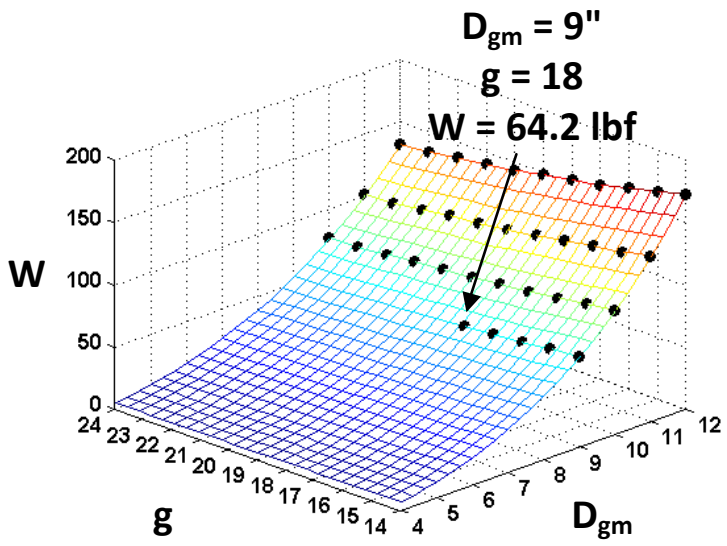

Figure 4-4: Design Map - Weight

The weight corresponding to the chosen design solution is 64.2 *lbf*. Note that the nominal design requirements in Table 4-1 did not include any constraint on the maximum allowable weight. Suppose that the weight is now constrained to a maximum of 42 *lbf*. The new, more demanding set of design requirements are summarized in Table 4-5.

Table 4-5: Summary of Updated Design Requirements

Design Requirement	Value
Rated Torque	833 *ft-lbf*
Output RPM	7.5 RPM
Gear Ratio	18
Max. Diameter	11 *in*
Max. Length	5 *in*
Weight	42 *lbf*
Life	10^7 revolutions at the output

A discussion on basic gear nomenclature, as well as a description of the AGMA stress equations and related terms, was provided in Chapter 2. Section 3.2 listed a set of design knobs that a designer could tune in order to arrive at a satisfactory set of design maps. Based on the gear design background provided in Chapter 2 and Chapter 3, the problem at hand can be tackled.

It should be apparent that, since a design solution with reduced weight is sought, it is necessary to try and increase the torque density of the gear train designs. Based on the discussion in Section 2.1.3, a designer should see that there are two ways to do this. The first is to increase the pressure angle in the gear teeth. The second is to increase the helix angle; i.e., use helical gears. Note that the values for helix angles ψ_1 and ψ_2 in Table 3-2 were equal to zero; i.e., spur gears were specified. Also, in Table 3-2, the values for the pressure angles φ_1 and φ_2 were equal to 25^o (high). Although increasing the pressure angle further would result in greater rated torque capacity, doing so would require custom cutting tools for gear manufacturing. For the purposes of this design

problem, let us assume that the gear train is to be designed as a one-off design, and not for mass manufacturing. Specifying pressure angles higher than 25^o would therefore result in prohibitively high cost. Therefore, this option is ruled out. With the constraint on material in Section 4.1.2, using Grade 2 material is not an option. Therefore, the only design knobs that a designer is now free to tune are the ones for helix angles. Geometry factor information is available from AGMA (AGMA 908-B89) for helix angles of 0^o, 10^o, 15^o, 20^o, 25^o and 30^o. Therefore, this report will be restricted to the use of these values. [ref] states that helix angles of 15^o generally have maximum bending strength. Strength in pitting (contact stress) is approximately equal for teeth with helix angles 10^o and greater. The findings of the current research are that the torque capacity significantly increases when the helix angle is increased from 0 to 10^o. The use of helix angles greater than 10^o does not significantly affect the rated torque capacity (an indication that contact stresses are limiting) but does have a significant effect on bearing thrust loads and tooth contact ratios. This will be shown in a later section. For the present design problem, the design knobs ψ_1 and ψ_2 are set to 10^o. The resulting design map for weight W is shown in Figure 4-5.

Table 4-6: Tuning of Design Knobs - Helix Angles (Tooth System)

Design Knob	Previous value	New Value
ψ_1	0^o	10^o
ψ_2	0^o	10^o

As Figure 4-5 shows, with the required gear ratio fixed at 18, a design solution with a weight W equal to 44.6 *lbf* is available for a D_{gm} of 8". However, consider the corresponding design map for rated torque shown in Figure 4-6. A quick glance at the design map in Figure 4-6 should give a designer the following insight: For a gear ratio of 18, the rated torque value (1059 *ft-lbf*) for the solution with a D_{gm} of 8" lies well above

the reference plane. The rated torque value for the solution with the same gear ratio but a D_{gm} of 7" (point A in Figure 4-6) lies just below the reference plane.

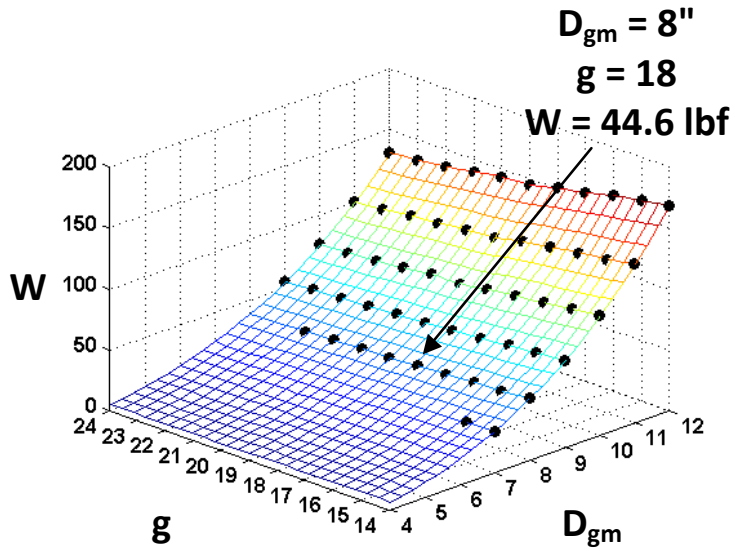

Figure 4-5: Design Map (With design knobs ψ_1 and ψ_2 tuned) - Weight

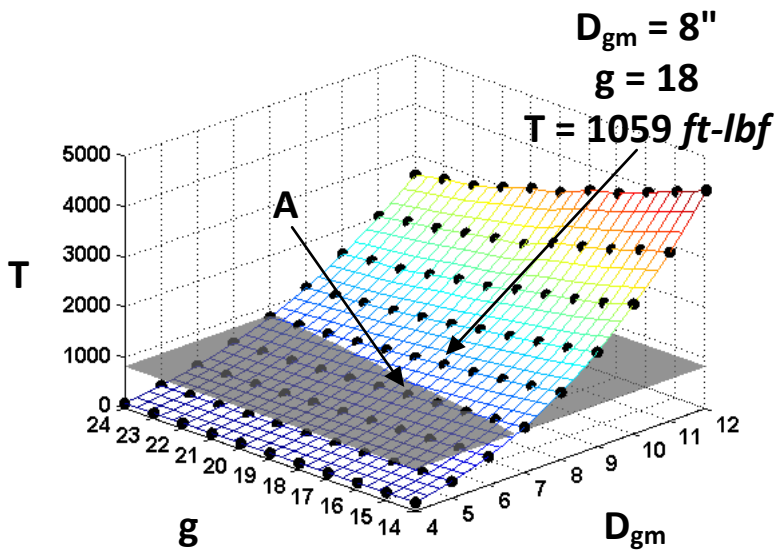

Figure 4-6: Design Map (With design knobs ψ_1 and ψ_2 tuned) - Rated Torque

Therefore, the next step is to tune the design knobs D_{gm} so that the range of D_{gm} values between 7” and 8” may be investigated. In other words, the designer is narrowing down on a satisfactory design solution. With the rest of the design knobs unchanged, D_{gm} is set to range from 7” to 8” in increments of 0.1”.

Table 4-7: Tuning of Design Knobs - Diameter (Geometric)

Design Knob	Previous value	New Value
D_{gm}	4” to 12” in increments of 1”	7” to 8” in increments of 0.1”

The design map for rated torque corresponding to the updated values of the design knobs is shown in Figure 4-7. Note that the rated torque is 841.2 *ft-lbf*, much closer to the required rated torque of 833 *ft-lbf* compared to the previous design solution (1059 *ft-lbf*). Therefore, the updated design knobs ensure that the gear train is not overdesigned.

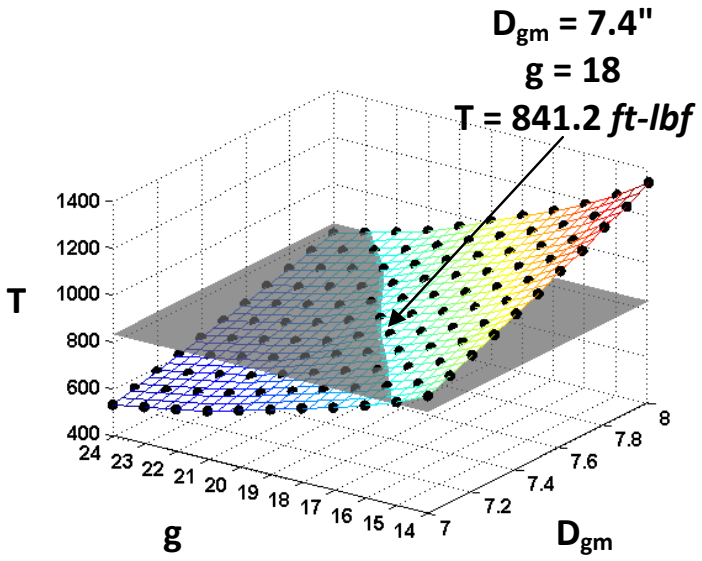

Figure 4-7: Design Map (With design knob D_{gm} tuned) - Rated Torque

The design maps for length L and weight W corresponding to the updated design knobs are shown in Figure 4-8. The weight W can be seen to be just 35.48 *lbf* which is well within the maximum allowed (42 *lbf*).

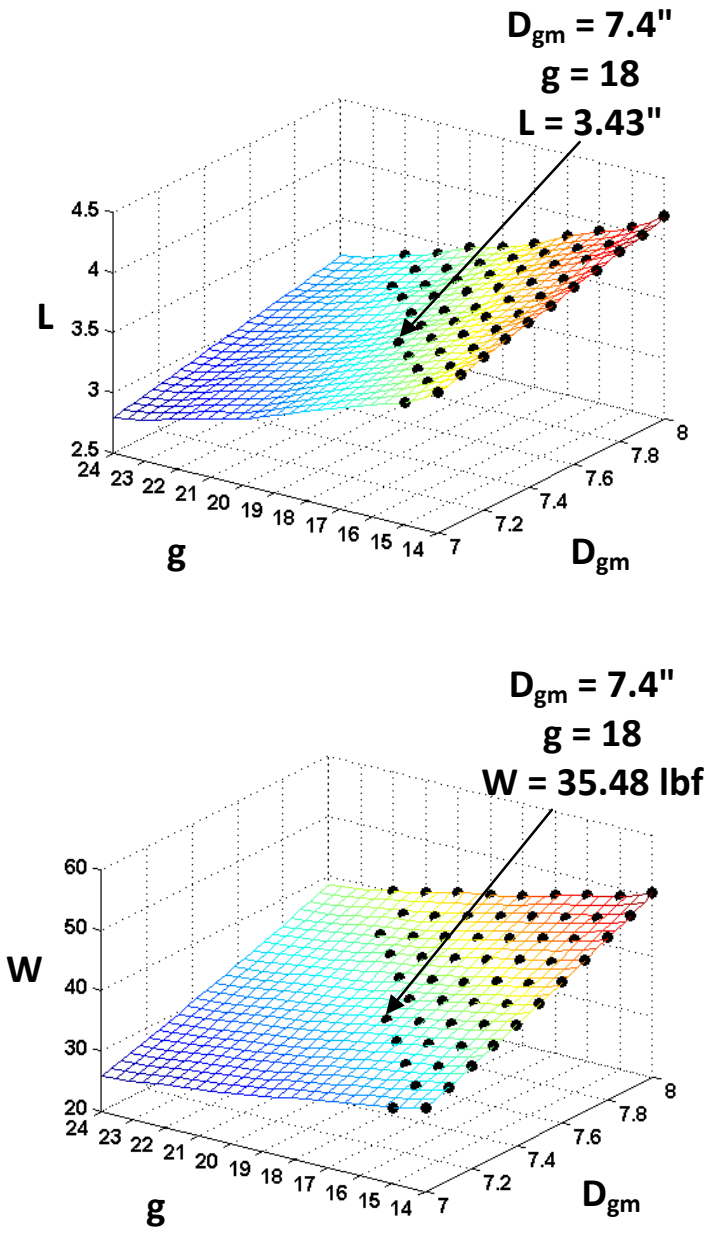

Figure 4-8: Design Map (Design knob D_{gm} tuned) - Length (above) and Weight (below)

Comparing the new design solution obtained using helical gears (Figure 4-7 and Figure 4-8) with the older solution using spur gears (Figure 4-3 and Figure 4-4); a very important observation is made. In this design problem, the use of helical gears instead of spur gears resulted in a significant reduction in weight of approximately *44%* (64.2 *lbf* down to 35.48 *lbf*). An assessment of the benefit offered by helical gears in comparison to spur gears can be made by creating design maps for the Torque Density T_D for both the spur (design knobs ψ_1 and ψ_2 equal to zero) and helical gear train (ψ_1 and ψ_2 equal to 10) designs for the present valve actuator gear train design problem.

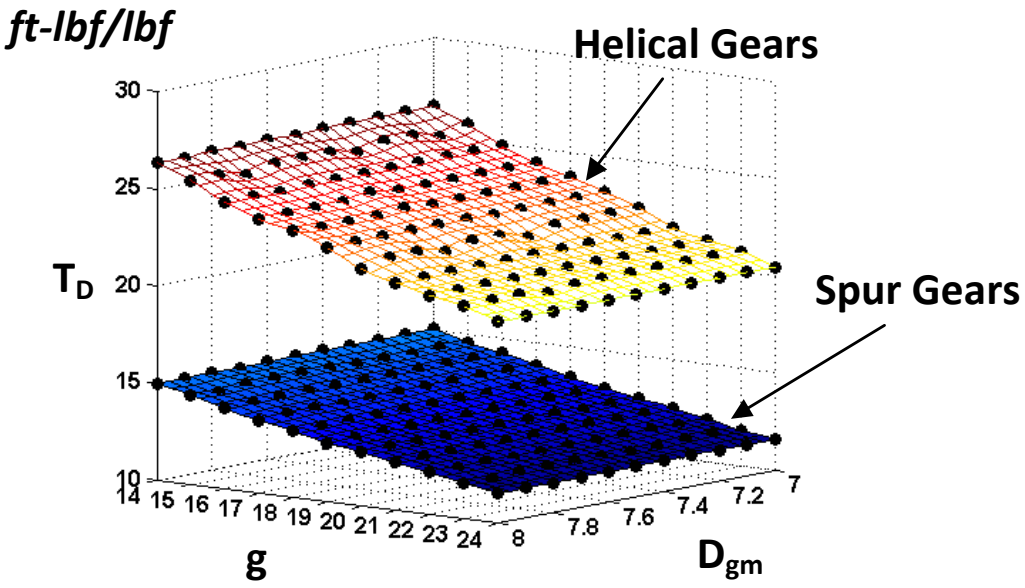

Figure 4-9: Design Map - Torque Density Comparison

The design maps in Figure 4-9 indicate that the torque density for the gear train with helical gears is, on average, 1.75 times higher than that for the spur gear. The current research found that this is roughly true for any 1-Stage SCGT. Generally speaking, for a

1-Stage SCGT, all other parameters being the same, the torque density increases by 1.6-1.75 times when helical gears are used instead of spur gears.

4.1.4 Addition of Tooling Constraint for Reduced Cost

So far, a set of nominal design requirements was first presented. Then, two constraints (see Section 4.1.2 and Section 4.1.3) were added to increase the difficulty of finding an improved design solution for the given design problem. At this stage, another constraint is added to make the problem harder still.

Typically, diametral pitch values are restricted to whole numbers (ref). Thus far however, no effort was made to ensure that the diametral pitches were whole numbers (see Table 4-3). Although gears can be cut with any diametral pitch values, the cost for special tooling can be avoided if a designer only specifies commonly available diametral pitches. Therefore, this constraint will be added to the previous list of design requirements. A summary of the design requirements for the valve actuator gear train at this stage is shown in Table 4-8.

Table 4-8: Summary of Updated Design Requirements

Design Requirement	Value
Rated Torque	833 *ft-lbf*
Output RPM	7.5 RPM
Gear Ratio	18
Max. Diameter	11 *in*
Max. Length	5 *in*
Weight	42 *lbf*
Life	10^7 revolutions at the output

So far, design maps have been updated by changing the values for the design knobs. The design knobs provide a designer with high-level decision making ability. Examples of this are the ability to decide whether to use helical gears or spur gears, the ability to choose gear materials appropriate to a given application and the ability to

control the overall geometry (D_{gm} and g (See Section 3.4.2.1)). In order to give the designer the power to control lower level decisions such as the diametral pitch, the concept of filtered designs was discussed in Section 2.7.5.

In the proposed design procedures in Chapter 2, for a given D_{gm} and g, a Design Solution Set containing numerous gear configurations is generated. By filtering the Design Solution Set through *constraint addition,* only design solutions with particular characteristics can be retained for use in design map generation. A list of useful criteria that may be used to filter the Design Solution Set was listed in Section 2.7.5. For the current design problem, design maps are generated with the diametral pitches constrained to integer values. With no change in the design knob values from Section 4.1.3, maps for the rated torque T, length L and weight W are generated.

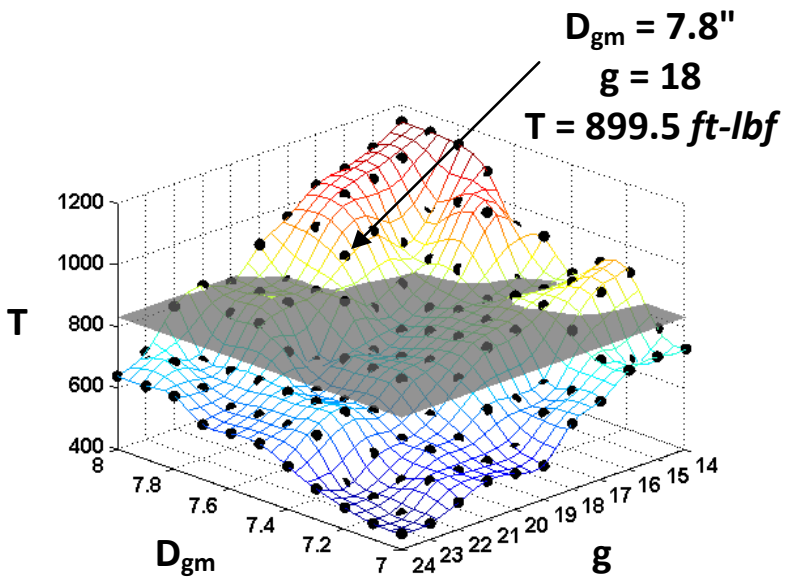

Figure 4-10: Design Map (With Constrained Diametral Pitches) - Rated Torque

These are shown in Figure 4-10 and Figure 4-11. Note how the addition of the constraint on diametral pitch leads to numerous 'dimples' in the design maps. The dimples occur because the diametral pitch constraint results in a limited number of gear tooth number and pitch diameter configurations, which suit some particular D_{gm} and g combinations better than others.

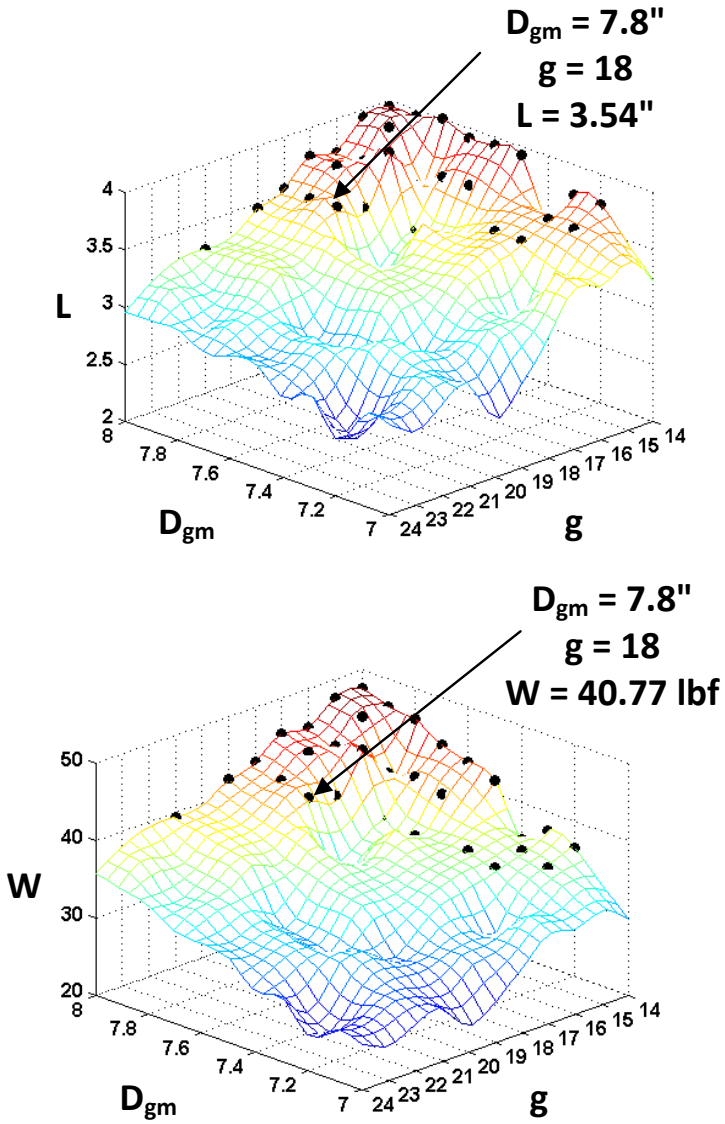

Figure 4-11: Design Maps (With Constrained Diametral Pitches) - Length (above) and Weight (below)

The chosen design solution (see Figure 4-10 and Figure 4-11) satisfies all of the current design requirements (Table 4-8). Major design parameters corresponding to the chosen solution are shown in Table 4-9. Thus, with 4 changes to the initial set of design knobs and the addition of one filter constraint, a design solution that satisfies all design requirements is found. Only a basic understanding gear nomenclature was necessary to be able to understand how to tune the design knobs.

Table 4-9: List of Design Parameters corresponding to the chosen Design Solution

N_P	No. of teeth on the Input Pinion	34	
N_{LS}	No. of teeth on the Large Star gears	131	
N_{SS}	No. of teeth on the Small Star gears	15	
N_R	No. of teeth on the Ring gear	70	
D_P	Pitch Diameter of the Input Pinion	0.89	inch
D_{LS}	Pitch Diameter of the Large Star gear	3.41	inch
D_{SS}	Pitch Diameter of the Small Star gear	1.17	inch
D_R	Pitch Diameter of the Ring gear	5.47	inch
P_{d1}	Diametral Pitch in Mesh 1	39.000	$inch^{-1}$
P_{d2}	Diametral Pitch in Mesh 2	13.000	$inch^{-1}$
F_1	Face width of gears in Mesh 1	0.89	Inch
F_2	Face width of gears in Mesh 2	1.14	inch
D_{gm}	Gear Mesh Diameter	7.8	inch
g	Gear Ratio	18	
T	Rated Torque Capacity	899.53	ft-lbf
L	Length	3.55	inch
W	Approximate Weight	40.77	lbf
TD	Torque Density	22.06	ft-lbf/lbf
I	Inertia	1.94E-03	$lbm\text{-}in^4$
R_I	Input Responsiveness	1.44E+04	rad/s^2
R_O	Output Responsiveness	44.37	rad/s^2
A	Aspect Ratio	0.45	

4.1.5 Notes on Design Problem 1

Design maps for the Inertia and Responsiveness were not presented in Section 4.1 because they were not necessary for the given design problem. In Design Problem 3, presented in the Section 4.3, these two performance criteria will be considered.

4.2 DESIGN PROBLEM 2 – WIND TURBINE GEAR AMPLIFIER (P-TYPE 2-STAGE SCGT)

The goal is to develop an unusually compact geared speed amplifier (about 90:1, to produce high power generator speeds from low turbine blade speeds). The Pancake Type 2-Stage Star Compound Gear Train offers great simplicity, symmetry, small diameter bearings in rugged stationary support structures, and ease of design and manufacture to accomplish this objective. Specifically, the wind turbine gear amplifier must have a rated torque capacity of 100,000 *ft-lbf* and run continuously at 20 rpm (at the Ring gear) for 20,000 hours. The power output (assuming no loss) is therefore 380 hp. In order to generate 1800 rpm at the motor shaft, a speed increase ratio of 90:1 is necessary. These design requirements were obtained based on wind turbine specifications from [ref] and [ref]. A summary of the design requirements is shown in Table 4-10.

Table 4-10: Summary of Design Requirements

Design Requirement	Value
Rated Torque	100,000 *ft-lbf*
RPM at Ring Gear	20 RPM
Gear Ratio	90
Max. Diameter	40 *in*
Max. Length	10 *in*
Weight	42 *lbf*
Life	24×10^6 rev at the Ring Gear

The primary aim in presenting these design problems is to demonstrate how the design procedures (Chapter 2) and design maps (Chapter 3) developed in this report simplify SCGT gear train design. Therefore, for the current design problem, both

versions of the P-Type 2-Stage SCGT (P-Type (6) and P-Type (3)) will be designed. Both versions of the P-Type SCGT's will be compared to see the relative benefits of one over the other, in the light of the current design requirements.

4.2.1 P-Type 2-Stage SCGT with 3 Amplifier Gears (P-Type-3)

Transmission in wind turbines are usually fabricated using high quality materials and small tolerances. Therefore, the design knobs for the Allowable stresses (s_t and s_c) will be set to those corresponding to AGMA Grade 2 Steel (70 *ksi* and 225 *ksi*). Since the rotational speeds are not high, initially spur gears will be specified. Note that, noise in spur gears can be reduced to a large extent using certain crowning techniques [ref]. The design knobs controlling maximum face-width (F_{rule}*'s*) will be set to 1. The length L (and aspect ratio A) will be controlled by adding a constraint to filter the Design Solution Set. The range for gear ratio g will be 60 to 120 is increments of 5. The range for D_{gm} will initially be 30" to 40" in increments of 1". Gears with 20^o pressure angles will be initially used to reduce bearing loads (see Section 2.1.3). The initial set of design knobs are listed in Table 4-11. With these design knob values, and the a priori parameters as in Table 3-2, the design map for rated torque obtained for a P-Type-3 SCGT is shown in Figure 4-12.

Table 4-11: Initial Set of Design Knobs for Design Problem 2

Design Knobs		
D_{gm}	Diameter	30" to 40" in increments of 1"
g	Gear Ratio	60 to 120 in increments of 5
$F_{rule1}.F_{rule2},F_{rule3}$	Rule for max. face-width	1,1,1
$\varphi_1,\varphi_2,\varphi_3$	Pressure Angles	25^o,25^o,25^o
ψ_1,ψ_2,ψ_3	Helix Angles	0^o,0^o,0^o
s_t	Allowable Bending Stress	70,000 psi
s_c	Allowable Pitting Stress	225,000 psi

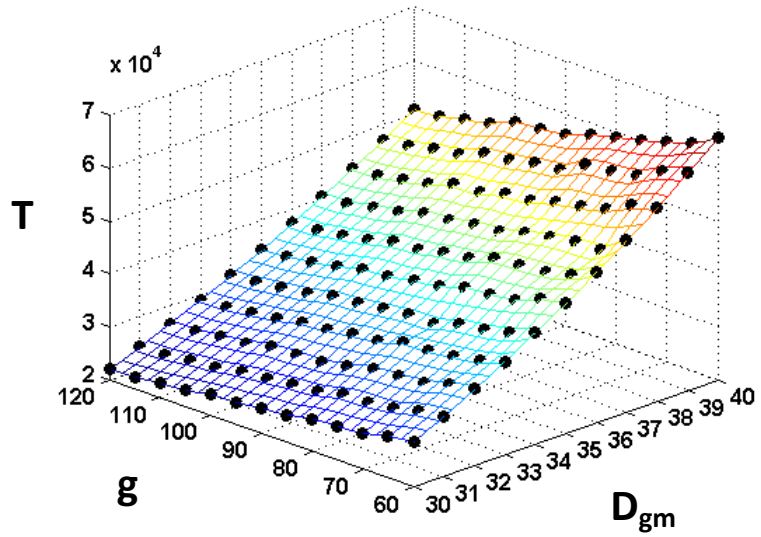

Figure 4-12: Design Map - Rated Torque

A glance at Figure 4-12 shows that the rated torque capacity is inadequate for the current design problem (maximum rated torque in the design map is about 70,000 *ft-lbf*). Therefore, a decision is made to use helical gears. Instead of switching all the gear meshes to helical, suppose only the design knob ψ_3 is set to 10^o. Therefore, the gears in Mesh 3 are helical but the others are gear meshes contain spur gears. This is primarily done to demonstrate to the reader that the design knobs can be changed individually. Also, some design insight is gained. To elaborate, consider the updated design map for the rated torque shown in Figure 4-13. When compared with the previous design map in Figure 4-12, it is apparent that the rated torque capacity with helical gears in Mesh 3 is significantly higher than when only spur gears were used. This indicates that the gears in Mesh 3 were limiting the rated torque capacity in Figure 4-12. Thus, by changing a single design knob and looking at an updated design map, a designer may gain some insight into a particular design problem. However, the required rated torque capacity is still not achieved. The entirety of the design map lies below the reference plane (100,000 *ft-lbf*).

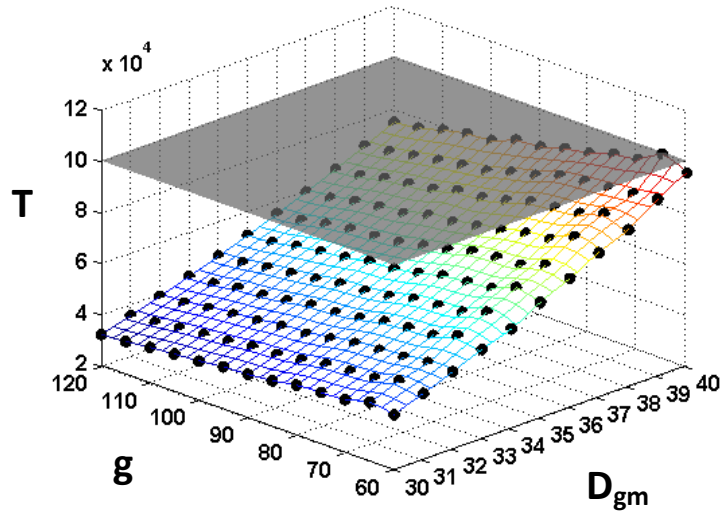

Figure 4-13: Design Map (Updated) -Rated Torque

Suppose that all three gear meshes are now specified with helical gears ($\psi_3 = \psi_3 = \psi_3 = 15^o$). The updated design map corresponding to the new set of design knobs is shown in Figure 4-14. The only design solution that achieves a gear ratio of 90 and the required rated torque has a D_{gm} of 40". The estimated actual diameter D is therefore 44".

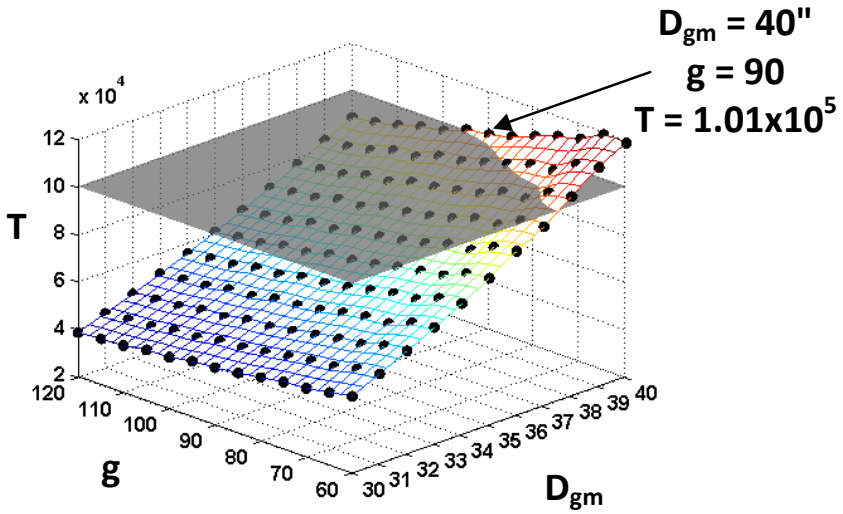

Figure 4-14: Design Map (with design knobs tuned) - Rated Torque

Based on the design map in Figure 4-14, a designer may choose one of two options. The first concerns the maximum face-widths. Although the recommended value for F_{rule} in this report is 1, it was mentioned in Section 2.2.1 that if high quality gearing and tight manufacturing tolerances are specified, it is possible to set F_{rule} as high as 1.25. In the AGMA technical paper titled "The Effect of Gearbox Architecture on Wind Turbine Enclosure Size" [ref], a value of 1.25 is used. The second option is to stop the P-Type-3 design and evaluate the P-Type-6 gear train performance. A decision is made to first explore the former option. With the F_{rule}*'s* set to 1.25, the design map shown in Figure 4-15 is obtained. The diameter D corresponding to the chosen design solution in Figure 4-15 is 41.25"; i.e., outside the maximum diameter allowed (see Table 4-10). Therefore, a designer is left with two options: the first is to use Grade 3 Steel in an effort to get higher torque density. The second option is to ignore the recommendation for the maximum face-width and use a value greater than 1.25 for F_{rule}.

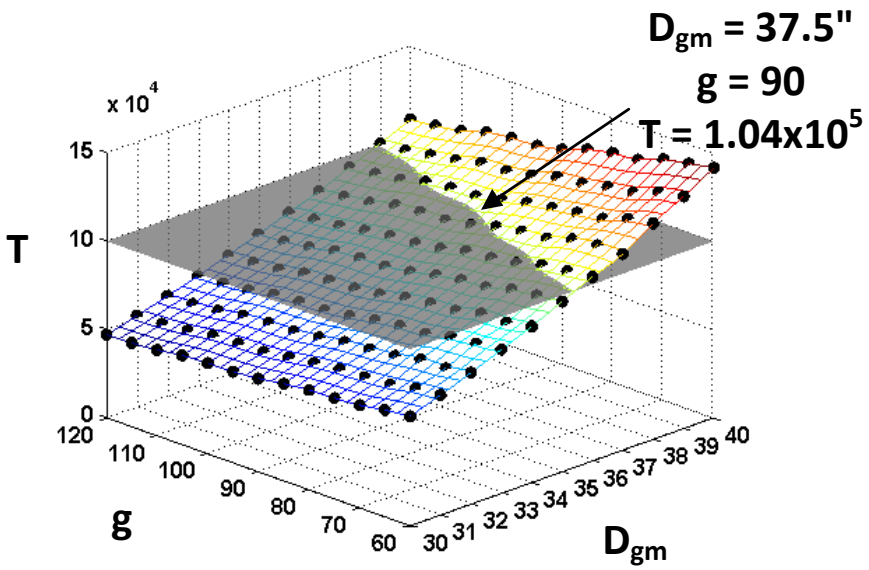

Figure 4-15: Design Map (with F_{rule} Updated) - Rated Torque

For the purpose of the current discussion, let us assume that neither of these options is viable. Using Grade 3 steel would result in prohibitively high cost and using longer face-widths might reduce service life due to non-uniform loading across the width of the gear teeth. Therefore, a decision is made to stop the P-Type-3 design at this stage and instead evaluate the P-Type-6 design.

4.2.2 P-Type 2-Stage SCGT with 6 Amplifier Gears (P-Type-6)

The design knobs for the P-Type-6 gear train are shown in Table 4-12. The corresponding design map for rated torque is shown in Figure 4-16. The design map shows that, even with the F_{rule} values set to 1, the P-Type-6 SCGT easily achieves the required rated torque within the maximum diameter constraint (40"). By checking the corresponding design map for length L (shown in Figure 4-17), it is seen that length L of the current design (10.2") is *just* outside what is allowed (see Table 4-10).

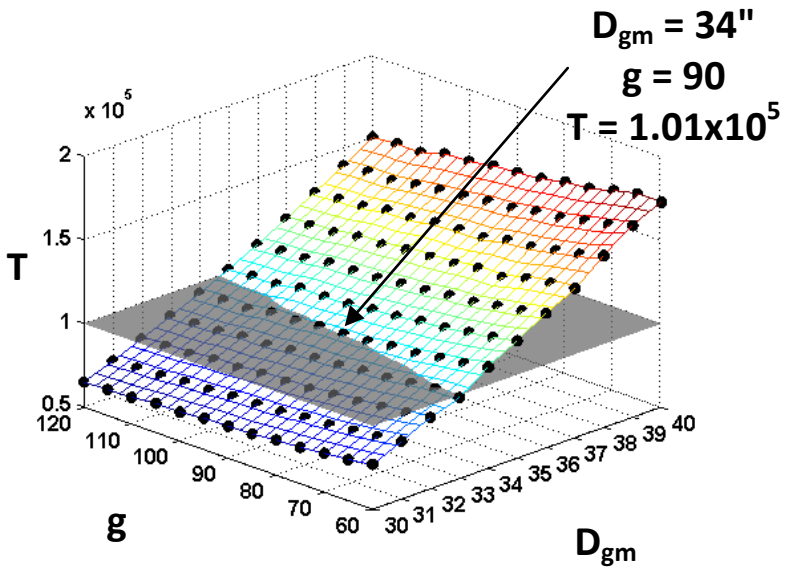

Figure 4-16: Design Map (P-Type-6) - Rated Torque

Table 4-12: Initial Set of Design Knobs for the P-Type-6 Design Maps

Design Knobs		
D_{gm}	Diameter	30” to 40” in increments of 1”
g	Gear Ratio	60 to 120 in increments of 5
$F_{rule1}.F_{rule2},F_{rule3}$	Rule for max. face-width	1,1,1
$\varphi_1,\varphi_2,\varphi_3$	Pressure Angles	25^o,25^o,25^o
ψ_1,ψ_2,ψ_3	Helix Angles	10^o,10^o,10^o
s_t	Allowable Bending Stress	70,000 psi
s_c	Allowable Pitting Stress	225,000 psi

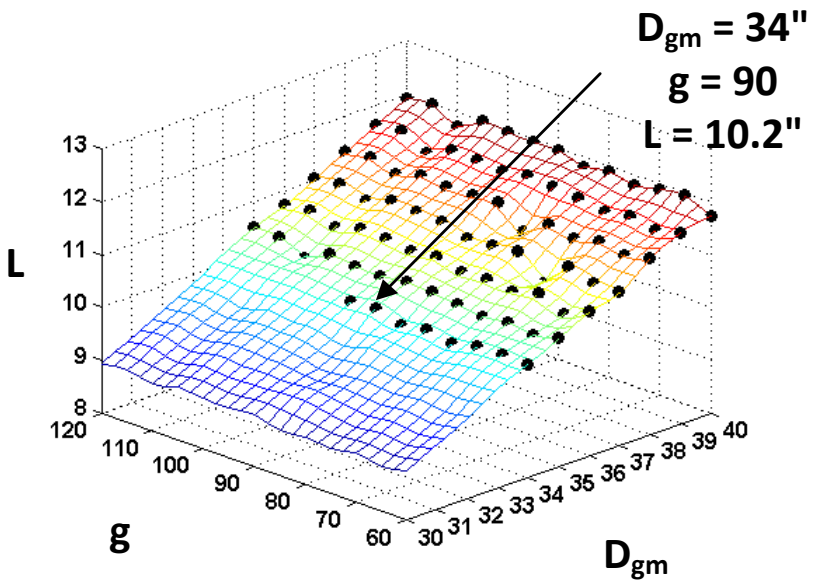

Figure 4-17: Design Map (P-Type-6) - Length

Recall from Section 3.4.2 that the length L was estimated by multiplying the sum of the face-widths (F_2 and F_3, in case of a P-Type SCGT (See Figure 2.22)) by a multiplication factor of 1.75. However, it was mentioned that this multiplication factor ranged between 1.5 and 2 depending on factors such as the thrust load on bearings and bearing type. If the resultant thrust load is large, tapered roller bearings are necessary to

support the gears. If the resultant thrust load is minimized, angular contact or even deep-groove ball bearings may be used. Both angular contact and deep groove ball bearings are in general smaller than tapered roller bearings. If resultant thrust loads are reduced such that they are almost zero, it may even be possible to use needle-roller bearings (radial load) together with a snap ring (thrust load) to support the gears. Thus, by making an effort to avoid the use of tapered roller bearings for the amplifier gears in SCGT's, it is possible to use a multiplication factor of around 1.5 for estimating the length L. Since at this stage of the current design problem, the length L is slightly greater than what is allowed, effort will be made to reduce the resultant thrust load in the amplifier gears. A detailed discussion on bearing types is beyond the scope of the current report. For the benefit of the reader, a brief discussion on calculating the resultant thrust load on the amplifier gear is presented.

4.2.3 Resultant Thrust Load in the Amplifier Gears

The axial (thrust) load generated at a helical gear tooth with a helix angle of ψ, given a tangential transmitted load of f^t is given by:

$$f^a = f^t \tan\psi \tag{3.19}$$

Recall that in the design procedures described in Chapter 2, the tangential transmitted loads in all gear meshes are known. Using Equation 4.1, the axial loads generated on the Large Star Gear (Mesh i) and the Small Star gear (Mesh i+1) can be obtained using:

$$f_i^a = f_i^t \tan\psi_i \tag{3.20}$$

$$f_i^a = f_i^t \tan\psi_i \tag{3.21}$$

Note that the index i can have values of either 1 or 2, depending on whether the 1st or the 2nd Amplifier gear is under consideration. The axial loads calculated using Equation 4.2 and Equation 4.3 can be made to oppose each other by choosing appropriate helix hands (see Appendix A). The magnitude of the resultant thrust load (f_{res}^{a}) on the amplifier gear is therefore given by:

$$f_{res}^{a} = f_i^{a} - f_{i+1}^{a} = f_i^{t} \tan\psi_i - f_{i+1}^{t} \tan\psi_{i+1} \tag{3.22}$$

In order to completely nullify the resultant thrust load, we have:

$$f_{res}^{a} = f_i^{a} - f_{i+1}^{a} = f_i^{t} \tan\psi_{i+1} - f_i^{t} \tan\psi_{i+1} = 0$$
$$\Rightarrow \frac{f_{i+1}^{t}}{f_i^{t}} = \frac{\tan\psi_i}{\tan\psi_{i+1}} \tag{3.23}$$

Substituting the amplification factor r_A in Equation 4.5, we finally get:

$$r_{Ai} = \frac{\tan\psi_i}{\tan\psi_{i+1}} \tag{3.24}$$

Thus, a powerful result obtained from Equation 4.6 is that, the resultant thrust load in an amplifier gear can be nullified if the helix angles ψ_i and ψ_{i+1} are chosen such that the ratio of the tangents of the helix angles equals the amplification factor. Note that, if a designer is constrained to specify only commonly available helix angles, he or she should choose them such that the ratio of the tangents of the helix angles is as close to the amplification factor as possible.

4.2.4 Design Refinement

At this stage of the current design problem, the goal is to try to reduce the length L of the gear train (10.2" currently) in order to satisfy the maximum length constraint (10") specified in the design requirements (see Table 4-10). The result obtained in

Section 4.2.3 can be used to achieve this goal. To illustrate, consider the 2nd Amplifier gear in the current design problem (see Figure 2-2). Since the tangential transmitted load is amplified in each amplifier gear, the tangential transmitted loads on the 2nd amplifier gear are higher than those in the 1st. Therefore, effort will be made to minimize the resultant thrust load in the 2nd amplifier gear. The resultant thrust load in the 2nd amplifier gear, with the current values ψ_2 and ψ_3, is shown in Figure 4-18.

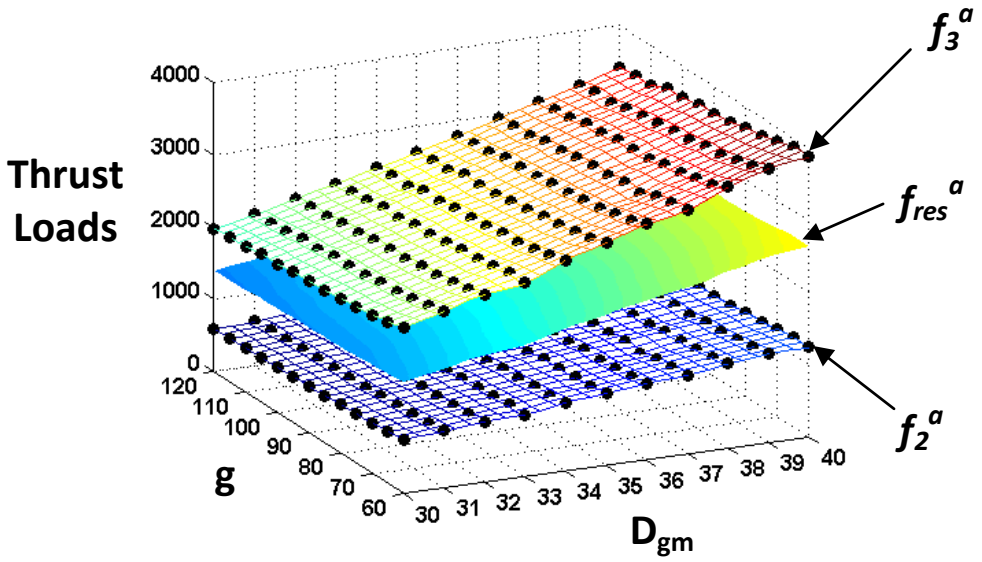

Figure 4-18: Design Map - Thrust Loads on the Second Amplifier Gear

A design map of r_{A2}; i.e., the amplification factor in the 2nd amplifier gear is shown in Figure 4-19. In Figure 4-19, only design solutions which have a gear ratio g of 90 are shown for clarity. As shown, the amplification factor r_{A2} is 3.284. A list of helix angles and the tangents of those helix angles are shown in Table 4-13.

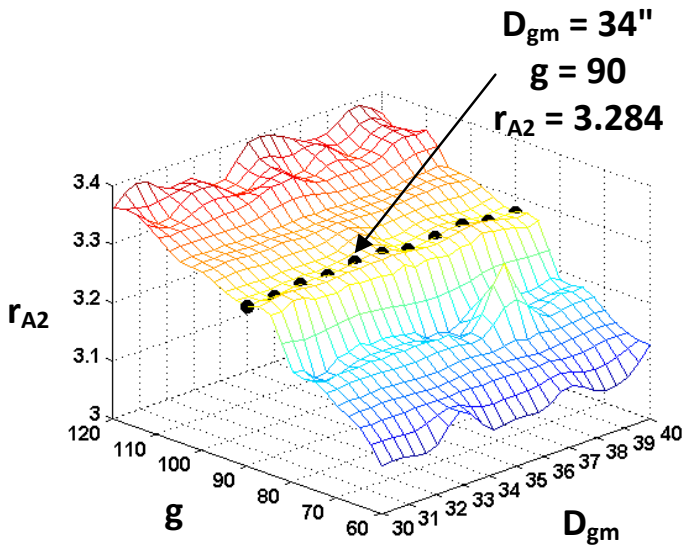

Figure 4-19: Amplification factor in the Second Amplifier Gear

Table 4-13: List of Helix Angles and Corresponding Tangent Values

ψ	$tan(\psi)$
0	0
10	0.1763
15	0.2679
20	0.3640
25	0.4633
30	0.5744

At the current stage of design, ψ_2 and ψ_3 are each equal to 10^o. From Table 4-13, the following observation may be made:

$$\frac{\tan 30^o}{\tan 10^o} = 3.2743 \qquad (3.25)$$

The value of 3.2743 shown in Equation 4.7 is very close to the value of r_{A2} (3.284) obtained from Figure 4-19. Using the result obtained from Equation 4.6, we can conclude that in order to minimize the resultant thrust load in the 2nd Amplifier gear, the design knob ψ_2 should be changed to 30^o. The updated design map is shown in Figure 4-20. It

can be seen that the resultant thrust load in the 2nd Amplifier gear is reduced almost to zero. This implies that, with regard to load capacity and noise, the design solution gains the full benefit of using helical gearing, while almost nullifying the undesirable thrust loads generated due to the helical gear teeth.

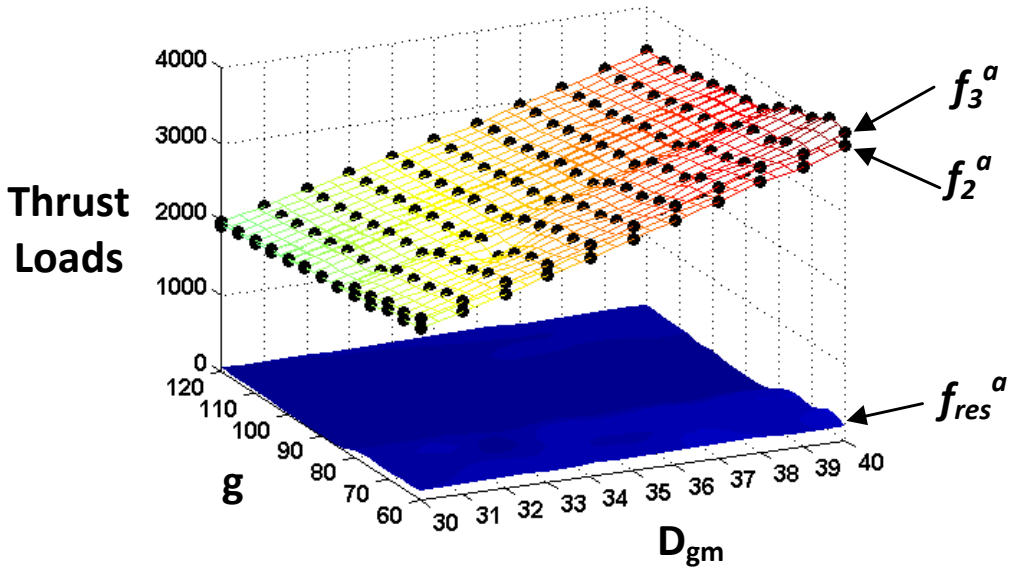

Figure 4-20: Design Map (with Updated Design Knobs) - Thrust Loads on the Second Amplifier Gear

Thus, it is possible to use simple deep groove ball bearings rather than large tapered roller bearings to support the 2nd Stage amplifier gears. As a result of this, it is possible to use a multiplication factor of 1.5 rather than 1.75 when estimating the gear train length *L* (See Section 4.2.2). The length obtained using a multiplication factor of 1.5 is 8.74".

Therefore, all of the design requirements specified in Table 4-10 are met. The design solution chosen in Figure 4-16 may be chosen and pursued to a more detailed design stage.

4.3 DESIGN PROBLEM 3 – C-TYPE 2-STAGE SCGT FOR A MDW ACTUATOR

Two preliminary Coffee-Can Type 2-Stage Star Compound Gear Trains are to be designed for use in a multi-speed drive wheel (MDW) for a high-performance sports car. The basic idea is that a single designer should quickly generate two alternative preliminary designs. The discussion in this section will demonstrate the design process developed in this report to allow a single designer to handle this task with ease. The alternative designs can then be compared and the better one chosen for detailed design by a multi-person team.

The gear trains must have a rated torque T of 750 ft-lbs and an overall gear ratio g of 48 ± 0.5. The maximum output speed is 1000 rpm. The maximum input speed for both of the 1st (Front End) and 2nd stages (Back End) is 15000 rpm. The splitting of the overall gear ratio g between the two stages (g_f and g_b) for each of the design alternatives is shown in Table 4-14.

Table 4-14: Distribution of Gear Ratio between the First and Second Stages

Gear Ratio per Stage	Alternative-1	Alternative-2
g_f (Front End)	4.8	3.4
g_b (Back End)	10	14

The gear trains are to last for a 100,000 miles. It is essential to keep weight as low as possible. Therefore, an aggressive maximum weight constraint of 50 lbs is set. The MDW must be fit within the wheels of the vehicle. Therefore, the maximum diameter D of the gear trains must not exceed 10". The length L should be limited to 5.25" to be able to incorporate the driving motor within the wheel volume. Effort should be made to keep noise low. A summary of the design requirements are shown in Table 4-15.

Table 4-15: Summary of Design Requirements for the MDW Gear Trains

Design Requirement	Value
Rated Torque	750 *ft-lbf*
Output RPM	1000 RPM
Gear Ratio	48
Max. Diameter *D*	10 *in*
Max. Length *L*	5.25 *in*
Life	100,000 miles

For a 24" wheel diameter, the life requirement translates to 84 million output revolutions N for the gear trains. With regard to the a priori parameters, this number N affects the stress life cycle factors (See Section 2.2.1.11) used in the AGMA stress equations. The effect of the output speed is incorporated into the AGMA stress equations through the dynamic factor K_v (See Section 2.4.1.2). The list of a priori parameters shown in Table 3-2 is unchanged apart from the stress cycle and dynamic factors mentioned above. With regard to the design knobs, the following can be said: As mentioned is Section 2.6, the suggested approach to the design of a C-Type 2-Stage SCGT is to design the 2nd Stage first and then design an appropriate 1st Stage. The design process for the 2nd Stage is exactly the same as for the 1-Stage SCGT. Since D is to be less than 10", D_{gm} should approximately less than 9". Suppose that the range for the design knobs for D_{gm} is initially 4" to 8" in increments of 0.5". The range for g is 8 to 16, thus encompassing the required g_b values. Due to the high input speeds and requirement for low noise, a decision is made to use helical gearing. The design knobs ψ_1 and ψ_2 are set initially to 10^o. Hardened and carburized Grade 2 Steel will be used for high performance. A summary of these initial values for the design knobs is shown in Table 4-16.

Table 4-16: Summary of the Initial Set of Design Knobs

Design Knobs		
D_{gm}	Diameter	4” to 8” in increments of 0.5”
g (g_b)	Gear Ratio	8 to 16 in increments of 1
F_{rule1}, F_{rule2}	Rule for max. face-width	1,1
φ_1, φ_2	Pressure Angles	25^o,25^o
ψ_1, ψ_2	Helix Angles	10^o, 10^o
s_t	Allowable Bending Stress	70,000 psi
s_c	Allowable Pitting Stress	225,000 psi

The design map for rated torque corresponding to the current set of a priori and design knob parameters is shown in Figure 4-21. It appears that solutions with D_{gm} values around the range of 4.5-6.5 achieve the required rated torque capacity (750 *ft-lbf*). A designer could thus make a decision to narrow down the D_{gm} range and look at an updated design map. An updated design map for the rated torque with D_{gm} ranging from 4.4” to 6.4” in increments of 0.2” is shown in Figure 4-22.

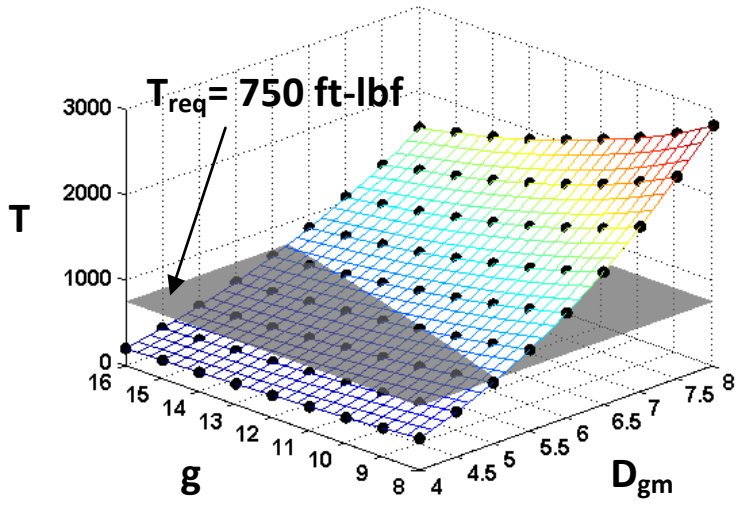

Figure 4-21: Design Map - Rated Torque

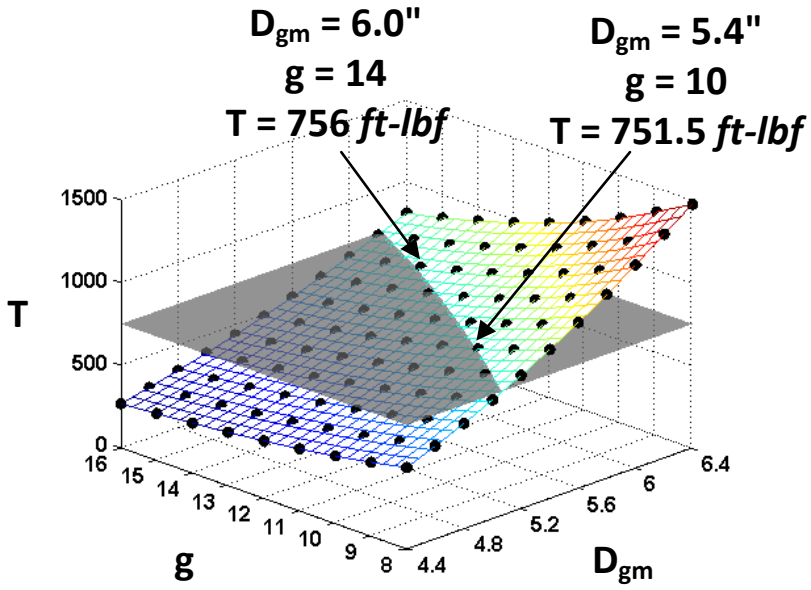

Figure 4-22: Design Map (With D_{gm} Tuned) - Rated Torque

As Figure 4-22 shows, a single design map can be used to compare the two alternative design solutions. Alternative-1 with a gear ratio of 10 can be realized with a gear train with D_{gm} equal to 5.4" whereas Alternative-2 requires a gear train with a D_{gm} of 6" to achieve the required rated torque capacity. In Section 4.1, information about the length of the gear train was obtained by looking at design maps for length L. For the current problem however, an alternative approach that a designer may use is presented. As Figure 3-26 showed, unless otherwise restricted, the aspect ratio A was found to be purely a function of the gear ratio g. By consulting the plot for the aspect ratio A (shown in Figure 4-23), the following observations are made: When g equals 10, the aspect ratio A is 0.65 and when g equals 14, the aspect ratio A is 0.55. Thus, the length L for a given D_{gm} and g can be easily calculated by multiplying D_{gm} by A. Therefore, the same design map from Figure 4-22 is shown in Figure 4-24 with additional information on length L.

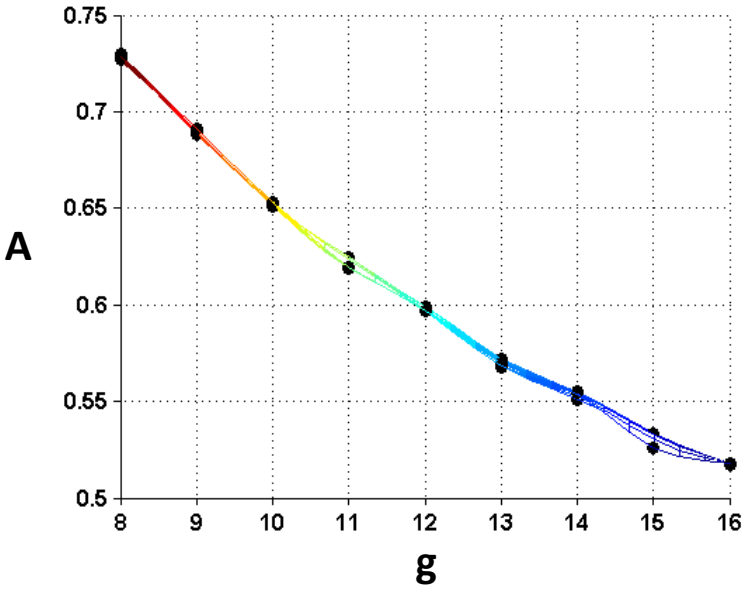

Figure 4-23: Plot of Aspect Ratio *A* versus Gear Ratio *g*

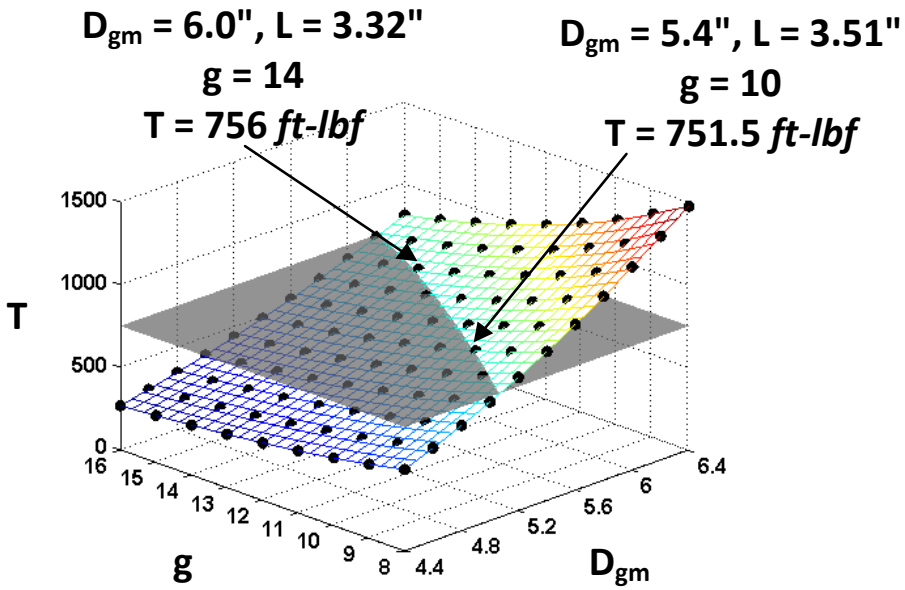

Figure 4-24: Design Map (With D_{gm} tuned) - Rated Torque

At this stage, it is clear that both the gear trains being designed are easily able to meet the constraint on maximum diameter (see Table 4-15). At this stage of the design process, the lengths of the 2nd stage gear trains are known, but it is as yet unknown if the 1st stage gear trains can be accommodated within the length constraint in Table 4-15. The same can be said regarding the weight *W*. The design map for weight W (Figure 4-25) shows the weights of the 2nd stages for the competing alternatives.

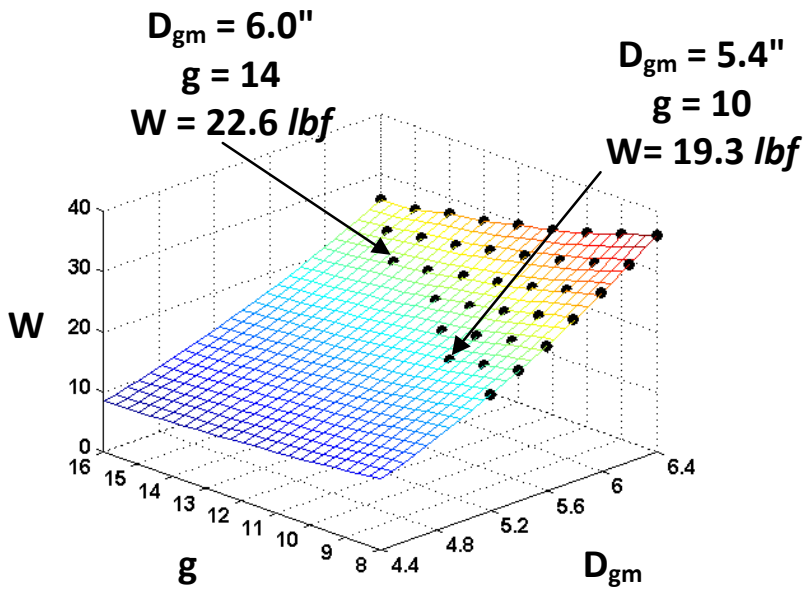

Figure 4-25: Design Map - Weight

When designing for appropriate 1st stage gear trains, it is necessary to know the *total* length, weight or torque density of the C-Type 2-Stage SCGT's. Therefore, a method by which information about the whole gear train can be visually presented to a designer is shown in Section 4.3.1. By doing this, selection of the appropriate 1st stage gear train for a given 2nd stage gear train is greatly simplified.

4.3.1 Combined First and Second Stage Gear Train Performance Visualization

The 2nd Stage gear trains for the two competing alternatives have been chosen at this stage in the design process. It is understood that the torque required at the input to the 2nd stage gear trains must be provided at the output of the 1st stage gear trains. This is because the two gear train stages in a C-Type 2-Stage SCGT are serially connected. Therefore, the required rated torque from the 1st stage gear train (Front End) equals the rated torque capacity of the 2nd gear train (Back End) divided by the gear ratio g_2. Thus, the required rated torque from the Front End equals the rated torque capacity of the MDW gear train (750 *ft-lbf*) divided by the gear ratio in the Back End; 10 and 14 for the two alternatives being considered for this design problem. Consider the design map for the Rated Torque in the Front End shown in Figure 4-26.

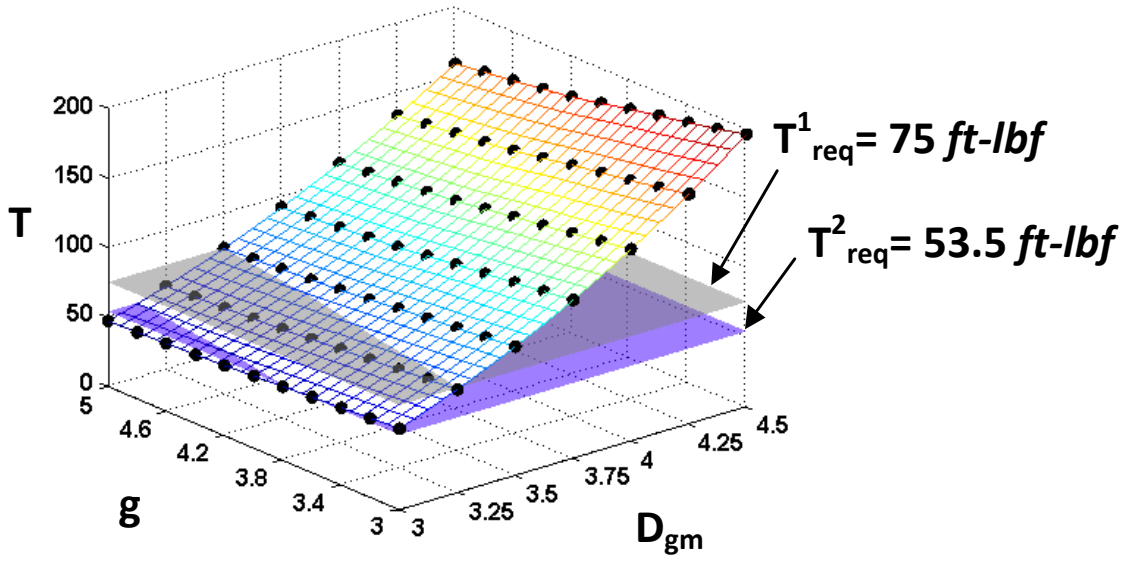

Figure 4-26: Design Map - Rated Torque in the Front End

The design map in Figure 4-26 corresponds to the design knobs shown in Table 4-17.

Table 4-17: Summary of Design Knobs for the Front End

Design Knobs		
D_{gm}	Diameter	3" to 4.5" in increments of 0.25"
g	Gear Ratio	3 to 5 in increments of 0.2
F_{rule1}, F_{rule2}	Rule for max. face-width	1,1
φ_1, φ_2	Pressure Angles	25^o,25^o
ψ_1, ψ_2	Helix Angles	10^o, 10^o
s_t	Allowable Bending Stress	70,000 psi
s_c	Allowable Pitting Stress	225,000 psi

The design knobs in Table 4-17 are obtained using the same reasoning as that used to obtain the initial design knobs for the Back End (see Table 4-16).

The important observation to make in Figure 4-26 is that there are *two* reference planes. Each reference plane indicates the rated torque required from the Front End design solutions, given chosen design solutions for the Back End. To elaborate, the upper reference plane (75 *ft-lbf*) in Figure 4-26 indicates the rated torque required from the Front End, for the Back End corresponding to Alternative-1 (g_b = 10). Any design solutions lying above this plane indicate possible Front End solutions for the Back End from Alternative-1. The lower reference plane (53.5 *ft-lbf*) is the rated torque required from the Front End, for the Back end corresponding to Alternative-2 (g_b = 14). Therefore, any design solutions lying above this plane indicate possible Front End solutions for the Back End from Alternative-2. This is illustrated more clearly in Figure 4-27. With the observation that a large portion of the design maps in Figure 4-26 lie above the reference planes, a decision is made to use Grade 1 Steel instead of Grade 2 Steel. This helps reduce the cost of the MDW gear train. Note that the 'grade' does not affect the surface finish of the gears. Therefore, using steel of a lower grade reduces rated torque capacity but factors such as noise are not affected. The design knobs s_t and s_c are set equal to those

corresponding to AGMA Grade 1 Steel (see Table 4-18) to generate an updated design map for rated torque in the Front End.

Table 4-18: Tuning of Design Knobs – Allowable Stresses (Material)

Design Knob	Previous value	New Value
s_t	70 ksi	55 ksi
s_c	225 ksi	180 ksi

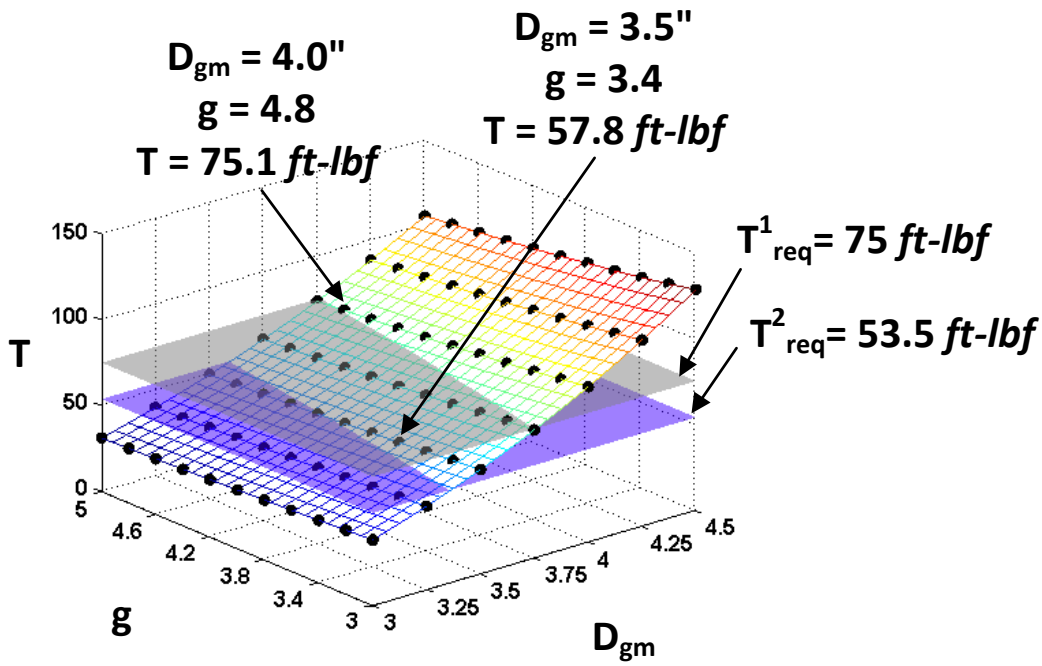

Figure 4-27: Design Map - Rated Torque in the Front End

Looking at the design map shown in Figure 4-27, it is possible to choose appropriate Front End solutions for each of the two competing alternative MDW gear trains. Corresponding design maps for the length L and weight W in the Front End are shown in Figure 4-28. As shown, it is easy to obtain information for both alternatives from a single map. From Figure 4-24 and Figure 4-28, it is possible to simply add the length of the corresponding 1st and 2nd stages to obtain the length of the whole C-Type 2-

Stage SCGT. Similarly, from Figure 4-25 and Figure 4-28, the weight of the entire gear train can be calculated by summing up the weights of the individual stages. The length and weights of the two competing alternatives are shown in Table 4-19.

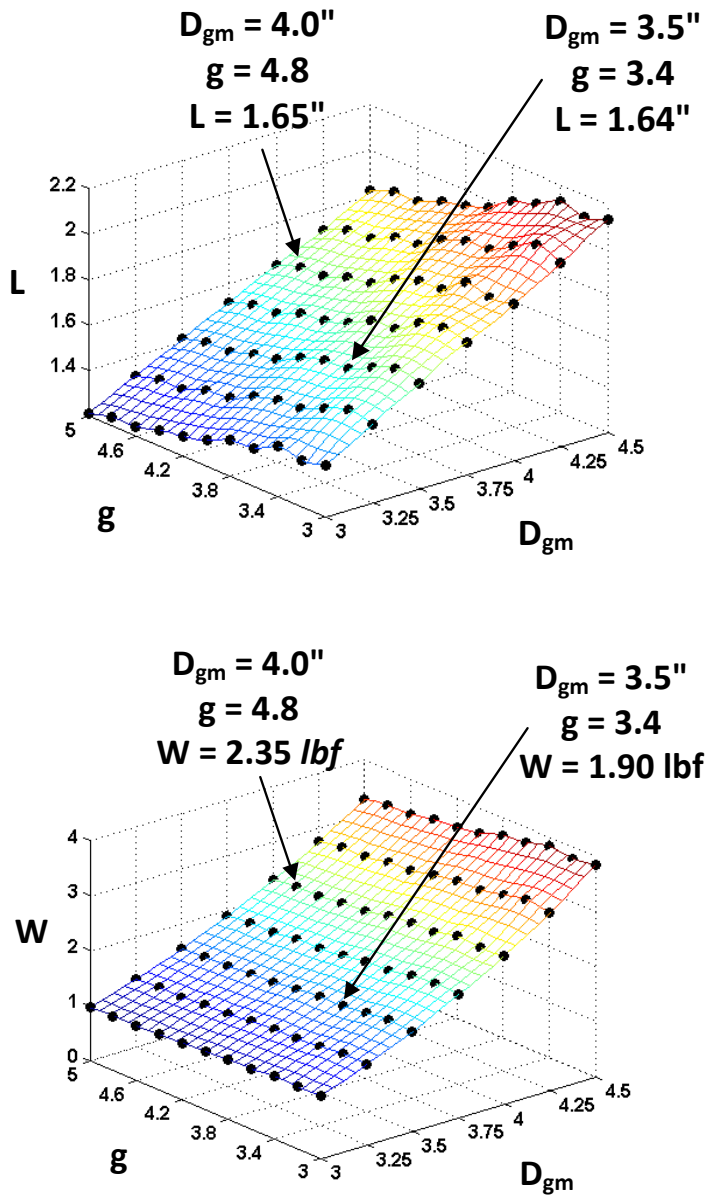

Figure 4-28: Design Maps (Front End) - Length (above) and Weight (below)

Table 4-19: Comparison between the Competing Design Alternatives

	Alternative-1	Alternative-2
g_f	4.8	3.4
g_b	10	14
D_{gm}	6”	5.4”
L	4.96” (3.32 + 1.64)	5.15”
W	21.65 *lbf* (19.3 + 2.3)	24.5 lbf (1.9 + 22.6)
T	751.5 *ft-lbf*	756 *ft-lbf*
T_D	34.7 *ft-lbf/lbf*	30.85 *ft-lbf/lbf*

4.3.2 Demand for Low Inertia

As Table 4-19 shows, both the design Alternatives satisfy the design requirements shown in Table 4-15. Assume that the Alternative which has lower inertia (and therefore greater responsiveness) is to be chosen as the final design solution. The Inertia (reflected to the input) in the Front End can be obtained using the following equation (compare with Equation 3.10):

$$I_{FrontEnd} = I_P + 3 \times \frac{(I_{LS} + I_{SS})}{g_1^2} + \frac{I_O}{g_f^2} \tag{3.26}$$

In Equation 4.8, the bearing inertias are not considered because they are generally insignificant compared to the gear components [Vaculik and Tesar, 2008]. All of the terms used in Equation 4.8 are those related to the Front End gear train. Since the Front End and Back End in a C-Type 2-Stage SCGT are serially connected, the inertia in the Back End simply has to be added to the inertia of the output gear of the Front End, in order to be able to calculate the inertia of the whole C-Type 2-Stage SCGT.

$$I_{C-Type} = I_P + 3 \times \frac{(I_{LS} + I_{SS})}{g_1^2} + \frac{I_O + I_{BackEnd}}{g_f^2} \tag{3.27}$$

Comparing Equation 4.8 and Equation 4.9, it can be seen that it is possible to express the inertia of a C-Type 2-Stage SCGT using the formula:

$$I_{C-Type} = I_{FrontEnd} + \frac{I_{BackEnd}}{g_f^2} \tag{3.28}$$

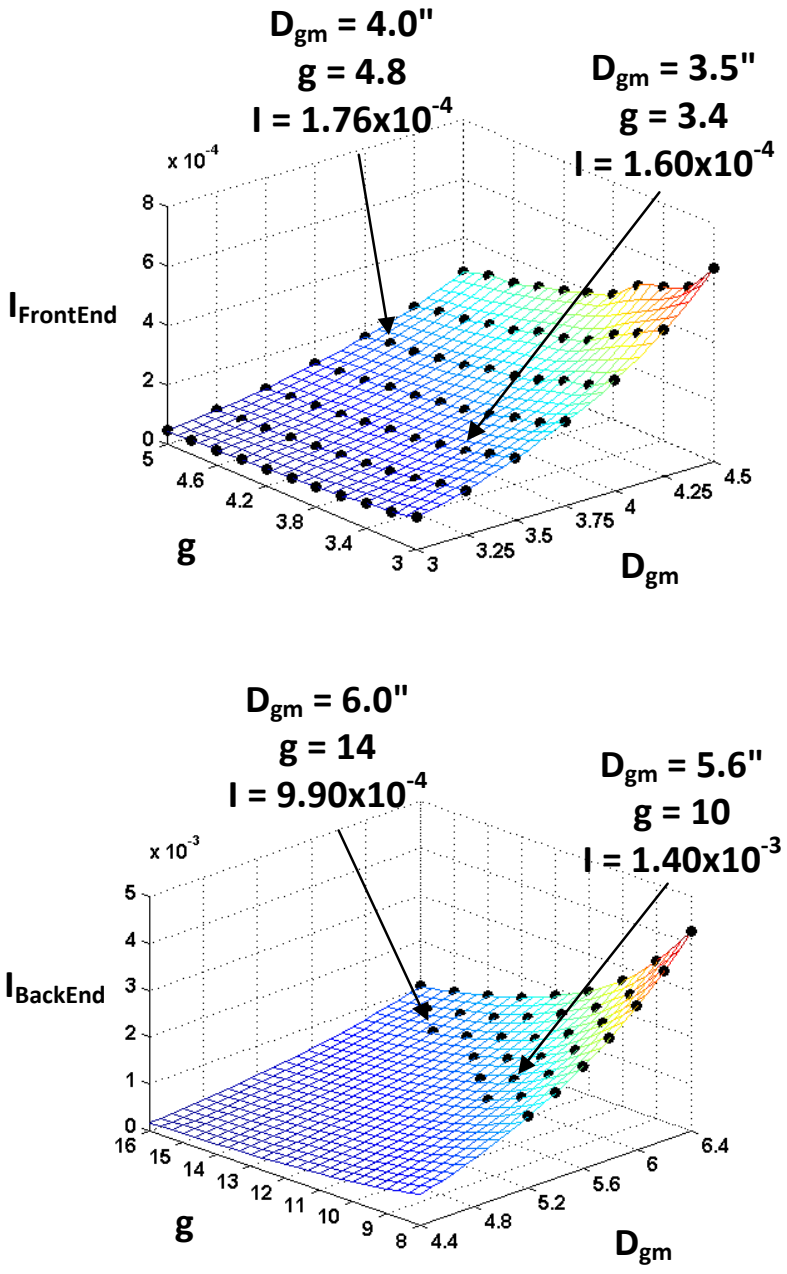

Figure 4-29: Design Maps - Inertia in the Front End (above) and Back End (below)

As shown in Chapter 3, design maps for the Inertia for both the Front end and Back End can be obtained using the design procedures developed in this report. These are shown in Figure 4-29. With the Inertia values obtained from Figure 4-29, the Inertia of the two alternative C-Type 2-Stage SCGT's can be calculated. These are shown in Table 4-20. The responsiveness at the input is also shown.

Table 4-20: Comparison between the Competing Design Alternatives

	Alternative-1	Alternative-2
g_f	4.8	3.4
g_b	10	14
D_{gm}	6"	5.4"
L	4.96" (3.32 + 1.64)	5.15"
W	21.65 *lbf* (19.3 + 2.3)	24.5 lbf (1.9 + 22.6)
T	751.5 *ft-lbf*	756 *ft-lbf*
T_D	34.7 *ft-lbf/lbf*	30.85 *ft-lbf/lbf*
I	$2.37\text{x}10^{-4}$ *lbm-in*^{4}	$2.46\text{x}10^{-4}$ *lbm-in*^{4}
R_I	$9.85\text{x}10^4$ *rad/s*	$9.54\text{x}10^4$ *rad/s*

4.3.2 Notes on Design Problem 3

By looking at Table 4-20, it can be seen that with regards to Inertia, both the design alternatives are not significantly different. Alternative-1 may be chosen for more in-depth development by a multi-person team. Alternative-1 only has slightly lesser inertia that Alternative-2. However, with regards to weight and torque density, design Alternative-1 can be said to more desirable than Alternative-2. Therefore, Alternative-1 may be picked for further design development. Note that the design problem was presented primarily to demonstrate to the reader, the efficacy of the design procedures developed in Chapter 2 and the design maps described in Chapter 3. Therefore, no effort was made to perform a detailed design of the MDW gear trains considered in the current design problem. Section 4.3.1 and Section 4.3.2 demonstrate that a single designer can

use the design maps and design knobs to quickly arrive at preliminary designs for two competing alternatives simultaneously.

4.4 CHAPTER SUMMARY

Three different design problems were presented in Chapter 4. The steps that a designer may take to tackle the given design problems were described. Although the specific steps necessary will vary depending on the application, it is possible to summarize the basic steps for the visual design approach as shown in Figure 4-30.

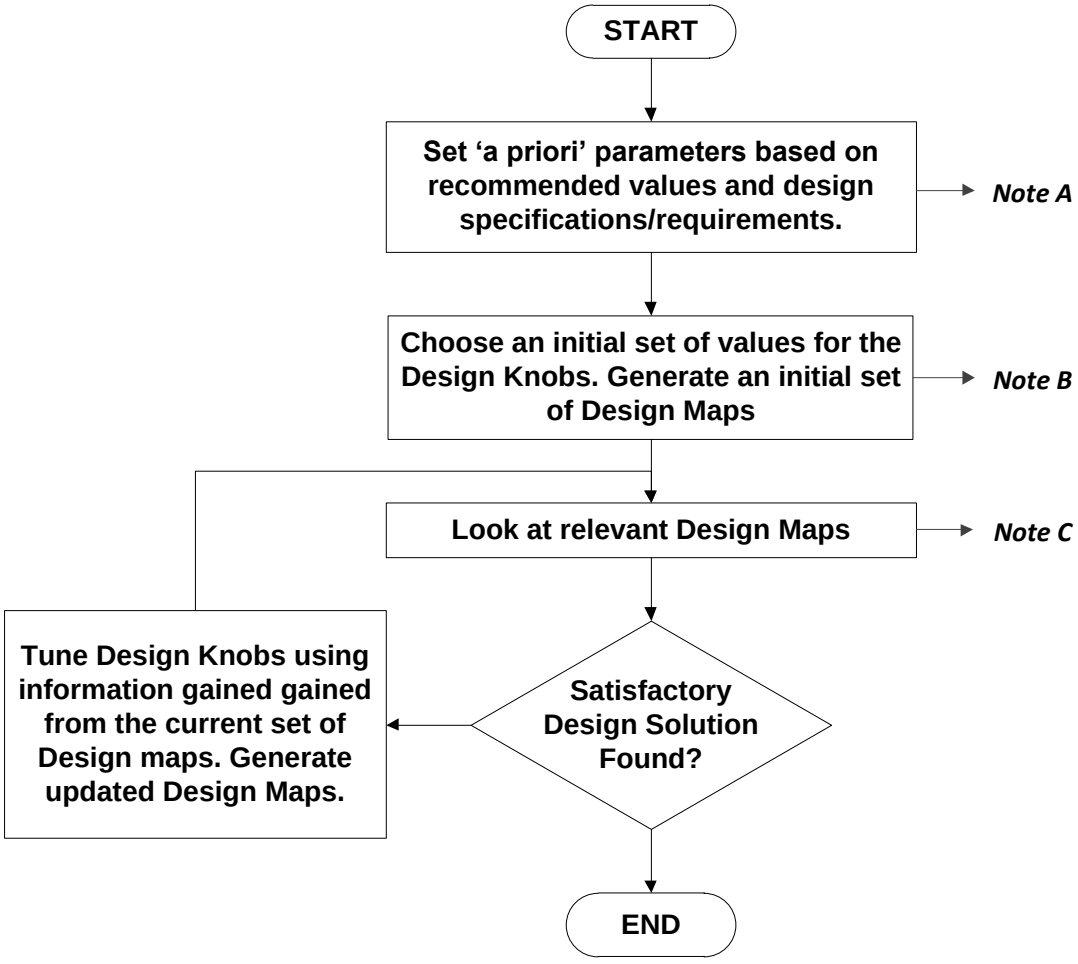

Figure 4-30: Flowchart Illustrating the Visual Approach to SCGT Design

The steps outlined in Figure 4-30 indicate the recommended approach a designer may employ when using the design maps for SCGT design. . Note A, Note B and Note C contain information relevant to the steps marked in Figure 4-30. They are shown below:

- **Note A:** The majority of A Priori parameters are the stress modification factors in the AGMA Strength Equations Some of these factors (such as K_v, K_o) are fixed by the design requirements while others (such as Safety Factors) depend upon the nature of the designer (aggressive or conservative (see Section 2.2). The values for the A Priori parameters used in this report are listed in Table 3-2.
- **Note B:** The initial set of Design Knobs together with the A Priori parameters are used to generate an initial set of Design Maps. Recommended values for the initial set of Design Knobs were provided in Section 3.2.1 and listed in Table 3-2.
- **Note C:** The relevant design maps are specific to the application being designed for. For example, if Inertia or Responsiveness is not important for a given application, Design maps for these parameters need not be considered. A novice designer may look only at Design Maps related to performance criteria (See Section 2.3). A more experienced designer may look at secondary criteria such as resultant thrust loads, amplification factors etc.

In summary, the recommended approach is to first generate a set of initial design maps by setting design knobs to values that are thought to be appropriate for the given design problem. If the design solutions obtained from the initial set of design maps are found not to satisfy the design requirements for a given problem, the design knobs are tuned so as to obtain updated design maps. Each set of design maps provides sufficient visual information for a designer to be able to understand what design knobs are to be tuned next. Thus, a designer may be able to obtain a design solution that satisfies a set of design requirements within minutes.

Chapter 5 : Summary and Conclusions

There is a growing tendency in the world today to replace traditional forms of actuation (e.g. hydraulic) with electromechanical (EMA) actuators (Budinger et al.). (Koran and Tesar 2008) suggest that the field of intelligent actuators has been developing for mechanical systems in a manner that parallels the computer chip for electronic systems. In order to improve EMA technology to meet increasingly demanding requirements, it is necessary for gear transmission technology to improve (Park 2005). The University of Texas Robotics Research Group (D.Tesar) has been pursuing in-depth actuator development since 1975 as documented in a 330 page listing entitled: Electromechanical Actuator Architecture (EMAA) The goal of the current research is to develop a design process for Star Compound Gear Trains (SCGT's), for use in a class of low complexity rotary actuators that can be mass produced at low cost while still maintaining a high level of performance.

5.1 Need for the Present Research

5.1.1 Shortcomings of traditional design methodologies

(Chong 2002) identifies a fundamental drawback of traditional gear train design methodologies. Although gear standards organizations and researchers provide methods for estimating gear sizing, these methods generally do not take into account the gear train configuration and arrangement. Methods for optimizing strength in single cylindrical pairs of gears are available (Kang and Choi 2009; V Spitas and C Spitas 2007)but are not very useful for multi-stage gear train design considered in the present research. It was found that researchers studying multi-stage gear train design have recently tended towards the use of optimization techniques (Savsani, Rao, and Vakharia 2010; Deb and Jain 2003; Huang, Tian, and Zuo 2005). However, one of the goals of the current

research was to develop a design process that a novice designer with perhaps a Bachelors degree in Mechanical Engineering would be able to use. Optimization techniques generally require an understanding of the optimization algorithms used in order to be effective.

5.1.2 Visual Decision-Making Environment

(Vaculik and Tesar, 2008) developed an electromechanical actuator framework with an emphasis on the development of preliminary visual decision-making tools. (Roos and Spiegelberg, 2005) make use of three-dimensional design surfaces as a tool to compare the relative merits of simple spur and planetary gear trains. (Simpson et al. 2007) state that visualization techniques are becoming more prevalently used in engineering design. A key focus of the current research, therefore, was to develop a relatively complete visual design process for Star Compound Gear Trains. The idea is that a designer may be able to make design decisions based on visual design information.

5.1.3 Interactive, Flexible Design Aid

(Tong and Walton 1987) describe an interactive program that guides a user towards a satisfactory design solution. The program ensures that assembly constraints such as center distance requirements are met. The end result is a complete design solution with all the information necessary for manufacture. It must be noted however, that their work deals with internal gear pairs; i.e., single mesh (not multi-stage reduction).

The ideas and background provided by the design tools/approaches discussed in Section 5.1.1, Section 5.1.2 and Section 5.1.3 indicated the need for a formal visual design process for the Star Compound Gear Trains studied in the current research. This became essential once it was realized that more than 20 basic design parameters must be

managed in terms of a broad range of gear train requirements (Rated torque capacity, Volume, Weight, Inertia, Responsiveness, Torque Density etc.) and assembly constraints.

5.2 SUMMARY OF THE PRESENT RESEARCH

5.2.1 Parametric Design

Procedures for the parametric design of three types of SCGT's considered in this report are developed and described in Chapter 2. Section 2.4 deals with the design procedure for a One-Stage SCGT. Section 2.5 presents the development of a design procedure for two variations of Pancake-Type 2-Stage SCGT's (P-Type 2-Stage SCGT's). The variation is in the number of amplifier gears (see Figure 2-22) in the second stage of the P-Type 2-Stage SCGT's. Pancake-Type SCGT's have low length to diameter ratio; i.e., low aspect ratio. Finally, Section 2.6 lays down the basic approach employed in the design procedure for a Coffee-Can Type 2-Stage SCGT. Coffee-Can Type SCGT's have much higher aspect ratios in comparison with P-Type SCGT's. A high-level summary of the SCGT design procedures is shown in Figure 5-1 (reproduced from Figure 2-15 in Chapter 2). The design procedure outlined in Figure 5-1 overcomes the shortcomings of traditional design methodologies discussed in Section 5.1.1. Configuration and dimensional design is integrated (Chong 2002) successfully for the multi-stage reductions occurring in SCGT's. This is done by using concepts from basic geometry coupled with a fundamental knowledge of gear train design. The reader is referred to Section 2.4 and Section 2.5 for an in-depth discussion of the development of parametric SCGT design procedures.

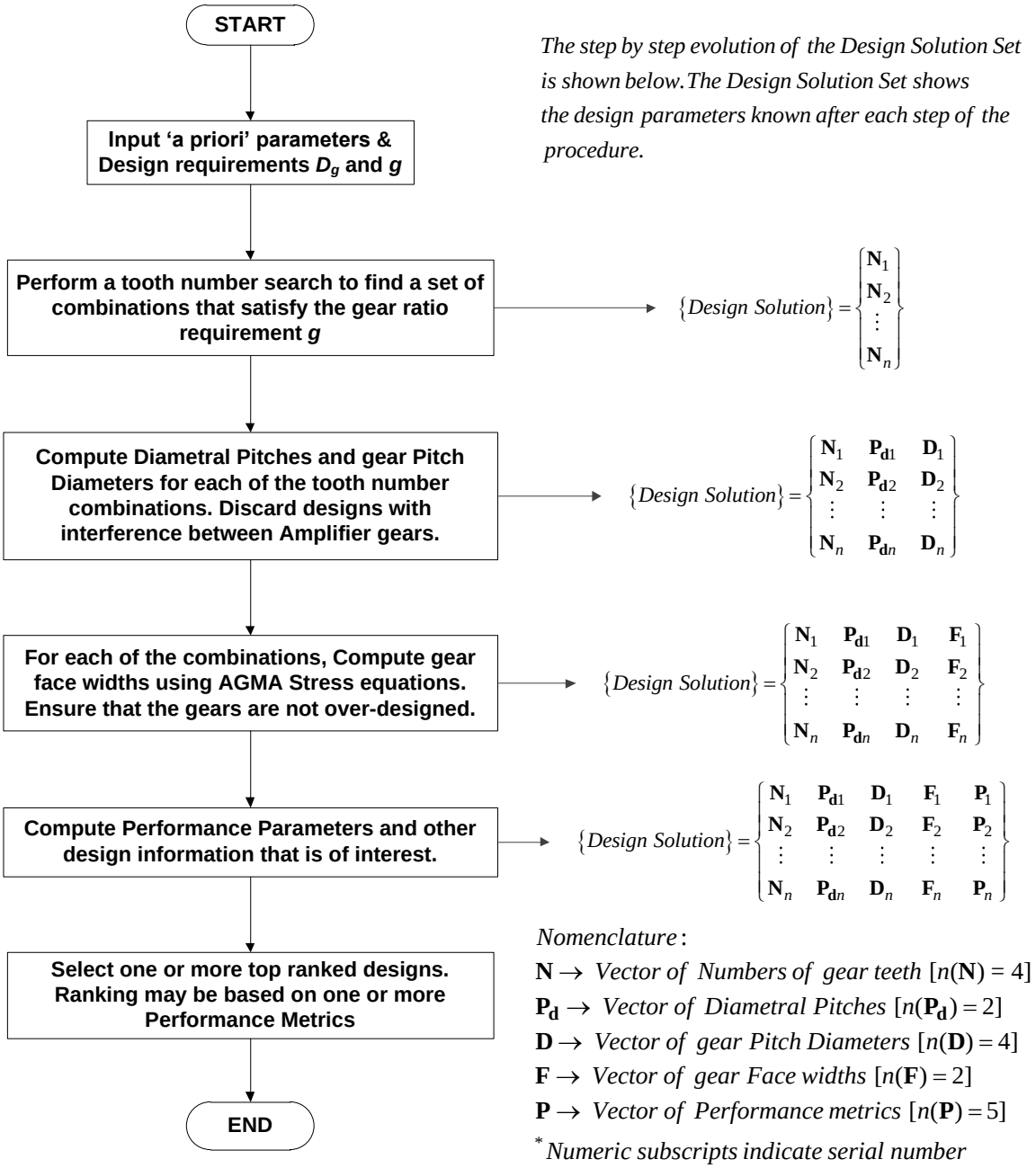

Figure 5-1: High Level Summary of SCGT Design Procedures

5.2.2 Design Maps

In Chapter 3, first design maps for One-Stage SCGT's are presented and analyzed in detail. In order to fully understand the shape of the design maps, curve-fitting in the form of power laws was done. The dependence of each of ther performance parameters (see Section 2.3) with the primary design knobs (gear mesh diameter *Dgm* and gear ratio g) (See Section 3.2.1) was thus explained. Six important design maps related to the 1-Stage SCGT are presented in Table 5-1 and Table 5-2. These design maps convey the design/performance parameter information that are generally useful for a novice designer to arrive at a design solution for a particular application. The reader may note that the six design maps shown in Table 5-1 and Table 5-2 are fully interactive when viewed on a computer screen. A designer can rotate and view them from any angle as well as select any of the design solutions in each map to obtain accurate design information. All six design maps are also linked. Each design map corresponds to the same set of design solutions. Therefore, when design knobs are changed, all six design maps are updated simultaneously. This characteristic is in keeping with the first of the key features for a visual decision-making environment (see Table 1-1) identified in Vaculik and Tesar, 2008.

The design maps shown in Table 5-1 and Table 5-2 relate to 1-Stage SCGT's For similar design maps related to P-Type 2-Stage SCGT's and the Front of the C-Type 2-Stage SCGT, the reader is referred to Section 3.5 and Section 3.6 from Chapter 3.

Table 5-1: Key Design Maps in a 1-Stage SCGT

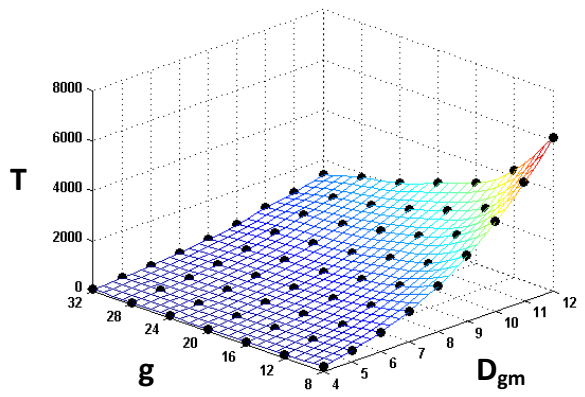	Rated Torque *(ft-lbf)*
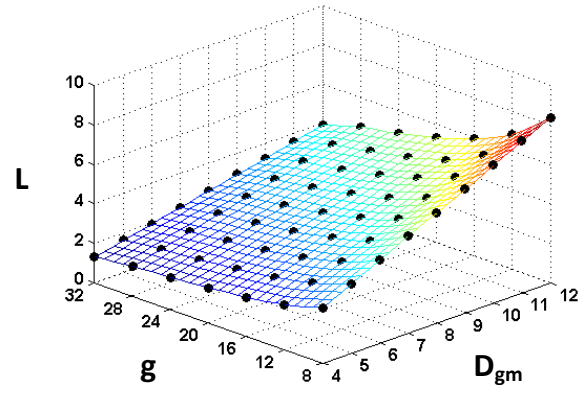	Length *(in)*
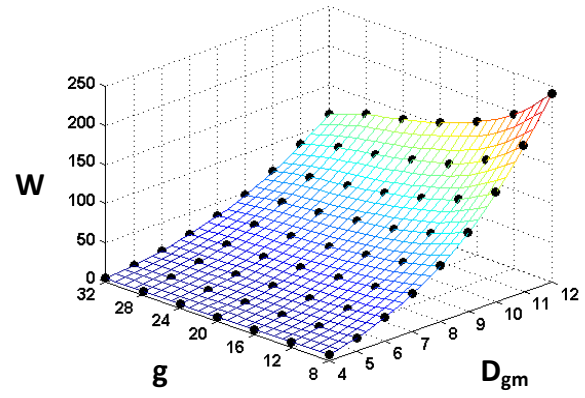	Weight *(lbf)*

Table 5-2: Key Design Maps in a 1-Stage SCGT (continued)

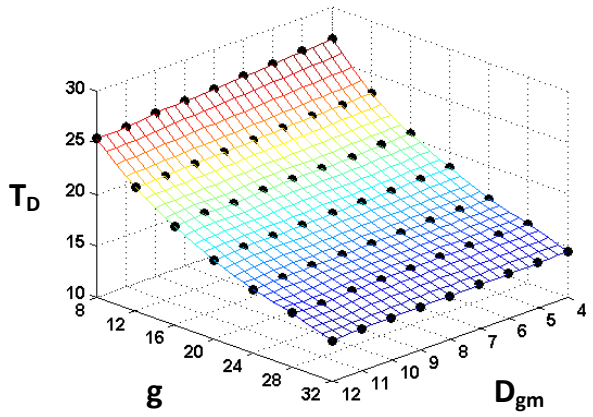	Torque Density *(ft-lbf/lbf)*
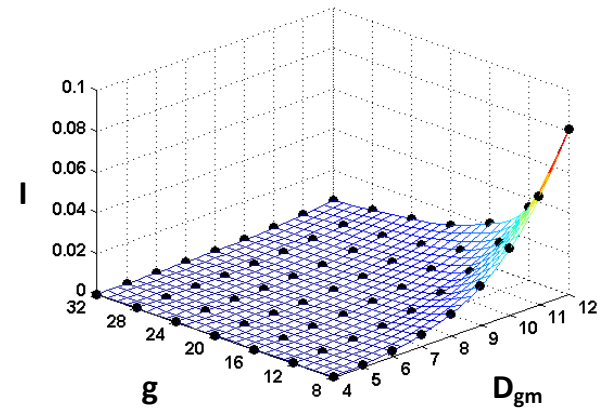	Inertia *(lbm-in2)*
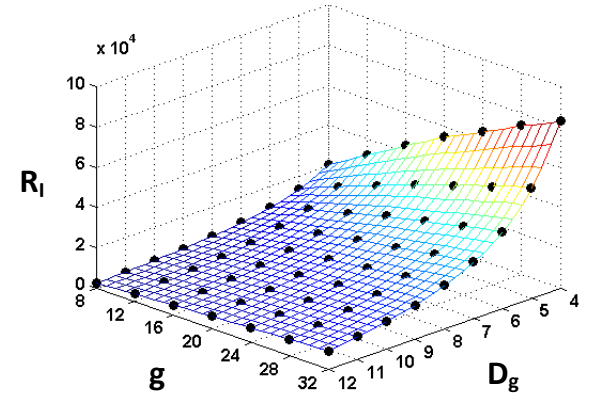	Input Responsiveness *(rad/s)*

An important goal of the current research is that the visual process must serve as a learning tool for a novice designer. The fact that the design information is conveyed visually to the designer is a key step towards meeting this goal. In order to illustrate this point, consider the design maps for rated torque capacity shown in Table 5-3 and Table 5-4. All of these design maps correspond to P-Type 2-Stage SCGT's with six amplifier gears in the second stage (P-Type-6). 'A Priori' parameters; i.e., design parameters that are fixed based on recommendations from the AGMA or based on the design requirements for all the design maps in Table 5-3 and Table 5-4 are kept constant. Only the design knobs (pressure angles, helix angles and gear material) are varied as described in the comments (see Table 5-3 and Table 5-4). The design maps shown in Table 5-3 and Table 5-4 provide a way for a novice designer to quickly assess the effect that basic design parameters have on the performance of the gear train. For clarity, a reference plane is drawn at 1000 lbf in the four design maps shown in Table 5-3 and Table 5-4. By comparing the area of the design maps that lie above the reference plane, it is possible to quickly assess the benefits of using helical gears versus spur gears, or higher pressure angles versus lower pressure angles for example.

Table 5-3: Design Maps as a Learning Tool – Rated Torque

Design Map	Comments
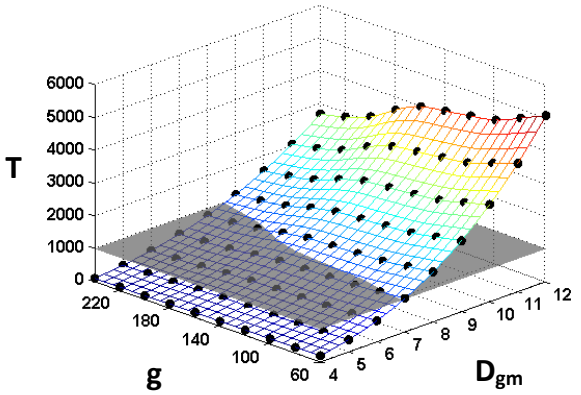	Material: Grade 2 Steel Gearing: Helical (15^o helix angle) Pressure Angle: 25^o
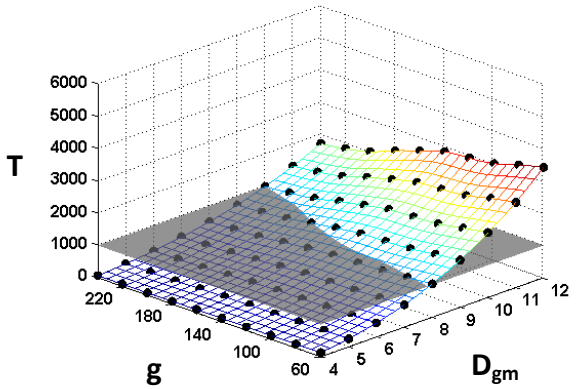	Material: Grade 1 Steel Gearing: Helical (15^o helix angle) Pressure Angle: 25^o
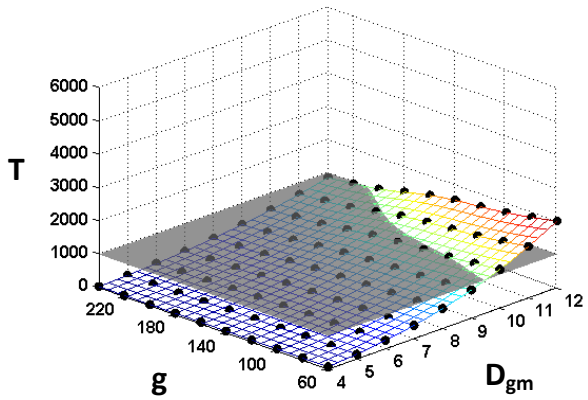	Material: Grade 1 Steel Gearing: Spur (0^o helix angle) Pressure Angle: 25^o

Table 5-4: Design Maps as a Learning Tool – Rated Torque (continued)

Design Map	Comments
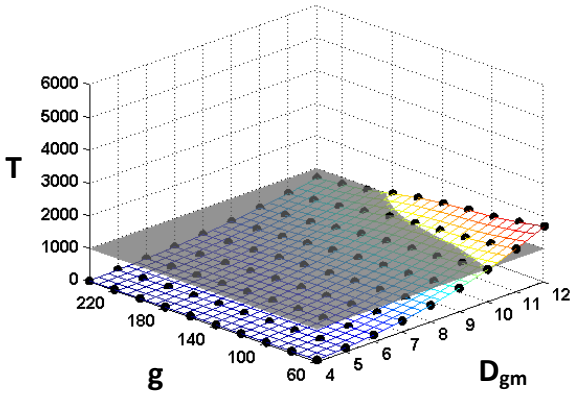	Material: Grade 1 Steel Gearing: Spur (0^o helix angle) Pressure Angle: 20^o

5.2.3 Visual Approach to SCGT Design

The discussions and design maps provided in this subsection should convince the reader of the benefits of presenting design information visually to a designer. For a full illustration on the use of the design maps in tackling a given design problem, the reader is advised to refer to Chapter 4. Three different design problems are presented in Chapter 4 and the visual decision making approach developed in the current research are used to find satisfactory solutions to the given design problems. The basic ideology employed in summarized in the flowchart shown in Figure 5-2.

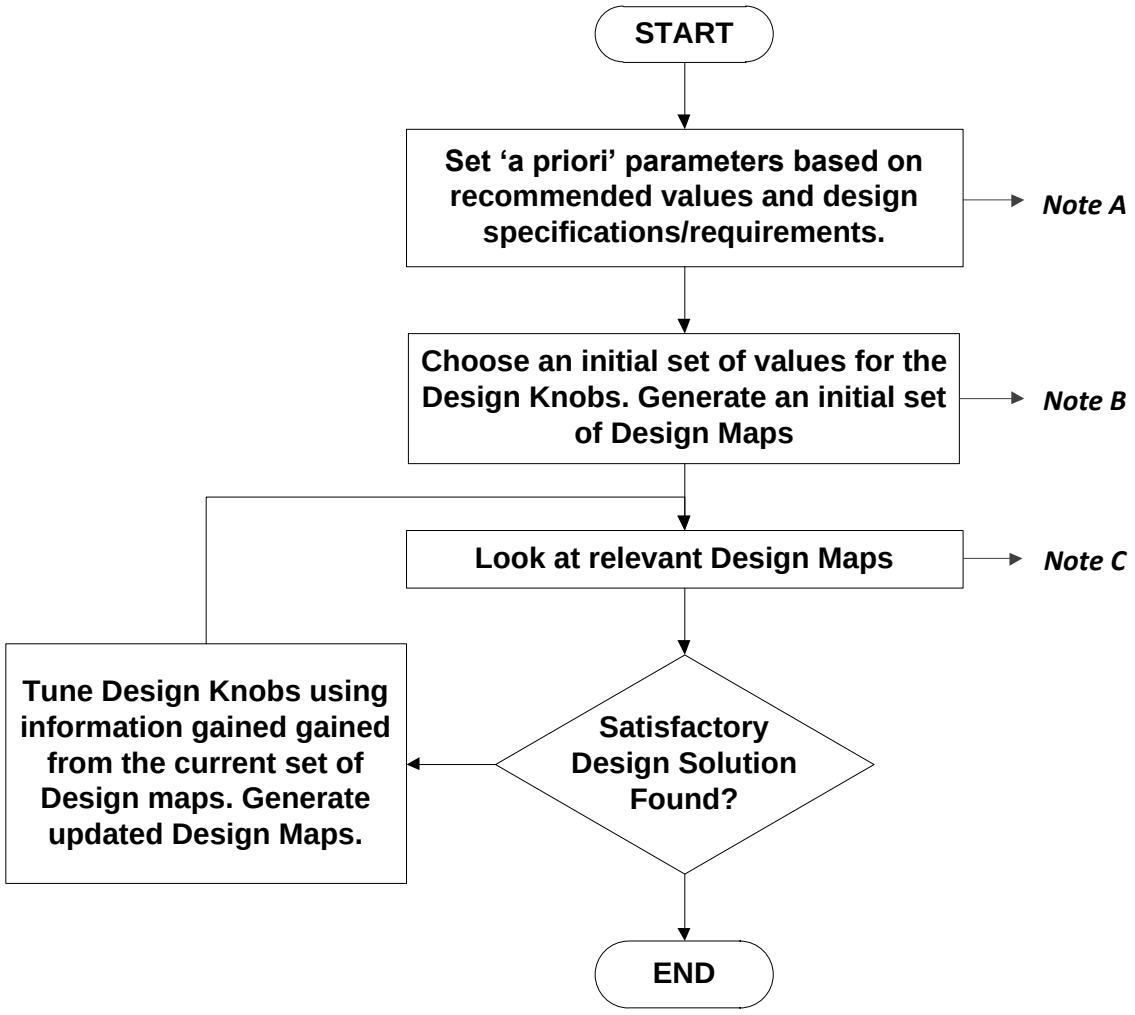

Figure 5-2: Flowchart illustrating the Visual Approach to SCGT Design (Reproduced from Figure 4-30)

A brief summary of Design Problem 1 from Section 4.1 (Chapter 4) is presented here to demonstrate to the reader, the value of the ideas embodied in Figure 5-2. A list of design requirements for the design problem under consideration is shown in Table 5-5. As outlined in Figure 5-2, the first two steps involve the setting and choosing of a priori

(fixed design parameters) and design knobs (design parameters free to be modified by the designer).

Table 5-5: Summary of Design Requirements

Design Requirement	Value
Rated Torque	833 *ft-lbf*
Output RPM	7.5 RPM
Gear Ratio	18
Max. Diameter	11 in
Max. Length	5 in
Life	10^7 revolutions at the output

A list of recommended a priori and initial design knob values is shown in Table 5-6 (reproduced from Table 3-2 in Chapter 3). The steps that follow are shown in Table 5-7 and Table 5-8. The reader may note that the steps shown as in keeping with the steps indicated in the flowchart for the visual design approach (Figure 5-2). The Table 5-7 and Table 5-8 show the set of relevant design maps obtained at each stage of the design. Comments are provided to help the reader understand how and which design knobs are tuned to generate the updated design maps.

Table 5-6: Summary of A Priori and Initial Design Knob Values

A Priori Parameters		
K_o	Overload Factor	1
K_v	Dynamic Factor	Calculated analytically
K_s	Size Factor	1
K_m	Load Distribution Factor	Calculated analytically
K_B	Rim Thickness Factor	1
C_f	Surface Condition Factor	1
K_T	Temperature Factor	1
K_R	Reliability Factor	1
S_F and S_H	Safety Factors	1.3
Y_N and Z_N	Stress Cycles Factors	Calculated corresponding to 10^7 mesh cycles at the output gear
J and I	Geometry Factors	Calculated analytically
C_P	Elastic Co-efficient	2300 (Both pinion and gear made of Steel)
C_H	Hardness Ratio Factor	1 (Pinion and gear equally strong)
Q_v	AGMA Accuracy Number	11
Design Knobs		
D_{gm}	Diameter	4” to 12” in increments of 1”
g	Gear Ratio	8 to 32 in increments of 4
F_{rule1}, F_{rule2}	Rule for max. face-width	1,1
φ_1, φ_2	Pressure Angles	25^o,25^o
ψ_1, ψ_2	Helix Angles	0^o,0^o
s_t	Allowable Bending Stress	70,000 psi
s_c	Allowable Pitting Stress	225,000 psi

Table 5-7: Initial Set of Design Maps

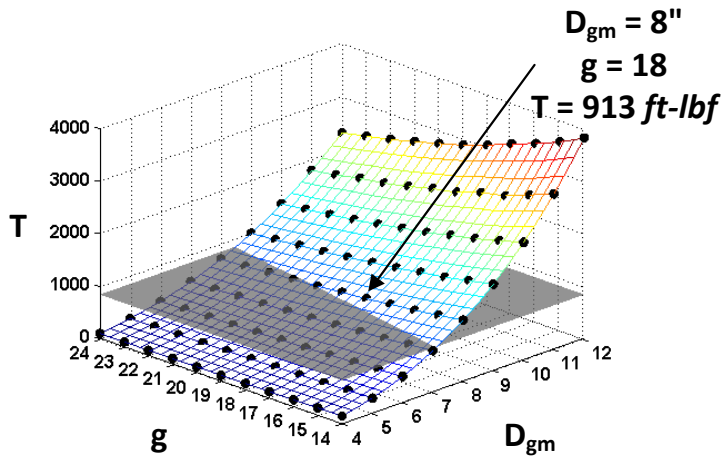

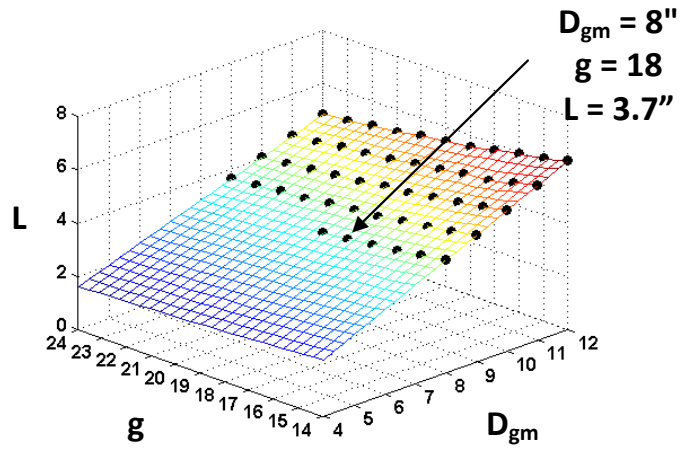

Comments

With regard to the upper design map for rated torque, all design solutions that lie above the horizontal reference plane achieve the required rated torque capacity. Looking at the smallest D_{gm} value corresponding to the desired gear ratio (18), a design solution 8” in diameter is seen to be a valid solution. The length L obtained from the lower design map is shown to satisfy the given length constraint.

It is observed from the design map for rated torque that the chosen design solution lies well above the reference plane indicating the required rated torque. It can also be seen that the solution corresponding to D_{gm}-g of 7”-18 lies below the reference plane (indicating inadequate torque capacity) whereas the chosen design solution with a D_{gm}-g combination of 8”-18 is well above the reference plane. Therefore, it is concluded that a design solution between the D_{gm} range of 7” to 8” might be more desirable.

Table 5-8: Updated Set of Design Maps

<table>
<tr>
<td> 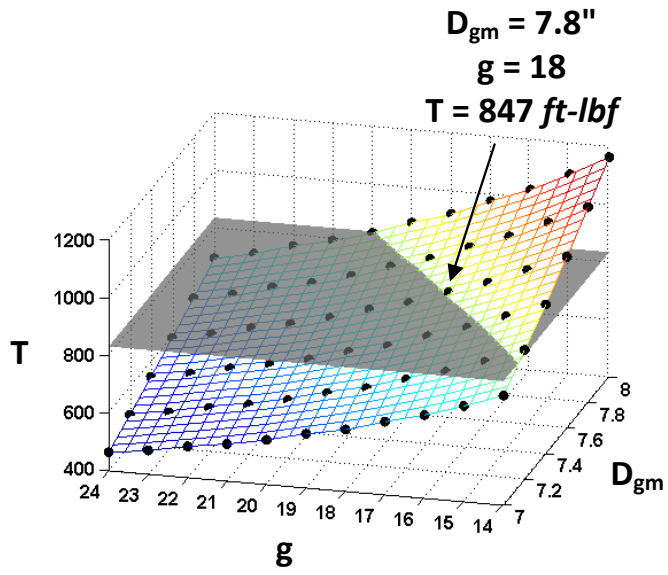
</td>
<td rowspan="2">Comments

Design Knob D_{gm} is modified to 7” to 8” and the updated design maps obtained are shown on the left. The design map for rated torque now indicates that a design solution with a D_{gm} of 7.8” (and gear ratio g of 18) is capable of providing the required rated torque capacity. The design solution obtained from this updated set of design maps can be seen to be smaller in volume than the earlier one. (both D_{gm} and L are smaller than previously)</td>
</tr>
<tr>
<td> 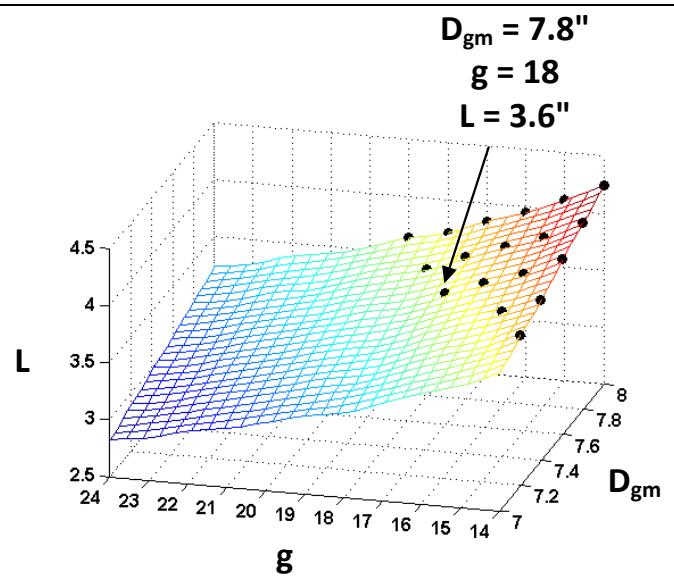
</td>
</tr>
<tr>
<td colspan="2">The design maps and comments presented in Table 5-7 and Table 5-8 illustrate a simple case of how design information conveyed visually to the designer is sufficient for him/her to understand how and which design knobs are to be tuned to arrive at a refined solution. The reader may refer to Section 4.1 to learn how the design solution can be further refined.</td>
</tr>
</table>

5.3 RECOMMENDED FUTURE WORK

Recommendations for future work will be divided into two categories. The first set of recommendations will relate to the Star Compound Gear Trains studied in this report. The second set of recommendations will relate to EMA's in general.

5.3.1 Recommendations for Future Work on Star Compound Gear Trains

The design procedures developed for the SCGT's studied in this research took into account more design parameters than generally considered for preliminary design. For instance, defer the choice of pressure and helix angles to a more detailed design stage. However, it is beneficial if a large number of design parameters can be selected in a preliminary design stage by a single designer if possible. Therefore, a possible extension of the design procedures developed in Chapter 2 of this report will be to include tooth modification parameters (addendum or dedendum modification) in order to obtain better design solutions at a preliminary design stage.

Another important area for future work is in the quantitative comparison of the SCGT's studied in this report with conventionally used planetary gear systems. Qualitatively, there is reason to expect that the Star Compound Gear Trains are superior to planetary gear systems at least in terms of inertia content and torque density.

It will be highly beneficial if a visual design process similar to the one developed in this report can be developed for bearing selection. This would require the availability of a full set of commercial bearing data. The combination of the two may be expected to significantly reduce the time taken to obtain a good preliminary gear train design for a given set of design requirements.

5.3.1 Recommendations for Future Work on Electro-mechanical Actuators

The Star Compound Gear Trains studied in the present research represent a class of low complexity gear trains. However, to be able to truly push EMA technology forward, visual design processes such as the one developed in this report should be developed for other gear train architectures as well. Two examples are UT RRG's Parallel Eccentric Gear Train (PEGT) and the Hypocyclic Gear Train (HGT). It is possible to envision the development of a complete visual design process that can handle the design of all these different gear architectures. Such a tool would be very useful for the development of these technologies in the future.

Further is an expanded architecture of actuators with layered control and position, (dual control - force and motion control, layered velocity control etc.). In other words, this design field is only beginning.

Appendix A

$$K_v = \begin{cases} \left(\dfrac{A+\sqrt{V}}{A}\right)^B & V \text{ in ft/min} \\ \left(\dfrac{A+\sqrt{200V}}{A}\right)^B & V \text{ in m/s} \end{cases}$$

where

$$A = 50 + 56(1 - B)$$

$$B = 0.25(12 - Q_v)^{2/3}$$

and the maximum velocity, representing the end point of the Q_v curve, is given by

$$(V_t)_{\max} = \begin{cases} [A + (Q_v - 3)]^2 & \text{ft/min} \\ \dfrac{[A + (Q_v - 3)]^2}{200} & \text{m/s} \end{cases}$$

Figure A.3: Calculation for the Dynamic Factor *Kv* (Extracted from Collins (2002))

$$K_m = C_{mf} = 1 + C_{mc}(C_{pf}C_{pm} + C_{ma}C_e)$$

$$C_{mc} = \begin{cases} 1 & \text{for uncrowned teeth} \\ 0.8 & \text{for crowned teeth} \end{cases}$$

$$C_{pf} = \begin{cases} \dfrac{F}{10d} - 0.025 & F \le 1 \text{ in} \\ \dfrac{F}{10d} - 0.0375 + 0.0125F & 1 < F \le 17 \text{ in} \\ \dfrac{F}{10d} - 0.1109 + 0.0207F - 0.000\,228F^2 & 17 < F \le 40 \text{ in} \end{cases}$$

Note that for values of $F/(10d) < 0.05$, $F/(10d) = 0.05$ is used.

$$C_{pm} = \begin{cases} 1 & \text{for straddle-mounted pinion with } S_1/S < 0.175 \\ 1.1 & \text{for straddle-mounted pinion with } S_1/S \ge 0.175 \end{cases}$$

$$C_{ma} = A + BF + CF^2 \qquad \text{(see Table 14–9 for values of } A, B, \text{ and } C)$$

$$C_e = \begin{cases} 0.8 & \text{for gearing adjusted at assembly, or compatibility} \\ & \text{is improved by lapping, or both} \\ 1 & \text{for all other conditions} \end{cases}$$

Figure A.4: Calculations of Load Distribution Factor K_m (Extracted from Collins (2002))

$$K_R = \begin{cases} 0.658 - 0.0759\ln(1 - R) & 0.5 < R < 0.99 \\ 0.50 - 0.109\ln(1 - R) & 0.99 \le R \le 0.9999 \end{cases}$$

Table 14–10

Reliability Factors K_R (Y_Z)

Source: ANSI/AGMA 2001-D04.

Reliability	K_R (Y_Z)
0.9999	1.50
0.999	1.25
0.99	1.00
0.90	0.85
0.50	0.70

Figure 5: Calculation and Look-up table for Reliability Factor K_R

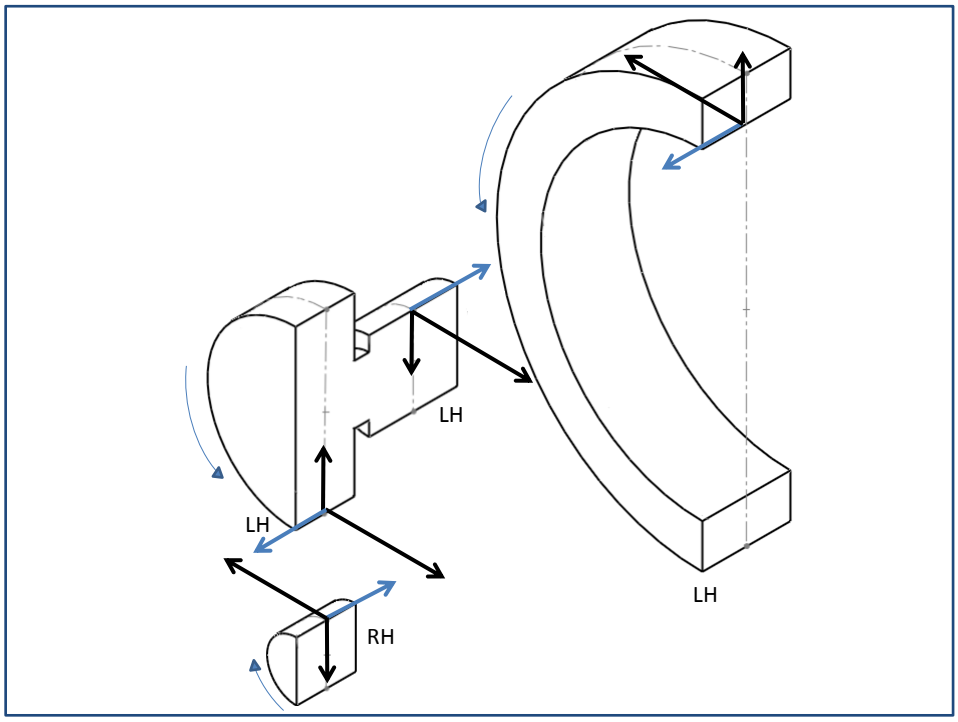

Figure 6: Shows appropriate choice of Helix Hands that oppose Amplifier Thrust Load
(LH - Left Hand Helix, RH - Right hand Helix)

References

Anon. Pitch Circle. http://www.diracdelta.co.uk/science/source/g/e/gear design/source.html.

Arikan, M. 2002. Direct calculation of AGMA geometry factor J by making use of polynomial equations. *Mechanics Research Communications* 29, no. 4 (August): 257-268. doi:10.1016/S0093-6413(02)00249-5. http://linkinghub.elsevier.com/retrieve/pii/S0093641302002495.

Ashok, Pradeepkumar. 2007. Math Framework For Decision Making In Intelligent Electromechanical Actuators. *Philosophy*. The University of Texas at Austin.

Budinger, M, J Liscouet, S Orieux, and J-ch Maré. Automated preliminary sizing of electromechanical actuator architectures 5, no. C.

Budynas, Richard, and Keith Nisbett. 2010. *Shigley's Mechanical Engineering Design*. 9th ed. McGraw-Hill Science/Engineering/Math, January.

Chong, T. 2002. A new and generalized methodology to design multi-stage gear drives by integrating the dimensional and the configuration design process. *Mechanism and Machine Theory* 37, no. 3 (March): 295-310. doi:10.1016/S0094-114X(01)00078-7. http://linkinghub.elsevier.com/retrieve/pii/S0094114X01000787.

Collins, Jack A. 2002. *Mechanical Design of Machine Elements and Machines: A Failure Prevention Perspective*. Wiley, November.

Deb, Kalyanmoy, and Sachin Jain. 2003. Multi-Speed Gearbox Design Using Multi-Objective Evolutionary Algorithms. *Journal of Mechanical Design* 125, no. 3: 609. doi:10.1115/1.1596242. http://link.aip.org/link/JMDEDB/v125/i3/p609/s1&Agg=doi.

Gonzalo. 2009. Higher Contact Ratios for Quieter Gears. *Gear Solutions.* http://www.gearsolutions.com/article/detail/5865/higher-contact-ratios-for-quieter-gears

Gonzalo, González Rey, Pablo Frechilla Fernández, and Roberto José García Martín. 2007. Estimating Gear Fatigue Life. *Gear Solutions*. http://www.gearsolutions.com/article/detail/5356/estimating-gear-fatigue-life.

Huang, Hong-Zhong, Zhi-Gang Tian, and Ming J. Zuo. 2005. Multiobjective optimization of three-stage spur gear reduction units using interactive physical programming. *Journal of Mechanical Science and Technology* 19, no. 5 (May):

1080-1086. doi:10.1007/BF02984029. http://www.springerlink.com/index/10.1007/BF02984029.

Kang, Ju Seok, and Yeon-Sun Choi. 2009. Optimization of helix angle for helical gear system. *Journal of Mechanical Science and Technology* 22, no. 12 (January): 2393-2402. doi:10.1007/s12206-008-0804-z. http://www.springerlink.com/index/10.1007/s12206-008-0804-z.

Kawalec, Andrzej, Jerzy Wiktor, and Dariusz Ceglarek. 2006. Comparative Analysis of Tooth-Root Strength Using ISO and AGMA Standards in Spur and Helical Gears With FEM-based Verification. *Journal of Mechanical Design* 128, no. 5: 1141. doi:10.1115/1.2214735. http://link.aip.org/link/JMDEDB/v128/i5/p1141/s1&Agg=doi.

Koran, L.R., and D. Tesar. 2008. Duty Cycle Analysis to Drive Intelligent Actuator Development. *IEEE Systems Journal* 2, no. 4 (December): 453-463. doi:10.1109/JSYST.2008.2004848. http://ieeexplore.ieee.org/lpdocs/epic03/wrapper.htm?arnumber=4682613.

Letaief, M R, F Chaari, and M Haddar. 2008. Influence of Internal Gears Rim Thickness and Design on Gearmesh Stiffness. *Mechanical Engineering* 2, no. December 2007: 62-68.

Lewicki, David G, Gregory F Heath, Robert R Filler, Stephen C Slaughter, and Jason Fetty. 2007. *RDS – 21 Face-Gear Surface Durability Tests*. *Society*.

Li, X, G R Symmons, and G Cockerham. 1996. Optimal Design Of Involute Profile Helical Gears. *Science* 31, no. 6: 717-728.

McCarthy, David L. 1996. A better way to rate gears. *Machine Design* 68, no. 5: 125.

Mott, Robert L. 2003. *Machine Elements in Mechanical Design*. 4th ed. Prentice Hall, July.

Norton, Robert L. 2010. *Machine Design*. 4th ed. Prentice Hall, February.

Oberg, Erik Et Al. 2000. *26th Edition Machinery's Handbook*. Industrial Press.

Park, Sang-hyun. 2005. Fundamental Development of Hypocycloidal Gear Transmissions. *Power*. The University of Texas at Austin. http://catalog.lib.utexas.edu/search/X?SEARCH=fundamental+development+hypocycloidal.

Pedrero, J.I, A Fuentes, and M Estrems. 2000. Approximate Method for the Determination of the Bending for External Spur and Helical. *Journal of Mechanical Design* 122, no. September: 331-336.

Pope, J Edward. 1996. *Rules of Thumb for Mechanical Engineers*. Ed. J Edward Pope. Gulf Professional Publishing. http://www.amazon.com/dp/0884157903.

Roos, F, H Johannson, and J Wikander. 2006. Optimal selection of motor and gearhead in mechatronic applications. *Mechatronics* 16, no. 1 (February): 63-72. doi:10.1016/j.mechatronics.2005.08.001. http://dx.doi.org/10.1016/j.mechatronics.2005.08.001.

Roos, Fredrik, and Christer Spiegelberg. 2005. Relations between size and gear ratio in spur and planetary gear trains by. *Trains*: 1-35.

Savsani, V., R.V. Rao, and D.P. Vakharia. 2010. Optimal weight design of a gear train using particle swarm optimization and simulated annealing algorithms. *Mechanism and Machine Theory* 45, no. 3 (March): 531-541. doi:10.1016/j.mechmachtheory.2009.10.010. http://linkinghub.elsevier.com/retrieve/pii/S0094114X09001943.

Schultz, C.D. 2009. The Effect of Gearbox Architecture on Wind Turbine Enclosure Size. In .

Shigley, Joseph, Charles Mischke, and Thomas Brown. *Standard Handbook of Machine Design*. McGraw-Hill Professional. http://www.amazon.com/Standard-Handbook-Machine-Design-Shigley/dp/0071441646.

Simpson, Timothy W., Kimberly Barron, Ling Rothrock, Mary Frecker, Russell R. Barton, and Chris Ligetti. 2007. Impact of response delay and training on user performance with text-based and graphical user interfaces for engineering design. *Research in Engineering Design* 18, no. 2 (July): 49-65. doi:10.1007/s00163-007-0033-y. http://www.springerlink.com/index/10.1007/s00163-007-0033-y.

Spitas, V, and C Spitas. 2007. Optimizing involute gear design for maximum bending strength and equivalent pitting resistance. *Proceedings of the Institution of Mechanical Engineers, Part C: Journal of Mechanical Engineering Science* 221, no. 4 (January): 479-488. doi:10.1243/0954406JMES342. http://journals.pepublishing.com/openurl.asp?genre=article&id=doi:10.1243/0954406JMES342.

Tong, B.S., and D. Walton. 1987. A computer design aid for internal spur and helical gears. *International Journal of Machine Tools and Manufacture* 27, no. 4: 479-489.

doi:doi: DOI: 10.1016/S0890-6955(87)80020-2. http://www.sciencedirect.com/science/article/B6V4B-4HMGVTK-7/2/9dab4951bcc58f4d13204c1e4d051421.

Vaculik, Stewart Andrew. 2008. A Framework For Electromechanical Actuator Design. *Office*. The University of Texas at Austin.

Weimer, J.a. 2003. The role of electric machines and drives in the more electric aircraft. *IEEE International Electric Machines and Drives Conference, 2003. IEMDC'03.* 11-15. doi:10.1109/IEMDC.2003.1211236. http://ieeexplore.ieee.org/lpdocs/epic03/wrapper.htm?arnumber=1211236.

Wilson, Charles E., and J. Peter Sadler. *Kinematics and Dynamics of Machinery (3rd Edition)*. Prentice Hall.

Winer, E.H., and C.L. Bloebaum. 2001. Visual design steering for optimization solution improvement. *Structural and Multidisciplinary Optimization* 22, no. 3 (October 1): 219-229. doi:10.1007/s001580100139. http://www.springerlink.com/openurl.asp?genre=article&id=doi:10.1007/s001580100139.